UNIVERSITY OF SOUTHAMPTON

FACULTY OF ENGINEERING AND APPLIED SCIENCE
CIVIL ENGINEERING DEPARTMENT

MANAGEMENT OF STREAM-AQUIFER SYSTEMS

by

Ahmed Mohamed Rashad Khater, B.Sc., M.Sc.

A thesis submitted to the Civil Engineering
Department for the degree of
Doctor of Philosophy

Southampton, January 1988

To My Wife Magda

UNIVERSITY OF SOUTHAMPTON

ABSTRACT

FACULTY OF ENGINEERING AND APPLIED SCIENCE
CIVIL ENGINEERING DEPARTMENT

Doctor of Philosophy

MANAGEMENT OF STREAM-AQUIFER SYSTEMS

By **Ahmed Mohamed Rashad Khater**

The term stream-aquifer system is used to denote a system of an alluvial aquifer which is in hydraulic connection with a stream. The system considered is of a deterministic nature and subject to conditions where a linear groundwater model can be applied. In the management problem of the system, management decisions are mainly concerned with the hydraulics of the system. The main objective is to safely optimize, on intra-annual basis, the yield of the system. Thus, the management problem essentially involves optimization of abstraction in space and time. Mathematical models which solve the management problem of the system and provide the information requested by the decision-making process involved in the operation of such system are developed in this work.

In order to solve the management problem, one must first be able to predict the response of the system to any proposed operational policy. A computer model, which is based on analytical solutions, has been developed to examine stream-aquifer interaction and to assess excitation-response relationships in general. The Boundary Element Method is then employed to solve forecasting problem of the system for steady and transient flow conditions.

The chosen approach to develop the management model is the combined simulation-optimization one. The response function technique is used to establish a link between simulation and optimization. The case study used to demonstrate the application of the model is that of the stream-aquifer system in the new land reclamation areas south-east of the Nile delta in Egypt.

ACKNOWLEDGEMENTS

The author gratefully acknowledges the advice and guidance provided by Dr. J.R. Rydzewski, who supervised this work.

The author would also like to thank Dr. Z. Svehlik (Institute of Irrigation Studies), Dr. R. Herbert (Hydrogeology Group, British Geological Survey), and Dr. S. Syngellakis (Civil Engineering Department) whose interest, discussions, comments and advice have been a great help in bringing this work to a conclusion.

The effort of Dr. T. Lock and the computation facilities provided by the Civil Engineering Department are also acknowledged.

The author would also like to express his sincere gratitude to the Water Research Centre and the Research Institute for Groundwater, Egypt, for providing the scholarship.

The financial support provided through the Dutch aid to Egypt, in the framework of the Project "Development and Management of Groundwater Resources in the Nile Valley and Delta", is gratefully acknowledged.

The author should also like to thank The Dutch Project team (IWACO) in Rotterdam and Cairo for the continuous support provided by Mrs. H.R. Jansen (Deputy Director, IWACO), Mr. S.J. de Jong (Regional Director, IWACO) and A. Tuinhof (Project Manager, Cairo, IWACO).

Finally, the author wishes to thank Mrs. G.J.Cooper for an excellent job of typing this thesis.

CONTENTS

	Page No
Abstract	i
Acknowledgements	ii
Contents	iii
CHAPTER 1 INTRODUCTION	1
1.1 Statement of the Problem	2
1.2 Objectives of Research	5
1.3 Approaches to Solution of the Problem	6
1.4 Method of Solution Adopted	10
1.5 Scope of Present Study	11
CHAPTER 2 A MATHEMATICAL MODEL OF STREAM-AQUIFER INTERACTION	15
2.1 Introduction	16
2.2 Theoretical Approach and Model Formulation	17
2.2.1 Stream Depletion During Pumping	17
2.2.2 Stream Depletion After Cessation of Pumping	20
2.2.3 Boundary Conditions in Real Systems	22
2.3 Computer Implementation of the Model	23
2.3.1 Computation Schemes	23
2.3.2 Evaluation of Mathematical Functions	25
2.3.3 Computer Programs	27
2.4 Excitation-Response Relationships	27
CHAPTER 3 MANAGEMENT OF A STREAM-AQUIFER SYSTEM	41
3.1 Introduction	42
3.2 Management Modelling of Aquifer Systems	44
3.2.1 Aquifer Simulation Approach	44
3.2.2 Combined Simulation-Optimization Approach	44

3.3 Stream-Aquifer Management Approach 47
3.3.1 Stream-Aquifer Response Functions 47
3.3.2 Hydraulic Management of the System 53

3.4 Formulation of the Management Model 55
3.4.1 Statement of the Optimization Problem 56
3.4.2 Solution of the Optimization Problem 58

CHAPTER 4 FORMULATION OF BOUNDARY ELEMENT SOLUTION FOR THE SIMULATION MODEL 59

4.1 Introduction 60

4.2 Boundary Element Solution For Transient Conditions 64
4.2.1 Governing Equations 64
4.2.2 The Fundamental Solution 65
4.2.3 Boundary Element Formulation 66
4.2.4 Solution of the Boundary Element Equation 71
4.2.4.1 Temporal Discretization 71
4.2.4.2 Spatial Discretization 73
4.2.4.3 Evaluation of the Integrals 85
4.2.4.4 Formation of the Matrices and Solution of Algebraic Equations 92

4.3 Boundary Element Solution for Steady-State Conditions 93
4.3.1 Governing Equations 93
4.3.2 The Fundamental Solution 94
4.3.3 Boundary Element Formulation 95
4.3.4 Solution of the Boundary Element Equation 98
4.3.4.1 Boundary Element Discretization 98
4.3.4.2 Domain discretization 100
4.3.5 Evaluation of the Integrals 102
4.3.5.1 Boundary Integrals 102
4.3.5.2 Domain Integrals 104
4.3.6 Solution of Algebraic Equations 104

4.4 Treatment of Discontinuity Problems 105
4.4.1 Treatment of Corners 105
4.4.2 Treatment of Zones 108

CHAPTER 5 COMPUTER IMPLEMENTATION OF THE BOUNDARY ELEMENT MODEL 110

5.1 Introduction 111

5.2 Input Data Section 111
5.2.1 Implementation of Spatial Discretization 111
5.2.2 Specification of Boundary Conditions 114
5.2.3 Specification of Parameters and Coefficients 117

5.3 The Boundary Element Solver 118
5.3.1 Evaluation of Integrals 118
5.3.2 Assembly of Equations 118
5.3.3 Solution of Equations 119
5.3.4 Interior Solutions 120

5.4 The Computer Program "SABEM" 120
5.4.1 Program Description 120
5.4.2 Sample Problems 125

CHAPTER 6 CASE STUDY: THE STREAM-AQUIFER SYSTEM SOUTH-EAST OF THE NILE DELTA DESCRIPTION OF SYSTEM 133

6.1 Introduction 134

6.2 Physical Setting 134
6.2.1 Location and Topography 134
6.2.2 Climate 137
6.2.3 Physiography 137
6.2.4 Geology 137

6.3 Hydrogeology 143
6.3.1 Hydrogeological Setup 143
6.3.2 Regional Flow of Groundwater 145
6.3.3 Quality of Groundwater 148
6.3.4 Salt Water Intrusion 148

6.4 The Ismailia Canal 152
6.4.1 Existing Conditions 152
6.4.2 Future Development 154
6.4.3 Canal Seepage 155

CHAPTER 7 CASE STUDY: MANAGEMENT OF THE STREAM-AQUIFER SYSTEM 158

7.1 Introduction 159

7.2 The Management Problem 161
7.2.1 Optimal Yield of the System 161
7.2.2 Development Considerations and Constraints 162
7.2.3 The Management Model 163

7.3 Simulation Modelling 163
7.3.1 Input Data 163
7.3.2 Calibration of the Model 165
7.3.3 Application of the Model 176

7.4 Hydraulic Management of the System 178
7.4.1 Alternative Operating Policies 178
7.4.2 Application of the Management Model 180
7.4.3 Feedback Verification 187

CHAPTER 8 CASE STUDY: RESULTS OF THE MANAGEMENT MODEL ANALYSIS 189

8.1 Introduction 190

8.2 Optimal Solution 191
8.2.1 Operating Policy 1 191
8.2.2 Operating Policy 2 197
8.2.3 Operating Policy 3 201
8.2.4 Operating Policy 4 207

8.3 Feedback Verification 212
8.3.1 Steady State Drawdowns 212
8.3.2 Location of the Interface 212

8.4 Concluding Remarks 221

CHAPTER 9 CONCLUSIONS AND RECOMMENDATIONS 222

9.1 Conclusions 223

9.2 Recommendations 226

REFERENCES 228

APPENDICES

CHAPTER 1

INTRODUCTION

1.1 Statement of the Problem

1.2 Objectives of Research

1.3 Approaches to Solution of the Problem

1.4 Method of Solution Adopted

1.5 Scope of Present Study

CHAPTER 1
INTRODUCTION

1.1 Statement of the Problem

In developing countries, in semi-arid and arid regions, where water resources are not only limited, but mostly improperly operated, regional planning for efficient agricultural expansion is a complex undertaking. Basic to this problem is making an optimal development of the available water resources. The rapid expansion of population and the increasing needs for agricultural development has brought about a substantial rise in the demand for groundwater use to supplement surface water supplies.

In Egypt, over the next two decades, the government has planned to expand the agricultural sector by reclaiming new lands to meet the incessantly growing population and the pressing needs for economic development. Egyptian agriculture is wholly dependent on the Nile water. At present, Egypt's annual quota of the Nile water ($55.5 \times 10^9 m^3$) is almost fully consumed. Groundwater constitutes additional resources that are not fully utilized. The Ministry of Irrigation and other agencies of the government have a strong desire to improve their capability to manage the water resources of the country. Thus, research studies are needed to guide the available water resources towards optimal development. The need for such studies is clearly spelled in the five years research plan of the Water Research Centre of the Ministry of Irrigation.

The advocacy of multi-disciplinary approach to optimal development of water resources by engineers, researchers and administrators has created a demand for management tools which could accommodate all the components of the complex

problem including size of the physical system, the necessity for regulating the usage and distribution on a short term basis. The present study aims to develop an efficient management tool for the development of groundwater resources in an alluvial aquifer which is in hydraulic connection with a stream, a natural system which is referred to herein as the "stream-aquifer system". The main objective of management here is to safely optimize, on intra-annual basis, the yield of the system so that optimal development policy or policies are available on hand for the planning of an efficient agricultural expansion. The management problem of the system essentially involves optimization of abstraction points in space and time. The study introduces the concept of considering the stream-aquifer interaction as a manageable component of the system.

The case study which is considered in application of the management model is that of the stream-aquifer system in the new land reclamation areas south east of the Nile delta. Namely, the unconfined part of the Quaternary alluvial aquifer of the Nile delta and the Ismailia canal. The stream flows, natural recharge to the aquifer and other factors affecting water balance in the system are of deterministic nature. Head levels in the stream and the discharges are controlled. The interaction between the stream and the aquifer is assumed to be such that, there is sufficient flow in the stream at all times so that withdrawals directly from the stream or losses from the stream to the aquifer do not affect the head levels in the stream, and likewise, normal seasonal variations in stream head levels produce negligible interaction. The saturated thickness of the aquifer is always large compared to that of any drawdown; hence transmissivity is independent of head. There is no subsidence, and groundwater is instantly released from storage. Under these conditions a linear groundwater model is applicable.

Future agricultural development in Egypt asks for an integrated policy for allocation of the available water resources and careful planning for the development of groundwater resources so that groundwater usage is maximised in those areas where aquifers have excellent properties and the saved surface water could be transported to other areas where groundwater has low potentiality. It is evident that, waterlogging and salinization problems associated with the previous experience of reclaiming desert uplands in the vicinity of the Nile delta and valley stem from neglecting interaction between surface and groundwater and the assumed independence of water resources. If a development plan for groundwater resources in those areas was available at that time, these problems could be quantitatively appreciated and minimised in the planning stage, and much would be gained. In a stream-aquifer system, the answer to these problems is to deal with the integrated structure of the system by considering the mutual interaction between the super-structure on the surface represented by the stream and the sub-structure being the aquifer. In this sense, seepage from the stream into the aquifer is viewed as natural diversion into the aquifer which acts as a natural reservoir as well as a distribution network of a certain capacity that can be assessed and optimally utilized. Thus, the aimed control on the system is not achieved by eliminating the stream-aquifer interaction but by extending the imposed manipulation to handle the integrated system.

Hence, a management model which is capable of determining optimal areal and temporal quantitative distribution of groundwater withdrawals in the system is the tool to be developed, and how much could be utilized, where and when are the unknowns to be determined.

1.2 Objectives of Research

In view of the limited water resources, in Egypt as well as in many parts of the world, research studies are needed to guide the available water resources towards optimal development. The substantial rise in the demand for groundwater use to supplement surface water supplies asks for efficient management tools that could provide planning schemes for optimal development of aquifer systems.

One of the most reliable means of solving management problems of aquifer systems and providing the information requested by the decision-making process involved in planning, designing and running these systems is the use of mathematical models. Therefore, the primary objective of this work is to develop a management model for groundwater resources in a natural system which exists wherever an aquifer is in hydraulic connection with surface water. The system is referred to in this study as a "stream-aquifer system".

Another objective which is concerned with the development of the model is to employ the Boundary Element method in solving the forecasting problem of a stream-aquifer system to overcome the problems associated with scarce data and the need to construct a model which simulates the real system. In this respect, the boundary element method holds a promise for reducing computational effort and the initial amount of data required to run a problem with comparable numerical accuracy as that achieved by the alternative methods.

The other objectives considered in this work are concerned with

- defining the role of stream-aquifer interaction as a manageable component of the system,
- highlighting the fact that, a stream-aquifer system

should be managed and operated as a unit to achieve various goals beyond serving as just a source of water,

- and applying the developed model to a case study related to the new land south-east of the Nile Delta to provide an accessible source of water in the desert uplands where large-scale land reclamation projects are planned.

1.3 Approaches to Solution of the Problem

The natural system of an aquifer traversed by a stream in hydraulic connection with it is recognised in literature as stream-aquifer system. Management of such a system requires evaluation of the interaction between the stream and the aquifer. Groundwater abstraction from a stream-aquifer system implies that water is derived from storage in the aquifer as well as from induced seepage from the stream. The need to estimate the flow from a stream to an aquifer caused by pumping near the stream was early identified by Theis (1941). He presented an analytical solution to obtain the ratio of water lost from a stream to the amount of water pumped from a single well in an idealized system. Glover and Balmer (1954) derived an analytical expression for the ratio of water lost from river and flow of well using the relationship between the quantity pumped and the corresponding aquifer drawdown. Hantush (1955), and Hantush and Jacob (1955) derived an expression for the same ratio. Hantush (1964, 1965) introduced a modification which made the derived expression approximately applicable when the stream bed is semi-pervious and partially penetrating the aquifer. Jenkins (1968a) used the previous work of Glover and Balmer (1954) and Hantush (1964) to produce a set of dimensionless curves and tables which could be used to estimate the rate of stream depletion during the pumping period or after cessation of pumping from

a nearby well. In this study Jenkins also introduced the concept of a system descriptor which expresses the effects of hydraulic properties of the aquifer and the location and types of boundaries; he names this descriptor as the stream depletion factor. In later studies by Jenkins (1968b), Moulder and Jenkins (1969), and Jenkins and Taylor (1974) the stream depletion factor was evaluated for real stream-aquifer systems using electric analogs and finite difference digital models.

Mathematical treatment of groundwater flow and bank storage in response to a sinusoidal change in stream stage was presented by Cooper and Rorabaugh (1963). Hornberger, Ebert and Remson (1970) used a finite difference scheme to solve the Boussinesq's equation in one dimension for stream-aquifer interaction considering groundwater recession and groundwater flow in response to changes in stream stage. Hall and Moench (1972) treated the stream-aquifer system as a linear system and derived a general approach to handle flood pulses using the convolution equation. They used the analytical expressions derived by Carslaw and Jaeger (1959) and Cooper and Rorabaugh (1963) to generate the unit step response functions for four idealized cases of finite and semi-finite aquifers, with and without semi-pervious stream banks.

The role of mathematical models as tools to solve management problems associated with groundwater systems is now fully realised. When dealing with a groundwater management problem, it is necessary to assess the aquifer responses to different operation alternatives. Numerical simulation methods have provided a framework for conceptualizing and evaluating aquifer systems. It is unlikely that optimal management alternatives will be discovered using simulation techniques alone, what is required is a combined simulation and optimization approach. A guide to a broad range of groundwater models, including

management models, was presented by Bachmat et al (1980). A comprehensive review of distributed parameter groundwater management modelling methods was presented by Gorelick (1983).

Several hydrologic models of stream-aquifer systems have been developed in the past; Glover (1960), Eshett and Bittinger (1965). These models were designed to predict the hydraulic behaviour of the system in response to particular sets of numerical values of excitations rather than provide a functional relation between the response and the excitation. Aquifer simulation models are distributed parameter models based on diffusion type partial differential equations with suitably defined initial and boundary conditions. They are difficult to couple explicitly with optimization techniques. Two reported pioneer endeavours to couple simulation with optimization were introduced to a management model of a stream-aquifer system. Martin, Burdak and Young (1969) used a linear programming model indirectly coupled with an electric analog groundwater model. Bredehoeft and Young (1970) replaced the electric analog with a digital model and in a single study they have combined a physically realistic hydrologic model of a stream-aquifer system with a description of the economic behaviour of the water users. Morel-Seytoux and Daly (1975) reported that "A definite evolution in the modelling of stream-aquifer system is apparent. At first the hydrologic model was viewed primarily as an end itself. Now it is viewed as a necessary intermediate component of a more complex system. Since the role of hydrologic model has changed, should not its design also be modified?" In a series of papers, Maddock (1972, 1973, 1974) has developed and applied a Green's function representation which involved the distributed aquifer behaviour directly in the optimization through a set of response functions. He referred to these response functions as the algebraic technological functions. A similar aquifer response

approach has been adopted by Morel-Seytoux and Daly (1975) and Morel-Seytoux (1975). The basic procedure is to use the response function of the physical components of the system to simulate the behaviour of the whole system when subject to different excitations. The approach is based on the theory of linear systems and it is known in literature as 'response function' by Venetis (1968), 'influence coefficients or functions' by Schawarz (1971), and 'technological functions' by Maddock (1972).

The recent work of Bathala (1980), Heidari (1982), and Illangasekare and Morel-Seytoux (1982, 1983 and 1984) have demonstrated that the response functions approach is applicable to real world systems and is a valuable tool for evaluating groundwater management policies. Thus, the response functions approach is chosen to be used in developing the management algorithm for the considered stream-aquifer system in this work.

Computer based numerical methods are practically the major tool for solving large scale groundwater forecasting problems as encountered in practice. In recent years, parallel to the advance in computer technology, effort has been devoted to the development of the techniques of numerical simulation. Among specialised literature on this subject, one may mention those of Remson et al (1971), who deal mainly with finite difference techniques, Pinder and Gray (1977), who deal with finite element method, and Huyakorn and Pinder (1983) who deal with the various numerical approaches. Finite differences were used extensively in the 1960s. In the 1970s finite elements began to replace finite differences as the dominant techniques. Lately, the boundary integral equation method has emerged as a contender in the computation rally under the name Boundary Elements. The term 'boundary elements' was originated within the Department of Civil Engineering at Southampton University where the method has been presented

in a form attractive to engineering analysts by Brebbia (1978), Brebbia and Walker (1980), and Butterfield and Banerjee (1981). The boundary element method holds promise for reducing computational efforts and the data required to run a problem, yet the numerical accuracy is generally greater than that of finite elements. Thus, boundary element techniques are employed in this study.

The other literature related to theories and approaches used in this study are cited and referenced at the proper places in the text.

1.4 Method of Solution Adopted

The ability to predict the response of a system to any implemented decision is an intrinsic part of the procedure for determining a management policy. Mathematical models are often employed to solve the forecasting problem of water resources systems. Information derived from solving the forecasting problem serves as an input to the management problem.

A mathematical model, based on analytical solutions for the case of pumping a single well in a stream-aquifer system, is developed to investigate the stream-aquifer interaction in terms of excitation-response relationships. The model provides the facility to perform sensitivity analysis and make a quantitative assessment of the role of the various variables which should be on hand before seeking management of the system. The forecasting problem in a stream-aquifer system, being a regional problem of practical interest, is likely to be solved by numerical methods. However, in this analytical model, the author makes an identification of those relationships that should help in the development of the management statement.

Modelling of aquifer systems is an area of current research. As such, new techniques and applications continually evolve. In addition to being influenced by the necessity to solve certain problems, recent developments in modelling are influenced by the state of model evolution and computer capabilities. Referring to the present study, the author employs the boundary element method, being one of the recent developments in numerical modelling techniques, to solve the forecasting problem of the stream-aquifer system. The forecasting problem of the system is a time dependent one. Thus, the boundary element solution is for transient two-dimensional regional flow in the system. However, solution for steady-state condition is essential to calibrate the model and to generate the initial conditions for the transient solution.

In the management problem of the considered stream-aquifer system, management decisions are primarily concerned with the groundwater hydraulics of the system. Thus, the management model of the system, in the first level, is a hydraulic management one. The chosen approach to develop the management model is the combined simulation-optimization one. The response functions technique is selected to establish the link between the simulation model and the optimisation routine to form the developed management tool. The proposed management approach, modelling steps and operation are schematically shown on Figure (1.1).

1.5 Scope of Present Study

A mathematical model is developed to investigate the excitation-response relationships in a stream-aquifer system. The model formulation and the performed analysis are presented in Chapter 2.

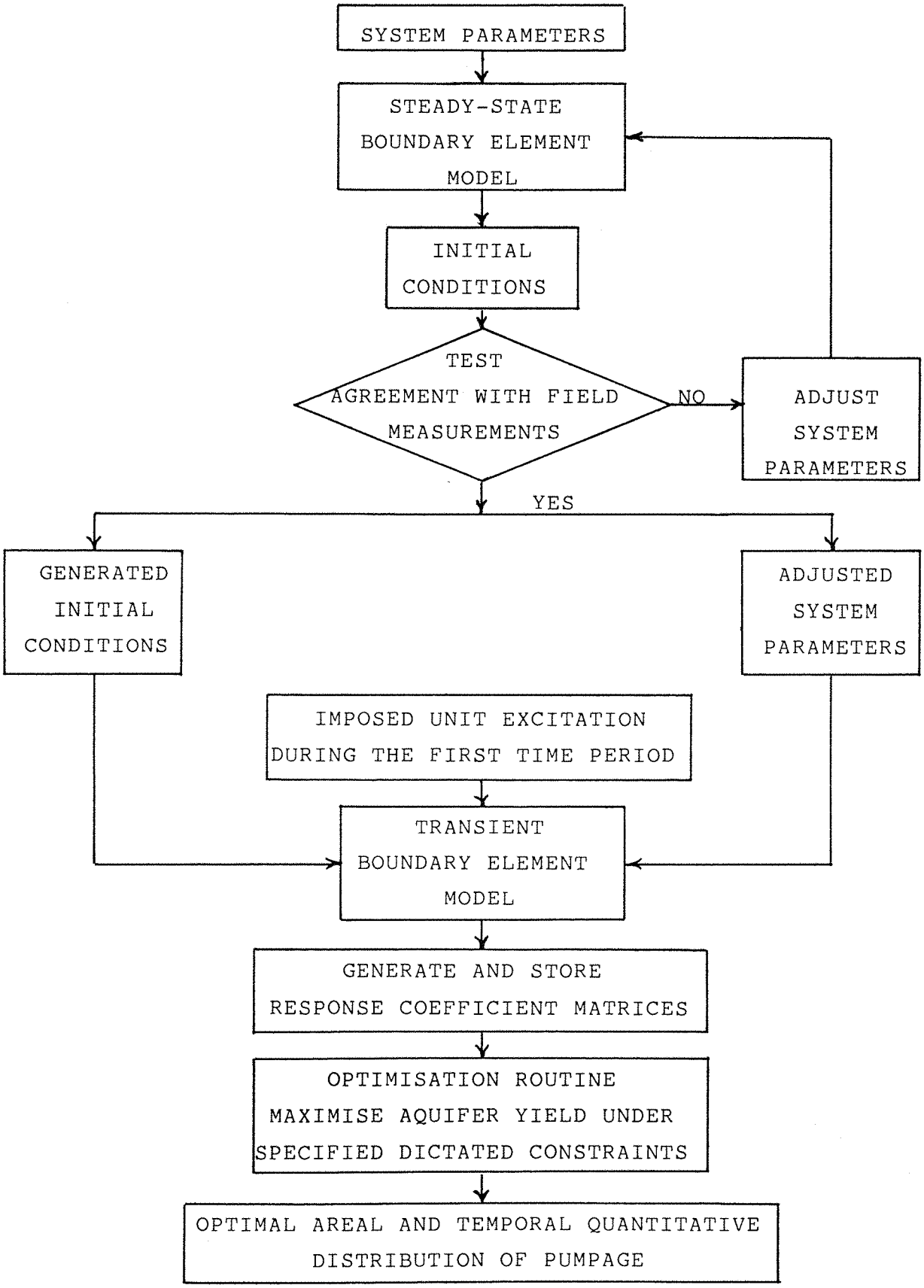

Figure 1.1: Schematic Representation of the Proposed Management Approach

Management modelling of a stream-aquifer system is discussed in Chapter 3. The response functions management approach is adopted to the management problem of the considered system. Expressions for the response coefficients and interaction parameters of the system are derived. Mathematical statement of the hydraulic management is formulated. The optimization problem and its solution using the linear programming technique are also presented.

The boundary element method is used to model regional stream-aquifer systems. The problem essentially involves the solution of the equations of two-dimensional transient and steady state flow of groundwater in a homogeneous and isotropic aquifer. Formulation of the boundary element solutions and the complete procedures of temporal and spatial discretization are presented in Chapter 4. Treatment of discontinuities in geometry and boundary conditions, associated with most practical problem, is also considered.

The full potential of the boundary element method cannot be realised unless it is programmed efficiently. The complete procedure of computer implementation of the boundary element solution is developed in Chapter 5. The procedure is tested by applying the algorithm to sample problems and the numerical solutions are compared with the exact analytical ones.

Simulation modelling of an aquifer system requires quantitative description of its physical setting and hydrogeology. For the case study of the stream-aquifer system south-east of the Nile delta, the system is described in Chapter 6.

In Chapter 7, the combined simulation-optimization management model is applied to the case study. Four alternative operating policies are considered in the hydraulic management of the system. Results of the

management model analysis are presented in Chapter 8.

Conclusions and recommendations are discussed in Chapter 9.

CHAPTER 2

A MATHEMATICAL MODEL OF STREAM-AQUIFER INTERACTION

2.1 Introduction

2.2 Theoretical Approach and Model Formulation
- 2.2.1 Stream Depletion During Pumping
- 2.2.2 Stream Depletion After Cessation of Pumping
- 2.2.3 Boundary Conditions in Real Systems

2.3 Computer Implementation of the Model
- 2.3.1 Computation Schemes
- 2.3.2 Evaluation of the Mathematical Functions
- 2.3.3 Computer Programs

2.4 Excitation-Response Relationships

CHAPTER 2

A MATHEMATICAL MODEL OF STREAM-AQUIFER INTERACTION

2.1 Introduction

A system may be defined as a set of objects which interacts in a regular interdependent manner. Since it is virtually impossible to isolate all interacting objects, the principal interacting elements are termed the system and those not included are considered through the specification of interactions with the environment in the form of inputs to and outputs from the system. Hall and Dracup (1970) state that any such system can be characterised by

i - A rule which determines whether any particular object is to be considered a part of the system or of the environment

ii - A statement of the input and output interactions with the environment

iii - A statement of the inter-relationships between the elements of the system

The system, including a region underlain by an alluvial aquifer and traversed by a hydraulically connected stream, composes a stream-aquifer system. A stream in such a system may contribute to or gain from the aquifer. With the stream and aquifer hydraulically connected, seepage from the stream into the aquifer or from the aquifer into the stream takes place with the seepage direction and rate are controlled by the pressure gradient across the boundary between the stream and aquifer. The flow in a

stream-aquifer system is described mathematically by the groundwater flow equation and the flow equation at the interface between the stream and aquifer.

The discharge of a well pumping in a stream-aquifer system is derived from aquifer storage as well as from induced seepage from the stream. During pumping, the stream flow is depleted at rates that depend on time, rate and place of withdrawal and also upon shape, size and hydraulic characteristics of the aquifer. On the other hand, after pumping stops the stream will continue to lose water, and if there is no capture of water from other sources, the total volume of induced seepage will approach the volume pumped as time approaches infinity. In order to investigate stream-aquifer interaction in terms of the behaviour of the stream flow depletion during and after cessation of pumping, the author has developed a mathematical model considering a case of pumping a single well in a stream-aquifer system. The model is based on the analytical solutions originated by Glover and Balmer (1954) and Hantush (1965). In this part of the study, the model is used to examine the role of stream-aquifer interaction, perform a sensitivity analysis and present excitation-response relationships of the system. However, it is fully realized that the forecasting problem in a stream-aquifer system, being a regional problem of practical interest, is generally intractable analytically, and it is likely to be solved by numerical methods.

2.2 Theoretical Approach and Model Formulation

2.2.1 Stream Depletion During Pumping

Glover and Balmer (1954) derived an analytical expression for the ratio of stream depletion to the total flow pumped from a well in an idealized stream-aquifer system. By an idealized system, it is meant that the

aquifer is isotropic, homogeneous and semi-infinite in areal extent, with a straight fully penetrating stream boundary and perfect hydraulic connection. The expression for this ratio is in the form

$$QR = q/Q = \text{erfc}[Z] \tag{2.1}$$

where QR is the ratio of stream depletion rate, q is the rate of stream depletion and Q is the pumping rate. The term erfc is called the complement of the error function and is defined as

$$\text{erfc}\,[Z] = 1 - \text{erf}[Z] \tag{2.2}$$

where erf is the error function and is defined by the probability integral

$$\text{erf}[Z] = \frac{2}{\sqrt{\pi}} \int_{o}^{Z} \exp[-U^2]\, dU \tag{2.3a}$$

Thus, the complement of the error function in equation (2.2) is given by

$$\text{erfc}[Z] = \frac{2}{\sqrt{\pi}} \int_{Z}^{\infty} \exp[-U^2]\, dU \tag{2.3b}$$

where

$$Z = X/\sqrt{4\alpha t} \tag{2.4a}$$

$$U = X/\sqrt{4\alpha(t-\tau)} \tag{2.4b}$$

$$\alpha = KD/S \tag{2.5}$$

and

D = saturated thickness of the aquifer

K = hydraulic conductivity of the aquifer

S = specific yield of the aquifer

X = the distance from the pumped well to the stream

t = time from beginning of pumping

τ = a time variable running between zero and t

Integration of equation (2.1) gives an expression for the ratio of total volume by which the stream is depleted to the total volume pumped during the time t;

$$VR = \int_o^t \frac{q}{Qt}\, dt \qquad (2.6)$$

where VR is the ratio of stream depletion volume. Analytical integration of equation (2.6) is shown by Glover (1960) as

$$\int_o^t \frac{q}{Qt}\, dt = 1 - \frac{2}{\sqrt{\pi}} \int_o^Z \exp[-U^2]dU - \frac{2Z^2}{\sqrt{\pi}} \int_Z^\infty \frac{\exp[-U^2]}{U^2}\, dU \qquad (2.7)$$

The line source integral $\left[\sqrt{\pi} \int_Z^\infty \frac{\exp[-U^2]}{U^2}\, dU\right]$ can be expressed in the form given in Abramowitz et al (1974) as

$$\frac{\exp[-Z^2]}{Z\sqrt{\pi}} - 1 + \frac{2}{\sqrt{\pi}} \int_o^Z \exp\,[-U^2]\, dU \qquad (2.8)$$

A compact form of the expression VR can be developed by substituting equation (2.3a) and expression (2.8) into equation (2.7) and rearrangement, hence

$$VR = 1 - (A\ erf[Z] + B) \qquad (2.9)$$

where

$$A = 1 + 2Z^2 \qquad (2.10a)$$

$$B = 2Z^2 \left[\frac{exp[-Z^2]}{Z\sqrt{\pi}} - 1\right] \qquad (2.10b)$$

2.2.2 Stream Depletion After Cessation of Pumping

The rate and volume of stream depletion at any time after cessation of pumping can be obtained by applying the method of superposition to the above derivation. This is by assuming that the pumping well continues to pump, and an imaginary recharge well at the same location is operated continuously at the same rate of the pumping well. This will nullify the flow of the well and the stream depletion can be computed as the algebraic sum of the effects of the pumping and recharge wells. Applying the method of superposition, the following expression for the ratio of stream depletion rate after cessation of pumping to the pumping rate can be obtained

$$RQR = qr/Q = erfc[ZTT] - erfc[ZTR] \qquad (2.11)$$

where

RQR = ratio of stream depletion after cessation of pumping

qr = rate of stream depletion after cessation of pumping

$ZTT = X/\sqrt{4\alpha(TT)}$

$TT = TP + TR$

TP = total time of pumping

TR = time after cessation of pumping

$ZTR = X/\sqrt{4\alpha(TR)}$

and the other symbols are as defined before.

An expression for the ratio of the total volume of stream depletion to the total volume pumped during a pumping time (TP) at any time (TR) after cessation of pumping, can be derived in a similar way. The volume of stream depletion (TVS), at any time after cessation of pumping, due to pumping for a time (TP) can be expressed in terms of the algebraic sum of the volume depleted during a pumping time (TT) and the volume gained due to an imaginary recharge well operated for a time (TR), where (TT) = (TP) + (TR), hence

$$(TVS) = Q[(VRTT)(TT) - (VRTR)(TR)] \qquad (2.12)$$

where (VRTT) and (VRTR) are the ratio of stream depletion volume at times (TT) and (TR), respectively. Substituting (TT) and (TR) in terms of (TP) and rearrangement, equation (2.12) gives,

$$(TRVR) = N[(VRTT) - (VRTR)] + (VRTT) \qquad (2.13)$$

where

$(TRVR)$ = ratio of stream depletion volume at any time after cessation of pumping

$= (TVS)/Q(TP)$

$N = (TR)/(TP)$

$(VRTT) = 1 - [(AT)\mathrm{erf}[ZTT] + (BT)]$

$(AT) = 1 + 2(ZTT)^2$

$$(BT) = 2(ZTT)^2\left[\frac{\exp[-(ZTT)^2]}{(ZTT)\sqrt{\pi}} - 1\right]$$

$(VRTR) = 1 - [(AR)\mathrm{erf}[ZTR] + (BR)]$

$$(AR) = 1 + 2(ZTR)^2$$

$$(BR) = 2(ZTR)^2 \left[\frac{\exp[-(ZTR)^2]}{(ZTR)\sqrt{\pi}} - 1 \right]$$

2.2.3 Boundary Conditions in Real Systems

The above analytical solutions are applicable to idealized systems as defined before. However, the solutions can be adapted for certain alterations in the boundary conditions of the idealized system. Two cases of the most common deviations of a real system from an idealized one will be considered.

In the first case, the assumption of semi-infinite areal extent of the aquifer is relaxed by introducing a no flow boundary parallel to the stream. The solution for this case can be achieved by applying the method of images so that the conditions on the recharge boundary, being the stream, and the no flow boundary are met. Theoretically speaking, the process is infinite since each change rectifies conditions at one boundary but disturbs them slightly at the other. The series are endless but convergent and each change improves the solution. Satisfactory results can be achieved by using a computer implemented scheme.

In the second case, the assumption of a perfect stream-aquifer hydraulic connection is relaxed by considering a semi-pervious stream bed. Hantush (1965) introduced a modification which made the above analytical solutions applicable to this case. The ratios of rate and volume of stream depletion expressed by equations (2.1) and (2.9) are altered and the resulting expressions considering imperfect hydraulic connection are given by

$$QR = \text{erfc}[Z] - \exp[-Z^2 + (Z+W)^2]\text{erfc}[Z+W] \qquad (2.14)$$

$$VR = 4i^2erfc[Z] + (1/W^2)\ (QR-2Wierfc[Z]) \qquad (2.15)$$

where

W = F/2Z

F = X/a

a = retardation factor = K/(k/b)

K = hydraulic conductivity of the semi-pervious layer

$i^n erfc$ = the nth repeated integral of the error function

2.3 Computer Implementation of the Model

2.3.1 Computation Schemes

Equations (2.1 to 2.15) form the mathematical model which is used to examine the role of stream-aquifer interaction and to present a general picture of the excitation-response relationships of the system. The following schemes are used.

i In order to investigate the behaviour of stream depletion during pumping, equations (2.1) and (2.9) are solved for an adequate range of the overall parameter (Z). The parameter (Z) is dimensionless and its value depends on location of pumping well, aquifer characteristics and pumping time. The equations are solved for values of (Z) running between zero and 2.0, where for greater values, rate and volume of stream depletion are found practically nil. Corresponding rates and volume of stream depletion are computed in dimensionless ratio terms, (QR) and (VR).

ii In the model formulation, the overall parameter (Z) is denoted as (ZTT) when it is calculated for the time span (TT) and is denoted (ZTR) when it is calculated for the

time (TR) after cessation of pumping. Rate of stream depletion after cessation of pumping is investigated by solving equation (2.11) for values of the parameter (ZTT) running between zero and 2.0, and the ratio of depletion rate (RQR) is calculated at a time (TR), where (TR) is expressed in terms of (TT) by introducing the time ratio (TR)/(TT), and the value of (ZTR) is determined implicitly in the computation process for each value of (ZTT). The solution is performed for selected values of the time ratio (TR)/(TT); (0.05, 0.10, 0.30, 0.70).

iii The total volume of stream depletion at any time after cessation of pumping is investigated by solving equation (2.13) using the time ratio (TR)/(TT) as a variable running between zero and 1.0 for selected values of the parameter (ZTT); (0.01, 0.10, 0.30, 0.50, 1.0, 1.50). Assuming that the aquifer does not capture water from other sources, the volume of stream depletion during a time (TR) after cessation of pumping will replace part of the volume released from aquifer storage during pumping. Equation (2.13) is used also to investigate the pattern of aquifer rewatering after cessation of pumping represented by the ratio of stream depletion volume during the time (TR) to the volume released from aquifer storage during pumping. The rewatering ratio (ARR) is calculated for the same values of (ZTT) and (TR)/(TT) which are used to calculated (TRVR).

iv In practice water is pumped intermittently and usually in cyclic patterns to fulfil a certain demand. In order to investigate the effect of cyclic pumping and its pattern on rate and volume of stream depletion equation (2.13) is solved for three different hypothetical patterns of cyclic pumping. In the first pattern, the well is pumped for 12 hours and then shut down for the next 12 hours, and the process is repeated four days a

week. In the second pattern, the well is pumped for one day, shut down the next day, and the process is repeated twice a week. In the third one, pumping continues for two days and then shuts down for the rest of the week. The pumping cycle in each pattern recurs weekly and the calculation is performed for the first successive four weeks.

v The effect of the presence of a no flow boundary on stream depletion is investigated by applying the method of images to the solution of equations (2.1) and (2.9). A parameter so called the boundary ratio (XB)/(XS) is introduced to express the location of the pumping well in the system, where (XB) is the distance from the well to the no flow boundary and (XS) is the distance from the well to the stream. The equations are then solved for selected values of the boundary ratio; (0.05, 0.50, 1.0, 3.0), with the parameter (Z) running between zero and 2.0.

vi The effect of a semi-pervious stream bed is investigated by solving equations (2.14) and (2.15) for selected values of the parameter (F); (0.1, 0.5, 1.0, 3.0), with the parameter (Z) running between zero and 2.0 as before.

2.3.2 Evaluation of the Mathematical Functions

Solution of the model equations involves evaluation of mathematical functions, namely, the error function, complement of the error function and the first and second repeated integral of the error function. Values of these functions are extensively tabulated in Abramowitz et al (1974). However, for computer implementation of the model, developing routines for evaluating these functions is a must.

The error function is defined by the probability integral of equation (2.3a) which can be evaluated by using an infinite series expansion (Fike, 1968). The result is in the form

$$\mathrm{erf}[Z] = \frac{2}{\sqrt{\pi}} \exp[-Z^2] \sum_{n=0}^{\infty} \frac{2^n Z^{2n+1}}{1.3\ldots(2n+1)} \qquad (2.16)$$

The complement of the error function is defined by equation (2.3b) and can be obtained from the relationship in equation (2.2), where

$$\mathrm{erfc}[Z] = 1 - \mathrm{erf}[Z]$$

But if the complement of the error function is always calculated by evaluating the error function using equation (2.16) and the above relationship, there will be large roundoff errors for arguments above 3. As the error function approaches unity, the complement approaches zero. Ultimately, all significant figures are lost. Furthermore, the computation time to evaluate equation (2.16) increases as the argument increases. One solution to this problem is incorporated into two separate routines, one for small argument and the other for larger arguments. Thus, the infinite series expansion of equation (2.16) is used to calculate the error function for arguments which are less than 2.0. The complement is then obtained by subtraction from unity. On the other hand if the argument is equal to or larger than 2.0, the complement is calculated with an asymptotic expansion algorithm (Fike, 1968). The algorithm is given by the expression,

$$\mathrm{erfc}[Z] = \frac{1/[1+V/\{1+2V/[1+3V/(1+\ldots)]\}]}{\sqrt{\pi}\ Z \exp[Z^2]} \qquad (2.17)$$

where

$$V = \frac{1}{2Z^2}$$

Equation (2.17) is expressed as a continued fraction, and the algorithm becomes more accurate as the argument increases.

Repeated integrals of the error function can be evaluated using the recurrence relation given in Abramowitz (1974) as

$$i^n\text{erfc}[Z] = -\frac{Z}{n}\, i^{n-1}\text{erfc}[Z] + \frac{1}{2N}\, i^{n-2}\text{erfc}[Z] \qquad (2.18)$$

For n=1, the first repeated integral is given by

$$i\ \text{erfc}[Z] = -Z\text{erfc}[Z] + \frac{1}{\sqrt{\pi}}\ \exp[-Z^2] \qquad (2.19)$$

and for n=2 the second repeated integral is given by

$$i^2\text{erfc}[Z] = \frac{1}{4}\ \text{erfc}[Z] + \frac{Z^2}{2} - \frac{Z}{2\sqrt{\pi}}\ \exp[-Z^2] \qquad (2.20)$$

Thus, the first and second repeated integrals of the error function which appear in equation (2.15) can be evaluated.

2.3.3 Computer Program

The above discussed computation schemes of the model are implemented by computer. Computer is also used to produce graphic output of the results. The computer programs are written in FORTRAN 77, and complete listing of the programs are given in Appendix A.

2.4 Excitation-Response Relationships

Excitation-response relationships obtained from the model are presented in dimensionless graphic format. Figure

(2.1) shows the behaviour of stream depletion, represented by the ratio of depletion rate (QR) and the ratio of depletion volume (VR), as a function of the overall parameter (Z). The value of (Z) is determined by location of pumping well, aquifer hydraulic characteristics and pumping time. The solution shows that the smaller the value of (Z) the higher is the rate and volume of depletion. The value of (Z) is mostly sensitive to changes in the distance of well from the stream. Since the hydraulic characteristics of an aquifer cannot be altered, and once the well is constructed it is almost impossible to change its location, and since the volume to be pumped is essentially a function of pumping time, thus determination of the proper pumping locations in a stream-aquifer system has a drastic influence on stream depletion response.

Changes in the ratio of depletion rate after cessation of pumping (RQR) are shown in Figure (2.2) as a function of the overall parameter (ZTT) and the time ratio (TR)/(TT). The outer curve represents the ratio of depletion rate immediately before pumping stops i.e. when (TR) = 0 and (TT) = (TP) , thus this curve is identical to the (QR) curve in Figure (2.1). The other curves are produced for the shown selected range of (TR)/(TT) being the curve parameter. Changes in the ratio of total volume of stream depletion (TRVR) as a function of (ZTT) and (TR)/(TT) are shown in Figure (2.3). The solution suggests that the total volume (TRVR) is much more sensitive to the changes in (ZTT) than the changes in (TR)/(TT) which emphasize the role of proper well location. The graphic output shown in Figure (2.4) represents the volume of aquifer rewatering after pumping stops expressed as ratio of stream depletion volume after cessation of pumping to the volume released from aquifer storage during pumping. The pattern of the rewatering ratio (ARR) suggests that (ZTT) and (TR)/(TT) should be considered in the design of operation schemes of stream-aquifer systems.

The results obtained from hypothetical example which investigates the effect of cyclic pumping on stream depletion are illustrated in Figures (2.5) to (2.7). The results show that for the same rate and volume of pumping the total volume of stream depletion during the first successive four weeks has increased by 0.9% and 2.6% when half day pumping cycle is replaced by one day cycle and two days cycle, respectively. Thus, stream depletion is slightly influenced by the change in cyclic pumping patterns.

Figures (2.8) and (2.9) show graphic output of the results obtained when a no flow boundary is introduced into the system. Altered rate and volume of stream depletion are given for the shown selected values of the boundary ratio (XB)/(XS). The presence of a no flow boundary tends to increase stream depletion according to the location of pumping well represented by the boundary ratio. However, values of (XB)/(XS) greater than 3.0 are found to yield practically nil effects. Figures (2.10) and (2.11) show the altered rate and volume of depletion for the case of semi-pervious stream bed. Results are given for the shown selected values of the parameter (F). It has been found that effective values of (F) are those less than 3.0. The parameter (F) drastically influences stream depletion tendency, thus special attention should be paid to the proper determination of this parameter in the field.

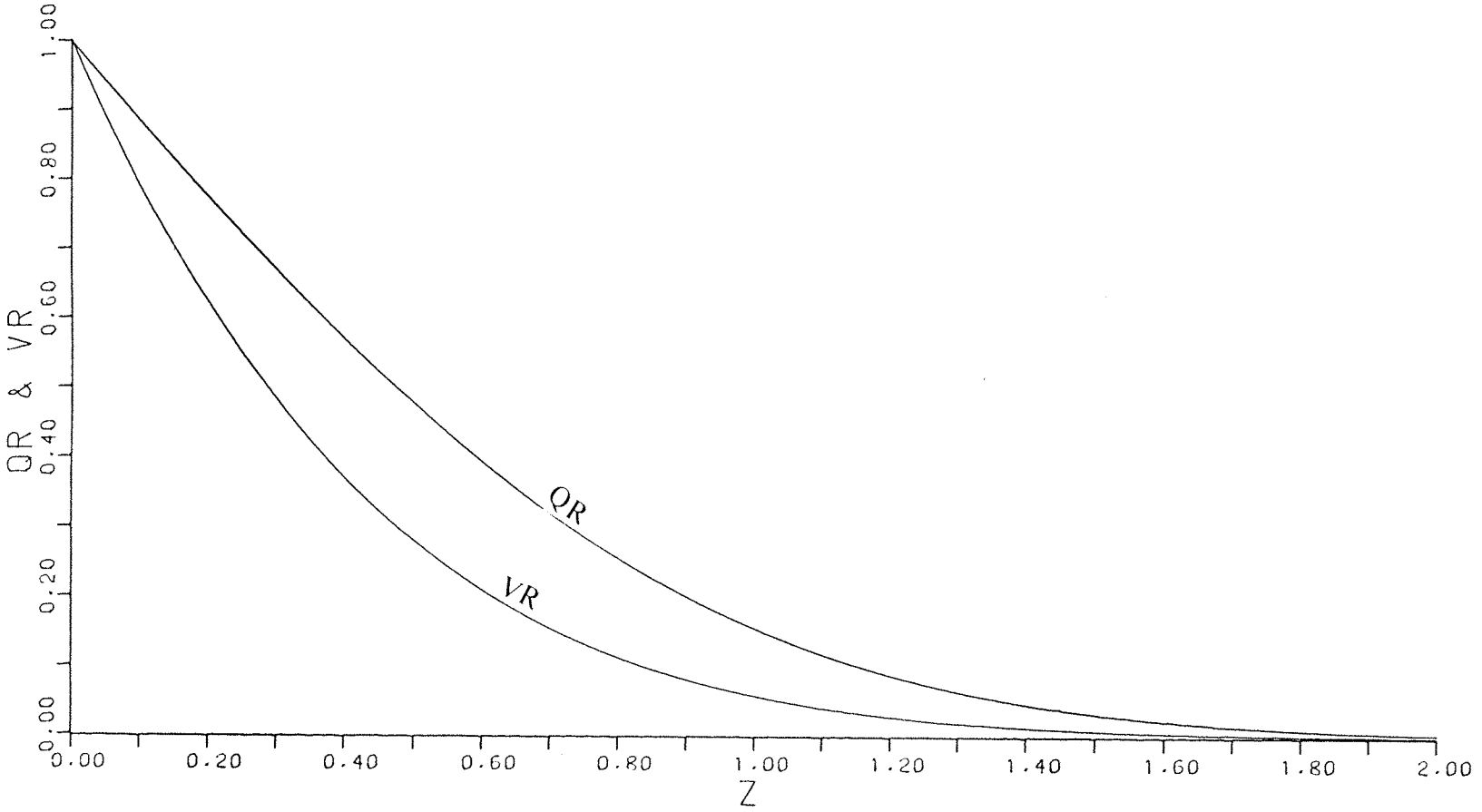

Figure (2.1) RATE AND VOLUME OF STREAM DEPLETION

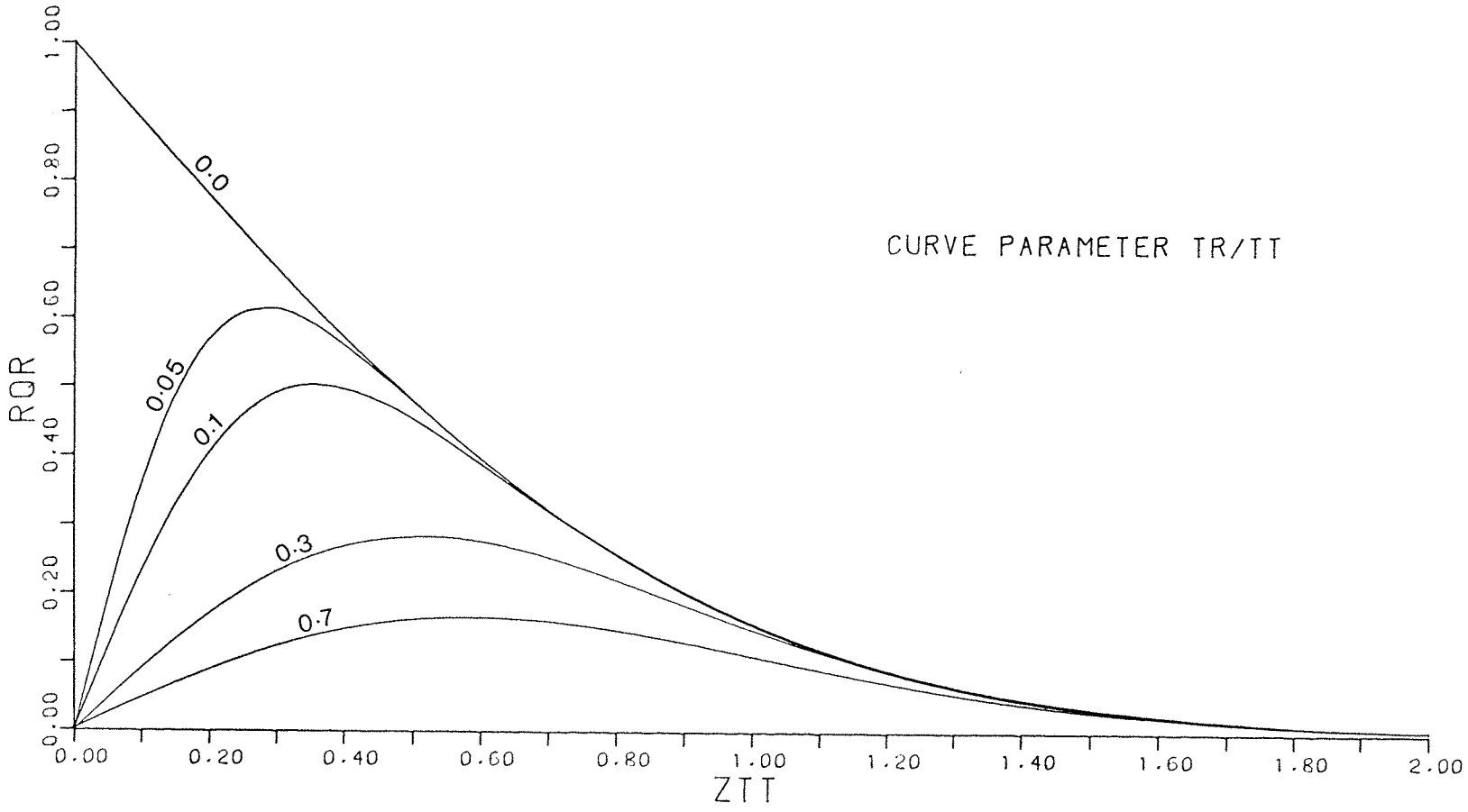

Figure (2.2) RATE OF STREAM DEPLETION AFTER CESSATION OF PUMPING

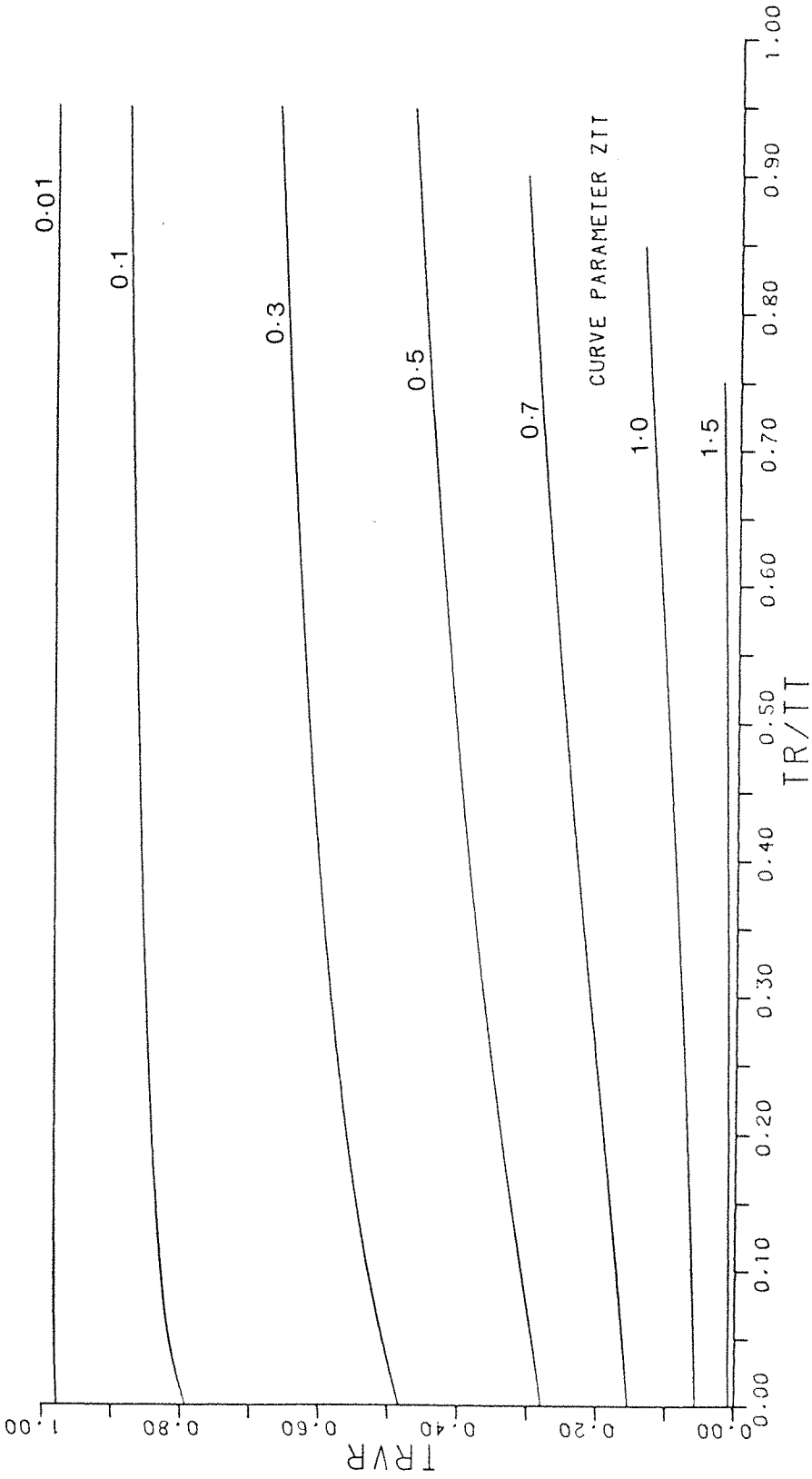

Figure (2.3) TOTAL VOLUME OF DEPLETION

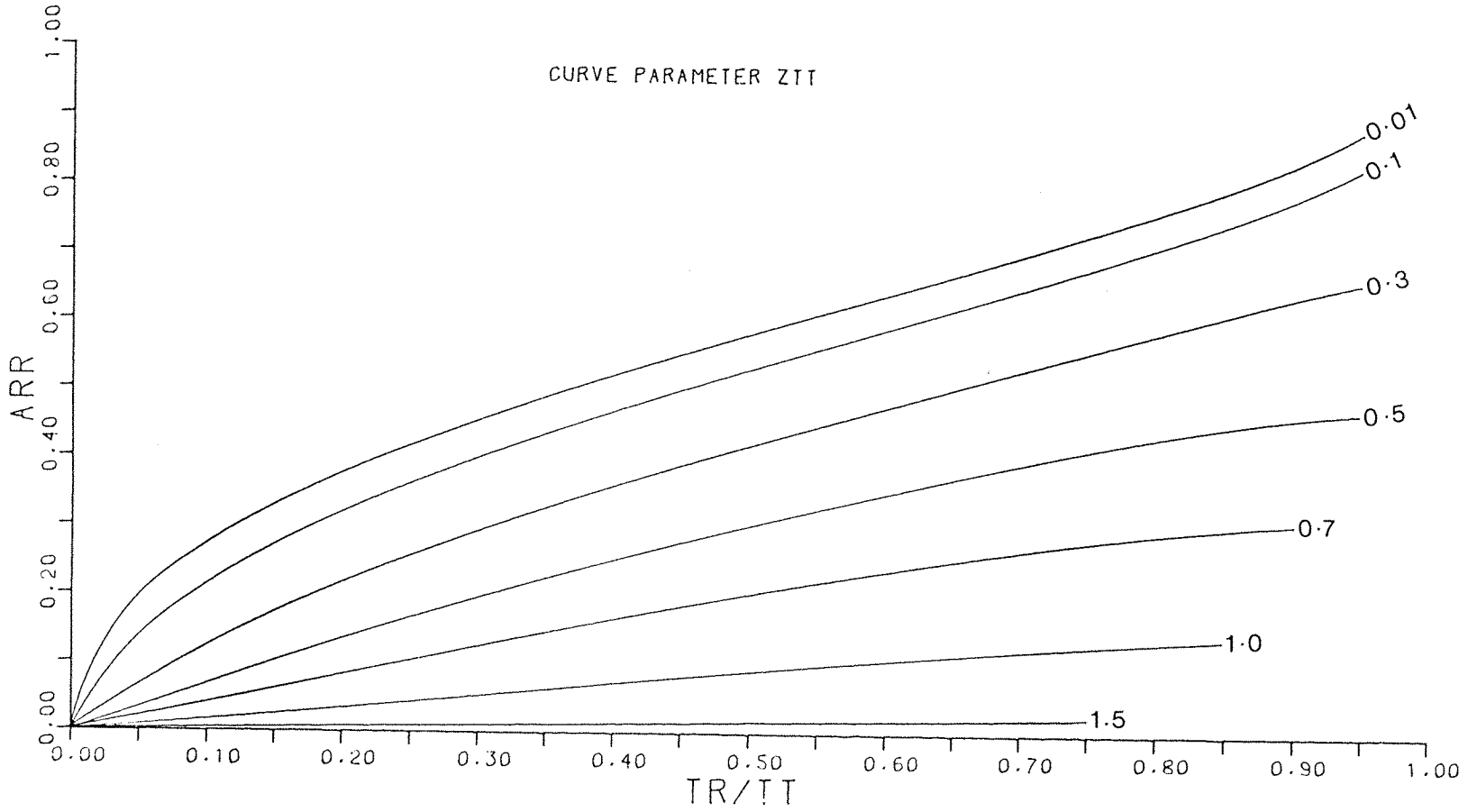

Figure (2.4) VOLUME OF AQUIFER REWATERING

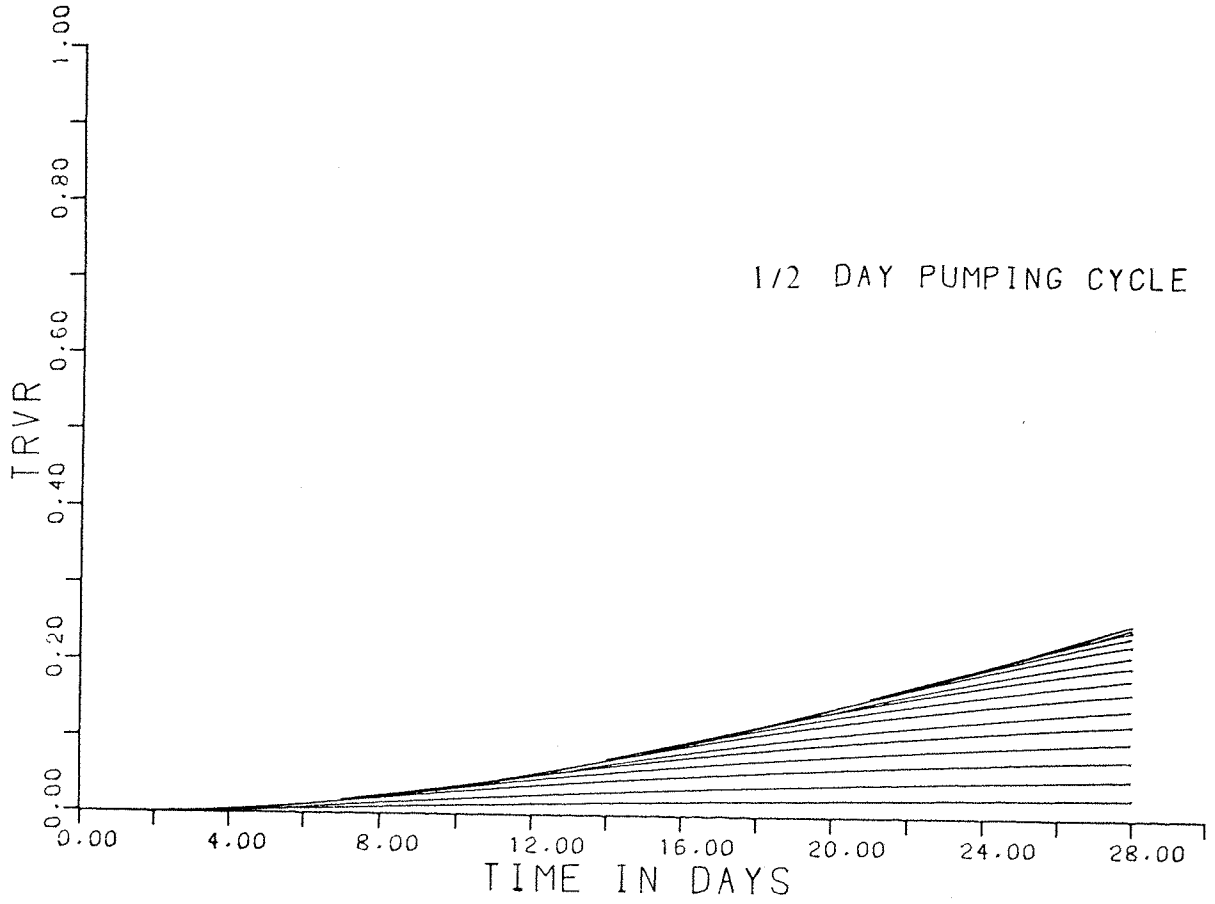

Figure (2.5) EXAMPLE OF CYCLIC PUMPING

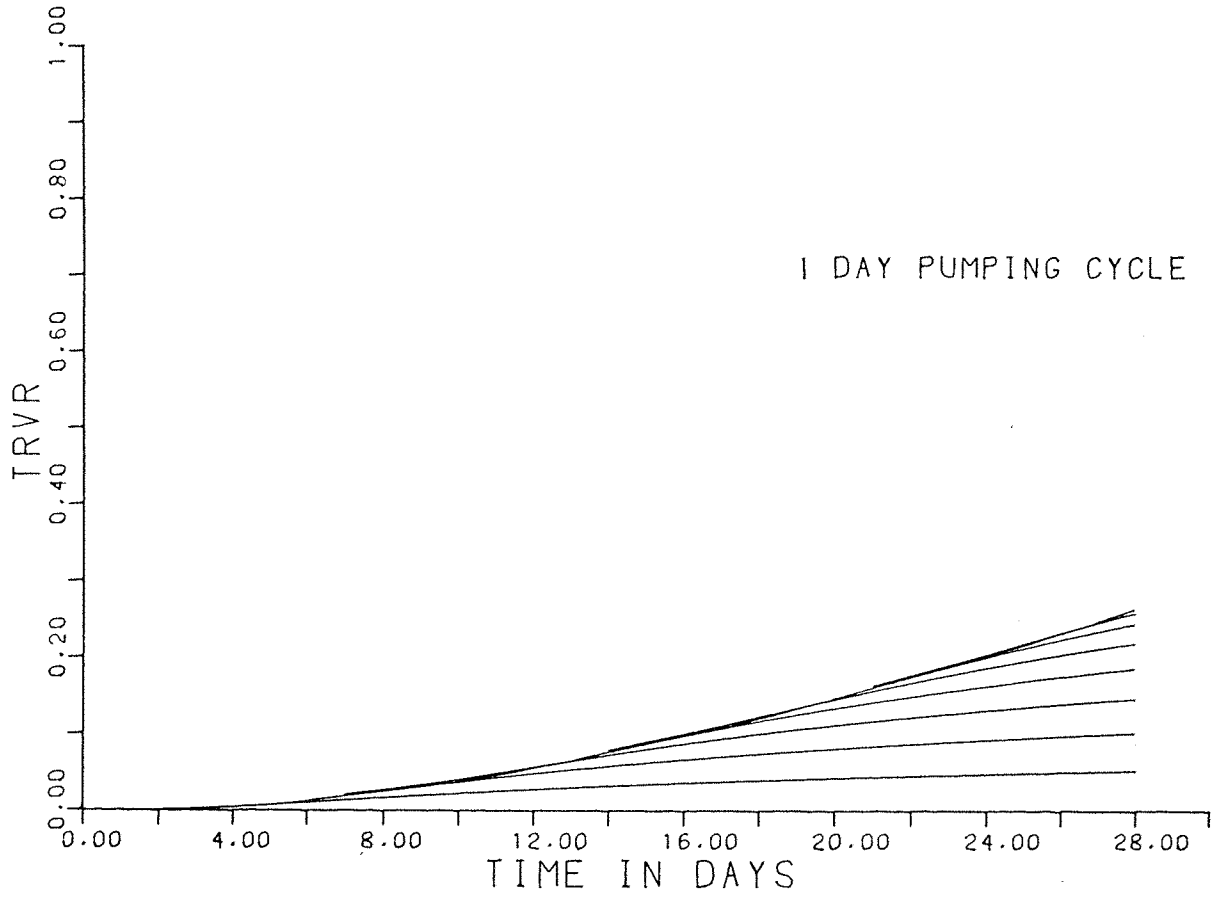

Figure (2.6) EXAMPLE OF CYCLIC PUMPING

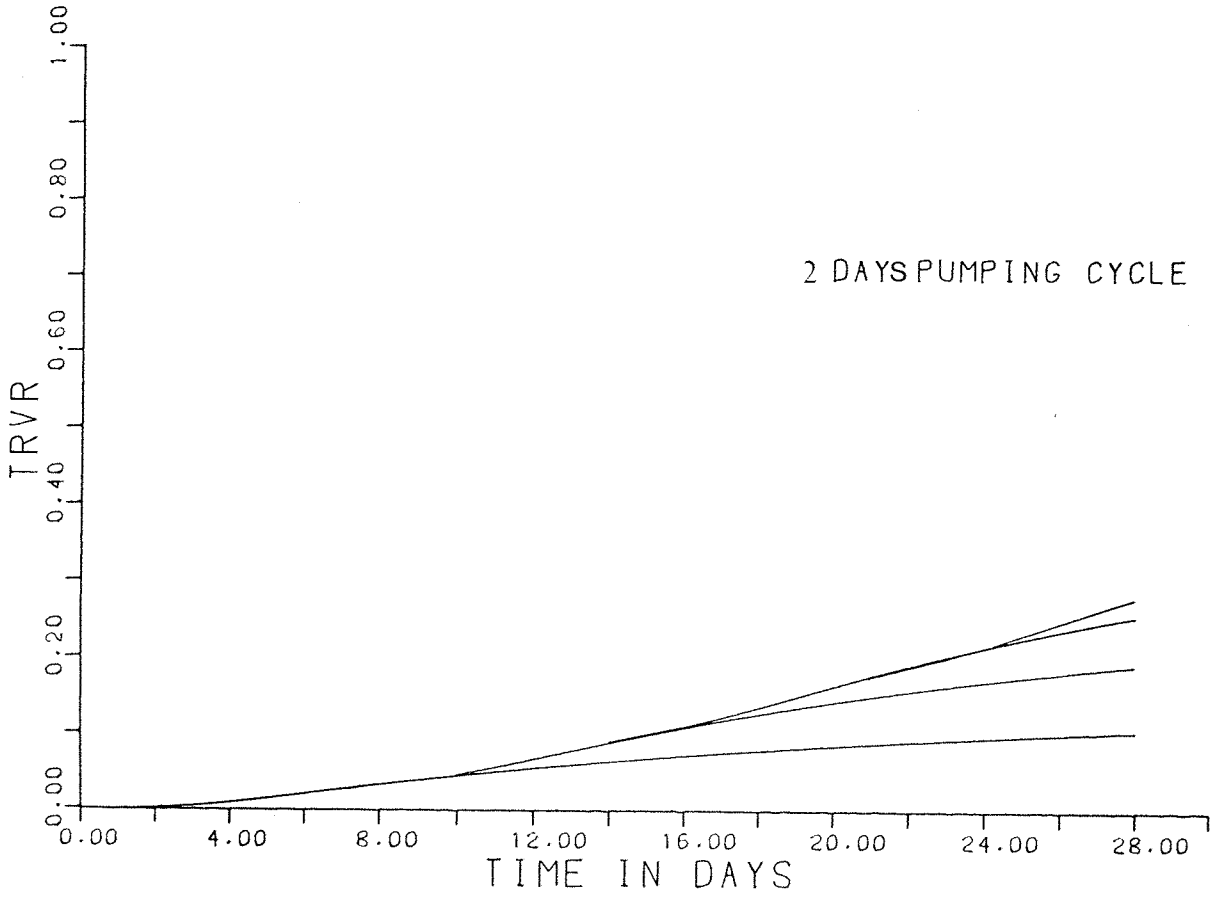

Figure (2.7) EXAMPLE OF CYCLIC PUMPING

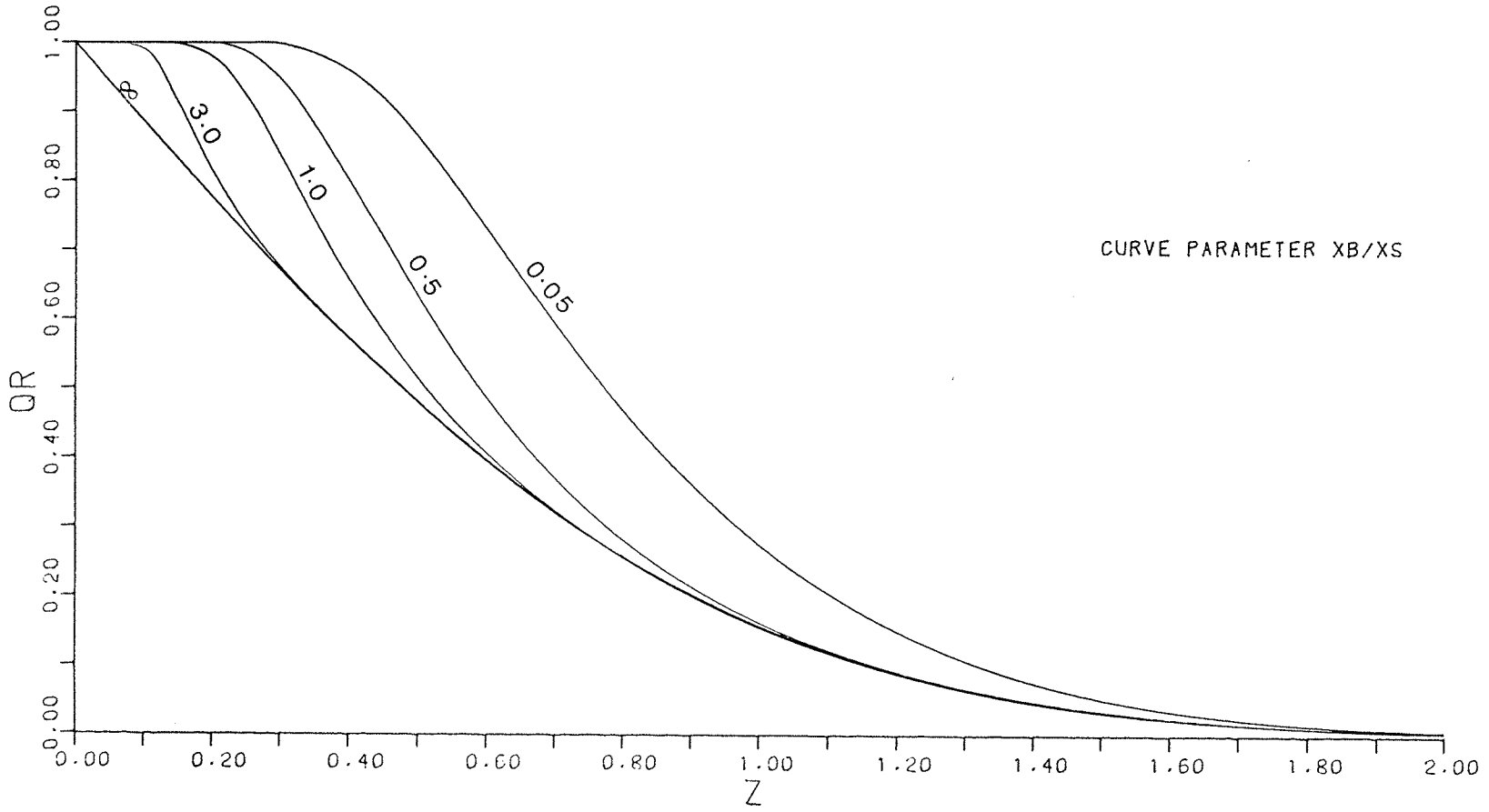

Figure (2.8) ALTERED RATE OF STREAM DEPLETION

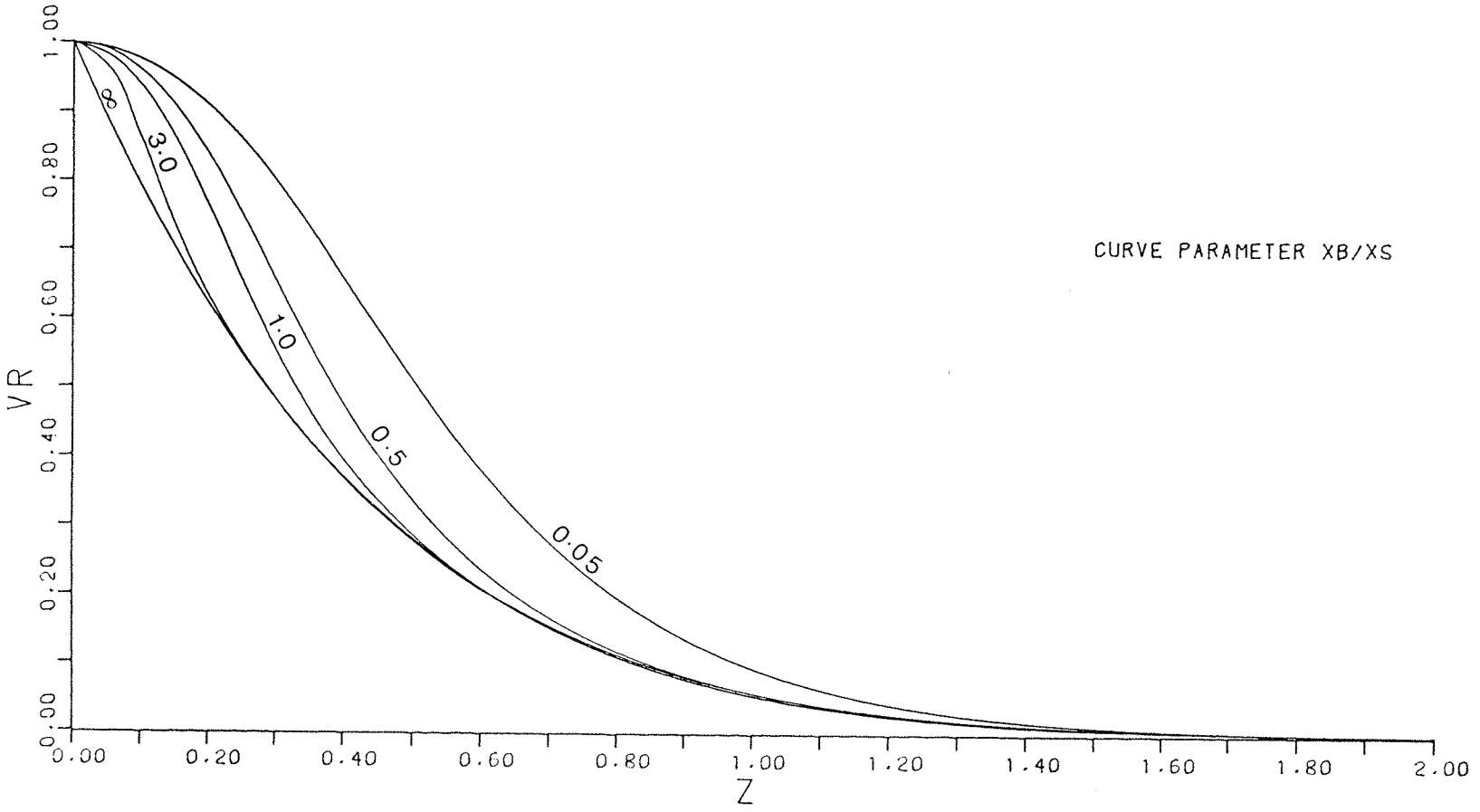

Figure (2.9) ALTERED VOLUME OF STREAM DEPLETION

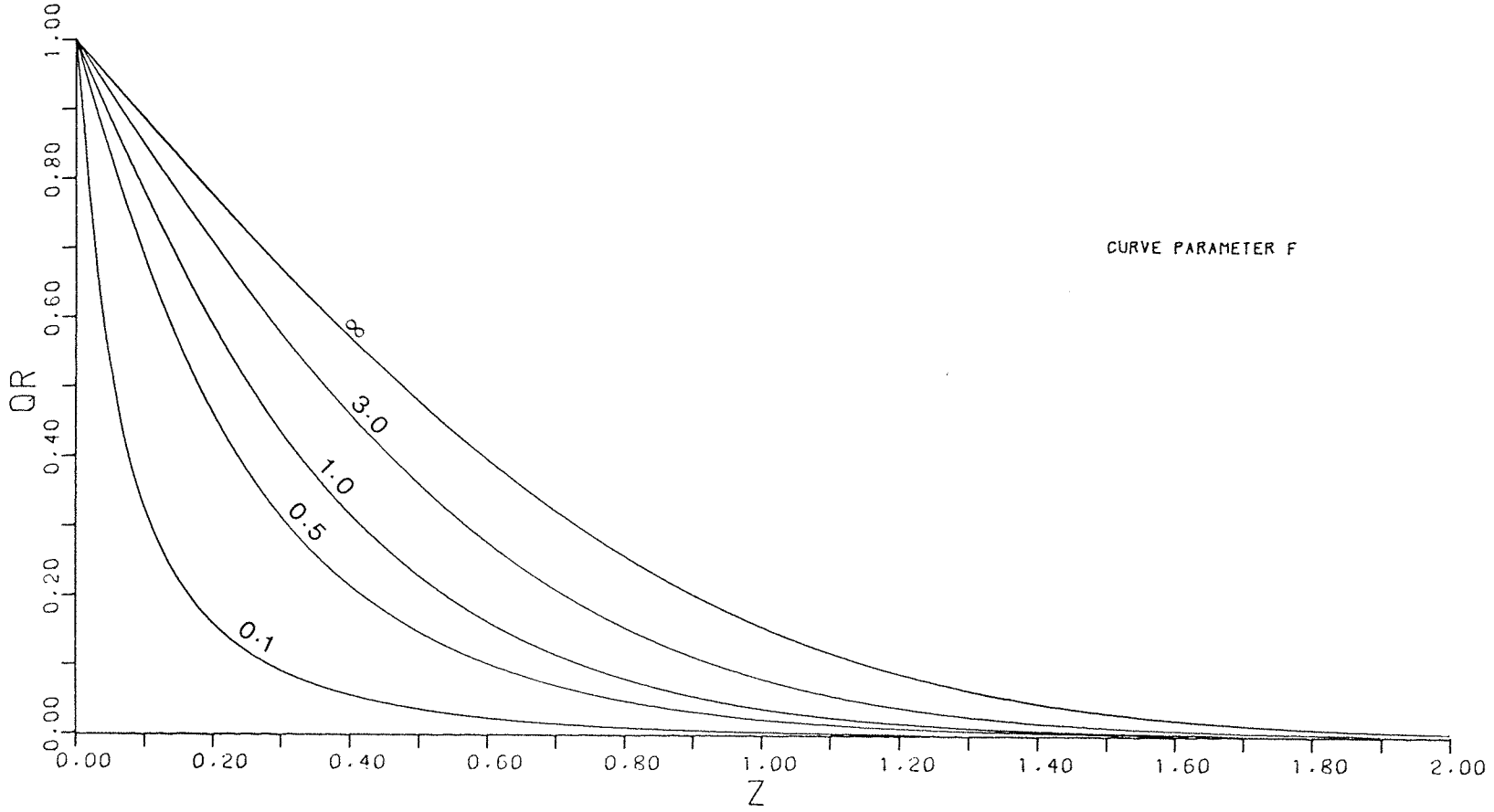

Figure (2.10) ALTERED RATE OF STREAM DEPLETION

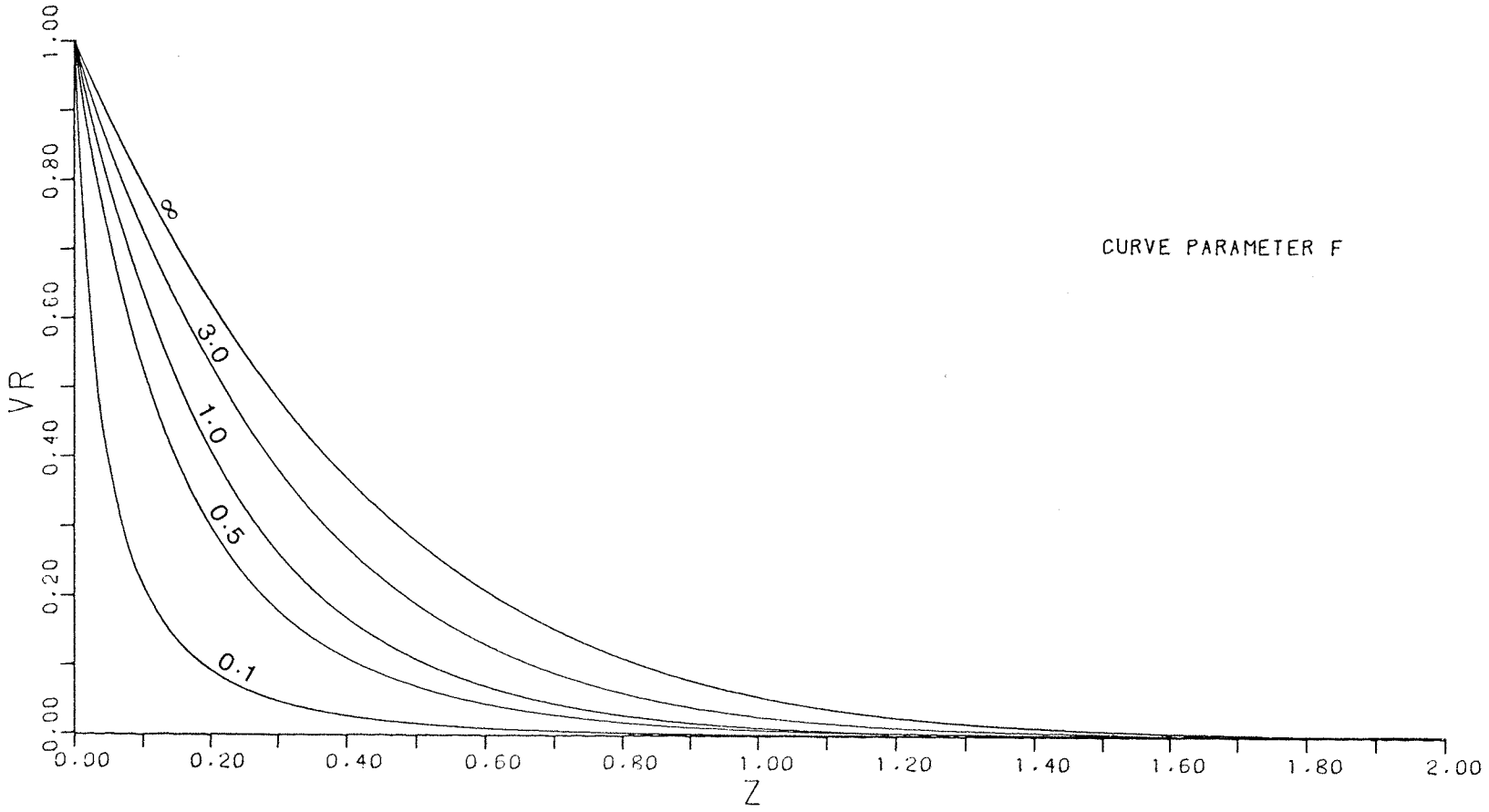

Figure (2.11) ALTERED VOLUME OF STREAM DEPLETION

CHAPTER 3

MANAGEMENT OF A STREAM-AQUIFER SYSTEM

3.1 Introduction

3.2 Management Modelling of Aquifer Systems
- 3.2.1 Aquifer Simulation Approach
- 3.2.2 Combined Simulation-Optimization Approach

3.3 Stream-Aquifer Management Approach
- 3.3.1 Stream-Aquifer Response Functions
- 3.3.2 Hydraulic Management of the System

3.4 Formulation of the Management Model
- 3.4.1 Statement of the Optimization Problem
- 3.4.2 Solution of the Optimization Problem

CHAPTER 3

MANAGEMENT OF A STREAM-AQUIFER SYSTEM

3.1 Introduction

Management of groundwater resources in an aquifer system aims at achieving certain goals through a set of decisions related to the operation of the system. Goals may be defined at different levels within the hierarchy of levels ranging from national ones to those at the level of individual users. The same goal or number of goals can be achieved by different policies. Therefore, management includes selection of the best policy which will lead to the achievement of the specified goals. The selection of the best policy is made according to some criteria or a measure of the relative effectiveness with which the different alternative policies meet or approach the specified goals. The function of the decision variables which measures the efficiency of the different alternative policies is called the objective function. Meanwhile, the feasibility of a policy has to be checked so that it does not violate specified constraints.

In order to solve the management problem of an aquifer system, we must be able to predict the response of the system to any proposed operation policy, and to obtain the modified state of the system. Since it is impossible to carry out experiments and tests in the real system itself to determine its response to activities proposed in the future, a model of the considered system has to be introduced. There is no need to elaborate on the fact that most real aquifer systems are indeed complicated beyond our capability to describe them and treat them exactly as they really are.

The very passage from the microscoping level of treating flow through porous media to the macroscoping level of treating it as a continuum involves already a certain simplification of the real world, and further simplifications are necessary. These take the form of a set of assumptions which should not be forgotten whenever the model is being employed in the course of investigations. On the basis of these assumptions, a conceptual model of the investigated system is to be constructed. Actually every considered system is usually only part of a larger system, with interactions between the sub-system and the rest of the system across the boundaries which define the considered sub-system. These interactions are referred to as the boundary conditions. Accordingly, any part of an aquifer system can be modelled, provided the boundary conditions of the considered sub-system are specified. A model of the system is always presented in the form of a set of mathematical equations, the solution of which yields the behaviour of the system. Due to the development of high-speed computers, the solution is often achieved by numerical techniques. Developing and testing a numerical model of the considered aquifer system requires sets of quantitative hydrogeological data that define the physical framework of the system and describe its hydrological stress. Obviously, the obtained solution cannot be more accurate than those data, a rule which emphasizes the role of an adequate identification of the system. Of equal importance is the calibration of the model; a process in which the various model parameters are verified.

Thus, a solution for the system's management problem cannot be achieved without solving first the forecasting problem, and no forecasting problem can be solved unless it is preceded by solving the system's identification problem.

3.2 Management Modelling of Aquifer Systems

3.2.1 Aquifer Simulation Approach

In the past two decades the field of groundwater hydrology has turned towards numerical simulation models to help evaluating groundwater resources. The application of numerical methods to groundwater flow equations has permitted complex, real world systems to be modelled. Numerical simulation models have enabled development of a better understanding of the behaviour of regional aquifers, and provided an efficient framework for conceptualizing and evaluating aquifer systems. Simulation models are often utilized to explore groundwater management alternatives. In such cases a model is executed repeatedly under various operation policies which attempt to achieve a particular objective. Use of such approach often avoids rigorous formulation of the management goals and fails to consider physical and operational constraints. It is unlikely that optimal management alternatives will be discovered using simulation techniques alone. What is required is a combined simulation and optimization model.

3.2.2 Combined Simulation Optimization Approach

Recently, joint simulation and optimization modelling approach has been developed. A combined model approach considers the particular behaviour of a given aquifer system and determines the best operating policy under the specified objectives and constraints. Gorelick (1983) presented a classification of groundwater management models where two categories have been defined; hydraulic management models and policy evaluation and allocation models. Hydraulic management models aim at managing aquifer stresses such as pumping and recharge. These models treat the stresses and hydraulic heads directly as management model decision variables. The physical decision variables, such as pumping

rates, may be interpreted as surrogate economic variables, however, some models may contain explicit economic factors, such as pumping and well costs. The second category involves models that can be used to inspect complex economic interactions and water allocation problems. These models do not explicitly determine regional operation policy but can be used in policy evaluation. In both categories the models employ optimization techniques to optimize a specified objective, such as maximisation of aquifer yield or minimisation of costs, and are subject to a set of constraints which limit or specify the values of decision variables such as drawdown, hydraulic gradients or pumping rates.

The management problem of the stream-aquifer system considered in this study belongs to the first category of hydraulic management models. Two techniques can be used to combine simulation with optimization in hydraulic management models. In the first technique, the simulation model is included in the optimization model directly as part of the constraint set of a linear programming model. This technique is known as the embedding method and was initially presented by Aguado and Remson (1974). The second technique is to combine an external simulation model with the optimization one. This is done by using the simulation model to develop response functions of the aquifer and the resulting response matrix is included in the optimization model. The response function technique has been established in the field of management of aquifer systems by the leading work of Maddock (1972) who developed and applied a response function of the distributed aquifer behaviour which he called an 'algebraic technological function'.

Some of the pros and cons of the two hydraulic management techniques are discussed in the review of groundwater management modelling methods presented by Gorelick (1983). In the embedding method, a complete

simulation model is solved as part of the management model. The embedded simulation model yields a great deal of information regarding aquifer behaviour. However, it will rarely occur that management involves all this information, which means that many of the decision variables and constraints will be unnecessarily contained in the optimization model. Therefore, for computational economy and avoidance of numerical difficulties, application of the embedding method should be restricted to small steady state problems. For cases in which hydraulic heads are constrained at many locations and many pumping sites are considered, the embedding method will be the more efficient. On the other hand, the response functions method yields relatively less information regarding system functioning but is generally a more economical technique. Development of a response matrix requires large initial expenditure of computational effort. However, the resulting response matrix is a highly efficient, condensed simulation tool. Constraints are included only for specified locations and times which means that unnecessary constraints and decision variables are not incorporated into the optimization model. Therefore the response functions method can handle large transient systems in an efficient manner.

The recent work of Bathala (1980), Heidari (1982), and Illangasekare and Morel-Seytoux (1982, 1983, 1984) has demonstrated that the response functions method is applicable to real world systems and is a valuable tool for evaluating groundwater management policies. Therefore, the response functions method, is adopted to handle the management problem in this study.

3.3 Stream-Aquifer Management Approach

3.3.1 Stream-Aquifer Response Functions

Functions relating systems response to a controlled input imposed on an aquifer are characterized by a set of partial differential equations with the associated boundary conditions. Evidently, it is inadequate to consider such a form of the system equations coupled with the optimization model and solved repeatedly for all possible patterns of values for the control variables. Based on this argument, the explicit relation between the system response and the control variables can be formulated in an algebraic form. This is possible provided an explicit solution to the system equation is available. However, only very simple cases with regular and symmetric boundaries maintain a specific analytical solution as demonstrated in Chapter 2. Most physical systems do not belong to the ideal simple cases, and a different approach is required. A variety of mathematical models approximating two-dimensional groundwater flow under different conditions is available in the literature; Todd (1959), DeWiest (1969), Bear (1972), Freeze (1979), and others. This can be justified when the vertical flow is insignificant and the drawdown is small compared to the aquifer thickness. Wherever one can justify the assumption that an aquifer system can be approximated by a linear model. Characteristics such as linear decomposition and superposition are valid and the system response can be approximated by a linear mathematical model. If this condition holds, as in our problem, once the system's response to one unit of input per unit of time is simulated, it is extended for any multiplication of input and time units in the range of the assumed existing linearity. Such explicit linear response functions can be easily coupled with the optimization model to form the management model of the system.

The equation governing the flow in the saturated zone of the considered aquifer system is given by the linearized differential equation of groundwater flow in two-dimensional regional phreatic aquifers. The equation is based on the mathematically advantageous formulation of horizontal flow proposed by Dupuit (1863) and the linear approximation justified by the relatively small departure in the hydraulic head compared to the initial saturated depth. The equation expressed in drawdown terms can be written in the form

$$\frac{\partial}{\partial X_1}\left(T\,\frac{\partial D}{\partial X_1}\right) + \frac{\partial}{\partial X_2}\left(T\,\frac{\partial D}{\partial X_2}\right) = S\,\frac{\partial D}{\partial t} + \sum_{\ell=1}^{L} N(\underset{\sim}{X}_\ell\ ,\ t)\ \delta(\underset{\sim}{X} - \underset{\sim}{X}_\ell) \qquad (3.1)$$

where D is the drawdown measured positive downward, T is the transmissivity, S is the specific yield, t is time, L is the number of pumping locations, $N(\underset{\sim}{X}_\ell\ ,\ t)$ is the aquifer pumping rate (chosen algebraically positive for a withdrawal excitation) at the ℓ^{th} location at time t, and δ is the Dirac delta function.

For a given set of initial and boundary conditions, the drawdown $D(\underset{\sim}{X}\ ,t)$ at any point $p(\underset{\sim}{X}\ )$ within the defined boundaries of the system, at any time t is given by

$$D(\underset{\sim}{X}\ ,t) = \sum_{\ell=1}^{L} \int_{o}^{t} G(\underset{\sim}{X} - \underset{\sim}{X}_\ell, t-\tau)\, N(\underset{\sim}{X}_\ell\ ,\ \tau)\, d\tau \qquad (3.2)$$

where $G(\underset{\sim}{X} - \underset{\sim}{X}_\ell, t-\tau)$ is the Green's function for equation (3.1) satisfying the particular initial and boundary conditions.

Under the linearity assumptions, algebraic functions which relate the quantity of water pumped to the drawdown,

averaged over a certain defined area, can be constructed. If t is divided into n time interval units so that the considered planning time horizon comprises exactly n time interval units, it can be shown that equation (3.2) may be represented by the algebraic response function D(k,n);

$$D(k,n) = \sum_{\ell=1}^{L} \sum_{i=1}^{n} \beta(k,\ell,n-i+1)\ N(\ell,i) \qquad (3.3)$$

The complete mathematical derivation of equation (3.3) is given in Maddock (1972), where it is shown that response functions exist even if the aquifer has irregularly shaped boundaries or non-homogeneous flow parameters. Equation (3.3) expresses the drawdown at the k^{th} location at the end of the n^{th} time period due to pumping in L locations, where $N(\ell,i)$ is the quantity of water pumped at the ℓ^{th} location over the i^{th} time period, and $\beta(k,\ell,n-i+1)$ is the response matrix for the n^{th} time period relating the drawdown at a location k to unit pumping at a location ℓ during the time period i. The coefficients $\beta(\ )$ are related to Green's function, having the advantage of the algebraic formulation characterizing the response function. However, the $\beta(\ )$ coefficients are not given explicitly by their derivation. Numerical values of the response coefficients $\beta(\ )$ are related to well hydraulics, aquifer characteristics, boundary and initial conditions, and the type of linear partial differential equation used as a model. Thus, the values of response coefficients are determined by using a simulation model of the considered system.

Considering the case of pumping in a stream-aquifer system where an aquifer is hydraulically connected with a stream, according to Maddock (1974), a set of response functions that relate the drawdown and interaction between the stream and aquifer due to pumping can be developed. The quantity of water removed from aquifer storage during pumping over time t, $V_s(t)$ can be determined by

multiplying equation (3.2) by the storage coefficient and integratng over the surface area of the system which yields

$$V_s(t) = \sum_{\ell=1}^{L} \int_o^t \varphi'_s(\underset{\sim}{X}_\ell , t-\tau)\, N(\underset{\sim}{X}_\ell ,\tau)d\tau \qquad (3.4)$$

where

$$\varphi'_s(\underset{\sim}{X}_\ell , t-\tau) = \iint S\, G(\underset{\sim}{X} - \underset{\sim}{X}_\ell , t-\tau)dX \qquad (3.5)$$

Equation (3.4) gives only the accumulated quantity of water removed from storage which does not represent the total quantity of water pumped from the well over the time t because part of the total quantity pumped is drawn from the stream into the aquifer by interaction. The quantity of water removed from storage and the stream by the pumping well over t is

$$V_p(t) = \sum_{\ell=1}^{L} \int_o^t N(\underset{\sim}{X}_\ell , \tau)d\tau \qquad (3.6)$$

Hence, the quantity of water removed from the stream by interaction over t is given by

$$V(t) = V_p(t) - V_s(t)$$

$$= \sum_{\ell=1}^{L} \int_o^t [1-\varphi'_s(\underset{\sim}{X}_\ell , t-\tau)]N(\underset{\sim}{X}_\ell , \tau)d\tau \qquad (3.7)$$

Under the assumption that the quantity of water pumped may vary from one time period to another, the quantity of water

induced from the stream into the aquifer is

$$I(n) = V(1) \qquad n=1 \tag{3.8a}$$

$$I(n) = V(n) - V(n-1) \qquad n>1 \tag{3.8b}$$

where

$$V(n) = \sum_{\ell=1}^{L} \sum_{i=1}^{n} \varphi'(\ell,n-i+1)\, N(\ell,i) \tag{3.9}$$

$$\varphi'(\ell,n-i+1) = 1-\varphi'_s(\ell,n-i+1) \tag{3.10}$$

The term $\varphi'(\ell,i)$ represents the response of the stream-aquifer interaction to pumping at the ℓ^{th} location during the i^{th} time period. If the ℓ^{th} location has undergone a unit pumping up to the i^{th} time period, then $\varphi'(\ell,i)$ is the fraction of water supplied by the stream, and $\varphi'_s(\ell,n-i+1)$ is the fraction supplied by aquifer storage.

From equations (3.8), (3.9) and (3.10) the quantity of water induced from the stream into the aquifer at time period n can be expressed as

$$I(n) = \sum_{\ell=1}^{L} \sum_{i=1}^{n} \varphi(\ell,n-i+1)\, N(\ell,i) \tag{3.11}$$

where the stream-aquifer interaction parameter $\varphi(\ell,n-i+1)$ is defined by the relation

$$\varphi(\ell,n-i+1) = \varphi'(\ell,n-i+1) - \varphi'(\ell,n-i) \tag{3.12}$$

As discussed in Chapter 2, the stream depletion takes place during pumping and after cessation of pumping the stream continues to lose water such that as time approaches infinity the total volume of stream depletion approaches the volume pumped, providing no capture of water from other sources. Considering an operation time horizon consists of n time interval units, the quantity of water supplied by the

stream I(n) can be divided into two components, the first one is that fraction of the volume induced during pumping at the i^{th} time interval, and the second is the rest of the volume induced after cessation of pumping during the complementary time (n-i). Thus, I(n) can be expressed as

$$I(n) = \sum_{\ell=1}^{L} \sum_{i=1}^{n} [I(\ell,1) + I(\ell,n-i)] \qquad (3.13)$$

where

$$I(\ell,1) = \varphi(\ell,1)\ N(\ell,i) \qquad (3.14)$$

$$I(\ell,n-i) = [\varphi(\ell,n-i+1) - \varphi(\ell,1)]\ N(\ell,i) \qquad (3.15)$$

In equations (3.14) and (3.15), $I(\ell,1)$ expresses nothing but the quantity of water supplied by the stream during pumping for the i^{th} time interval unit, and $I(\ell,n-i)$ is the quantity induced from the stream into the aquifer during the time interval units (n-i) after cessation of pumping, due to pumping at a location ℓ during the i^{th} time interval.

The stream-aquifer interaction parameters φ are related to the stream boundary conditions, the distance of pumping locations to the stream, and the factors affecting the response coefficients β. Numerical values of the φ parameters can be determined by using a simulation model of the considered stream-aquifer system.

The role of the simulation model as a component of the management model of the stream-aquifer system on hand is delineated by determining the response coefficients β and interaction parameters φ of the system. This is achieved by introducing one unit pumpage in a location point ℓ during the first time period and solving the system's equations to determine the resulting response where the β coefficients are the drawdowns due to that pumpage at all points k of interest at time intervals (n-i), and the φ parameters are

the induced flow from the stream into the aquifer due to the pumping at the i^{th} time interval. The procedure is repeated for all points and times of interest to generate the response matrices of β and φ.

3.3.2 Hydraulic Management of the System

In the management problem of the considered stream-aquifer system, management decisions are primarily concerned with the groundwater hydraulics of the system. Based on the above discussion of the management modelling approaches, the management model of the system is a hydraulic management one. Management decisions as well as simulation of the system's behaviour are to be accomplished simultaneously by using the response functions techniques. The aimed management of the system seeks determination of the best operating policy which maximises the aquifer yield under specific dictated constraints. Thus, the management model should be developed such that it is fully equipped to determine the optimal areal and temporal quantitative distributions of pumpage where the system is operated on intra-annual basis.

Mathematically speaking, the quantity of water to be pumped over an operation time horizon of n time interval units is given by

$$V_p(n) = \sum_{\ell=1}^{L} \sum_{i=1}^{n} N(\ell,i) \qquad (3.16)$$

where $N(\ell,i)$ is the pumping rate at the ℓ^{th} location during the i^{th} time interval unit. The quantity of water delivered on the surface at the ℓ^{th} location at the end of the i^{th} time interval is released from aquifer storage and stream depletion during pumping. Thus, $N(\ell,i)$ can be expressed as

$$N(\ell,i) = N_s(\ell,i) + N_d(\ell,i) \qquad (3.17)$$

where $N_s(\ell,i)$ is the quantity supplied by aquifer storage and $N_d(\ell,i)$ is that supplied by stream during pumping. Eventually, at the end of the n^{th} time interval and for all pumping locations, equation (3.17) becomes

$$V_p(n) = V_s(n) + V_d(n) \tag{3.18}$$

where $V_s(n)$ and $V_d(n)$ are the total quantities supplied by aquifer storage and stream depletion during pumping, respectively. The quantity of water necessary for release from aquifer storage $V_s(n)$, distributed over the one year operation time horizon at all pumping locations, is constrained by the fact that this quantity should be recovered at the end of the operation time horizon, so that the same quantity is always available for use every year.

The aquifer storage recovery is assumed to be covered by the stream natural seepage losses R(n) which take place with no pumpage imposed, and the induced stream depletion after cessation of pumping $V_r(n)$. Thus, $V_s(n)$ can be expressed in recovery balance terms as

$$V_s(n) = R(n) + V_r(n) \tag{3.19}$$

Using equation (3.15) to express $V_r(n)$ in terms of the stream-aquifer interaction parameters φ, equation (3.19) can be written as

$$V_s(n) = R(n) + \sum_{\ell=1}^{L} \sum_{i=1}^{n} [\varphi(\ell,n-i+1) - \varphi(\ell,1)]N(\ell,i) \tag{3.20}$$

Using equation (3.14), $V_d(n)$ can be expressed in the form

$$V_d(n) = \sum_{\ell=1}^{L} \sum_{i=1}^{n} \varphi(\ell,1)\ N(\ell,i) \tag{3.21}$$

Substituting equations (3.20) and (3.21) into equation (3.18) yields

$$V_p(n) = R(n) + \sum_{\ell=1}^{L} \sum_{i=1}^{n} \varphi(\ell, n-i+1)\, N(\ell, i) \qquad (3.22)$$

Equation (3.22) expresses the annual yield of the aquifer as a function of the assumed balance between the quantity of water released from aquifer storage and those supplied by natural seepage losses and stream depletion after cessation of pumping.

3.4 Formulation of the Management Model

Hydraulic management of the stream-aquifer system aims at maximising the annual yield from the aquifer. This is to be achieved through a set of decisions related to the operation of the system. The controllable and partially controllable inputs to the system are called decision variables. In the management of a system, when each decision variable is assigned a particular value, the resulting set of decisions is called a policy. In general, there will be constraints which will limit the number of possible policies. A policy which does not violate any constraints is a feasible policy. The subset of all feasible policies is termed the policy space which is quite variable over time and physical space. The condition of the system proper at anytime and place is represented by variables known as state variables.

Goals can be achieved by different policies. Therefore, management includes selection of the best policy or what is referred to as the optimal solution in an optimization problem. The concept of an optimal solution implies criteria whereby the effect of any feasible policy on the output from the system can be measured. This criterion is called the objective. Thus, an objective function is a mathematical statement by which the output of the system can be determined, given the policy, the initial values of the state variables and the system parameters.

Formulation of the management model is achieved by defining the statement of the objective, the statement of the optimization problem and the decision making technique to be used in solving the optimization problem.

3.4.1 Statement of the Optimization Problem

The optimization problem is defined by means of the proper set of variables, coefficients and parameters and by the equations able to represent in mathematical terms the evolution of the system's components. Of equivalent importance in the optimization problem is the set of constraints and bounds imposed on the variables of the system.

The annual yield of the aquifer is expressed in terms of quantitative distribution of pumping in time and space by equation (3.16). The management objective is to maximise this yield. However, providing no surface storage facilities are available, in order to ensure that the maximised quantity of water pumped from the aquifer at any time interval is fully utilized, temporal distribution of pumpage over the one year cycle should be achieved according to the temporal distribution of a specific annual demand. Adoption of a specific demand to develop a certain part of the system is beyond the scope of this study since the model is a regional one and the main objective is to maximise the overall yield of the system. In order to circumvent this situation, the author introduces the use of a representative demand density function for the system. Such function or set of functions can be developed using information about irrigation water requirements for the various cropping patterns which are practised in the region of the system and are likely to be adopted in the system. Thus the aquifer yield distributed in time according to certain demand density function is given by

$$V_p(n) = \sum_{\ell=1}^{L} [N^*(\ell) \sum_{i=1}^{n} \alpha(\ell,i)] \qquad (3.23)$$

where $N^*(\ell)$ is the quantity of water withdrawn from the aquifer at the ℓ^{th} location during the time interval of maximum demand, i.e. the time interval during which the value of the demand density function $\alpha(\ell,i)$ is maximum.

The annual yield of the aquifer constrained by equation (3.22) can also be expressed using the demand density function as

$$V_p(n) = R(n) + \sum_{\ell=1}^{L} [N^*(\ell) \sum_{i=1}^{n} \varphi(\ell,n-i+1)\alpha(\ell,i)] \qquad (3.24)$$

Substituting equation (3.24) into the left-hand term of equation (3.23) and rearranging yields

$$\sum_{\ell=1}^{L} [N^*(\ell) \sum_{i=1}^{n} 1-\varphi(\ell,n-i+1)\ \alpha(\ell,i)] = R(n) \qquad (3.25)$$

The aquifer yield is also constrained such that the resulting drop in groundwater levels, as expressed by equation (3.3), should not exceed certain allowable drawdowns, $D_a(k,n)$, to protect the aquifer against undesirable effects, such as salt water intrusion. Introducing the demand density function into equation (3.3), the constraint on drawdowns can be expressed by

$$D(k,n) = \sum_{\ell=1}^{L} [N^*(\ell) \sum_{i=1}^{n} \beta(k,\ell,n-i+1)\alpha(\ell,i)] \leq D_a(k,n) \qquad (3.26)$$

Mathematically, the optimization problem can be stated as follows. Determine the values of L decision variables $N^*(\ell)$, ($\ell = 1,2,...L$), which will maximise the objective function $V_p(n)$ expressed by equation (3.23), subject to the constraint on the decision variables defined by equation (3.25) and the constraints on the state variables expressed by equation (3.26).

3.4.2 Solution of the Optimization Problem

The decision making technique to be used in solving the optimization problem essentially depends on the type of the problem. Based on the nature of equations (3.23), (3.25) and (3.26), the optimization problem is a linear programming problem. The principles and techniques of solving linear programming problems are well established in the literature, e.g., Hadley (1962), Dantzing (1963) and Gass (1969).

The problem expressed in the usual linear programming form is: Determine $N^*(\ell)$, $(\ell = 1,2,\ldots,L)$ such that

$$\left.\begin{aligned} &\text{Maximise } V_p(n) = \sum_{\ell=1}^{L} c(\ell)N^*(\ell) \\ &\text{Subject to the m constraints} \\ &\sum_{\ell=1}^{L} a_1(\ell)N^*(\ell) \leq b_1 \\ &\sum_{\ell=1}^{L} a_2(\ell)N^*(\ell) \leq b_2 \\ &\sum_{\ell=1}^{L} a_m(\ell)N^*(\ell) \leq b_m \\ &\text{and the non-negativity restriction} \\ &N^*(\ell) \geq 0, \quad \ell = 1,\ldots,L \end{aligned}\right\} \qquad (3.27)$$

Once the problem has been cast into the standard linear programming form (3.27), the common algebraic procedure for solving it is the Simplex method. This procedure is well suited for solution by digital computers. Packages for solving linear programming by modified and advanced Simplex methods are available in most computer libraries. The H01ADF routine available in the NAG computer library is an example of the standard procedure for solving the linear programming problem using the Revised Simplex method.

CHAPTER 4

FORMULATION OF BOUNDARY ELEMENT SOLUTION FOR THE SIMULATION MODEL

4.1 Introduction

4.2 Boundary Element Solution for Transient Conditions
- 4.2.1 Governing Equations
- 4.2.2 The Fundamental Solution
- 4.2.3 Boundary Element Formulation
- 4.2.4 Solution of the Boundary Element Equation

4.3 Boundary Element Solution for Steady-State Conditions
- 4.3.1 Governing Equations
- 4.3.2 The Fundamental Solution
- 4.3.3 Boundary Element Formulation
- 4.3.4 Solution of the Boundary Element Equation

4.4 Treatment of Discontinuity Problems
- 4.4.1 Treatment of Corners
- 4.4.2 Treatment of Zones

CHAPTER 4

FORMULATION OF BOUNDARY ELEMENT SOLUTION FOR THE SIMULATION MODEL

4.1 Introduction

It has been pointed out in the previous chapters that a simulation model of the considered stream-aquifer system is required as a component of the management model to solve the forecasting problem of the system.

Owing to the difficulties of obtaining analytical solutions to complex groundwater flow problems, there has long been a need for techniques that enable meaningful solutions to be found. Such techniques exist nowadays in the form of numerical modelling. Of the general variety of numerical techniques, all of them have in common that an approximate solution is obtained by replacing the basic differential equations that describe the flow system by another set of discrete equations that can easily be solved by a digital computer. The model which is presented in this study is based on one of these techniques; the boundary element method.

Engineers are nowadays very familiar with the numerical methods which tackle the differential equations directly in their original derived forms without any further mathematical treatment. This is often done either by approximating the differential operators in the equations by simpler, localised algebraic ones valid at a series of nodes within the domain, as in finite difference techniques, or by representing the domain itself by finite elements and the governing equations are approximated for each element by localised functions which satisfy the boundary conditions and are approximate in the domain, and the resulting equations are assembled to provide an approximation to the

real system, as in finite element techniques. Finite differences approach has been applied successfully to the simulation of aquifer systems over the last twenty years. The first application of finite differences to groundwater flow appears to have been made by Remson et al (1965).* The popularity of finite differences stems from the fact that the method is conceptually straightforward and does not require advanced training in applied mathematics. By far the most popular numerical approach at present is the finite element techniques. Ten years ago, finite elements began to replace finite differences as the dominant technique. The classic papers by Javandel and Witherspoon (1968) and Zienkiewicz et al (1966), appear to be the first two publications describing the use of finite element theory in porous media flow. The finite element technique has now reached such a stage of development and popularity, that one might well doubt whether there is any other approach which can offer comparable power. In the methods of finite differences and finite elements, the techniques are applied on the domain, therefore they are called the domain methods.

Another equally versatile numerical approach which is based on mathematical manipulation of the differential equations, before either introducing any approximation or performing any discretization, is the boundary integral equation method. The essence of this method is the transformation of the differential equations into an equivalent set of integral ones. Such an operation would yield a set of equations which involve only values of the variables on the boundaries of the domain. This, in turn, would imply that any discretization scheme needed would only involve the domain's boundaries. Application of the boundary integral approach to groundwater flow has been pioneered by Liggett (1977). The important components and steps of model development for the domain methods and the boundary element method are shown in Figure (4.1). Among other reasons, the relative mathematical complexity involved in the development

* Based on earlier work on flow in porous media by Shaw and Southwell (1941)

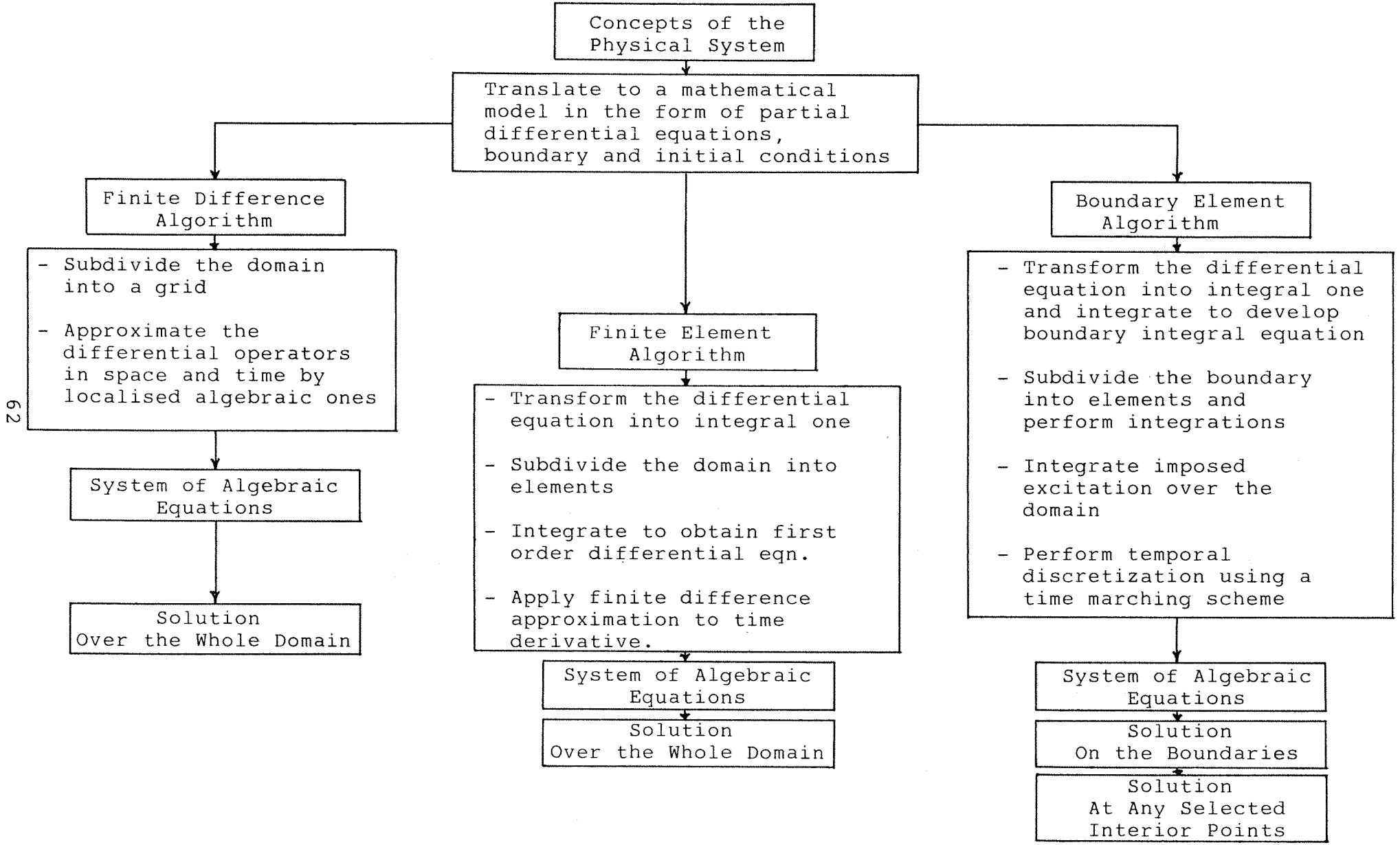

Fig. (4.1) Generalized model development by domain and boundary element methods

and solution of the boundary integral equations, compared to the domain methods, has been the cause of the slow development in employing the boundary element method. However, over the last few years, the boundary element method has been re-examined and re-introduced in the literature without mathematical bias and in a form amenable to problems in engineering and applied science. The boundary element method is now gaining considerable popularity as an economic and elegant alternative to the domain methods.

In principle the boundary element method is applicable to any problem for which the governing differential equation is linear or incrementally linear. In problems involving elliptic differential equations, the solutions are direct, whereas for parabolic ones marching process in time has to be introduced. The most outstanding virtue of the boundary element method is that the algorithm reduces the domain of calculation by one dimension and hence computation effort and time. If in a homogeneous domain problem, imposed excitation on the system has to be included, as in our problem, then the boundary integrals have to be augmented by a domain integral involving arbitrary discretization of the interior of the domain. However, in this case the internal discretization does not result in any increase in the order of the final system of algebraic equations to be solved and the advantage remains with the method. Thus for the great majority of practical problems the algorithm leads to a very much smaller system of simultaneous equations than any of the domain methods. The boundary element method involves modelling only the boundary geometry of the system. Once the boundary integrals have been derived, values of the solution variables can be calculated at any subsequently selected interior points. Furthermore, the solution is fully continuous throughout the interior of the domain. Both of these features appear to be unique to the boundary element method among the possible alternatives. However, the

boundary element method does not replace the finite element method in all cases. For problems in which inhomogeneity is so great that very large numbers of homogeneous zones are needed to model it adequately, the boundary element method and finite element method becomes virtually indistinguishable from each other. On the other hand, finite elements or finite differences are attractive in problems where there are high degrees of either geometrical or material non-linearity. Therefore for some problems, it may be advantageous to use a combination of more than one method in what is often called a hybrid solution.

The present study employs the boundary element method to solve the forecasting problem of the considered stream-aquifer system. The problem is essentially time dependent, thus the boundary element solution is to be formulated for transient flow conditions in the system. However, steady state solution is also needed to perform the model calibration and to generate the initial conditions for the transient solution.

4.2 Boundary Element Solution for Transient Conditions

4.2.1 Governing Equations

The governing equation to be solved is the linearized parabolic differential equation of time-dependent horizontal groundwater flow in a homogeneous and isotropic phreatic aquifer. The equation can be written in the form

$$T \frac{\partial^2 H}{\partial X_i \partial X_i} = S \frac{\partial H}{\partial t} + N \qquad (4.1)$$

where the function H corresponds to the hydraulic head, T and S are the average transmissivity and specific yield of the phreatic aquifer, respectively, and N is the recharge (-ve) or withdrawal rate (+ve) per unit area.

The flux $q(X,t)$ across any boundary defined by its outward normal $n_i(X)$ is

$$q(X,t) = -T \frac{\partial H(X,t)}{\partial X_i} n_i = -T \frac{\partial H}{\partial n} \qquad (4.2)$$

In a well posed problem the boundary conditions associated with equation (4.1) will be

i $H(X,o) = H_o$, the associated initial conditions specified throughout the solution domain Ω at time $t=0$.

ii $H(X_o,t) = h(X_o,t)$, specified over part (Γ_1) of the boundary Γ at all times, ($X_o \varepsilon \Gamma$).

iii $-T \frac{\partial H(X_o,t)}{\partial n} = q(X_o,t)$, specified over the remainder (Γ_2) of the boundary Γ.

iv alternatively, a linear combination of H and q, might be specified over part of the boundary Γ.

4.2.2 The Fundamental Solution

The fundamental solution for this type of problem, being a diffusion one, is given by Carslaw and Jaeger (1959) as

$$G(r,t-\tau) = \frac{1}{4\pi T(t-\tau)} \exp\left[\frac{-r^2 S}{4T(t-\tau)}\right], \qquad (4.3)$$

where $r = [(X_1-\xi_1)^2 + (X_2-\xi_2)^2]^{\frac{1}{2}}$
and ξ_1, ξ_2 are the coordinates of the fixed base point. Physically, the function G represents the hydraulic head distribution at time t resulting from instantaneous application of a unit point source at ξ_i at time τ in an

infinite domain. It can be shown that the function G satisfies the equations

$$T \frac{\partial^2 G}{\partial X_i \partial X_i} - S \frac{\partial G}{\partial t} = o \qquad t>\tau \qquad (4.4a)$$

and

$$T \frac{\partial^2 G}{\partial X_i \partial X_i} + S \frac{\partial G}{\partial \tau} = o \qquad \tau>t \qquad (4.4b)$$

In addition, G has the property

$$G(X_i, \xi_i, t-\tau=o) = \frac{1}{S} \delta(X_1-\xi_1)\delta(X_2-\xi_2)\delta(t-\tau) \qquad (4.4c)$$

where δ is the Dirac delta function which its limit is zero everywhere except at $\xi_i=X_i$ where it is infinite.

4.2.3 Boundary Element Formulation

Boundary element solution can be formulated directly using the consequences of the divergence theorm known as Green's identities (Appendix B). Green's second identity can be expressed in the form

$$\int_\Omega \left[H \frac{\partial^2 G}{\partial X_i \partial X_i} - G \frac{\partial^2 H}{\partial X_i \partial X_i} \right] d\Omega = \int_\Gamma \left[H \frac{\partial G}{\partial n} - G \frac{\partial H}{\partial n} \right] d\Gamma \qquad (4.5)$$

The problem in hand is time dependent, thus Green's second identity, equation (4.5), has to be integrated with respect to time. This can be expressed as

$$\int_o^t \int_\Omega \left[H \frac{\partial^2 G}{\partial X_i \partial X_i} - G \frac{\partial^2 H}{\partial X_i \partial X_i} \right] d\Omega d\tau$$

$$= \int_o^t \int_\Gamma \left[H \frac{\partial G}{\partial n} - G \frac{\partial H}{\partial n} \right] d\Gamma d\tau \quad , \qquad (4.6)$$

where Ω and Γ are the interior and the boundary of the solution domain.

Rewriting equation (4.1) in terms of τ as

$$T \frac{\partial^2 H}{\partial X_i \partial X_i} = S \frac{\partial H}{\partial \tau} + N \qquad (4.7)$$

Using equations (4.4b) and (4.7) to substitute for the left-hand terms of equation (4.6), gives

$$- \int_o^t \int_\Omega \left[S\left(H \frac{\partial G}{\partial \tau} + G \frac{\partial H}{\partial \tau}\right) + G N \right] d\Omega d\tau$$

$$= \int_o^t \int_\Gamma T \left[H \frac{\partial G}{\partial n} - G \frac{\partial H}{\partial n} \right] d\Gamma d\tau \qquad (4.8)$$

Integration of the left-hand terms of equation (4.8) by parts yields

$$- \left[\int_\Omega S H G \, d\Omega \right]_{\tau=o}^{\tau=t} - \int_o^t \int_\Omega G N \, d\Omega d\tau \qquad (4.9a)$$

Substituting for H and G, at $\tau = o$ and $\tau = t$, in expression (4.9a) gives

$$-H(\xi_1, \xi_2, t) + \int_\Omega S H_o G(r,t) \, d\Omega - \int_o^t \int_\Omega G N \, d\Omega d\tau \qquad (4.9b)$$

Replacing the left-hand terms of equation (4.8) by the expression (4.9b) and rearranging, thus equation (4.8) becomes

$$H(\xi_1,\xi_2,t) = T\int_o^t\int_\Gamma\left[G\frac{\partial H}{\partial n} - H\frac{\partial G}{\partial n}\right]d\Gamma d\tau$$

$$+\int_\Omega S\,H_o G(r,t)\,d\Omega - \int_o^t\int_\Omega G\,N\,d\Omega d\tau \qquad (4.10)$$

Equation (4.10) gives the value of H at a fixed point $p(\xi_1,\xi_2)$ at time t. This solution is valid as long as $p(\xi_1,\xi_2)$ lies in the interior of the solution domain. When p is moved on the boundary Γ, it must at one stage coincide with the field point, i.e. $\xi_i,=X_i$, leading to r=o which cause the boundary integral to have a singularity at p. This can be treated by excluding the point p from the domain by a small circular arc c with a radius which in the limit shrinks to zero. Integration along the circular arc c can be evaluated as

$$\int_o^t\int_c G\frac{\partial H}{\partial n}\,d\Gamma d\tau - \int_o^t\int_c H\frac{\partial G}{\partial n}\,d\Gamma d\tau \qquad (4.11)$$

Substituting for G and $\frac{\partial G}{\partial n}$, integrating with respect to time and taking the limit when the radius tends to zero, the first term in expression (4.11) yields a zero value and the second term gives $H\frac{\theta}{2\pi}$, where θ is the interior angle enclosed by the boundary at (ξ_1, ξ_2). Considering the boundary integrals due to the singularity at p, expression (4.11), thus equation (4.10) can be written in a general form as

$$\lambda H(\xi_1,\xi_2,t) = T\int_o^t\int_\Gamma\left[G\frac{\partial H}{\partial n} - H\frac{\partial G}{\partial n}\right]d\Gamma d\tau$$

$$+\int_\Omega S\,H_o G(r,t)\,d\Omega - \int_o^t\int_\Omega G\,N\,d\Omega d\tau \qquad (4.12)$$

where

$$\lambda = \begin{cases} 1 & \text{if } (\xi_1,\xi_2) \text{ is in } \Omega \\ \frac{1}{2} & \text{if } (\xi_1,\xi_2) \text{ is on } \Gamma \text{ and the boundary is smooth} \\ \frac{\theta}{2\pi} & \text{if } (\xi_1,\xi_2) \text{ is on } \Gamma \text{ and the boundary is not smooth} \end{cases}$$

Equation (4.12) is the complete statement of the boundary element solution to the problem. The boundary element statement of equation (4.12) can also be derived as a particular application of the Weighted Residual techniques (Brebbia, 1980). In this approach, the potential function H is approximated and the introduced error is minimized by weighting the governing equation by the function G which is the fundamental solution of the equation.

Weighting equation (4.1) and integrating with respect to time gives

$$\int_o^t \int_\Omega \left[T \frac{\partial^2 H}{\partial X_i \partial X_i} - S \frac{\partial H}{\partial t} - N \right] G \, d\Omega d\tau$$

$$= \int_o^t \int_{\Gamma_2} \left[T \frac{\partial H}{\partial n} - q \right] G \, d\Gamma d\tau - \int_o^t \int_{\Gamma_1} \left[H-h \right] T \frac{\partial G}{\partial n} \, d\Gamma d\tau \quad (4.13)$$

where $o \leq \tau \leq t$

Integrating equation (4.13) by parts twice yields

$$\int_o^t \int_\Omega \left[T \frac{\partial^2 G}{\partial X_i \partial X_i} - S \frac{\partial G}{\partial t} \right] H \, d\Omega d\tau - \int_o^t \int_\Omega G \, N \, d\Omega d\tau - \left[\int_\Omega S \, H \, G \, d\Omega \right]_{\tau=o}^{\tau=t}$$

$$= T \int_o^t \int_\Gamma H \frac{\partial G}{\partial n} \, d\Gamma d\tau - T \int_o^t \int_\Gamma G \frac{\partial H}{\partial n} \, d\Gamma d\tau \quad (4.14)$$

The fundamental solution G is given by equation (4.3) and possesses the properties

$$T \frac{\partial^2 G}{\partial X_i \partial X_i} - S\frac{\partial G}{\partial t} = o \text{ in } \Omega \text{ for all } \tau,$$

and for $\tau = t$

$$\int_\Omega G \, d\Omega = \begin{cases} o \text{ for } r \neq o \\ \\ 1 \text{ for } r = o \end{cases}$$

Substituting the fundamental solution into equation (4.14) after rearrangement and taking the point $p(\xi_1, \xi_2)$ to the boundary and considering the singularity as before, equation (4.14) yields the boundary element statement as expressed by equation (4.12) which is derived using Green's second identity approach.

Equation (4.12) can be written in a compact form as

$$\lambda H(\xi_1, \xi_2, t) = \int_o^t \int_\Gamma H \, q^* \, d\Gamma d\tau - \int_o^t \int_\Gamma G \, q \, d\Gamma d\tau + \int_\Omega S \, H_o G(r,t) d\Omega - \int_o^t \int_\Omega G \, N \, d\Omega d\tau, \qquad (4.15)$$

where q is given by equation (4.2) and q^* is defined as

$$q^* = - T \frac{\partial G}{\partial n} \qquad (4.16)$$

where q^* can be directly evaluated by deriving equation (4.3) which gives

$$q^* = \frac{d \, S}{8\pi T(t-\tau)^2} \exp\left[\frac{-r^2 S}{4T(t-\tau)}\right] \qquad (4.17)$$

where d is the distance from $p(\xi_1, \xi_2)$ normal to the boundary. Thus, the key problem is the solution of the Boundary Element equation (4.15) using the specified boundary values and internal sources or sinks to solve for the remaining unknown boundary data. Once all the boundary data are known then back substitution into equation (4.10) will yield the potential at any internal point.

4.2.4 Solution of the Boundary Element Equation

In all the foregoing development no approximations have been made. If equation (4.15) could be integrated in a closed form then the solution for $H(\xi_1, \xi_2, t)$ would be exact. However, this is virtually impossible in practical problems and approximations have to be introduced. These approximations are in the form of numerical discretization and integration.

4.2.4.1 Temporal Discretization

In order to circumvent the problem related to time integration in equation (4.15), the stepwise integration procedure is employed (Brebbia and Wrobel, 1980). In this procedure, the integration is performed with the assumption that H, q and N do not vary over small time intervals. Then, equation (4.15) becomes

$$\lambda H(\xi_1,\xi_2,t_{\ell+1}) = \int_\Gamma H \int_{t_\ell}^{t_{\ell+1}} q^* \, d\tau d\Gamma - \int_\Gamma q \int_{t_\ell}^{t_{\ell+1}} G \, d\tau d\Gamma$$

$$+ \int_\Omega S \, H_\ell \, G(r, t_\ell - t_{\ell+1}) \, d\Omega - \int_\Omega N \int_{t_\ell}^{t_{\ell+1}} G \, d\tau d\Omega \qquad (4.18)$$

where $t_\ell \leq \tau \leq t_{\ell+1}$ and H_ℓ is the value of H at time level ℓ. Denoting the time level ℓ as t_1 and the time level $\ell+1$ as t_2, the first time integral in equation (4.18) can be

evaluated using equation (4.17) as

$$\int_{t_1}^{t_2} q^* \, d\tau = \frac{d}{2\pi} \int_{t_1}^{t_2} \frac{S}{4T(t_2-\tau)^2} \exp\left[\frac{-r^2S}{4T(t_2-\tau)}\right] d\tau$$

$$= \frac{d}{2\pi r^2} \exp\left[\frac{-r^2S}{4T(t_2-t_1)}\right] \qquad (4.19)$$

Defining the variables

$$X = \frac{r^2S}{4T(t_2-\tau)} \qquad (4.20)$$

$$dX = \frac{r^2S}{4T(t_2-\tau)^2} \, d\tau \qquad (4.21)$$

The second and third time integrals in equation (4.18) can be evaluated using equations (4.3), (4.20) and (4.21) as follows

$$\int_{t_1}^{t_2} G \, d\tau = \int_{t_1}^{t_2} \frac{1}{4\pi T(t_2-\tau)} \exp\left[\frac{-r^2S}{4T(t_2-\tau)}\right] d\tau$$

$$= \frac{1}{4\pi T} \int_a^{\infty} \frac{1}{X} \exp[-X] \, dX$$

$$= \frac{1}{4\pi T} \mathrm{Ei}[a] \qquad (4.22)$$

where a is defined as

$$a = \frac{r^2S}{4T(t_2-t_1)} \qquad (4.23)$$

and Ei[a] is the exponential integral function which can be evaluated by series.

Substituting equations (4.19), (4.22) and (4.23) into

equation (4.18) yields for a particular time step

$$\lambda H(\xi_1,\xi_2,t_2) = \frac{1}{2\pi}\int_\Gamma H\,\frac{d}{r^2}\exp[-a]\,d\Gamma - \frac{1}{4\pi T}\int_\Gamma q\,Ei[a]d\Gamma$$

$$+\int_\Omega S\,H_{t1}\,G(r,t_2-t_1)\,d\Omega - \frac{1}{4\pi T}\int_\Omega N\,Ei[a]\,d\Omega \qquad (4.24)$$

We begin the solution at the first time step by using equation (4.24) with $t_1 = o$ and $H_{t1} = H_o$ as the initial condition. At the end of the time step the value of H_{t2} is determined and used as the initial condition for the second time step. The solution procedure is then repeated until the final time step is reached.

4.2.4.2 Spatial Discretization

Equation (4.2) is not homogeneous in the sense that the solution is not entirely in terms of boundary integration but the initial conditions and the applied sources and sinks are integrated over the domain. The boundary and domain integration can be achieved by means of spatial discretization. The boundary integrals are approximated by using the linear element discretization scheme with linear interpolation functions. The integration over the domain is performed by dividing the domain into a series of triangular internal cells.

i - Boundary element discretization:

The boundary element discretization algorithm involves the selection of a finite number of node points, $P_j(j=1,2,3,\ldots,N)$, on the boundary Γ, such that the boundary is divided into a number of linear elements, $\Gamma_e(e=1,2,3,\ldots,N)$. It is assumed that over an element Γ_e between a pair of boundary node points (P_j,P_{j+1}),

the distribution of the potential and its normal derivative is linear. The integration is performed for all elements with reference to a number of base points, $P_i (i=1,2,3,\ldots,N)$.

Introducing the local coordinate system (n, ℓ) for each element and considering an element Γ_e defined by the two nodes P_j and P_{j+1}, as shown in Figure (4.2) thus, H and q at any point on the element can be represented by

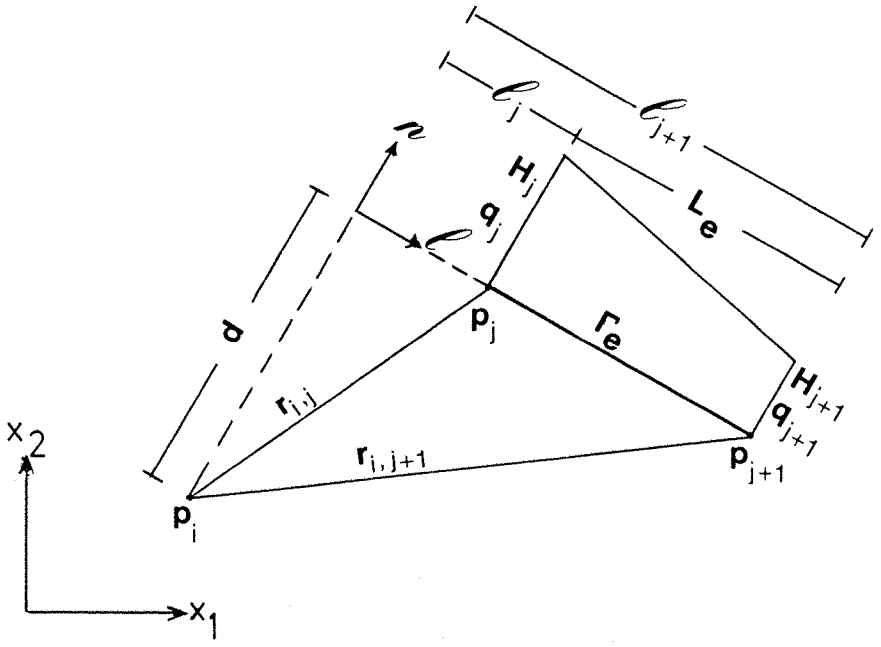

Fig. (4.2) Linear element and the local coordinate system (ℓ, n).

$$H = F_j H_j + F_{j+1} H_{j+1} \tag{4.25}$$

$$q = F_j q_j + F_{j+1} q_{j+1} \tag{4.26}$$

where F_j and F_{j+1} are linear interpolation functions defined as

$$F_j = \frac{1}{L_e} (\ell_{j+1} - \ell) \tag{4.27a}$$

$$F_{j+1} = \frac{1}{L_e} (\ell - \ell_j) \tag{4.27b}$$

where L_e is the length of the element Γ_e, i.e. $L_e = (\ell_{j+1} - \ell_j)$.

In equation (4.24), the boundary integral contributed by an element Γ_e with reference to a base point P_i is given by

$$\begin{aligned} C^e &= \frac{1}{2\pi} \int_{\Gamma_e} H \frac{d}{r_i^2} \exp[-a]\, d\Gamma - \frac{1}{4\pi T} \int_{\Gamma_e} q\, Ei[a]\, d\Gamma \\ &= \frac{1}{2\pi} \int_{\ell_j}^{\ell_{j+1}} (F_j H_j + F_{j+1} H_{j+1}) \frac{d}{r_i^2} \exp[-a]\, d\ell \\ &\quad - \frac{1}{4\pi T} \int_{\ell_j}^{\ell_{j+1}} (F_j q_j + F_{j+1} q_{j+1})\, Ei[a]\, d\ell \end{aligned} \tag{4.28}$$

Introducing the dimensionless coordinate system η for each element as shown in Figure (4.3), ℓ can be expressed in terms of η, hence

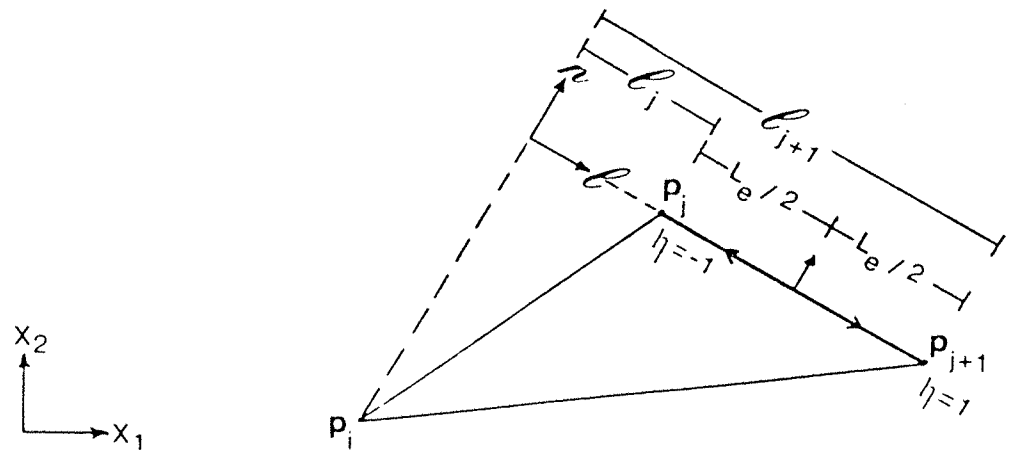

Fig. (4.3) Local dimensionless coordinate system (η)

$$\ell = \ell_j + \frac{L_e}{2}(1+\eta) \tag{4.29}$$

Deriving equation (4.30) gives

$$d\ell = \frac{L_e}{2} d\eta \tag{4.30}$$

Rewriting the integrals in equation (4.28) in terms of η, equation (4.28) can be expressed in the form

$$C^e = A^e_{i,j}H_j + A^e_{i,j+1}H_{j+1} + B^e_{i,j}q_j + B^e_{i,j+1}q_{j+1} \tag{4.31}$$

where

$$A^e_{i,j} = \frac{L_e}{8\pi}\int_{-1}^{1}(1-\eta)\frac{d}{r_i^2}\exp[-a]\,d\eta \tag{4.32a}$$

$$A^e_{i,j+1} = \frac{L_e}{8\pi}\int_{-1}^{1}(1+\eta)\frac{d}{r_i^2}\exp[-a]\,d\eta \tag{4.32b}$$

$$B^e_{i,j} = -\frac{L_e}{16\pi T}\int_{-1}^{1}(1-\eta)\,Ei[a]\,d\eta \tag{4.33a}$$

$$B^e_{i,j+1} = -\frac{L_e}{16\pi T}\int_{-1}^{1}(1+\eta)\,Ei[a]\,d\eta \tag{4.33b}$$

Considering the associated boundary conditions, for boundaries of specified head and/or specified flux, equations (4.28) to (4.33) are directly applicable. However, if the boundary condition is expressed as a linear combination of the head H and the flux q over part of the boundary, as in the condition of a hydraulically connected stream-aquifer boundary, as shown in Figure (4.4), the above analysis will have to be extended. The condition over a mixed boundary can be expressed in terms of the boundary flux q, the head on the external side of the boundary H^*, the head on the internal side of the boundary H and the

coefficient of hydraulic connection, σ, as

$$q = -T \frac{\partial H}{\partial n} = \sigma (H^* - H) \qquad (4.34)$$

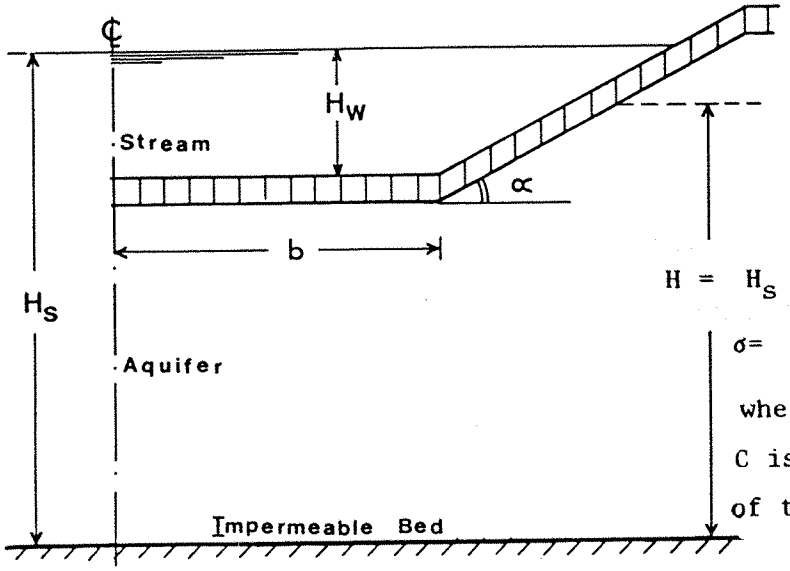

$$H = H_s - 0.5H_w^2/(b \sin\alpha + H_w) - q/\sigma$$

$$\sigma = (b + H_w/\sin\alpha)/C$$

where

C is the hydraulic resistance of the stream-aquifer boundary.

Fig. (4.4)

Hydraulically connected stream_aquifer boundary (Khater, 1980)

Substituting equation (4.34) into equation (4.28) yields

$$C^e = \frac{1}{2\pi} \int_{\Gamma_e} H \left[\frac{d}{r_i^2} \exp[-a] + \frac{\sigma}{2T} Ei[a] \right] d\Gamma$$

$$- \frac{1}{4\pi T} \int_{\Gamma_e} H^* \left[\sigma Ei[a] \right] d\Gamma$$

$$= \frac{1}{2\pi} \int_{\ell_j}^{\ell_{j+1}} (F_j H_j + F_{j+1} H_{j+1}) \left[\frac{d}{r_i^2} \exp[-a] + \frac{\sigma}{2T} Ei[a] \right] d$$

$$- \frac{1}{4\pi T} \int_{\ell_j}^{\ell_{j+1}} (F_j H_j^* + F_{j+1} H_{j+1}^*) \left[\sigma Ei[a] \right] d\ell \qquad (4.35)$$

Defining the variables

$$\nu = \frac{\sigma}{2T} \tag{4.36}$$

$$u = \sigma \tag{4.37}$$

and rewriting the integrals in equation (4.35) in terms of η, as before, equation (4.35) can be expressed in the same form as equation (4.31)

$$C^e = A^e_{i,j} H_j + A^e_{i,j} H_{j+1} + B^e_{i,j} H^*_j + B^e_{i,j+1} H^*_{j+1} \tag{4.38}$$

where

$$A^e_{i,j} = \frac{L_e}{8\pi} \int_{-1}^{1} (1-\eta) \left[\frac{d}{r_i^2} \exp[-a] + \nu \, Ei[a] \right] d\eta \tag{4.39a}$$

$$A^e_{i,j+1} = \frac{L_e}{8\pi} \int_{-1}^{1} (1+\eta) \left[\frac{d}{r_i^2} \exp[-a] + \nu Ei[a] \right] d\eta \tag{4.39b}$$

$$B^e_{i,j} = -\frac{L_e}{16\pi T} \int_{-1}^{1} (1-\eta) \, u \, Ei[a] \, d\eta \tag{4.39c}$$

$$B^e_{i,j+1} = -\frac{L_e}{16\pi T} \int_{-1}^{1} (1+\eta) \, u \, Ei[a] \, d\eta \tag{4.39d}$$

In fact, equation (4.38) and (4.39) are the general form of equations (4.31), (4,32) and (4.33) for, specified head and flux boundary conditions, with $H^*_j = q_j$, $H^*_{j+1} = q_{j+1}$, $\nu = 0$ and $u = 1$. Hence, equation (4.38) and (4.39) are directly applicable to the associated boundary conditions of specified head, specified flux and mixed type. In matrix notation equation (4.38) can be written as

$$\{C\}^e = [A]^e \{H\}^e + [B]^e \{H^*\}^e \tag{4.40}$$

where

$$[A]^e = [A^e_{i,j} \ , \ A^e_{i,j+1}] \tag{4.41a}$$

$$[B]^e = [B^e_{i,j} \ , \ B^e_{i,j+1}] \tag{4.41b}$$

$$\{H\}^e = \begin{Bmatrix} H_j \\ \\ H_{j+1} \end{Bmatrix} \tag{4.41c}$$

$$\{H^*\}^e = \begin{Bmatrix} H^*_j \\ \\ H^*_{j+1} \end{Bmatrix} \tag{4.41d}$$

and where for a specified head and flux boundary conditions $\{H^*\}^e$ is defined as

$$\{H^*\}^e = \{q\}^e = \begin{Bmatrix} q_j \\ \\ q_{j+1} \end{Bmatrix} \tag{4.41e}$$

Summing up all elemental contribution $\{C\}^e$ with reference to the base point P_i gives

$$\sum_{e=1}^{N} \{C\}^e = \sum_{e=1}^{N} [A]^e \{H\}^e + \sum_{e=1}^{N} [B]^e \{H^*\}^e \tag{4.42}$$

Equation (4.42) is the expression for the boundary integrals with reference to a particular base point.

ii - Domain discretization

If the domain Ω is approximated by a number of triangular internal cells Ω_c (C=1,2,3,...,M), a discrete approximation of the domain integrals in equation (4.24) can be achieved. It is assumed that the potential is linearly distributed over the internal cells. Considering an internal cell Ω_c defined in the (X_1,X_2) global coordinate system by the coordinate of the triangle apices (P(1), P(2) and P(3)), and introducing the local oblique coordinates (η_1, η_2) as shown in Figure (4.4) the global coordinates of an arbitrary point within triangular cell can be expressed in terms of its oblique coordinates (η_1, η_2) as follows,

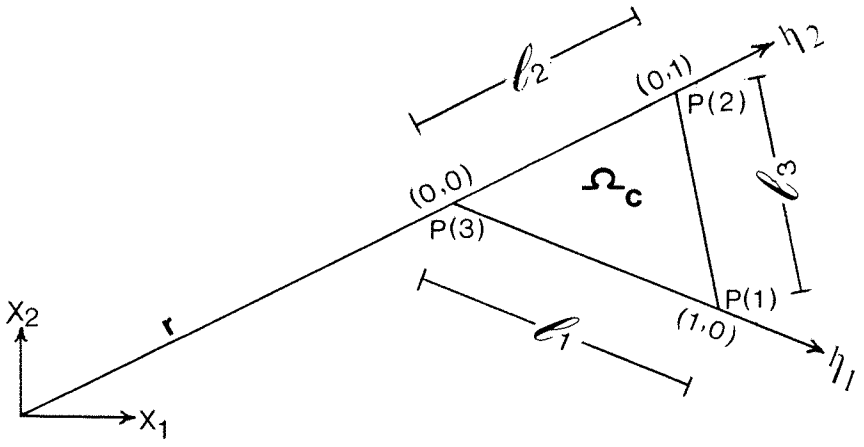

Fig. (4.5) Triangular cell and the local coordinate system (η_1,η_2)

$$X_1 = X_1(1)\eta_1 + X_1(2)\eta_2 + X_1(3)(1-\eta_1-\eta_2) \qquad (4.43a)$$

$$X_2 = X_2(1)\eta_1 + X_2(2)\eta_2 + X_2(3)(1-\eta_1-\eta_2) \qquad (4.43b)$$

where

$(X_1(1),X_2(1))$, $(X_1(2),X_2(2))$ and $(X_1(3),X_2(3))$ are the global coordinates of the triangle apices P(1), P(2) and P(3), respectively.

Equation (4.43) can be inverted to obtain

$$\eta_i = \frac{1}{2A} (\alpha_i+\beta_i X_1+\gamma_I X_2) \qquad (4.44)$$

where

$$\alpha_i = X_1(j)\ X_2(k) - X_1(k)X_2(j) \qquad (4.45a)$$

$$\beta_i = X_2(j) - X_2(k) \qquad (4.45b)$$

$$\gamma_i = X_1(k) - X_1(j) \qquad (4.45c)$$

and $i = 1,2$ for $j = 2,3$ and $k = 3,1$

$$A = \text{area of triangle} = \tfrac{1}{2}(\beta_1\gamma_2 - \beta_2\gamma_1) \qquad (4.46)$$

Thus, an arbitrary point within the triangle cell can be identified by specifying its local coordinates (η_i) as given by equation (4.44). Furthermore, these coordinates fulfil the requirement of shape functions, and for linear variation of the potential H at any point can be expressed as

$$H = H_1\eta_1 + H_2\eta_2 + H_3(1-\eta_1-\eta_2) \qquad (4.47)$$

where H_1, H_2 and H_3 are the potential heads at the triangle apices p(1), p(2) and p(3), respectively.

In equation (4.24) the domain integrals contributed by a triangular cell Ω_c, with reference to a particular base point p_i, is given by

$$C^c = \int_{\Omega_c} S\, H_{t1} G(r, t_2 - t_1)\, d\Omega - \frac{1}{4\pi T} \int_{\Omega_c} N\, Ei[a]\, d\Omega \qquad (4.48)$$

Substituting equation (4.47) into equation (4.48) and rewriting the integrations with respect to X_i, yields

$$C^c = \iint S(H_1\eta_1 + H_2\eta_2 + H3(1-\eta_1-\eta_2))t_1\, G(r, t_2 - t_1)\, dX_1 dX_2$$

$$- \frac{1}{4\pi T} \iint N\, Ei[a]\, dX_1 dX_2 \qquad (4.49)$$

Performing the transformation from the global cartesian space X_i to the local one η_i, the differential components will be interrelated by the Jacobian of transformation, J, which is given by the determinant of

$$J = \begin{vmatrix} \frac{\partial X_1}{\partial \eta_1} & \frac{\partial X_1}{\partial \eta_2} \\ \frac{\partial X_2}{\partial \eta_1} & \frac{\partial X_2}{\partial \eta_2} \end{vmatrix} \qquad (4.50)$$

partial derivation of equations (4.43) yields

$$J = X_1(1)(X_2(2) - X_2(3)) + X_1(2)(X_2(3) - X_2(1)) + X_1(3)(X_2(1) - X_2(2)) \qquad (4.51a)$$

which gives, $J = 2A$ (4.51b)

Whence, equation (4.49) becomes

$$C^C = \int_o^1 \int_o^{1-\eta_2} S(H_1\eta_1 + H_2\eta_2 + H_3(1-\eta_1-\eta_2)_{t1}\, G(r,t_2-t_1)\, J\, d\eta_1 d\eta_2$$

$$- \frac{1}{4\pi T} \int_o^1 \int_o^{1-\eta_2} NEi[a]\, J\, d\eta_1 d\eta_2 \qquad (4.52)$$

Equation (4.52) can be expressed in the form

$$C^C = D^C_{i,1} H_{1_{t1}} + D^C_{i,2} H_{2_{t1}} + D^C_{i,3} H_{3_{t1}} + E^C_{i,c}\, N_c \qquad (4.53)$$

where

$$D^C_{i,1} = \int_o^1 \int_o^{1-\eta_2} S\, G(r,t_2-t_1)\, J\eta_1\, d\eta_1 d\eta_2 \qquad (4.54a)$$

$$D^C_{i,2} = \int_o^1 \int_o^{1-\eta_2} S\, G(r,t_2-t_1)\, J\eta_2\, d\eta_1 d\eta_2 \qquad (4.54b)$$

$$D^C_{i,3} = \int_o^1 \int_o^{1-\eta_2} S\, G(r,t_2-t_1)\, J\, (1-\eta_1-\eta_2)\, d\eta_1 d\eta_2 \qquad (4.54c)$$

$$E^C_{i,c} = \int_o^1 \int_o^{1-\eta_2} -\frac{1}{4\pi T}\, Ei[a]\, J\, d\eta_1 d\eta_2 \qquad (4.54d)$$

In matrix notation equation (4.53) may be written as

$$\{C\}^C = [D]^C \{H\}^C_{t_1} + [E]^C \{N\}^C \qquad (4.55)$$

where

$$[D]^C = [D^C_{i,1},\ D^C_{i,2},\ D^C_{i,3}] \qquad (4.56a)$$

$$[E]^C = [E^C_{i,c}] \qquad (4.56b)$$

$$\{H\}^c_{t_1} = \begin{Bmatrix} H_1 \\ H_2 \\ H_3 \end{Bmatrix}_{t_1} \tag{4.56c}$$

$$\{N\}^c = \{N_c\} \tag{4.56d}$$

Summing up all the cellular contribution, with reference to the base point p_i, as expressed in equation (4.55) gives

$$\sum_{C=1}^{M} \{C\}^c = \sum_{C=1}^{M} [D]^c \{H\}^c_{t_1} + \sum_{C=1}^{M} [E]^c \{N\}^c \tag{4.57}$$

Hence, the spatially discretized version of equation (4.24) is given by the summation of equations (4.42) and (4.57) as,

$$\lambda H(\xi_1, \xi_2, t_2) = \sum_{e=1}^{N} [A]^e \{H\}^e + \sum_{e=1}^{N} [B]^e \{H^*\}^e + \sum_{c=1}^{M} [D]^c \{H\}^c_{t_1} + \sum_{c=1}^{M} [E]^c \{N\}^c \tag{4.58}$$

By writing equation (4.58) at each boundary node for a particular instant of time, a system of algebraic equations that describes the entire global system can be obtained with λH^e being absorbed into the diagonal elements of $[A]^e$. Thus the following matrix equation can be obtained

$$[A]\{H\} + [B]\{H^*\} = [D]\{H\}_{t_1} + [E]\{N\} \tag{4.59}$$

where [A], [B], [D] and [E] are the global coefficient matrices defined as

$$[A] = \sum_{e=1}^{N} [A]^e \tag{4.60a}$$

$$[B] = \sum_{e=1}^{N} [B]^e \tag{4.60b}$$

$$[D] = -\sum_{c=1}^{M} [D]^c \qquad (4.60c)$$

$$[E] = -\sum_{c=1}^{M} [E]^c \qquad (4.60d)$$

4.2.4.3 Evaluation of the Integrals

In order to construct the matrices for the global system of equation (4.59) it is necessary to evaluate the spatially discretized boundary and domain integrals. The integrations can be carried out numerically by applying Gauss quadrature formulae. Numerical integration formulae, the underlying mathematic and the tables can be found in Lanczos (1961) and Stroud and Secrest (1966).

i - Boundary integrals

The boundary integrals involved are given by equations (4.39). The integrals can be evaluated numerically with a highly acceptable accuracy by applying a four points Gauss quadrature formula. The boundary integrals of equation (4.39) can be approximated by the summation

$$BI = \int_{-1}^{1} f(\eta)\, d\eta \approx \sum_{i=1}^{n} W_i f(\eta_i) \qquad (4.61)$$

where W_i is a weighting factor, η_i is the coordinate of the i^{th} integration point and n is the total number of integration points. For a four points Gauss quadrature integration, η_i and W_i are listed in Table (4.1).

	n	i	η_i	W_i
Table (4.1)		1	+0.86113631	0.34785485
(Four points		2	-0.86113631	0.34785485
Gaussian	4	3	+0.33998104	0.65214515
quadrature)		4	-0.33998104	0.65214515

In order to evaluate $f(\eta_i)$ for each integration point the values of the variables in equations (4.39) should be calculated. This can be achieved according to the following definitions:

L_e; the length of a boundary element Γ_e is given by

$$L_e = \sqrt{(X_1(1)-X_1(2)^2 + (X_2(1)-X_1(2))^2} \qquad (4.62)$$

where $(X_1(1),X_2(2))$ and $(X_1(2),X_2(2))$ are the global coordinates of the boundary nodes P_j and P_{j+1} which define the element Γ_e.

d; the distance defined by the normal from the base point under consideration to the boundary element tangent is given by

$$d = \sqrt{(X_1(p)-X_1(d))^2 + (X_2(p)-X_2(d))^2} \qquad (4.63)$$

where $(X_1,(P), X_2(p))$ and $(X_1(d),X_2(d))$ are the global coordinates of the considered base point and its normal projection on the boundary element tangent, respectively. The coordinates $(X_1(d),X_2(d))$ are given by

$$X_1(d) = \frac{1}{2(X_1(2)-X_1(1))}\left[\left(\frac{r_1^2-r_2^2}{1+Z^2}\right) + (X_1^2(2)-X_1^2(1))\right] \qquad (4.64a)$$

$$X_2(d) = \frac{1}{2(X_2(2)-(X_2(1))} \left[Z^2 \left[\frac{r_1^2-r_2^2}{1+Z^2} \right] + (X_2^2(2)-X_2^2(1)) \right] \quad (4.64b)$$

where $(X_1(1), X_2(1))$ and $(X_1(2), X_2(2))$ as defined above and

$$r_1^2 = \left[(X_1(1) - X_1(p))^2 + (X_2(1) - X_2(p))^2 \right] \quad (4.65a)$$

$$r_2^2 = \left[(X_1(2) - X_1(p))^2 + (X_2(2) - X_2(p))^2 \right] \quad (4.65b)$$

$$Z = \left[\frac{X_2(2)-X_2(1)}{X_1(2)-X_1(1)} \right] = \frac{DX_2}{DX_1} \quad (4.65c)$$

with the special conditions

$DX_1 = o$, hence, $X_1(d) = X_1(1)$ and $X_2(d) = X_2(p)$ which leads to

$$d = \left| (X_1(p)-X_1(1)) \right| \quad (4.66a)$$

or, $DX_2 = o$, hence, $X_1(d) = X_1(p)$ and $X_2(d) = X_2(1)$

which leads to

$$d = \left| (X_2(p)-X_2(1)) \right| \quad (4.66b)$$

r_i; the distance from the base point under consideration to the i^{th} integration point is given by

$$r_i^2 = \left[d^2 + \ell_i^2 \right] \quad (4.67)$$

where

$$\ell_i = L + \frac{L_e}{2}(1+\eta_i) \qquad (4.68a)$$

$$L = \sqrt{(X_1(1)-X_1(d))^2 + (X_2(1)-X_2(d))^2} \qquad (4.68b)$$

and η_i is the local coordinate of the i^{th} integration point, and the other notations as defined above

The variable [a] is given by equation (4.23) as

$$a = \frac{r_i^2 S}{4T(t_2-t_1)}$$

where r_i as defined above

Ei[a] is the exponential integral function which can be evaluated by series as

for $a \leq 5$

$$Ei[a] = -c-Ln[a] + \sum_{n=1}^{\infty} (-1)^{n-1} \frac{[a]^n}{n.n!} \qquad (4.69a)$$

where c is the Euler's constant; c = 0.57721566...

for a >5 equation (4.69a) requires a great number of terms in the calculation, to overcome this difficulty, the following approximate series can be used

$$Ei[a] = \exp[-a] \sum_{n=1}^{\infty} (-1)^{n-1} \frac{(n-1)!}{[a]^n} \qquad (4.69b)$$

Calculating the values of the above defined variables for each integration point, the boundary integrals of equation (4.39) can be evaluated using the Gauss quadrature formula expressed by equation (4.61).

ii - Domain integrals

The domain integrals involved are given by equation (4.54). The integrals can be evaluated by applying the numerical integration formula suggested by Hammer and Stroud using a seven points quadrature scheme. The domain integrals of equation (4.54) can be approximated by the summation

$$DI = \int_0^1 \left[\int_0^{1-\eta_2} f(\eta_1,\eta_2,(1-\eta_1-\eta_2))\, d\eta_1 \right] d\eta_2$$

$$= \tfrac{1}{2} \sum_{i=1}^{n} W_i f(\eta_1^i, \eta_2^i, (1-\eta_1^i-\eta_2^i)) \qquad (4.70)$$

where W_i is a weighting factor, (η_1^i, η_2^i) are the coordinates of the i^{th} integration point and n is the total number of integration points. For a seven points quadrature scheme, (η_1^i,η_2^i) and W_i are listed in table (4.2) below

	n	i	η_1^i	η_2^i	$(1-\eta_1^i-\eta_2^i)$	W_i
Table		1	0.33333333	0.33333333	0.33333333	0.22500000
(4.2)		2	0.79742699	0.10128651	0.10128651	0.12593918
seven		3	0.10128651	0.79742699	0.10128651	0.12593918
points	7	4	0.10128651	0.10128651	0.79742699	0.12593918
quadr-		5	0.05971587	0.47014206	0.47014206	0.13239416
ature		6	0.47014206	0.05971587	0.47014206	0.13239416
scheme)		7	0.47014206	0.47014206	0.05971587	0.13239416

The following definitions of the variables in equations (4.54) can be used to evaluate $f(\eta_1^i, \eta_2^i, (1-\eta_1^i-\eta_2^i))$ for each integration point

The variable $G(r, t_2-t_1)$ is defined by equation (4.3) as,

$$G(r,t_2-t_1) = \frac{1}{4\pi T(t_2-t_1)} \exp\left[\frac{-r_i^2 S}{4T(t_2-t_1)}\right]$$

The variable [a] is given by equation (4.23) as

$$a = \frac{r_i^2 S}{4T(t_2-t_1)}$$

where r_i is the distance from the base point under consideration and the i^{th} integration point, r_i is given by

$$r_i^2 = \left[(X_1(P) - X_1(i))^2 + (X_2(P)-X_2(i))^2\right] \qquad (4.71)$$

where $(X_1(P), X_2(P))$ and $(X_1(i), X_2(i))$ are the global coordinates of the base point and the i^{th} integration point, respectively. Substituting the coordinates of the i^{th} integral point in terms of local coordinates (η_1^i, η_2^i) as given by equation (4.43), the rearranged expanded form of equation (4.71) is

$$r_i^2 = \eta_1^2\ell_1^2 + \eta_2^2\ell_2^2 + \eta_1(\alpha-\ell_1^2) + \eta_2(\beta-\ell_2^2)$$

$$+ \eta_1\eta_2(\ell_1^2+\ell_2^2-\ell_3^2) + \gamma \qquad (4.72)$$

where ℓ_1, ℓ_2 and ℓ_3 are the lengths of the sides of a triangular cell, which are given in terms of the global coordinate of the triangle apices as

$$\ell_1^2 = \left[(X_1(1)-X_1(3))^2 + (X_2(1)-X_2(3))^2\right] \qquad (4.73a)$$

$$\ell_2^2 = \left[(X_1(2)-X_1(3))^2 + (X_2(2)-X_2(3))^2\right] \qquad (4.73b)$$

$$\ell_3^2 = \left[(X_1(1)-X_1(2))^2 + (X_2(1)-X_2(2))^2\right] \qquad (4.73c)$$

and α, β and γ are defined as

$$\alpha = (r_1^2 - r_3^2) \qquad (4.74a)$$

$$\beta = (r_2^2 - r_3^2) \qquad (4.74b)$$

$$\gamma = r_3^2 \qquad (4.74c)$$

where r_1, r_2 and r_3 are the distances between the base point and the triangle apices which are given by

$$r_i^2 = \left[(X_1(P)-X_1(1))^2 + (X_2(P)-X_2(1))^2\right] \qquad (4.75a)$$

$$r_2^2 = \left[(X_1(P)-X_1(2))^2 + (X_2(P)-X_2(2))^2\right] \qquad (4.75b)$$

$$r_3^2 = \left[(X_1(P)-X_1(3))^2 + (X_2(P)-X_2(3))^2\right] \qquad (4.75c)$$

J, the Jacobian of transformation is given by equations (4.51)

Ei[a], the exponential integral function which can be evaluated by equations (4.69)

Calculating the values of the above defined variables for each integration point, the domain integrals of equations (4.54) can be evaluated using the quintic quadrature scheme expressed by equation (4.70).

When the base point lies on the element Γ_e the evaluation of the integral $A^e_{i,i}$ can be avoided as it is possible to calculate the diagonal element of the global matrix $[A]^e$ indirectly by applying a uniform distribution of the function H to the global matrix equation (4.59), which will give zero normal fluxes at the boundaries. Thus, the coefficient of the diagonal of $[A]^e$ will be given by

$$A^e_{i,i} = - \sum_{j=1}^{N} A^e_{i,j} + \sum_{c=1}^{M} \{C\}^e \qquad (4.76)$$

4.2.4.4 Formation of the Matrices and Solution of Algebraic Equations

Once the boundary and domain integrals of equations (4.39) and (4.54) are evaluated the global coefficient matrices [A], [B], [D] and [E] can be constructed, the sizes of these matrices are NxN, NxN, NxM and NxM respectively. In equation (4.59), for a particular time step, the right-hand side is known since $\{H\}_{t1}$ are the given initial conditions and {N} are specified sources or sinks. In a well posed problem half of the boundary values {H} and $\{H^*\}$ will be known and therefore the remaining half can be obtained by solving the system of algebraic equations. Before the solution of the algebraic equations can be obtained, the known and unknown components of the nodal vectors {H} and $\{H^*\}$ must be separated and form the following system

$$[\Lambda]\ \{\chi\} = \{\xi\} \qquad (4.77)$$

where $[\Lambda]$ is a fully populated Nx1 matrix derived from [A] and [B], $\{\chi\}$ is a Nx1 vector containing the unknown boundary

values of $\{H\}$ and H^*, and $\{\xi\}$ is a Nx1 vector of known information compiled from multiplying the appropriate columns of [A] and [B] by the prescribed boundary values of $\{H\}$ and $\{H^*\}$ and the result is then transferred to join the known right-hand terms of equation (4.59) to form the vector of known information. This system of equations can be solved by using a Gaussian elimination scheme for a fully populated and asymmetric coefficient matrix.

Once all the nodal values of the potential and its normal derivative on the boundary are determined, it is possible to calculate the potential at the interior nodal points by using the interior nodal points as fixed base points with $\lambda = 1$. Thus a new $\{H\}_{t_{\ell+1}}$ vector is compiled and can be used as the initial conditions for the next time step. The solution procedure is then repeated until the final time step is reached.

4.3 Boundary Element Solution for Steady-State Conditions

4.3.1 Governing Equations

The steady-state aquifer conditions is described by the elliptic partial differential equation known as Poisson's equation written in the form

$$T \frac{\partial^2 H_o}{\partial X_i \partial X_i} = N_o \qquad (4.78)$$

where H_o is the steady-state potential, T is the average transmissivity of the aquifer and N_o is the steady recharge (-ve) or withdrawal rate (+ve) per unit area. The flux q_o across any boundary defined by its normal n_i is

$$q_o = - T \frac{\partial H_o}{\partial n} \qquad (4.79)$$

The boundary conditions associated with equation (4.78) will be

i - H_o specified over part Γ_1 of the boundary Γ

ii - q_o specified over the remainder Γ_2 of the boundary Γ

iii - a linear combination of H_o and q_o might be specified over part of the boundary Γ

4.3.2 The Fundamental Solution

The fundamental solution represented by the free space Green function which satisfies equation (4.78) (Greenberg 1971) is given by

$$G_o = \frac{1}{2\pi} \text{Ln } r_i \qquad (4.80)$$

in which r_i denotes the distance between the singular base point and another point on the boundary of the two dimensional domain.

where $r_i = \left[(X_1-\xi_1)^2 + (X_2-\xi_2)^2 \right]^{\frac{1}{2}}$

It can be shown that the function Ln r_i satisfies

$$\frac{\partial^2}{\partial X_i \partial X_i} (\text{Ln } r_i) = 2\pi \, \delta(X_1-\xi_1) \, \delta(X_2-\xi_2) \qquad (4.81a)$$

where (ξ_1,ξ_2) and (X_1,X_2) are the coordinates of the fixed base point and the variable field point, respectively.

The function G_o satisfies the equation

$$\frac{\partial^2 G_o}{\partial X_i \partial X_i} = o \qquad (4.81b)$$

4.3.3 Boundary Element Formulation

Boundary element solution can be formulated by using the consequences of the divergence theorm known as Green's identities. Green's second identity is given by

$$\int_\Omega \left[H_o \frac{\partial^2 G_o}{\partial X_i \partial X_i} - G_o \frac{\partial^2 H_o}{\partial X_i \partial X_i} \right] d\Omega$$

$$= \int_\Gamma \left[H_o \frac{\partial G_o}{\partial n} - G_o \frac{\partial H_o}{\partial n} \right] d\Gamma \qquad (4.82)$$

where Ω and Γ are the interior and boundary of the solution domain. Using equations (4.78) and (4.81b) to substitute for the left-hand side of equation (4.82) gives

$$\int_\Gamma \left[H_o \frac{\partial G_o}{\partial n} - G_o \frac{\partial H_o}{\partial n} \right] d\Gamma + \int_\Omega \frac{1}{T} N_o G_o \, d\Omega = o \qquad (4.83)$$

For a particular base point $p(\xi_1, \xi_2)$ on the boundary, substituting the fundamental solution given by equation (4.80), equation (4.83) can be expanded to give

$$\int_\Gamma \left[H_o \frac{\partial}{\partial n} (Lnr_i) - Lnr_i \frac{\partial H_o}{\partial n} \right] d\Gamma + \int_\Omega \frac{1}{T} N_o \, Lnr_i \, d\Omega = o \qquad (4.84)$$

The fundamental solution satisfies equation (4.81b) everywhere in Ω with the exception that it goes to infinity at the singular point $p(\xi_1, \xi_2)$. Thus in integrating along the boundary in equation (4.84) for any base point on

the boundary, as the field point moves around the boundary Γ it must at one stage coincide with the base point, leading to $r_i=o$. To avoid this difficulty the base point is excluded from the domain by a small circular arc with a radius which in the limit shrinks for zero. The integration along the small circular arc, a semi-circle when the boundary is smooth, gives a free term λ and the head at the base point is given according to Green's third identity by

$$\lambda H_o(\xi_1,\xi_2) = \int_\Gamma \left[H_o \frac{\partial}{\partial n}(Lnr_i) - Lnr_i \frac{\partial H_o}{\partial n}\right] d\Gamma + \int_\Omega \frac{1}{T} N_o Lnr_i \, d\Omega \qquad (4.85)$$

where the free term λ is given by

$$\lambda = \begin{cases} 1 & \text{if } P(\xi_1,\xi_2) \text{ is in } \Omega \\ \frac{1}{2} & \text{if } P(\xi_1,\xi_2) \text{ is on } \Gamma \text{ and the boundary is smooth} \\ \frac{\theta}{2\pi} & \text{if } P(\xi_1,\xi_2) \text{ is on } \Gamma \text{ and the boundary is not smooth} \end{cases}$$

and θ is the interior angle enclosed by the boundary at $P(\xi_1,\xi_2)$. Equation (4.85) is the complete statement of the steady state two dimensional boundary element solution. The statement of equation (4.85) can also be derived as a particular application of the Weighted Residual techniques (Brebbia, 1980). In this approach the potential function H_o is approximated and the introduced error is minimized by weighting the governing equation by the function G_o which is the fundamental solution. Weighting equation (4.78) gives

$$\int_{\Omega}\left[\frac{\partial^2 H_o}{\partial X_i \partial X_1} - \frac{N_o}{T}\right] G_o d\Omega = \int_{\Gamma}\left[\frac{\partial H_o}{\partial n} G_o - H_o \frac{\partial G_o}{\partial n}\right] d\Gamma \quad (4.86)$$

Integrating the left-hand terms by parts twice, equation (4.86) becomes

$$\int_{\Omega} \frac{\partial^2 G_o}{\partial X_i \partial X_i} H_o \, d\Omega - \int_{\Omega} \frac{N_o}{T} G_o d\Omega = \int_{\Gamma}\left[\frac{\partial H_o}{\partial n} G_o - H_o \frac{\partial G_o}{\partial n}\right] d\Gamma \quad (4.87)$$

the fundamental solution is given by equation (4.80) and has the property

$$\frac{\partial^2 G_o}{\partial X_i \partial X_i} = \delta(X_1-\xi_1)\ \delta(X_2-\xi_2)$$

where δ is the Dirac delta function.

Substituting the fundamental solution as the weighting function and taking the point $p(\xi_1,\xi_2)$ to the boundary, equation (4.87) will yield the boundary element solution statement as expressed by equation (4.85) which has been derived using Green's identities approach.

Deriving the function Lnr_i gives

$$d\ Lnr_i = \frac{1}{r_i} dr_i \quad (4.88)$$

Thus equation (4.85) can be expressed in the form

$$\lambda H_o(\xi_1,\xi_2) = \int_\Gamma H_o \frac{1}{r_i}\frac{\partial r_i}{\partial n}\, d\Gamma + \frac{1}{T}\int_\Gamma q_o \, Lnr_i \, d\Gamma + \frac{1}{T}\int_\Omega N_o \, Lnr_i \, d\Omega \qquad (4.89)$$

where q_o is defined by equation (4.79) as $q_o = -T\frac{\partial H_o}{\partial n}$

Hence, using the specified boundary values and internal sources or sinks equation (4.89) can be solved for the remaining unknown boundary data. Once all the boundary data are known then back substitution using the internal points as base points with $\lambda = 1$ will yield the potential at the internal points.

4.3.4 Solution of the Boundary Element Equation

4.3.4.1 Boundary element discretization

The boundary integral of equation (4.89) can be approximated by the summation of integrals over individual elements. Using a linear element discretization scheme and introducing the local coordinate system (ℓ ,n) for each element when ℓ is the direction of the boundary element tangent and n is its normal direction, thus, H_o and q_o at an arbitrary point on the element can be expressed by

$$H_o = F_j H_{oj} + F_{j+1} H_{oj+1} \qquad (4.90a)$$

$$q_o = F_j q_{oj} + F_{j+1} q_{oj+1} \qquad (4.90b)$$

where F_j and F_{j+1} are linear interpolation functions defined as

$$F_j = \frac{1}{L_e}(\ell_{j+1} - \ell) \qquad (4.91a)$$

$$F_{j+1} = \frac{1}{L_e} (\ell - \ell_j) \tag{4.91b}$$

where L_e is the length of the element Γ_e defined by the two nodes p_j and p_{j+1} ; $L_e = (\ell_{j+1} - \ell_j)$.

In equation (4.89) the boundary integral contributed by an element Γ_e with reference to a base point p_i is

$$\begin{aligned} C_o^e &= \int_{\Gamma_e} H_o \frac{1}{r_i} \frac{\partial r_i}{\partial n} d\Gamma + \frac{1}{T} \int_{\Gamma_e} q_o \, Lnr_i \, d\Gamma \\ &= \int_{\ell_j}^{\ell_{j+1}} (F_j H_{oj} + F_{j+1} H_{oj+1}) \frac{1}{r_i} \frac{\partial r_i}{\partial n} d\ell \\ &\quad + \frac{1}{T} \int_{\ell_j}^{\ell_{j+1}} (F_j q_{oj} + F_{j+1} q_{oj+1}) \, Lnr_i \, d\ell \end{aligned} \tag{4.92}$$

Equation (4.92) can be expressed in the form

$$C_o^e = A_{i,j}^e H_{oj} + A_{i,j+1}^e H_{oj+1} + B_{i,j}^e q_{oj} + B_{i,j+1}^e q_{oj+1} \tag{4.93}$$

where

$$A_{i,j}^e = \int_{\ell_j}^{\ell_{j+1}} F_j \frac{1}{r_i} \frac{\partial r_i}{\partial n} d\ell \tag{4.94a}$$

$$A_{i,j+1}^e = \int_{\ell_j}^{\ell_{j+1}} F_{j+1} \frac{1}{r_i} \frac{\partial r_i}{\partial n} d\ell \tag{4.94b}$$

$$B_{i,j}^e = \int_{\ell_j}^{\ell_{j+1}} \frac{1}{T} F_j \, Lnr_i \, d\ell \tag{4.94c}$$

$$B_{i,j+1}^e = \int_{\ell_j}^{\ell_{j+1}} \frac{1}{T} F_{j+1} \, Lnr_i \, d\ell \tag{4.94d}$$

In matrix notation equation (4.93) can be written as

$$\{C_o\}^e = [A]^e \{H_o\}^e + [B]^e \{q_o\}^e \tag{4.95}$$

where

$$[A]^e = [A^e_{i,j} \ , \ A^e_{i,j+1}] \tag{4.96a}$$

$$[B]^e = [B^e_{i,j} \ , \ B^e_{i,j+1}] \tag{4.96b}$$

$$\{H_o\}^e = \begin{Bmatrix} H_{oj} \\ H_{oj+1} \end{Bmatrix} \tag{4.96c}$$

$$\{q_o\}^e = \begin{Bmatrix} q_{oj} \\ q_{oj+1} \end{Bmatrix} \tag{4.96d}$$

Summing up all the elemental contribution $\{C_o\}^e$ with reference to the considered base point where e = 1,2,3,...,N.

$$\sum_{e=1}^{N} \{C_o\}^e = \sum_{e=1}^{N} [A]^e \{H_o\}^e + \sum_{e=1}^{N} [B]^e \{q_o\}^e \tag{4.97}$$

Equation (4.97) is the discretized expression for the boundary integrals of equation (4.89).

4.3.4.2 Domain discretization

A discrete approximation of the domain integral of equation (4.89) can be achieved by approximating the domain by a number of triangular internal cells Ω_c (C=1,2,3,...,M). Introducing the local oblique coordinates (η_1,η_2) and considering a triangular cell Ω_c, the domain integral in equation (4.89) is given by

$$C_o^c = \frac{1}{T} \int_{\Omega_c} N_o \ Lnr_i \ d\Omega = \frac{1}{T} \iint N_o \ Lnr_i \ dX_1 dX_2 \tag{4.98}$$

Performing the transformation from the global cartesian space (X_1, X_2) to the local one (η_1, η_2), equation (4.98) becomes

$$C_o^c = \frac{1}{T} \int_o^1 \int_o^{1-\eta_2} N_o \, Lnr_i J \, d\eta_1 d\eta_2 \tag{4.99}$$

where J is the Jacobian of transformation and is given by

$$J = 2A \tag{4.100}$$

where A is the area of the triangular cell.

Equation (4.99) can be expressed in the form

$$\{C_o\}^c = [E]^c \{N_o\}^c \tag{4.101}$$

where

$$[E]^c = \frac{1}{T} \int_o^1 \int_o^{1-\eta_2} Lnr_i \, J \, d\eta_1 d\eta_2 \tag{4.102}$$

Summing up all the cellular contributions with reference to the base point under consideration gives

$$\sum_{c=1}^{M} \{C_o\}^c = \sum_{c=1}^{M} [E]^c \{N_o\}^c \tag{4.103}$$

Hence, the spatially discretized version of equation (4.89) is given by equations (4.97) and (4.103) as

$$\lambda H_o(\xi_1, \xi_2) = \sum_{e=1}^{N} [A]^e \{H_o\}^e + \sum_{e=1}^{N} [B]^e \{q_o\}^e + \sum_{c=1}^{M} [E]^c \{N\}^c \tag{4.104}$$

By writing equation (4.104) at each boundary node a system of algebraic equations that describes the entire global system can be obtained with λH_o^e being absorbed into the diagonal elements of $[A]^e$. Thus the following global matrix equation can be obtained

$$[A]\{H_o\} + [B]\{q_o\} + [E]\{N_o\} = \{0\} \qquad (4.105)$$

where [A], [B] and [E] are the global coefficient matrices.

4.3.5 Evaluation of the Integrals

4.3.5.1 Boundary integrals

The boundary integrals involved are given by equations (4.94). These integrations can be evaluated analytically as follows:

$$A^e_{i,j} = \int_{\ell_j}^{\ell_{j+1}} \frac{1}{L_e}(\ell_{j+1}-\ell)\frac{1}{(d^2+\ell^2)^{\frac{1}{2}}}\frac{d}{(d^2+\ell^2)^{\frac{1}{2}}}\,d\ell \qquad (4.106)$$

Integration by substitution yields

$$A^e_{i,j} = \frac{1}{L_e}\left[-d\,\mathrm{Ln}(r_{i,j+1}/r_{i,j}) + \ell_{j+1}\left(\tan^{-1}\frac{\ell_{j+1}}{d} - \tan^{-1}\frac{\ell_j}{d}\right)\right] \qquad (4.107)$$

Similarly,

$$A^e_{i,j+1} = \frac{1}{L_e}\left[d\,\mathrm{Ln}(r_{i,j+1}/r_{i,j}) - \ell_j\left(\tan^{-1}\frac{\ell_{j+1}}{d} - \tan^{-1}\frac{\ell_j}{d}\right)\right] \qquad (4.108)$$

And,

$$B^e_{i,j} = \int_{\ell_j}^{\ell_{j+1}} \frac{1}{L_e}(\ell_{j+1}-\ell)\,\mathrm{Ln}\,(d^2+\ell^2)^{\frac{1}{2}}\,d\ell \qquad (4.109)$$

Integration by substitution yields

$$B^e_{i,j} = -\frac{1}{4L_e}\left[r^2_{i,j+1}\,(\mathrm{Ln}\, r^2_{i,j+1} - 1) - r^2_{i,j}\,(\mathrm{Ln}\, r^2_{i,j} - 1)\right.$$
$$-4\ell_{j+1}\left(\ell_{j+1}\,\mathrm{Ln}\, r_{i,j+1} - \ell_j\,\mathrm{Ln}\, r_{i,j} - L_e\right.$$
$$\left.\left. + d\,\left(\tan^{-1}\frac{\ell_{j+1}}{d} - \tan^{-1}\frac{\ell_j}{d}\right)\right)\right] \qquad (4.110)$$

Similarly,

$$B^e_{i,j+1} = \frac{1}{4L_e}\left[r^2_{i,j+1}\,(\mathrm{Ln}\, r^2_{i,j+1} - 1) - r^2_{i,j}\,(\mathrm{Ln}\, r^2_{i,j} - 1)\right.$$
$$-4\ell_j\left(\ell_{j+1}\,\mathrm{Ln}\, r_{i,j+1} - \ell_j\,\mathrm{Ln}\, r_{i,j} - L_e\right.$$
$$\left.\left. - d\,\left(\tan^{-1}\frac{\ell_{j+1}}{d} - \tan^{-1}\frac{\ell_j}{d}\right)\right)\right] \qquad (4.111)$$

where d is the distance defined by the normal from the base point to the boundary element tangent.

When the node i of the base point coincides with the node j of the field point on an element e, the boundary integrals are given by

$$A^e_{i,i} = -\theta/2 \qquad (4.112)$$

$$A^e_{i,j+1} = o \qquad (4.113)$$

$$B^e_{i,i} = -\frac{1}{4L_e}\left[L_e^2(\mathrm{Ln}\, L_e^2 - 1) - 4L_e^2(\mathrm{Ln}\, L_e - 1)\right] \qquad (4.114)$$

$$B^e_{i,j+1} = \frac{1}{4L_e}\left[L_e^2\,(\mathrm{Ln}\, L_e^2 - 1)\right] \qquad (4.115)$$

Similarly, when the node i coincides with the node j+1, the boundary integrals are given by the above equations with

$$A^{e}_{i,j} = A^{e+1}_{i,j},\ A^{e}_{i,i} = A^{e+1}_{i,i},\ B^{e}_{i,j} = B^{e+1}_{i,j+1} \text{ and } B^{e}_{i,i} = B^{e+1}_{i,i}.$$

4.3.5.2 Domain Integrals

The domain integral involved is given by equation (4.102). This integral can be evaluated numerically using a seven points quadrature scheme. The domain integral of equation (4.102) can be approximated by the summation

$$DI = \int_0^1 \left[\int_0^{1-\eta_2} f(\eta_1,\eta_2,(1-\eta_1-\eta_2)\, d\eta_1 \right] d\eta_2$$

$$= \tfrac{1}{2} \sum_{i=1}^{n} W_i\, f(\eta_1^i,\eta_2^i,\ (1-\eta_1^i-\eta_2^i)) \qquad (4.116)$$

where W_i is a weighting factor, (η_1^i, η_2^i) are the coordiantes of the i^{th} integration point and n is the total number of integration points.

4.3.6 Solution of Algebraic Equations

The system of algebraic equations resulting from the boundary element approximation can be solved by separating the known and unknown boundary values and form the following system

$$[\Lambda]\ \{\chi\} = \{\xi\} \qquad (4.117)$$

where $[\Lambda]$ is a fully populated NXN coefficient matrix derived from [A] and [B], $\{\chi\}$ is a NX1 vector containing the unknown boundary values and $\{\xi\}$ is compiled from the known information as a NX1 vector. This system of equations can be solved by using Gaussian elimination scheme.

4.4 Treatment of Discontinuity Problems

4.4.1 Treatment of Corners

In most practical problems discontinuities arise in the geometry and boundary conditions in the form of edges and corners. Rounding off edges and corners (Jaswon and Symm, 1977) cannot be considered a satisfactory solution to the problem since the results, even at some distance away from the rounded corners, must be affected.

If linear elements are used, the head will be uniquely defined but its normal derivatives will be multivalued at a corner node. This means that if the head H is specified at a corner node there will be two unknown fluxes at that node. One obvious approach to solve this indeterminacy of a Dirichlet problem is to assume that the corresponding unknown fluxes q_a and q_b, before and after the node, are equal, that is $q_a = q_b$. Lachat and Watson (1976) have found that the inconsistencies arising from this approach are important only in the case of sharp corners and the errors involved are mainly confined to the corners and are not significant even at points close to them.

In order to eliminate the ambiguities associated with a sharp corner node, Brebbia and Dominguez (1977) used a multiple independent node concept. In this approach, for two dimensional problems, two nodes are used in every sharp corner. The results are better than those previously obtained, however, this technique has the major drawback of being a potential source of instability unless a sufficient gap is left between the corner nodes so that the equations for them are really independent. Furthermore the multiple node solution also increases artificially the number of equations to be solved. A somewhat different multiple node concept was proposed by Alarcon et al (1978) who derived an additional set of equations to supplement the corner node

equation. For a Dirichelt problem, at a corner node the normal derivatives of the known head H can be expressed as

$$q_a = -T \frac{\partial H}{\partial X_i} n_{ai} = q \cos\alpha_a \qquad (4.118a)$$

$$q_b = -T \frac{\partial H}{\partial X_i} n_{bi} = q \cos\alpha_b \qquad (4.118b)$$

where q is the gradient modulus at the corner and α_a and α_b are the angles between the gradient and the boundary normals n_a and n_b respectively before and after the node as shown in Fig. (4.6). If the direction cosines of this dummy gradient are known the only remaining variable to be determined is q.

The gradient direction is obviously parallel to the vector $m = \left[\frac{\partial H}{\partial X_i}, \frac{\partial H}{\partial X_2}\right]$, it can therefore be calculated from the assumed linear distribution of the potential head H. If (i-1), (i) and (i+1) are there consecutive nodes where (i) is the corner node under consideration, the gradient of the plane defined by them can be calculated by using the relationship between the Cartesian and oblique coordinates as shown in Fig. (4.6). If these three nodes form a cell, the head H at any point in the defined plane can be expressed by Eq. (4.47), so that its spatial derivatives are given by

$$\frac{\partial H}{\partial X_1} = \frac{1}{2A} [H_{i+1}\beta_1 + H_{i-1}\beta_2 - H_i(\beta_1+\beta_2)] \qquad (4.119a)$$

$$\frac{\partial H}{\partial X_2} = \frac{1}{2A} [H_{i+1}\gamma_1 + H_{i-1}\gamma_2 - H_i(\gamma_1+\gamma_2)] \qquad (4.119b)$$

where

$$\beta_i = X_2(j) - X_2(k)$$

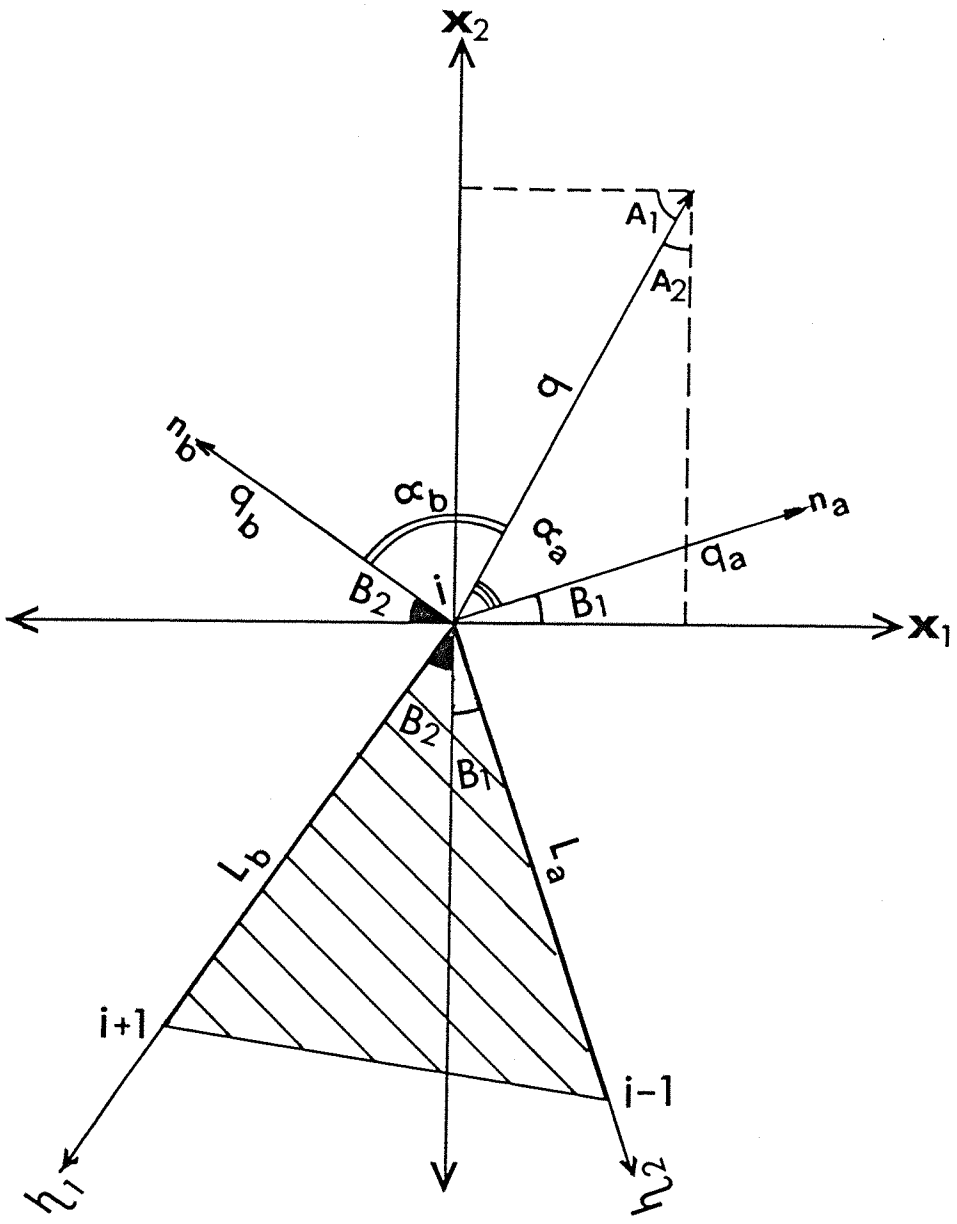

$$\cos\alpha_a = \cos(A_1 - B_1)$$

$$\cos\alpha_b = \cos(A_1 - B_2)$$

Fig. 4.6 The dummy gradient q at a corner point

$$\gamma_i = X_1(k) - X_1(j)$$

$$A = \text{area of triangle} = \tfrac{1}{2}(\beta_1\gamma_2 - \beta_2\gamma_1)$$

and $i = 1,2$ for $j = 2,3$ and $k = 3,1$

From the direction specified by Eq. (4.119a,b) and the known directions of the unit normals $\underset{\sim}{n}_a$, $\underset{\sim}{n}_b$, $\cos\alpha_a$ and $\cos\alpha_b$ can be evaluated. Thus the problem becomes determinate since it involves only one unknown, the dummy variable q at the corner.

4.4.2 Treatment of Zones

As formulated up to this point the boundary element solution applies to the flow of one liquid (fresh water) in a homogeneous and isotropic porous media. In groundwater problems where the aquifer is not homogeneous and/or involving two liquids (fresh and salt water), the problem domain is often divided into zones where the properties of the medium and the liquids are specified over these zones.

In fact the formulated solution is modular and could be extended to solve these problems by applying the formulated solution to the different zones. This can be illustrated by considering a domain divided into two zones or more such as shown in Figure (4.7). The potential is continuous across the dividing boundary Γ_D.

Thus,

$$H_1 = H_2 \text{ on } \Gamma_D \tag{4.120}$$

Across any element on the dividing boundary the amount of fluid leaving Zone 1 must equal the amount of fluid entering Zone 2. Thus,

$$T_1 \frac{\partial H_1}{\partial n} = - T_2 \frac{\partial H_2}{\partial n} \tag{4.121}$$

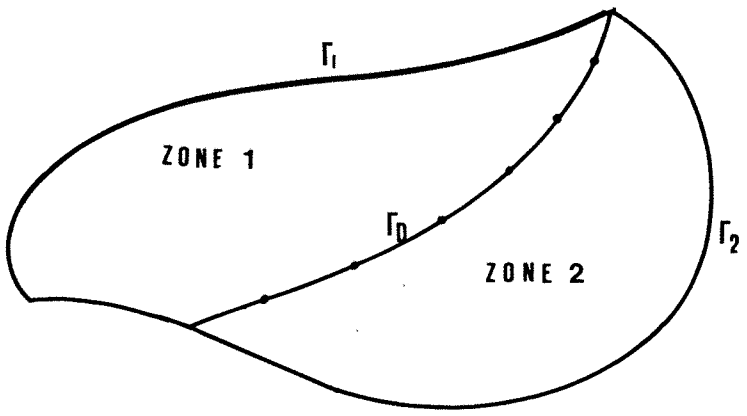

Fig. (4.7) A two-zone domain

Equations (4.120) and (4.121) form the compatibility equations and are used to supplement the formulated solution. Suppose that Zone 1 has N_1 boundary nodes, Zone 2 has N_2 boundary nodes, and there are M nodes on the dividing boundary. There is one equation and one unknown for each boundary node; on the dividing boundary each node has two unknowns and equations (4.120) and (4.121) are available. Thus the entire system can be assembled into an $N_1 + N_2 + 2M$ set of equations and unknowns. The solution of these equations completes the specification of the boundary data, and both H and $\partial H/\partial n$ are then known along the exterior and interior boundaries. Subsequent solutions for interior points need only consider one zone at a time.

The same idea can be extended to any number of zones in which case the total number of equation becomes $\sum N_i + 2\sum M_i$, where N_i is the number of exterior nodes on the i^{th} zone M_i is the number of nodes on i^{th} interior boundary.

CHAPTER 5

COMPUTER IMPLEMENTATION OF THE BOUNDARY ELEMENT MODEL

5.1 Introduction

5.2 Input Data Section
- 5.2.1 Implementation of Spatial Discretization
- 5.2.2 Specification of Boundary Conditions
- 5.2.3 Specification of Parameters and Coefficients

5.3 The Boundary Element Solver
- 5.3.1 Evaluation of Integrals
- 5.3.2 Assembly of Equations
- 5.3.3 Solution of Equations
- 5.3.4 Interior Solutions

5.4 The Computer Program "SABEM"
- 5.4.1 Program Description
- 5.4.2 Sample Problems

CHAPTER 5

COMPUTER IMPLEMENTATION OF THE BOUNDARY ELEMENT MODEL

5.1 Introduction

The full potential of a numerical method, no matter how powerful or elegant, cannot be realized unless the computer implementation is programmed efficiently. In fact, there is a wide gap between the first generation of boundary element programs, illustrated in the literature, and those required to solve complex problems of real physical systems. The available boundary element programs are mainly developed to solve simple problems in the process of introducing the method to the world of engineering problems.

However, these programs present the basic principles involved in developing computer implementation of boundary element solutions. There is no doubt that, over the next few years, research effort and further development and application of the boundary element method will lead to a wealth of efficient programs. The author hopes that the endeavour presented herein will contribute to the application of the method in the field of aquifer systems modelling.

5.2 Input Data Section

5.2.1 Implementation of Spatial Discretization

Spatial discretization of the solution domain is required to perform the boundary and domain integration developed in Chapter 4. Spatial discretization is

implemented by computer in the input data section of the program. The implementation scheme is developed such that large physical systems could be handled with the advantage that the input data defining the geometry of a system is generated internally with minimum effort from the user.

The boundary geometry of a system is defined in the input data section by specifying the number, (NCR), and the corordinates (CRX1(I),CRX2(I), I=1,2,...,NCR), of the corner points where geometrical change in directions and change in boundary conditions take place. The boundary geometry defined by the corner points comprises essentially a number of boundary sides equal to the number of corner points, (NCR). The solution, as formulated in Chapter 4, involves subdividing the boundary into linear elements. Thus, the number of boundary elements on each side should be specified in the input data. The boundary elements are generated by setting boundary nodes on each side. Obviously, the number of boundary nodes, (NSN(I)), required to subdivide a boundary side into a certain specified number of elements, (NSE(I)), is given by

$$NSN(I) = NSE(I)-1 \quad , \quad (I=1,2,...,NCR) \tag{5.1}$$

The coordinates of the boundary nodes are calculated by interpolation between the coordinates of the corner points. Actually, the corner points are also boundary nodes in common with the boundary sides. Considering the treatment of corner problems, as explained in Chapter 4, each corner point is represented in the model by a double node point. Thus, the total number of boundary nodes, (TNBN), i.e. the number of unknowns and also the number of equations to be solved is given by

$$TNBN = 2NCR + \sum_{I=1}^{NCR} (NSE(I) -1) \tag{5.2}$$

the above explained algorithm leaves the boundary of the domain discretized into a total number of boundary elements, NBE, equal to

$$NBE = \sum_{I=1}^{NCR} NSE(I) \qquad (5.3)$$

The boundary nodes, defined by their coordinates, and the boundary elements, defined by consecutive pairs of nodes, are then numbered in anticlockwise direction and stored in common arrays.

Internal discretization of the domain is also required to perform the integration over the domain. Discretization of the domain into triangular integration cells is implemented in the input data section of the program by means of an automatic mesh generation scheme. The mesh is generated by selecting a central point such that the boundary sides around that point are sufficiently convex in order that the lines connecting the central point to the corner point do not fall outside the domain. The central point in the developed scheme is selected at the midpoint of the longest chord between corner points. Coordinates of the central point, (COX1, COX2), are calculated by interpolation between the coordinates of the corner points. Lines are then extended from this point to each of the corner points dividing the domain into a number of triangular segments equal to the number of boundary sides. The lines connecting the central point to the corner ones are then divided into a number of equally spaced divisions (NDIV). The number of division points, (NDP), required to divide a connecting line into a certain specified number of divisions is given by

$$NDP = NDIV - 1 \qquad (5.4)$$

The central point is then used as the origin of the natural coordinate system for each triangular segment. Using the local natural coordinate system each triangular segment is

discretized into a number of triangular cells. The number of triangular cells, (NDBE), generated by this process is given by

$$NDBE = NCR*(NDP)^2 \qquad (5.5)$$

The number of cells generated along each of the boundary sides depends on the number of boundary elements on the side and the number of division points expressed by equation (5.4). Thus, including the cells generated along the boundary sides the total number of the internal cells (TNDBE) is given by

$$TNDBE = NDBE + \sum_{I=1}^{NCR} (NSE(I)+NDP) \qquad (5.6)$$

These cells are defined by the local coordinates of the generated internal nodes which form the apices of these triangles. Using the relationship between the global coordinate system and the local one as presented in Chapter 4 (equations (4.44), (4.45) and (4.46)). The coordinates of the internal nodes in the (X_1,X_2) plane can be calculated. Once the coordinates of internal nodes are calculated, each internal cell is defined by the coordinates of the triangle apices forming the cell. The cells are numbered and the coordinates defining each cell are stored in common arrays. A sample output of the automatic discretization scheme is shown in Figure (5.1).

5.2.2 Specification of Boundary Conditions

Three types of boundary conditions can be specified in the model; prescribe potential, prescribed flux and mixed boundary conditions. The type of boundary conditions at each boundary node is specified in the input data by using an identification code, (NCOD(J), J=1,2,...,TNBN), for each node of the total number of boundary nodes defined by equation (5.2). The NCOD(J) is expressed as

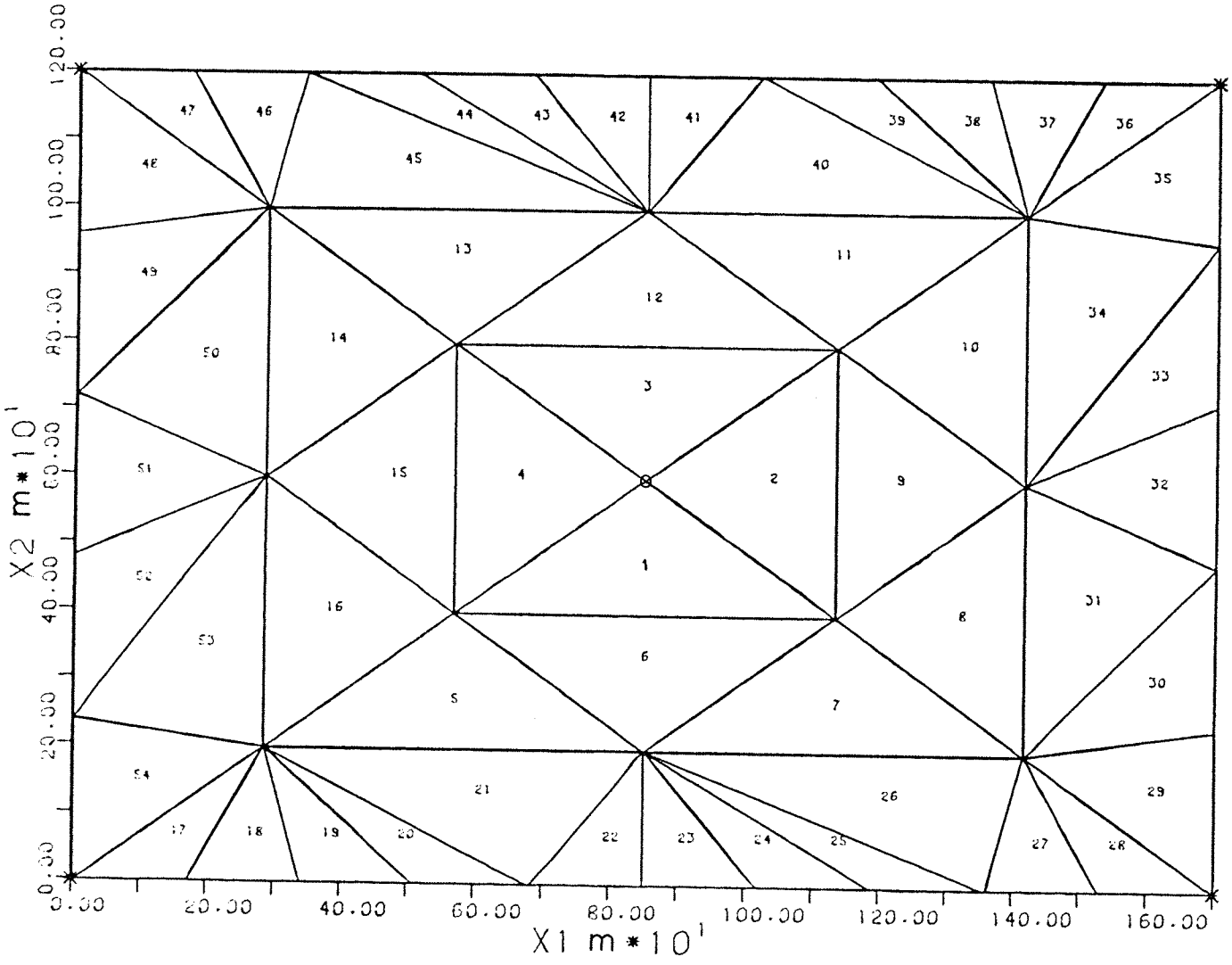

✳ corner point

⊗ central point

Fig. 5.1 SAMPLE OUTPUT

AUTOMATIC GENERATION OF BOUNDARY AND DOMAIN ELEMENTS

NCOD(J) = 1 if H is known and ∂H/∂n is to be computed
NCOD(J) = 2 if ∂H/∂n is known and H is to be computed
NCOD(J) = 5 if a linear combination of H and ∂H/∂n is specified

The identification code is also used to designate corner nodes. At a corner point the potential H will be uniquely defined but its normal derivative ∂H/∂n will be multivalued. Therefore, a corner point is represented by two nodes where the type of boundary conditions, approaching the point, is assigned to the first node and the type of boundary conditions, leaving the point, is assigned to the second node. A corner node is identified in the following way

NCOD(J) = 1 and NCOD(J+1) = 3

If H is prescribed when approaching the corner and ∂H/∂n is prescribed when leaving the corner

NCOD(J) = 4 and NCOD(J+1) = 1

If ∂H/∂n is prescribed when approaching the corner and H is prescribed when leaving the corner.

NCOD(J) = 1 and NCOD(J+1) = 15

If H is prescribed when approaching the corner and a mixed boundary condition is prescribed when leaving the corner

NCOD(J) = 51 and NCOD(J+1) = 1

If a mixed boundary condition is prescribed when approaching the corner and H is prescribed when leaving the corner.

NCOD(J) = 2 and NCOD(J+1) = 25

If $\partial H/\partial n$ is prescribed when approaching the corner and a mixed boundary condition is prescribed when leaving the corner

NCOD(J) = 52 and NCOD(J+1) = 2

If a mixed boundary condition is prescribed when approaching the corner and $\partial H/\partial n$ is prescribed when leaving the corner.

Prescribed values of the boundary conditions at each node are stored in arrays where the unknown boundary data is set to zero. These arrays are part of the basic input data to the model.

5.2.3 Specification of Parameters and Coefficients

The basic input data required to implement the model involves specification of parameters and coefficients which are related to the physical system. If a third type boundary condition is prescribed, then, three arrays, containing nodal values for the wetted perimeter of the canal, canal section property and the hydraulic resistance of the seepage surface, should be specified.

Obviously, hydraulic parameters of the aquifer; transmissivity and storativity, should be specified in the input data. The time step and the number of time steps required for the transient solution should also be included in the input data file. Point sources and/or sinks are specified by their values and coordinates. Any distributed excitation over the domain is specified by its strength over the generated internal cells.

5.3 The Boundary Element Solver

5.3.1 Evaluation of Integrals

In order to construct the matrices for the global system of equations explained in Chapter 4, it is necessary to evaluate the spatially discretized boundary and domain integrals for both the steady state and the transient flow conditions.

The steady state boundary integrals, (A1(I,J), A2(I,J), B1(I,J) and B2(I,J), I=1,2,...,NBE and J=1,2,...,NBE), are calculated analytically using the expressions derived in Chapter 4; equations (4.107), (4.108), (4.110) and (4.111). The boundary integrals for transient flow conditions, (A1T(I,J), A2T(I,J), B1T(I,J) and B2T(I,J), I=1,2,...,NBE and J=1,2,...,NBE), defined by equations (4.39) are evaluated numerically using expression (4.61).

The domain integral involved in the steady state solution (TDI(I), I=1,2,...,NBE), is defined by equation (4.102). The domain integrals involved in the transient flow solution, (TOTDI(I), I=1,2,...,NBE), are defined by equation (4.54). These integrals are evaluated numerically for both flow conditions using equation (4.70).

5.3.2 Assembly of Equations

Once the boundary and domain integrals are evaluated the global coefficient matrices can be constructed. For the steady state conditions the global coefficient matrices are constructed once whereas for transient flow conditions they are constructed for each time step. Assembly of equation is achieved by separating the known and unknown components of the nodal vectors {H} and {∂H/∂n}.

For the steady state solution the known information is compiled by multiplying the appropriate columns of [A1,A2] and [B1,B2] by the prescribed boundary values of {H} and {∂H/∂n}. The result is then added to the known terms of equation (4.105) to form the vector of known information {XI}. The unknown boundary values of H and ∂H/∂n are contained in the vector {CHI} and the coefficient matrix of these unknowns [ALPHA], is formed form the appropriate columns of [A1,A2] and [B1,B2]. The following system of equations is then formed

$$[ALPHA]\ \{CHI\} = \{XI\} \qquad (5.7)$$

For the transient flow solution the same process of separating the known and unknown components of the nodal vectors is repeated for each time step. The following system of equations is also formed

$$[ALPHAT]\ \{TCHI\} = \{TXI\} \qquad (5.8)$$

where [ALPHAT] is coefficient matrix of unknowns derived form [A1T,A2T] and [B1T,B2T], {TCHI} is the vector containing the unknown boundary values and {TXI} is the vector of known information compiled as described above and including the known right-hand terms of equation (4.59). The major part of computational work in the transient flow solution is in setting up the system of equations. This can be considerably reduced by using a uniform time step so that the global coefficient matrices are calculated for the first and then used for each subsequent time step.

5.3.3 Solution of Equations

The system of equations (5.7) and (5.8) can be solved by using a Gaussian elimination scheme for a fully populated andasymmetric coefficient matrix. The extended Gaussian scheme known as Gauss-Jordan elimination is used to solve

the equations. The solution yields the unknown nodal values of H and $\partial H/\partial n$ on the boundary.

5.3.4 Interior Solutions

Once all the boundary data is known it is possible to calculate the potential at the interior nodal points. This is achieved by back substitution in the main boundary element equation using the interior nodes as fixed base points. However, the process involves evaluation of the boundary and domain integrals with respect to the interior nodal points. These integrals are evaluated in the same way mentioned above.

5.4 The Computer Program "SABEM"

5.4.1 Program Description

The computer program, which is called "SABEM", is developed to implement the Stream-Aquifer Boundary Element Model. SABEM is designed to solve the equations of two-dimensional groundwater flow in homogeneous and isotropic aquifer for steady and transient conditions. The solution domain is essentially a closed one and may have arbitrary shape. The boundary conditions may be of the first type, second type, third type, or a mixture of them. The program is written in standard FORTRAN 77 and operated on a VAX-MS machine. The macro-flow chart of the program is shown in Figure (5.2).

SABEM consists of a main program and twenty three subroutines. The following twelve subroutines are called from the main program.

- SUBROUTINE BEIDAT forms the input data section where the basic input data is read into it. Five subroutine are called from BEIDAT to perform the automatic generation of

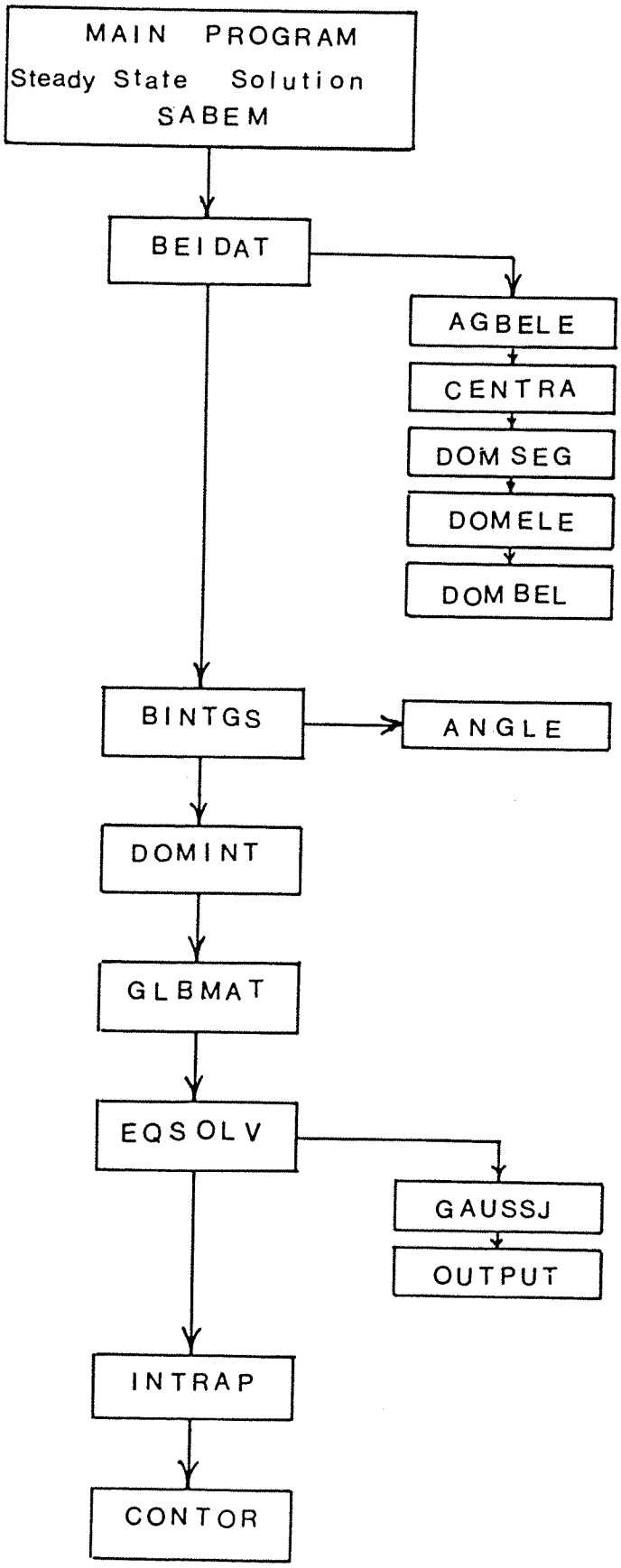

Fig. 5.2a Macro-Flow Chart

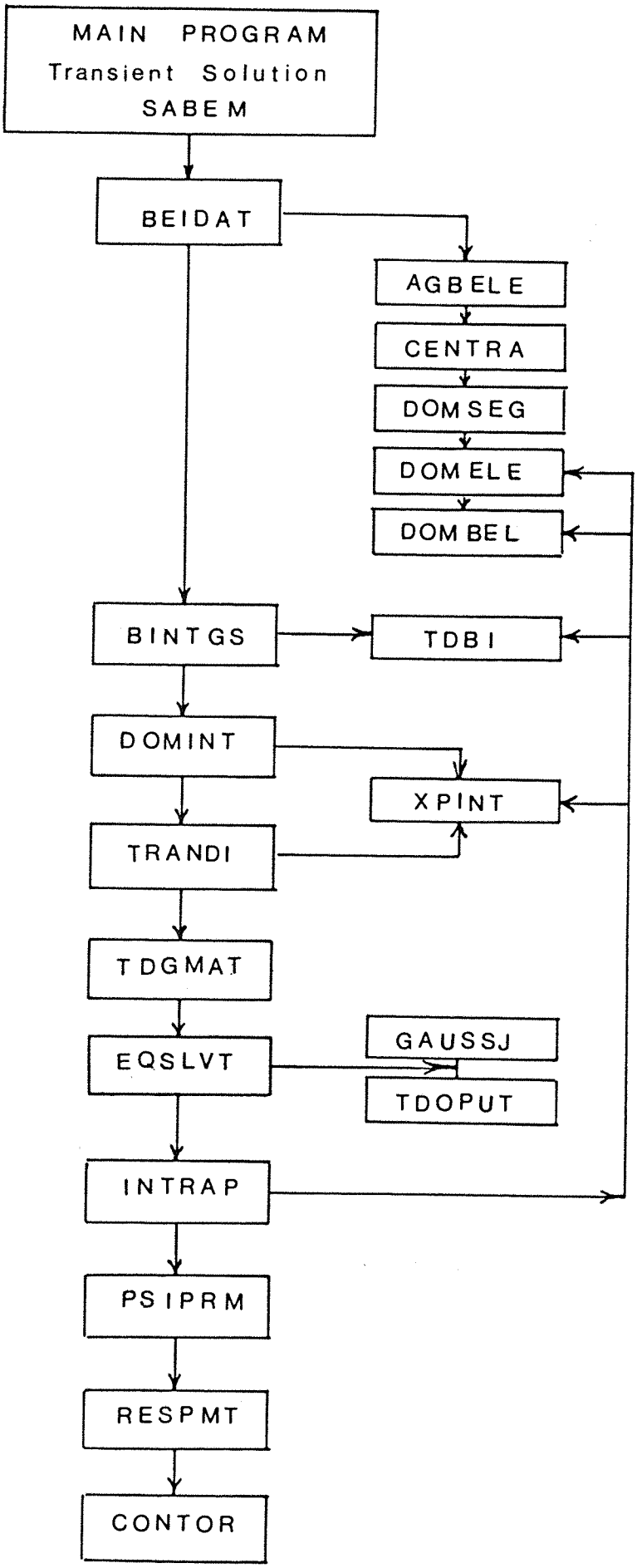

Fig. 5.2b Macro_Flow Chart

boundary elements and domain integration cells. Namely, Subroutine AGBELE to implement the automatic generation of boundary elements, Subroutine CENTRA to locate the central point, Subroutine DOMSEG to construct the domain segments and generate the domain internal nodes, Subroutine DOMELE to set the coordinates of the domain internal cells, and Subroutine DOMBEL to set the coordinates for the domain cells generated along the boundary.

- SUBROUTINE BINTGS calculates analytically the boundary integrals for steady state conditions. The process includes calling a subroutine named ANGLE which calculate the angle enclosed by the boundary at the base point. If the transient flow solution is required then Subroutine TDBI will be called from BINTGS to evaluate numerically the boundary integral for the time dependent solution.

- SUBROUTINE DOMINT evaluates the domain integrals for steady state flow conditions. If the problem is a time dependent one, existing point sinks and/or sources and distributed input to and output from the system, will be integrated over the domain. In this case Subroutine XPINT will be called to evaluate the exponential integrals.

- SUBROUTINE GLBMAT forms the global matrices and the system of algebraic equations for steady state conditions.

- SUBROUTINE EQSOLV solves the system of equations for steady state conditions by calling Subroutine GAUSSJ which performs the Gauss-Jordon elimination. The calculated unknown nodal values are then assigned to their nodes and the complete boundary data is stored in an output file by calling Subroutine OUTPUT.

- SUBROUTINE INTRAP performs the interior solutions and calculates the potential at the interior nodal points for steady state or transient solutions. Subroutine TDBI is

called to evaluate the time dependent boundary integrals using the internal nodes as fixed base points. Subroutine XPINT is called to evaluate the expotential integrals involved in evaluating the time dependent domain integrals. Subroutines DOMELE and DOMBEL are also called to set the calculated potentials at the internal nodes as initial conditions for the next time step.

- SUBROUTINE TRANDI evaluates numerically the time dependent domain integrals for the unit sink introduced into the system during the first time step to calculate the response coefficient and interaction parameters. And also evaluates numerically the integration of initial conditions over the domain. Subroutine XPINT is called to calculate the expotential integrals involved in evaluating the domain integrals.

- SUBROUTINE TDGMAT forms the global matrices and the system of algebraic equations for transient flow solution.

- SUBROUTINE EQSLVT solves the system of equations for transient flow solution. Subroutine GAUSSJ is called to perform the Gauss-Jordan elimination. The calculated unknown nodal values are then assigned to their boundary nodes and the complete boundary data at the end of each time step is stored in an output file by calling Subroutine TDOPUT.

- SUBROUTINE PSIPRM calculates the interaction parameters required by the management model and stores them in an output file.

- SUBROUTINE RESPMT formulate the response coefficient matrices required by the management model and stores them in an output file.

- SUBROUTINE CONTOR uses the calculated potential at

the internal nodes from INTRAP to produce a contour map of the groundwater levels. This is performed by linear interpolation between the internal nodes using a specified contour interval.

5.4.2 Sample Problems

In order to illustrate the effectiveness and test the performance of the algorithm discussed here, the solutions of two sample problems are presented. In the first problem, the effect of a discharging well on a nearby stream in a semi-infinite aquifer is analysed. The semi-infinite stream-aquifer system is represented by a block of medium having the configuration shown in Fig. (5.3). For large distances L and W, the domain is essentially infinite. However the computational domain of the problem is made finite by introducing far field artificial boundaries. Thus, the aquifer is bounded by a stream and artificial boundaries of impermeable rocks. The assumptions are made that the transmissivity T and storage coefficient S are constant. Fig. (5.3) shows a well discharging at a rate Q and at a distance a from the stream. The hydraulic head is everywhere zero initially and the boundary conditions are

$$H(X_1,0,t) = 0 \qquad (5.9a)$$

$$\frac{\partial H}{\partial n}\,(L,X_2,t) = 0 \qquad (5.9b)$$

$$\frac{\partial H}{\partial n}\,(X_1,W,t) = 0 \qquad (5.9c)$$

The objective is to find the subsequent variation of the flux $f = -T\,\partial H/\partial n(X_1,0,t)$ along the stream-aquifer boundary with time. The exact solution for this problem is given by Glover (1977) as

$$f\,\frac{a}{Q} = \frac{a^2}{X_1^2+a^2}\,\exp\left[-\frac{(X_1^2+a^2)}{4(T/S)\,t}\right] \qquad (5.10)$$

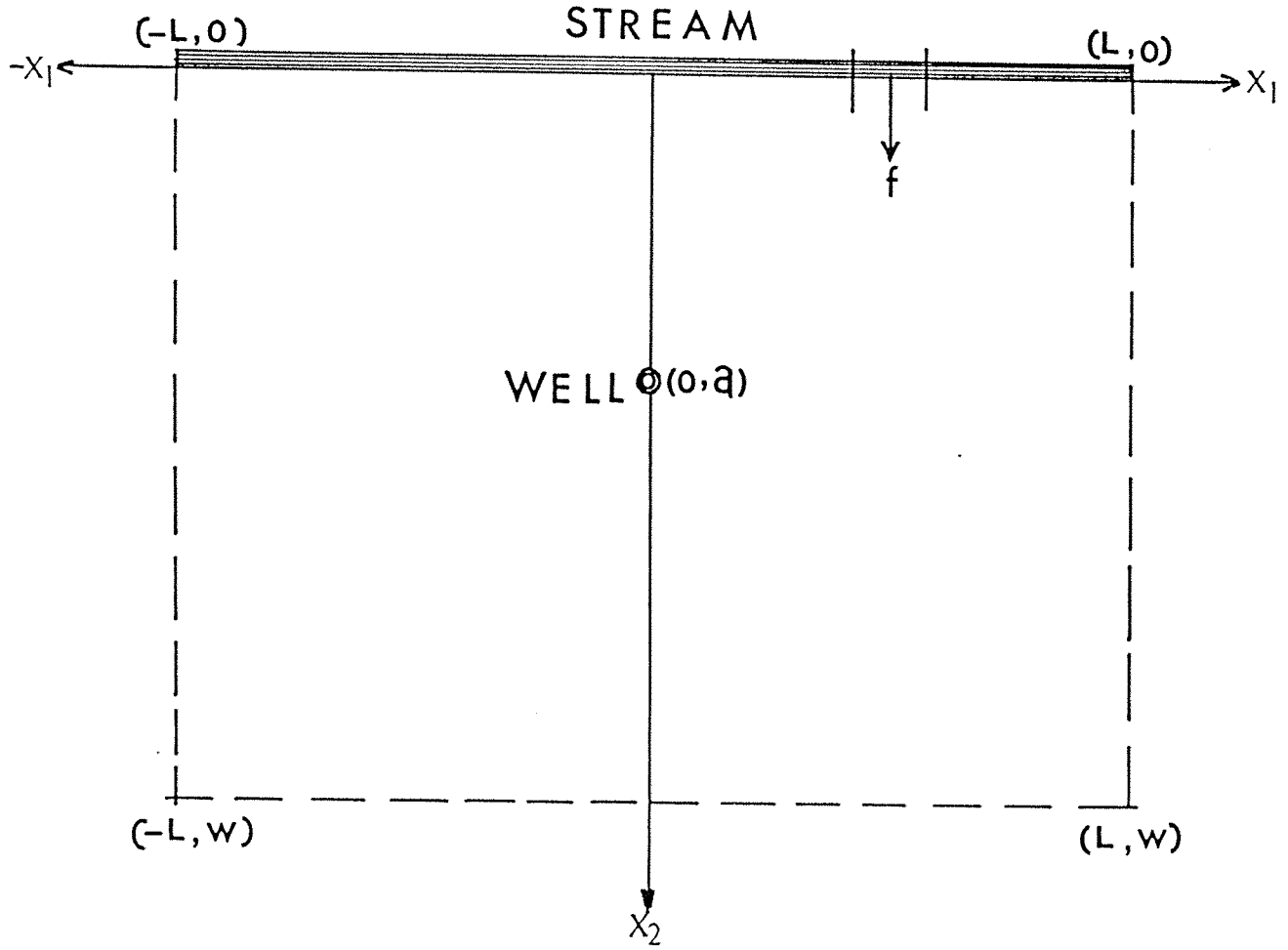

Fig. 5.3 Semi-infinite Stream-Aquifer System

where f is the flux per unit length of the stream boundary. The total flux can be determined by integrating over the whole stream length; in mathematical sense this will vary from $-\infty$ to $+\infty$. The depletion flow will be zero and $t = 0$ and will gradually rise toward Q as time increases. The depletion of the stream by the well, computed in this way is given in Chapter 2 by the expression

$$\frac{q}{Q} = \text{erfc}\ (z) \qquad (5.11)$$

where

$$z = \frac{a}{\sqrt{4(T/S)t}}$$

q is the rate of stream depletion and erfc is the complementary error function.

The problem is solved by the boundary element method to yield results in a general dimensionless form similar to that presented by Glover (1977). The stream boundary is discretized into 40 elements and the problem is solved for seven values of the time parameter z. The results of numerical calculation and the exact solution given by equations (5.10) and (5.11) are shown in Figs. (5.4) and (5. 5) respectively. Very good agreement is observed between the numerical and the exact analytical solutions.

The second problem considers the variation of hydraulic head with time in the vicinity of a discharging well in a rectangular stream-aquifer system. The problem domain is shown in Fig. (5.6). One pair of opposite boundaries are impermeable, the other are held at a head of 50 metres. Constant values of transmissivity $T = 0.1\ m^2/s$ and storage coefficient $S = 0.001$ are assumed. Initially the hydraulic head is 50 metres everywhere. A well discharging at a rate $Q = 0.5\ m^3/s$ is simulated at $X_1 = 1.2L$, $X_2 = 0.6L$ where L is a reference length equal to 1000

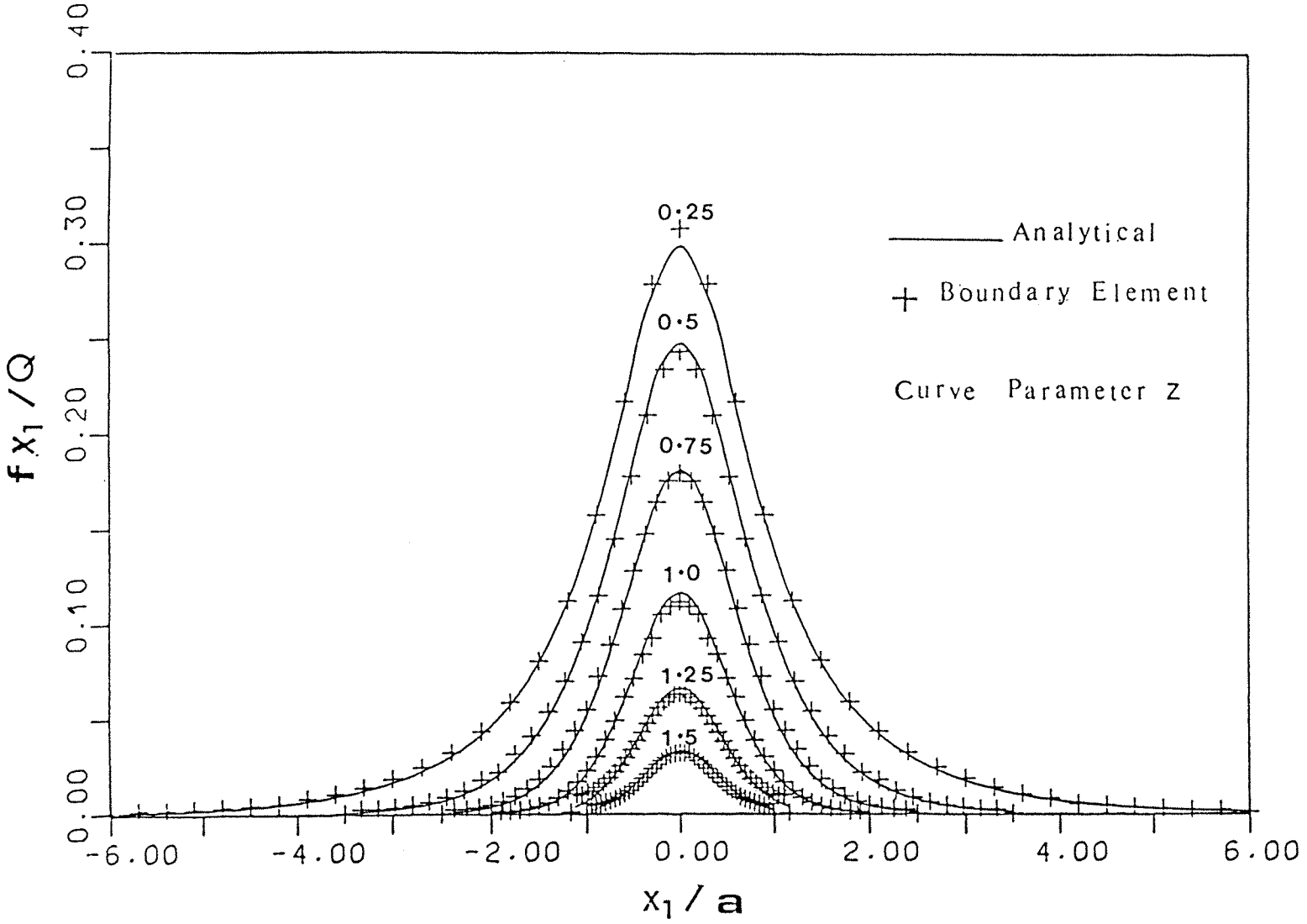

Fig. 5.4 Stream Depletion due to a Well

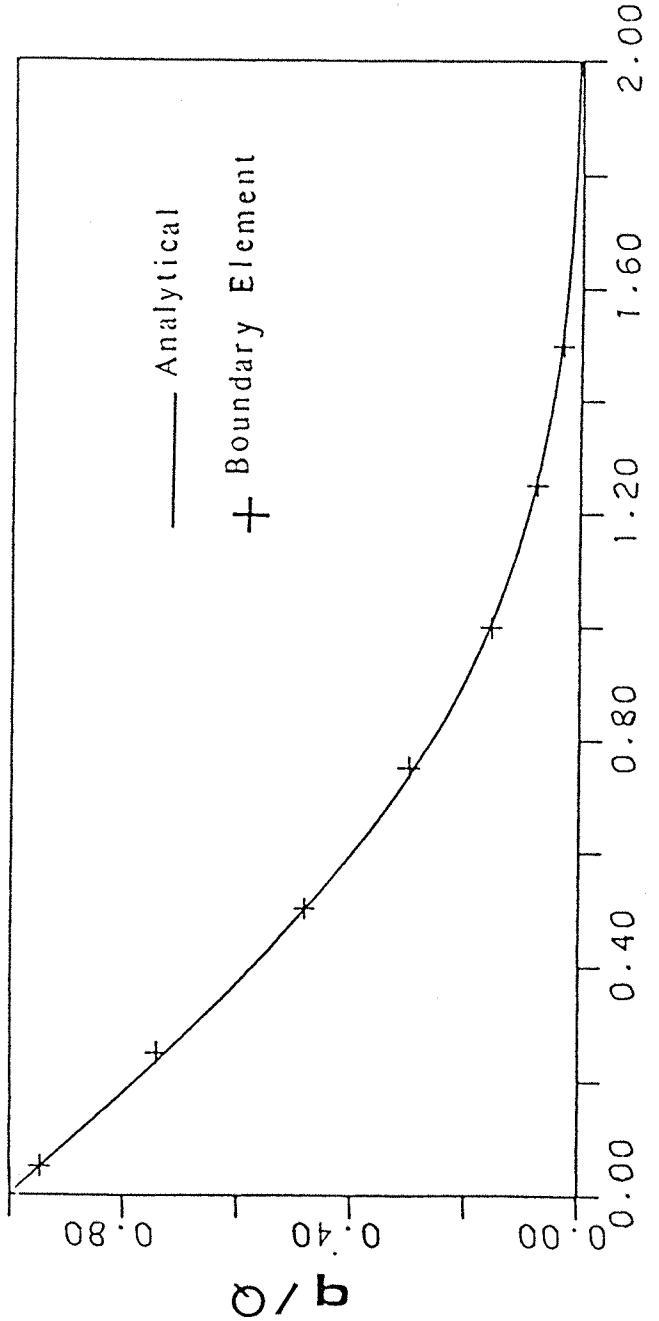

Fig. 5.5 Rate of Stream Depletion

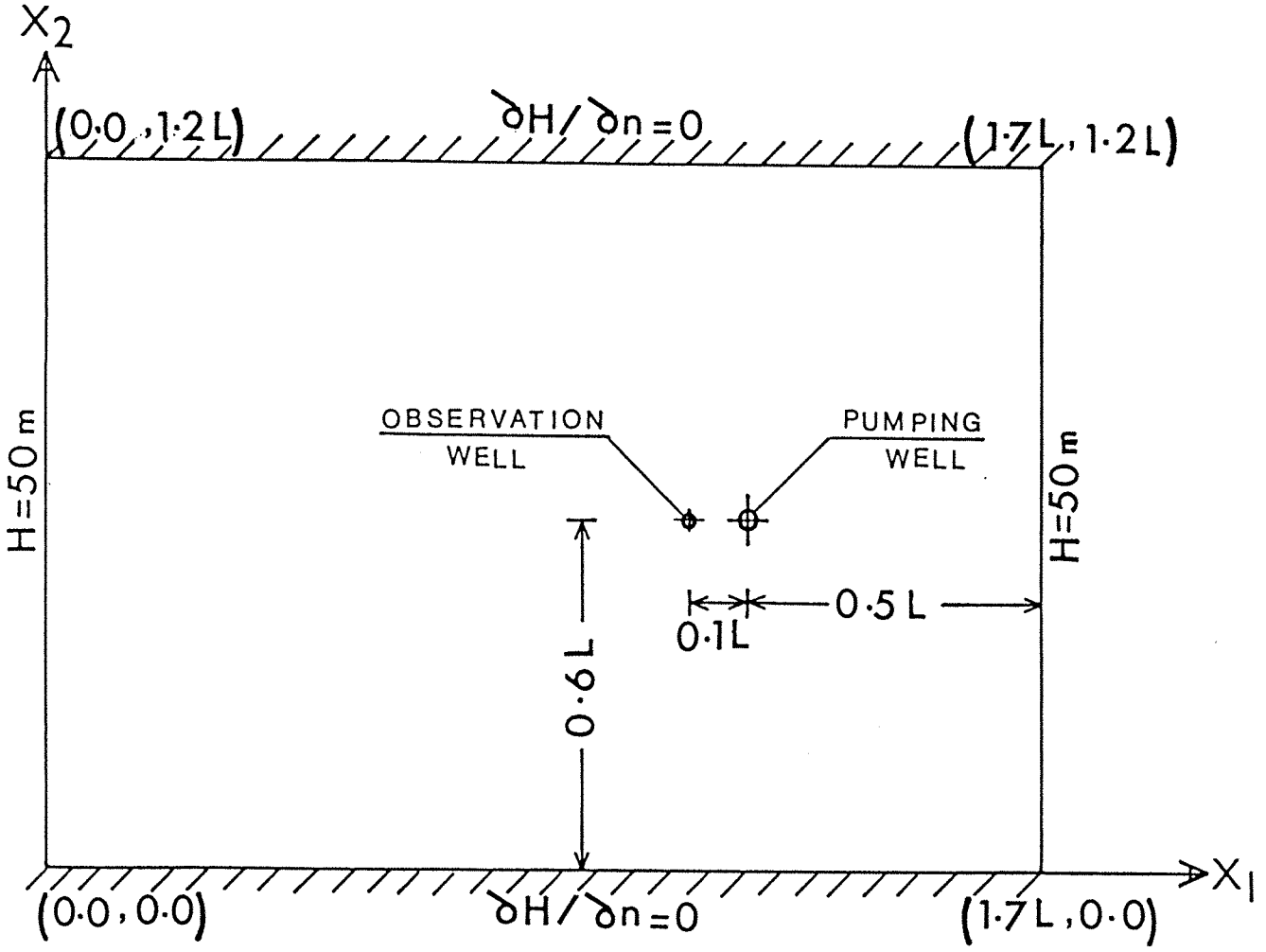

Fig. 5.6 Problem Domain

metres. Drawdowns in hydraulic heads are quoted at an observation well positioned at $X_1 = 1.1L$, $X_2 = 0.6L$.

A solution for this problem by the finite element method using a 35 node grid discretization is given in Kinzelbach (1986). The analytical solution is obtained by using the theory of images and the principle of superposition.

The problem is solved by the boundary element method where each side of the rectangular domain is divided into five elements, making a total of 25 boundary elements. Drawdowns at the observation well are calculated for 12 points on the time scale. The results of the boundary element solution, shown in Fig. (5.7) are in very good agreement with the analytical solution.

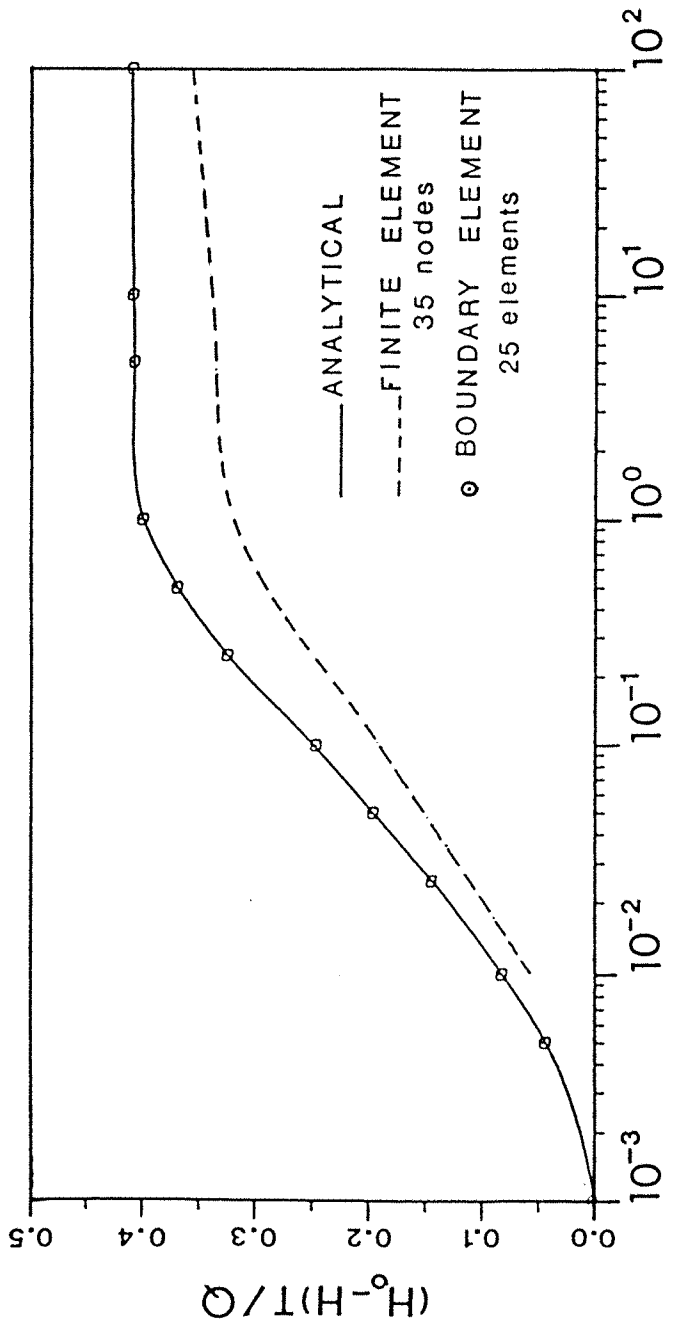

Fig. 5.7 Comparison of Drawdown versus Time

CHAPTER 6

CASE STUDY: THE STREAM-AQUIFER SYSTEM SOUTH-EAST OF THE NILE DELTA

- DESCRIPTION OF SYSTEM -

6.1 Introduction

6.2 Physical Setting
- 6.2.1 Location and Topography
- 6.2.2 Climate
- 6.2.3 Physiography
- 6.2.4 Geology

6.3 Hydrogeology
- 6.3.1 Hydrogeological Setup
- 6.3.2 Regional Flow of Groundwater
- 6.3.3 Quality of Groundwater
- 6.3.4 Salt Water Intrusion

6.4 The Ismailia Canal
- 6.4.1 Existing Conditions
- 6.4.2 Future Development
- 6.4.3 Canal Seepage

CHAPTER 6

CASE STUDY: THE STREAM-AQUIFER SYSTEM SOUTH-EAST OF THE NILE DELTA

- DESCRIPTION OF SYSTEM -

6.1 Introduction

The eastern region of the Nile Delta, map Figure (6.1), is one of the main areas of agricultural development in Egypt. About 30% of the total aimed area of land reclamation in the country are located in this region. Therefore, studies are needed to define the potentiality of aquifer systems in the region and to guide the available groundwater resources towards an optimal development.

The study area is the desert upland which occupies the southern part of this region. The area is bounded on the north and west by one of the major irrigation canals in the country, namely the Ismailia Canal, which cuts through the aquifer and thus forms a typical stream-aquifer system.

Simulation modelling of an aquifer system requires a set of quantitative data which describes physical setting and hydrogeology of the considered system. This set of data for the study area is summarized and presented herein.

6.2 Physical Setting

6.2.1 Location and Topography

The stream-aquifer system south-east of the Nile Delta covers an area of about 2000 square kilometres as shown in map Figure (6.2). The study area is bounded on the north and west by the Ismailia Canal, on the east by the Suez

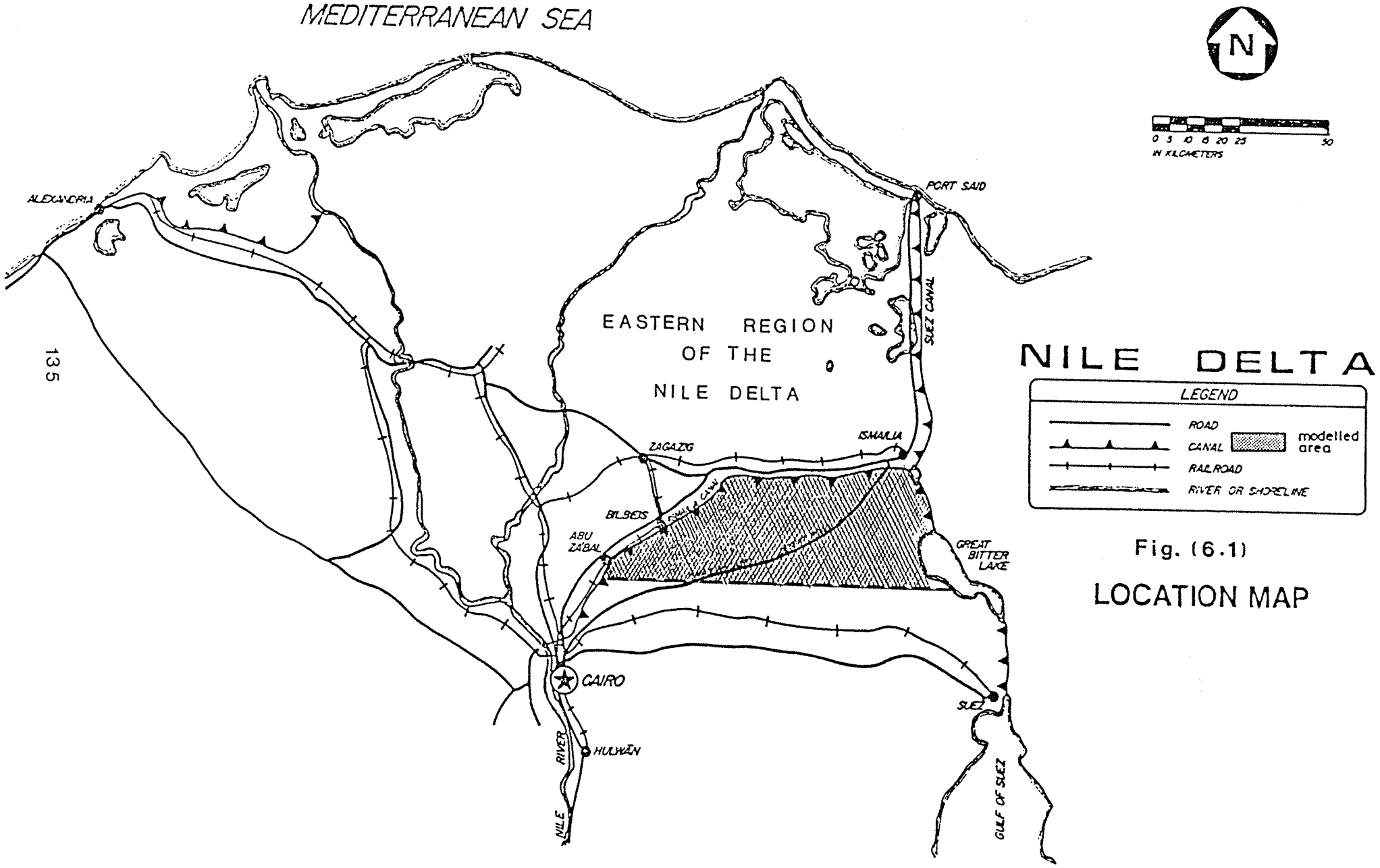

Fig. (6.1)

LOCATION MAP

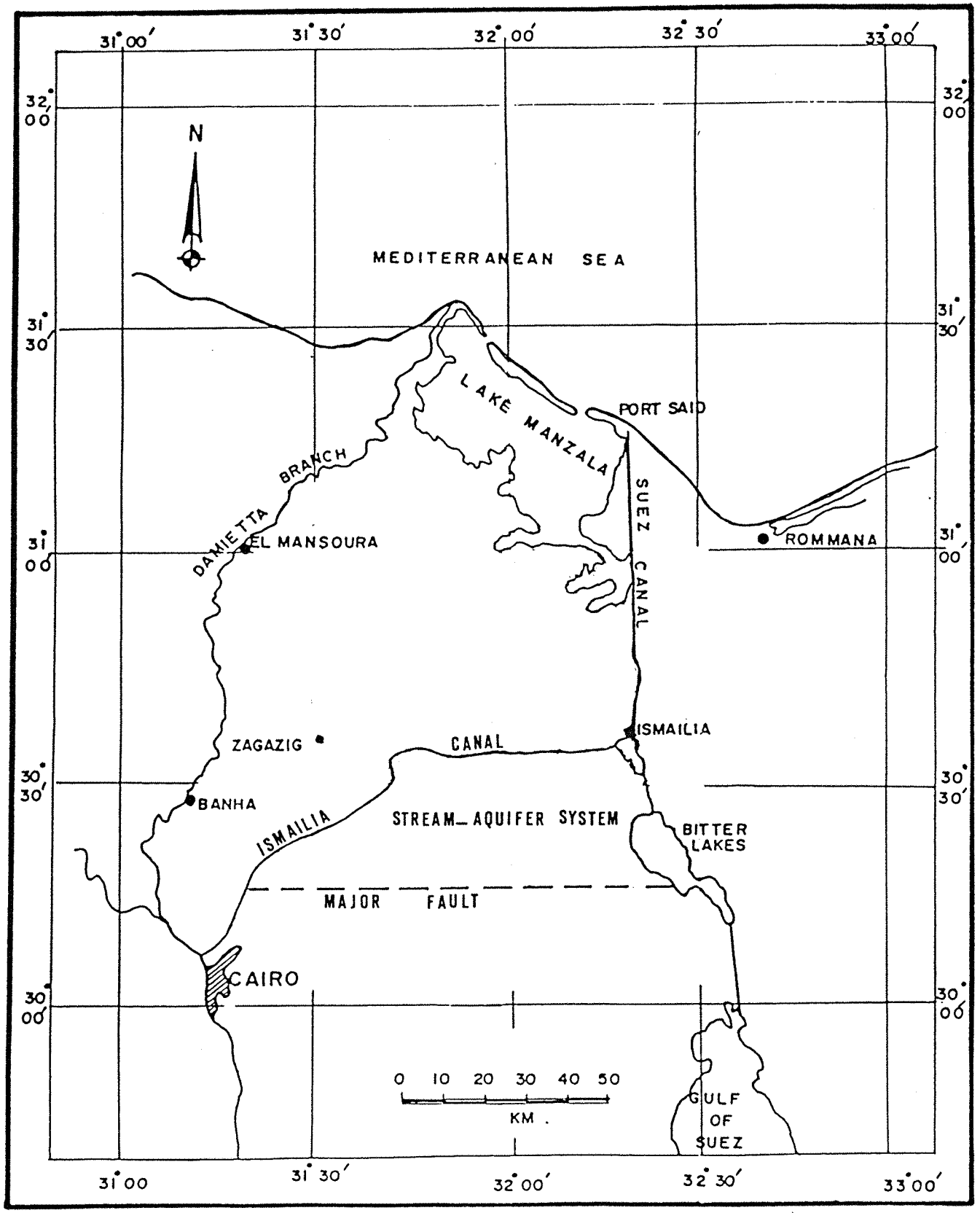

Fig.(6.2) THE STUDY AREA

Canal and the Bitter Lakes and on the south by a major fault which extends west-east direction towards the Bitter Lakes. Ground elevation varies from 12 metres above mean sea level in the vicinity of the Ismailia Canal to 150 metres above mean sea level in the southern part. Contour map of the ground surface in the study area is shown in Figure (6.3).

6.2.2 Climate

The climate of the area is a typical of semi-arid desert. Evaporation figures are high and winds come mainly from north and north-west. Precipitation is a minor factor in the area.

Meteorological data for the cities of Cairo and Ismailia are given in Tables (6.1) and (6.2).

6.2.3 Physiography

The physiographic provinces in the eastern region of the Nile Delta (El. Fayoumy, 1968) are shown in map Figure (6.4). The study area is dominated by the Rolling Plains where the terrain slopes from south to north. This province is traversed by an east-west elongated depression, known as Wadi El-Tumilat, in which the Ismailia Canal was originally dug. The Rolling Plains province is underlain by sandy and gravelly sediments belonging essentially to the old delta of the Nile. The western fringe of the study area is part of the Isthmus Basin which is a continuation of the Red Sea Rift Valley. In this part, the ground elevations is almost at sea level, and the surface is underlain by continental and shallow marine deposits.

6.2.4 Geology

A regional geological map of the eastern region of the Nile Delta is shown in Figure (6.5). The two major tectonic

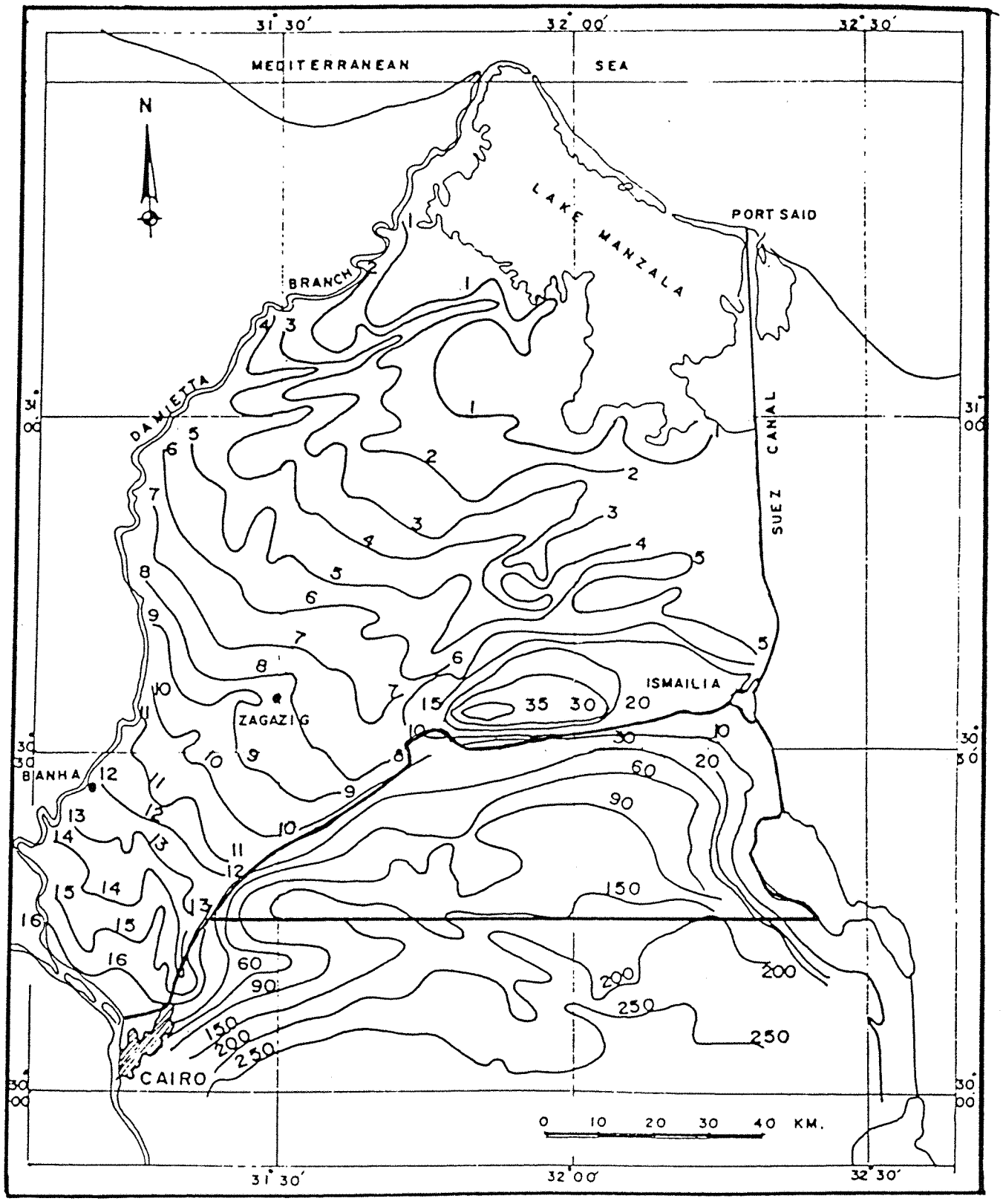

Fig. 6.3 MAP SHOWING THE CONTOUR LINES OF THE GROUND SURFACE IN THE EASTERN NILE DELTA REGION.

Table 6.1 : Meteorological Data - Cairo
Period 1947-1960 (windspeed 1956-1960)

Month	Temperature (°C) max.	min.	mean	Relative humidity (%)	Total sky cover (Oktas) 06.00	12.00	18.00	Mean wind-speed (knots)	Total rainfall (mm)	Evaporation (Piche) (mm/day)
Jan	19.1	8.6	13.7	59	2.9	3.6	1.9	6.7	3.7	7.0
Feb	20.7	9.1	14.9	56	3.0	3.8	2.0	6.9	4.2	7.9
Mar	23.7	11.3	17.3	52	2.9	3.5	1.6	7.4	2.3	10.2
Apr	28.2	13.9	20.9	48	2.7	2.5	1.2	7.7	0.6	12.4
May	32.4	17.4	24.8	44	2.6	2.4	1.6	7.5	0.5	14.6
Jun	34.5	19.9	27.0	48	2.0	0.5	0.2	6.8	0.3	14.6
Jul	35.4	21.5	28.1	52	2.7	0.4	0.1	4.9	0.0	13.4
Aug	34.8	21.6	27.9	56	3.0	0.3	0.1	5.0	Tr	12.1
Sep	32.3	19.9	25.8	58	2.3	1.0	0.2	5.6	Tr	10.8
Oct	29.8	17.8	23.5	58	2.4	2.1	0.8	5.7	0.1	9.7
Nov	25.1	13.9	19.3	61	2.7	3.6	1.4	6.1	3.5	7.3
Dec	20.7	10.4	15.3	64	3.6	4.1	2.1	5.8	8.6	6.1
Total	-	-	-	-	-	-	-	-	23.8	-
mean	28.1	15.4	21.5	55	2.7	2.3	1.1	6.3	-	10.5

Table 6.2: Meteorological Data - Ismailia
Period 1946-1956

Month	Temperature (°C)			Relative humidity (%)			Total sky cover (Oktas)			Mean wind-speed (knots)	Total rain-fall (mm)	Evaporation (Piche) (mm/day)
	max.	min.	mean	06.00	12.00	18.00	06.00	12.00	18.00			
Jan	20.4	8.1	14.2	70	41	66	3.3	4.1	2.2	3.5	4.4	4.7
Feb	21.7	9.1	15.4	68	37	63	3.6	4.3	2.2	4.0	4.7	5.4
Mar	23.9	11.0	17.4	60	33	58	3.6	4.4	2.2	4.7	3.0	6.8
Apr	27.6	13.6	20.6	61	30	56	3.4	3.5	1.3	4.1	1.1	7.0
May	32.1	17.3	24.7	58	26	52	3.4	3.6	2.1	3.8	0.8	9.8
Jun	34.8	20.2	27.5	63	28	56	2.5	1.5	0.2	3.2	0.0	9.7
Jul	36.4	22.2	29.3	68	29	56	2.4	1.0	0.0	3.8	0.0	9.3
Aug	36.5	22.5	29.5	68	31	59	2.7	1.1	0.0	3.5	0.0	8.6
Sep	33.9	20.7	27.3	69	35	65	2.1	1.9	0.2	3.0	0.0	7.5
Oct	30.7	17.8	24.2	70	38	67	2.5	3.0	0.8	3.2	2.2	6.4
Nov	26.6	13.9	20.2	74	43	71	3.1	4.2	1.4	2.6	4.7	4.7
Dec	21.5	10.0	15.8	78	48	72	3.9	4.6	2.3	3.2	8.5	3.8
Total	-	-	-	-	-	-	-	-	-	-	29.4	-
Mean	28.8	15.5	22.2	67	35	62	3.1	3.1	1.2	3.6	-	7.0

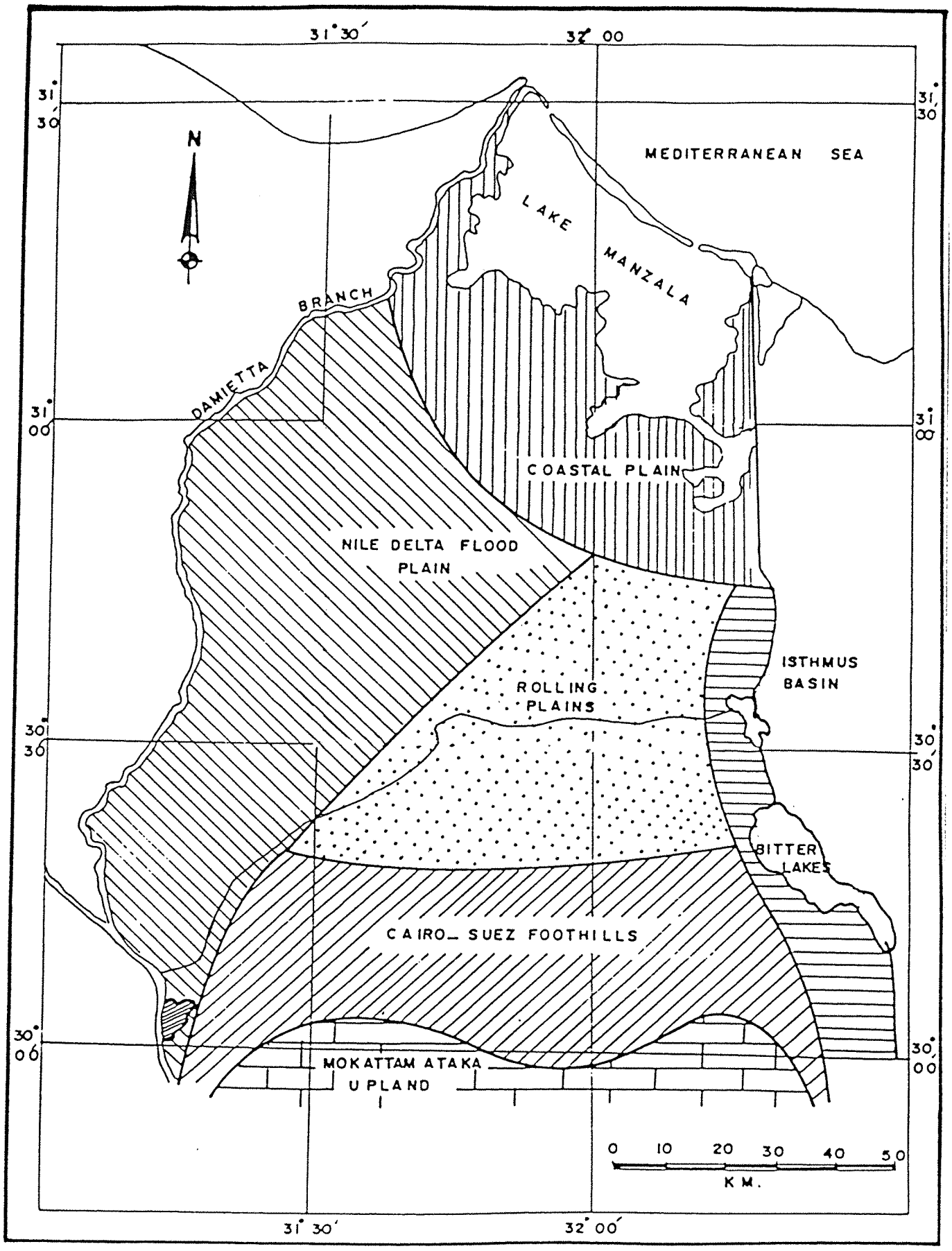

Fig. 6.4 MAP SHOWING THE PHYSIOGRAPHIC PROVINCES OF THE EASTERN NILE DELTA REGION (AFTER EL-FAYOUMY 1968)

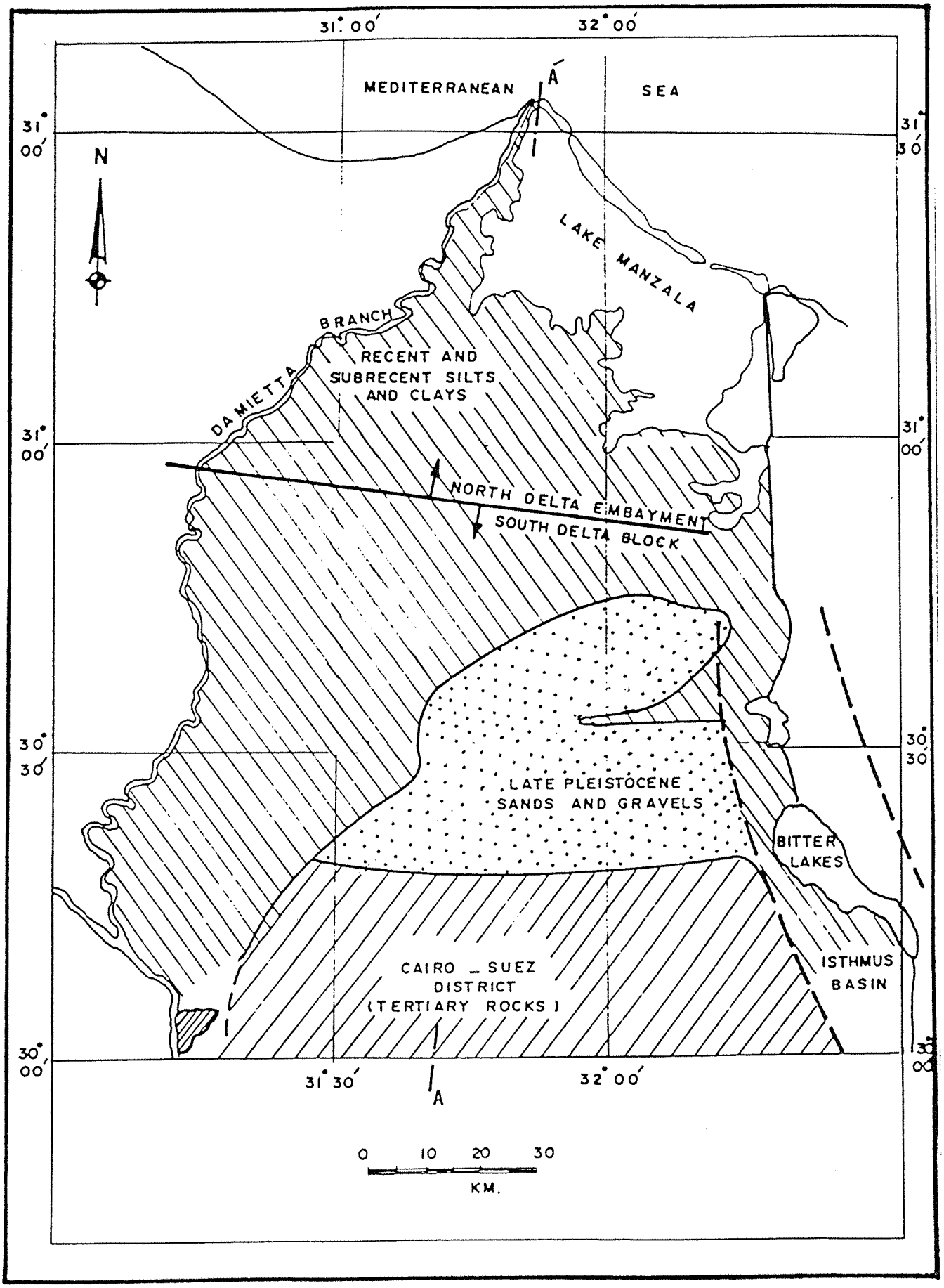

Fig 6.5 MAP SHOWING THE REGIONAL GEOLOGICAL SETTING OF THE EASTERN NILE DELTA REGION.

units in the region are the North Delta Embayment and the South Delta Block. The first unit was affected by the large scale tectonics of the Eastern Mediterranean. The second unit belongs to the stable African platform. An east-west running hinge zone which separates the two units is made up of a series of step faults (Said, 1981).

The study area is part of the South Delta Block. The area is occupied by unconsolidated Quaternary deposits which constitute the major aquifer. It is bounded on the east by part of the Red Sea Rift and on the south by Tertiary rocks outcropping in the Cairo-Suez district. The geological pattern of the region is summarised on the generalized geological profile shown in Figure (6.6).

6.3 Hydrogeology

6.3.1 Hydrogeological Setup

The aquifer in the study area is mainly unconfined and consists of Quaternary sands and gravels. The aquifer is underlain by virtually impervious beds consisting of fine grained Miocene deposits. The aquifer thickness varies from 200 metres in the north to 100 metres in the south. Hydrogeological investigations in the eastern region of the Nile Delta (RIGW, 1985) suggest that the assumption of a homogeneous and isotropic aquifer is a satisfactory approximation for the aquifer system in the study area. The aquifer consists of only one layer and not in direct connection with lower aquifers because of the thick impervious Miocene beds. Pumping tests performed in the study area indicate that values of 12000m^2/day and 0.012 are representative regional values for the transmissivity and storativity of the aquifer, respectively.

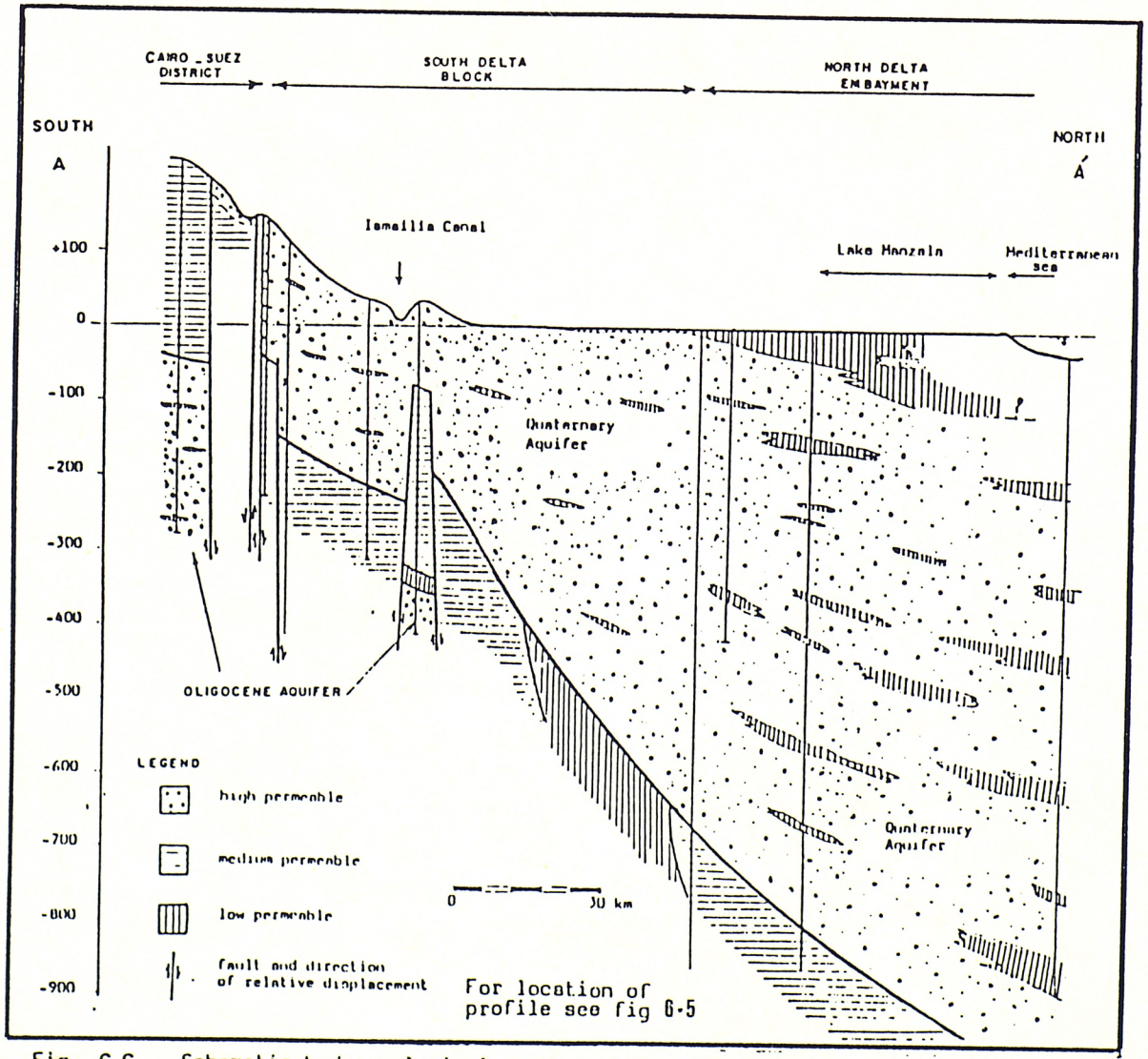

Fig. 6.6 Schematic hydrogeological north-south profile

6.3.2 Regional Flow of Groundwater

The aquifer in the study area is a natural extension of the Nile Delta main aquifer. This extension is situated between the Ismailia Canal and the major fault in the south. Groundwater levels in the study area are directly connected to those in the Nile Delta main aquifer and the water levels in the Ismailia Canal as well.

Contour maps of the measured groundwater levels in the Nile Delta main aquifer and in the study area are shown in Figures (6.7) and (6.8), respectively (RIGW, 1985). The contour maps indicate that the pattern of groundwater flow in the study area is mainly influenced by seepage from the Ismailia Canal and the flow from the Nile Delta main aquifer passing through the limited entrance between the canal and the major fault in the south. The regional hydraulic gradient in the area varies from 1/5000 to 1/10000 and the flow resultant is essentially eastward, i.e. towards the Suez Canal.

A pronounced groundwater ridge is present along the Ismailia Canal. Natural recharge to the aquifer in the study area mainly occurs by seepage from the canal. The aquifer loses water by natural discharge into the Suez Canal as well as some reaches of the Ismailia Canal.

Long-term data of groundwater levels in the study area shows a rise in water table of 0.4m to 0.9m between 1960 and 1980 (RIGW-IWACO, 1983). However, the average rise in water table during the period 1970-1980 is less than that of the period 1960-1970. Records of water table levels in the study area during the past decade suggest that the aquifer system is in a dynamic balance conditions, i.e. the flow is approaching steady state conditions.

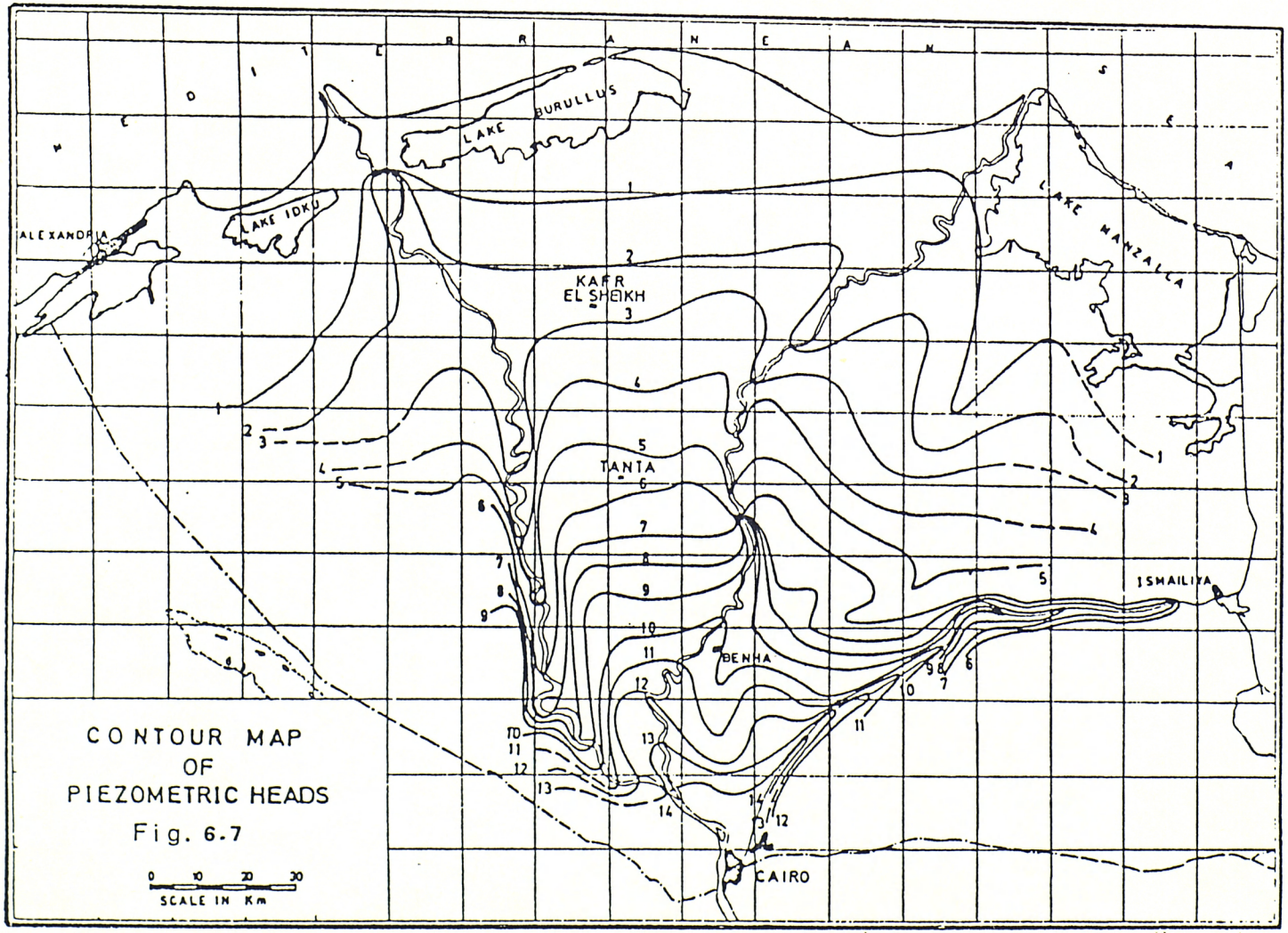
MEDITERRANEAN SEA
LAKE BURULLUS
LAKE IDKU
ALEXANDRIA
KAFR EL SHEIKH
LAKE MANZALLA
TANTA
ISMAILIYA
BENHA
CAIRO
CONTOUR MAP
OF
PIEZOMETRIC HEADS
Fig. 6.7
0 10 20 30
SCALE IN Km

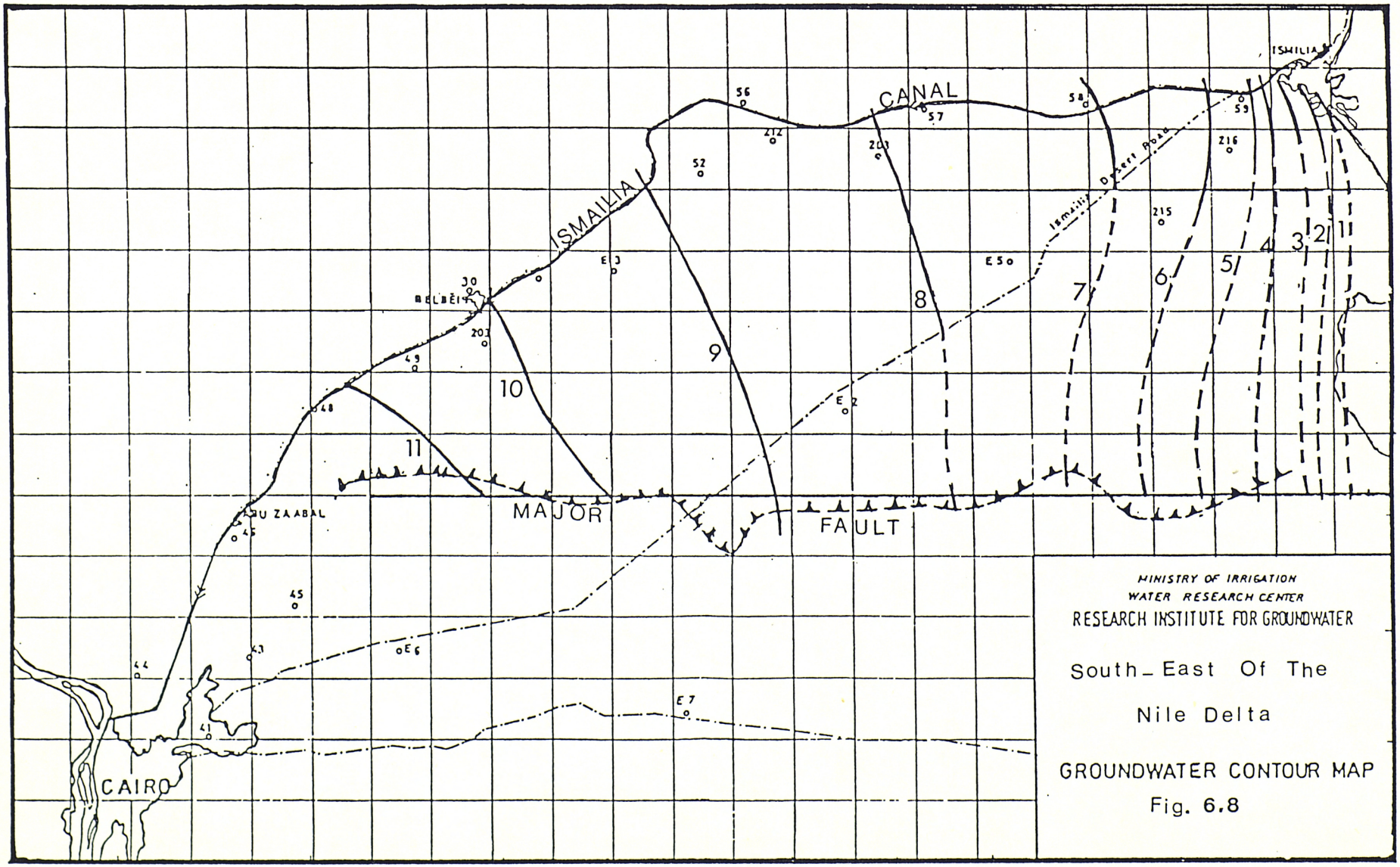
CANAL
ISMAILIA
MAJOR
FAULT
CAIRO
BELBEIS
ABU ZAABAL
ISHILIA
Ismailia Desert Road
MINISTRY OF IRRIGATION
WATER RESEARCH CENTER
RESEARCH INSTITUTE FOR GROUNDWATER
South_East Of The
Nile Delta
GROUNDWATER CONTOUR MAP
Fig. 6.8

6.3.3 Quality of Groundwater

Chemical analyses of water taken from the scattered observation wells in the study area imply a regional pattern of groundwater quality (RIGW, 1980) as shown in Figure (6.9). The overall pattern of water quality is controlled by recharge of fresh water from the Ismailia Canal. This is manifest by the good quality water of salinity less than 500p.p.m. of total dissolved solids, T.D.S., in the vicinity of the canal. The quality deteriorates gradually due south and east such that the zone south of the Cario-Ismailia desert road is generally of poor groundwater quality. Groundwater contained by the aquifer in the zone north of the road is generally of suitable quality for irrigation and domestic water supply.

6.3.4 Salt Water Intrusion

Aquifer formation on the eastern fringe of the study area contains salt water in the form of a wedge underneath the fresh water flowing to the Suez Canal. The zone of contact between fresh and salt water takes the form of a transition zone caused by hydrodynamic dispersion. However, the width of this zone is often relatively small and an abrupt interface approximation can be introduced.

Under the existing natural undisturbed conditions in the aquifer system, a state of equilibrium is maintained, with a stationary interface and a fresh groundwater flow to the Suez Canal. At every point on this interface, the elevation and slope are determined by the fresh water potential and gradient. If the water table in the vicinity of the Suez canal is lowered, by pumping from the aquifer, the interface will start to advance inland until a new equilibrium is reached. This phenomenon is known as salt water intrusion. Occurrence and mathematical description of salt water intrusion are discussed in Appendix C.

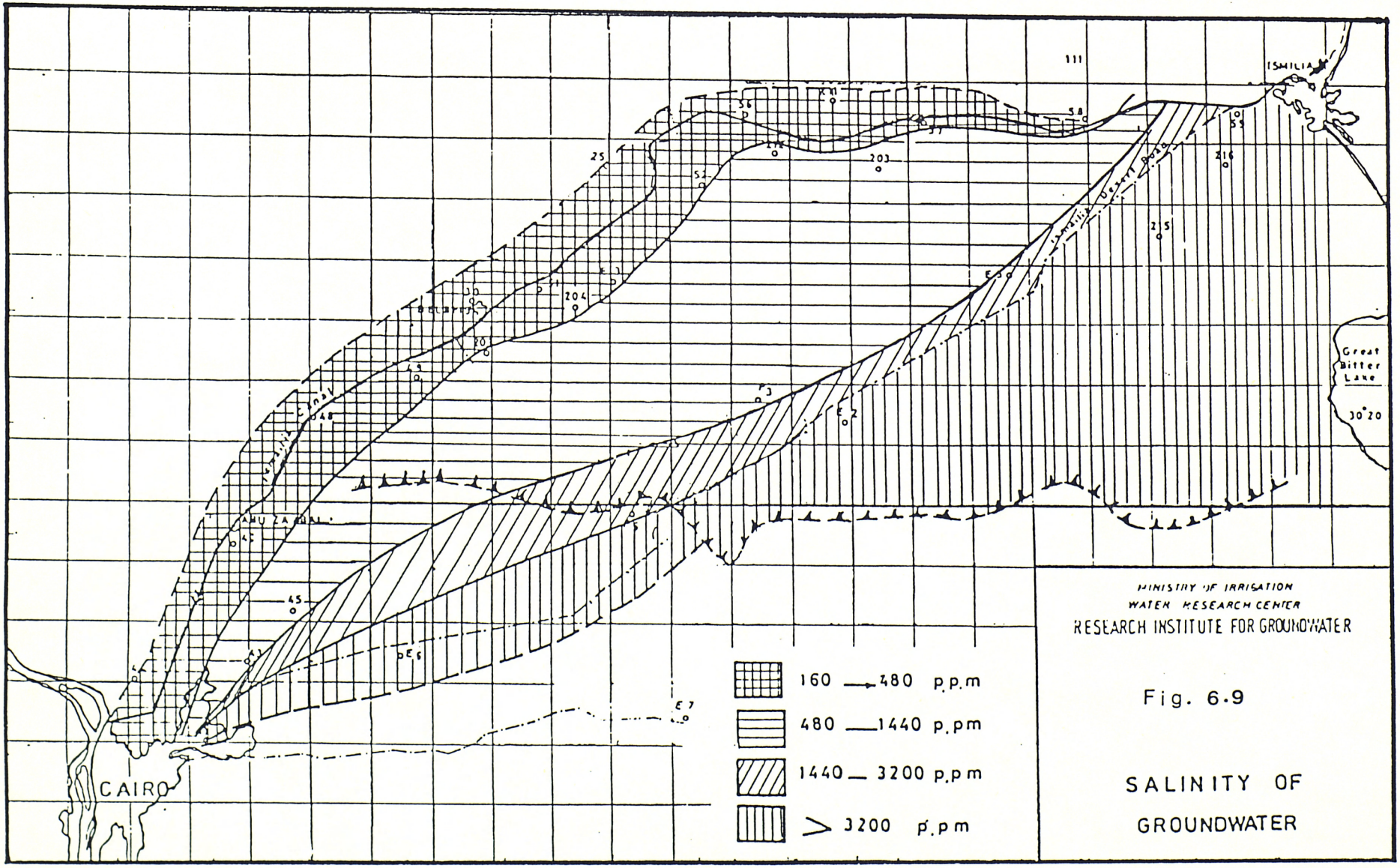
ISMILIA
Great Bitter Lake
30°20
CAIRO
160 → 480 p.p.m
480 — 1440 p.p.m
1440 — 3200 p.p.m
> 3200 p.p.m
MINISTRY OF IRRIGATION
WATER RESEARCH CENTER
RESEARCH INSTITUTE FOR GROUNDWATER
Fig. 6.9
SALINITY OF
GROUNDWATER

Unfortunately, no field investigations were carried out to determine the extent of salt water intrusion in the study area. However, information from exploratory drilling in the main aquifer of the Nile Delta (Farid, 1980 and Hassan, 1985) confirms the validity of Ghyben-Herzberg relationship. Providing the relationship is also valid for the study area, location of the interface could be defined. Using the nomenclature of Figure (6.10) and applying Ghyben-Herzberg relationship, the extent of salt water intrusion represented by the location of the toe point on the interface can be expressed as a function of the height of fresh groundwater above sea level as follows

$$H_f = D/(1 + (\gamma_f/\Delta\gamma))$$

where

$$\Delta\gamma = (\gamma_s - \gamma_f)$$

and $h_s = h_f(\gamma_f/\Delta\gamma)$ from Ghyben-Herzberg relationship

$$\left.\begin{aligned} h_s &= H_s \\ h_f &= H_f \\ D &= H_s + H_f \end{aligned}\right\} \text{ at the toe point}$$

In the study area, the average thickness D is 150 metres and the specific weights of fresh and salt water, γ_f and γ_s, are 1.0 gr/cm^3 and 1.025 gr/cm^3, respectively. Substituting these values in the above equation, the value of $H_f \approx 3.65$ metres above sea level is obtained. Thus the areal extent of salt water intrusion represented by the locus of the toe point along the coast can be detected by the locus of the fresh water elevation H_f.

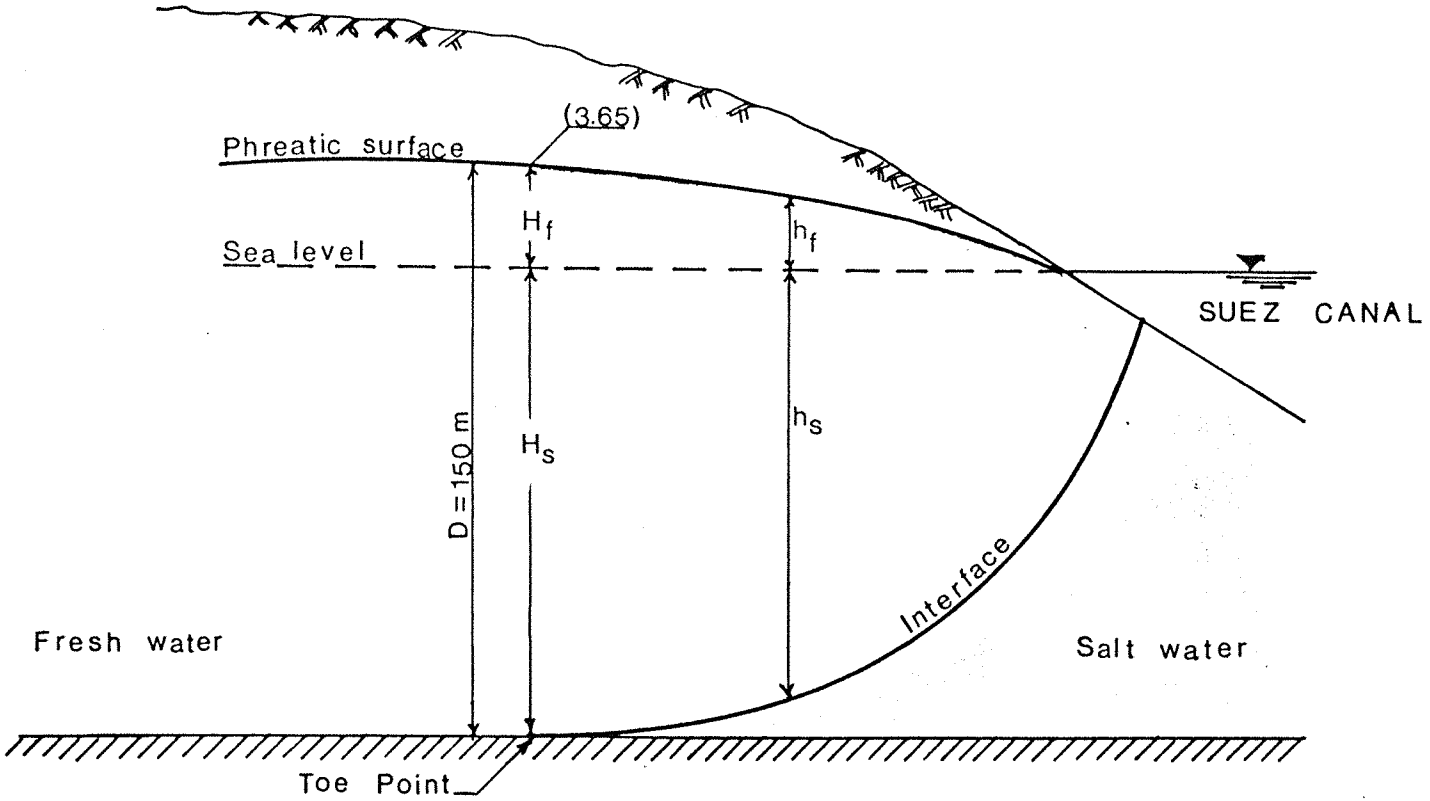

Fig. 6.10 SALT WATER INTRUSION

6.4 The Ismailia Canal

6.4.1 Existing Conditions

The Ismailia Canal was originally constructed between Zagazig and Ismailia in 1862 to carry fresh water to the Suez Canal towns of Port Said, Suez and Ismailia. In 1866 the canal was extended to Cairo. The total length of the canal from Cairo to Ismailia is 128 kilometres and the original canal size is reported to have been "eight feet deep and about sixty wide" (about 2.4m deep by 18m wide). The original excavation was through dry sandy strata and it is believe that the original canal leaked appreciably when first filled but the leakage diminished fairly quickly. During the past century the Ismailia Canal has been widened at various occasions (1920, 1957 and 1964). Figure (6.11) shows the route of the existing canal.

The canal at present has a width varying from 50 metres in the upper reaches to 30 metres at Ismailia with a depth of about 3.5 metres. The mean monthly flows through the headworks into the canal vary during the year from a maximum of about 135 cu.m/sec to 50 cu.m/sec. This water is used to irrigate an area of about 315,000 feddans (132,000 hectares), and to provide water for domestic and industrial use for parts of north Cairo, El-Abbasa region, Ismailia, Suez and Port Said.

Measured from the headworks, from Km 0 to Km 8, the canal passes through an industrial area and the banks are in clay. From Km 8 to Km 22 the canal passes through flat agricultural land and has a water level generally below the level of the adjoining ground or only slightly higher. Along this stretch Nile Delta clay deposits are exposed in the canal banks but the clay cap becomes thinner as it extends eastwards from the Nile. From Km 22 to Km 30 the canal is cut through sand lying between the Abu Zabal

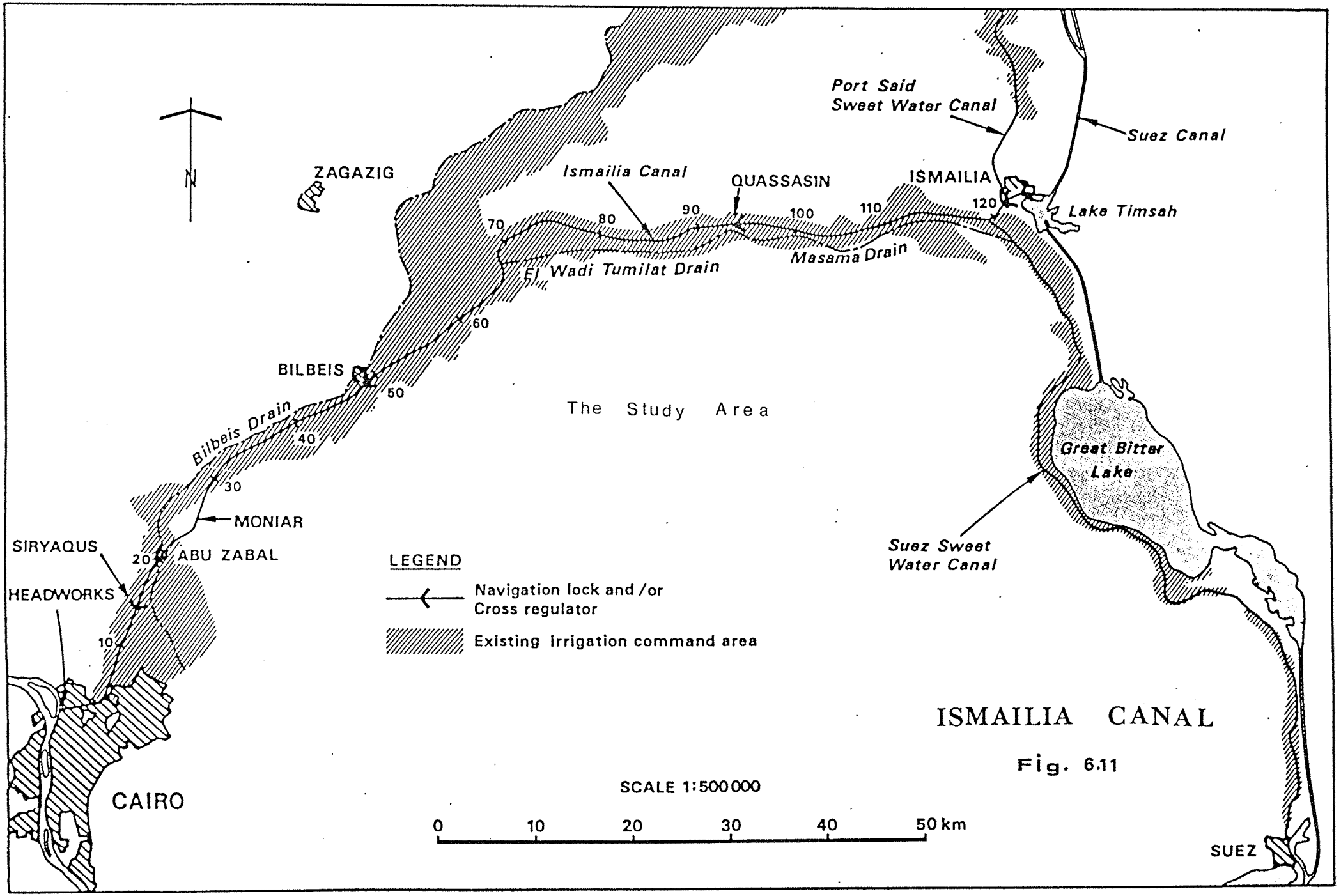

ISMAILIA CANAL

Fig. 6.11

basalt outlier and the desert. From Km 30 to Km 67 the canal runs close to the eastern edge of the Nile Delta. As far as Bilbeis (Km 50) the canal water level is generally about one metre above the adjoining ground. Beyond Km 50 this increases to as much as three metres. From Km 67 to 71 the canal crosses the top end of Wadi El-Tumilat. Here the canal water level is two to three metres above the level of neighbouring land. From Km 71 to Ismailia (Km 126) the canal generally runs along the northern edge of Wadi El-Tumilat. As far as Km 95 the canal water level is above the level of right bank abutting land by as much as 3 metres in places. From Km 95 to Ismailia the valley has a number of dune deposits and the canal water level is seldom much above the adjacent land.

Along the canal there are a number of areas of water-logged land. On the west side of the canal between Km 68 and Km 70 El-Eslah water logged area is about 500 feddans (214 ha). On the east side of the canal between Km 70 and 75 El-Abbasa water logged region has an area of 2,200 feddans (915ha). Much of this area is occupied by hunting lakes and fish farms. Elsewhere near the canal there are about 1600 feddans (660ha) of water logged land made up of many small areas.

6.4.2 Future Development

Over the next decade the Egyptian Government intends to expand agricultural production substantially in the Ismailia Canal Zone and elsewhere by reclaiming "new" lands and improving production on "old" lands. To this end, the Ismailia Canal is being widened to increase the canal capacity at the headworks from 135 cu.m/sec to 439 cu.m/sec so as to provide for the expansion of water supplies and to extend the area to be irrigated to 1.1 million feddans (436000ha). The planned development has already started and the Ismailia Canal in the near future will be considerably

wider (locally 90 metres instead of 50 metres) and deeper (locally 5.5 metres instead of 3.5 metres) than in the present situation.

During the canal widening in 1964, farmers complained about water-logging and salinization of the land adjacent to the widened stretches of the canal. Apparently, this was caused by increased seepage from the canal. However, such seepage decreased when, due to the silt bearing Nile water, a new skin of silt has been formed on the widened sections. Presently, the River Nile is no longer carrying and depositing any substantial amount of sediments, being trapped in the lake behind the Aswan High Dam. This means that after the present widening of the canal, the existing skin layer of deposited silt, which to a certain extent must have precluded seepage, will be removed leaving a seepage surface with relatively lower hydraulic resistance. This gives reason for increased seepage from the canal in the future and emphasizes the need for effective measures to control this seepage.

6.4.3 Canal Seepage

Seepage from the Ismailia Canal has been the subject of intensive investigation where different methods and techniques of quantitative assessment of seepage have been applied during the past decade Haskoning (1976), Hefny et al (1977), MOI (1978), Pontin et al (1978) and Binnie ' Partners (1980). More recently, a water balance study for Wadi El-Tumilate area using a finite element model, IWACO-RIGW (1986), has shown that the annual seepage rate from the Ismailia Canal between Km 46 and Km 124 amounts to 160 million cu.m. Though the various estimates of seepage rate from the canal are wide-ranging, they imply an agreement on the ratio by which the total seepage is subdivided into portions flowing away to the left and to the right of the canal. Seepage flow to the right of the canal

into the study area is estimated to be about 40% of the total canal seepage.

Natural seepage from the canal into the aquifer depends on a number of parameters which are related to both the canal and the aquifer. These parameters are the seepage surface represented by the wetted perimeter of the canal, the hydraulic connection between the canal and the aquifer expressed by the hydraulic resistance of the seepage surface and the head loss across the seepage surface determined by the difference between the water level in the canal and that in the aquifer out side the canal. Values of these parameters are required to define the conditions on the boundary which is referred to in the study as the stream-aquifer boundary. Numerical values of these parameters for the study area, along the Ismailia Canal from Km 28 to Km 128, are compiled in Figure (6.12).

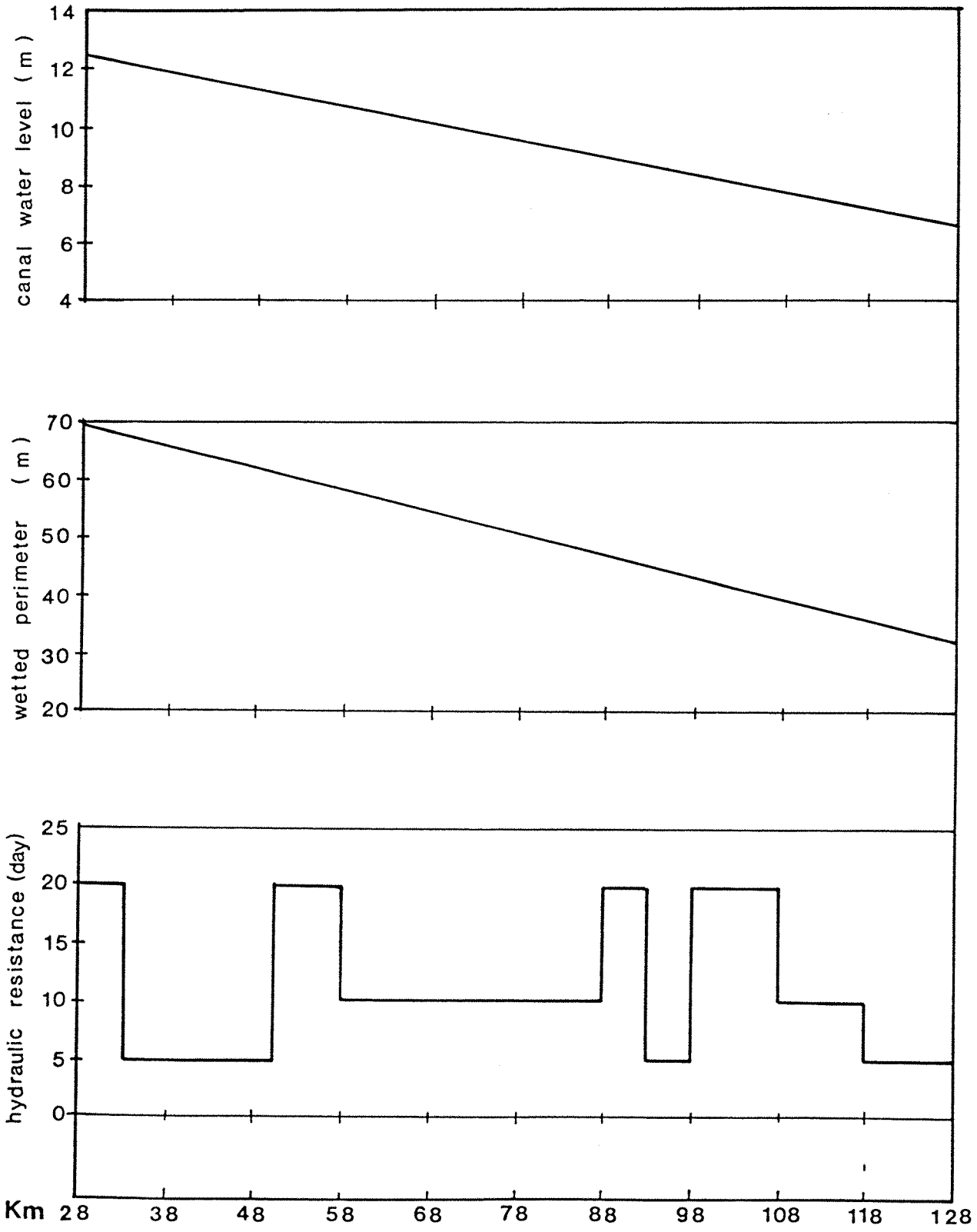

Fig. 6.12 ISMAILIA CANAL (from Km 28 to Km 128)

CHAPTER 7

CASE STUDY: MANAGEMENT OF THE STREAM-AQUIFER SYSTEM

7.1 Introduction

7.2 The Management Problem
- 7.2.1 Optimal Yield of the System
- 7.2.2 Development Considerations and Constraints
- 7.2.3 The Management Model

7.3 Simulation Modelling
- 7.3.1 Input Data
- 7.3.2 Calibration of the Model
- 7.3.3 Application of the Model

7.4 Hydraulic Management of the System
- 7.4.1 Alternative Operating Policies
- 7.4.2 Application of the Management Model
- 7.4.3 Feedback Verification

CHAPTER 7

CASE STUDY: MANAGEMENT OF THE STREAM-AQUIFER SYSTEM

7.1 Introduction

Agriculture expansion in Egypt asks for a thorough planning for the allocation of the available water resources. It is evident that, problems of water-logging and salinization associated with the previous experience of reclaiming desert uplands in the vicinity of the Nile Delta and the Valley stem from the assumed independence of water resources and not considering the interaction between surface water and groundwater. If development plans for groundwater resources in those areas were available at that time, these problems could be quantitively appreciated and minimised in the planning stage, and much would be gained. In a stream-aquifer system, the answer to these problems is to deal with the integrated structure of the system by considering the interaction between the super-structure on the surface represented by the stream and the sub-structure being the aquifer. In this sense, seepage from the stream into the aquifer is viewed as natural diversion into the aquifer which acts as natural reservoir as well as a distribution network of a certain capacity that can be assessed and optimally utilized. Thus, this system is controlled by extending the manipulation to handle the integrated system and not by eliminating the stream-aquifer interaction.

The case study considered in the application of the management model is that of the stream-aquifer system in the new land reclamation areas south-east of the Nile Delta, as described in Chapter 6. The stream flows, natural recharge to the aquifer and other factors affecting water balance in

the system are of deterministic nature. Water levels and discharges in the stream are controlled. The interaction between the stream and the aquifer is such that, there is sufficient flow in the stream at all times so that withdrawals directly from the stream or losses from the stream into the aquifer do not affect water levels in the stream, and likewise, normal seasonal variation in the stream water levels produce negligible interaction. The saturated thickness of the aquifer is always large compared to that of any drawdown; hence, transmissivity is assumed independent of head. There is no subsidence, and groundwater is instantly released from storage. Under these conditions a linear groundwater model is applicable.

In a stream-aquifer system, optimal development of groundwater resources is not only related to the physical characteristics of the system but also to the way the system is operated, as illustrated in Chapter 2. In the management problem of the considered system, management decisions are primarily concerned with the groundwater hydraulics of the system and the objective is to determine optimal quantitative distribution of groundwater abstraction in space and time. Thus, the management model, as presented in Chapter 3, is a hydraulic management one. The ability to predict the response of the system to any activities proposed in the future is an intrinsic part of the procedure for determining a management policy. Simulation modelling provides the tool to solve the forecasting problem of the system. The Boundary Element Model developed in Chapter 4 is used to solve the forecasting problem of the considered system. Computer implementation of the Boundary Element Model is that described in Chapter 5.

This chapter is devoted to the application of the developed combined simulation-optimization management model to the hydraulic management of the stream-aquifer system south-east of the Nile Delta.

7.2 The Management Problem

7.2.1 Optimal Yield of the System

Until recently, the definition of the yield of an aquifer system has often been based on the hydrological features of the physical system only. The concept of a safe yield, which is based on this approach, is often used by hydrologist to define the maximum annual withdrawal from an aquifer system which will not produce undesired results. Once the dynamic nature of an aquifer system, the excitation-response relationship, and the need to manage the system to achieve various goals are understood, it becomes obvious that the essentially hydrologic static concept of a safe yield is insufficient.

Obviously, the volume of water withdrawn from one aquifer system cannot exceed the aquifer's replenishment, unless mining of all or part of the volume of water in storage is taking place. However, from the quality view point, it is necessary to maintain certain rate of outflow of groundwater from the system. Accordingly the withdrawal from an aquifer is the difference between all inflows and outflows. Since inflow and outflow can be controlled by controlling water levels on which they depend, the yield of an aquifer system is a decision variable to be determined as part of its management. It is not necessarily a constant figure. It may vary from year to year or even during the year, depending on the state of the aquifer, the hydrologic constraints imposed on its operation and objective and constraints included in the management model. This is known as the optimal yield, or operational yield, of the system. The concept of optimal yield incorporates in it both the hydrological features of the physical aquifer system and those of the management model.

In the present study, the stream-aquifer system is to be managed on intra-annual basis. The stream-aquifer interaction is considered as a manageable component of the system, i.e. induced recharge is a controlled input. Thus, optimal yield of the system sought in the present study is a decision variable to be determined as part of its management.

7.2.2 Development Considerations and Constraints

Quality of groundwater plays a main role in the development of groundwater resources in the study area. Based on the regional pattern of groundwater quality, as described in Chapter 6, withdrawal from the aquifer system can only take place in that part north of the Cairo-Ismailia desert road. This a physical constraint which is satisfied in the management of the system by declaring the area north of the road as a productive zone and that south of the road as a non-productive zone. Another constraint related to quality aspects is the extent of salt water intrusion. This is controlled in the management model by controlling the rate of fresh water flowing to the Suez Canal boundary and the drawdowns in the system.

The maximum amount of water withdrawn from a certain area in the aquifer system is constrained by the maximum allowable capacity of a well, the allowable spacing between wells to avoid interference, the allowable regional drawdowns and the water demand. These are hydrological and operational constraints which are satisfied in the management model by specifying their limits. Pumping tests in the study area suggest a maximum well capacity of 4000 cu.m/day and a spacing of 1000 metres between wells, i.e. a maximum of one well, discharging at a rate of 250 cu.m/hr and operated for 16 hours per day, is allowed in the centre of an area of 1 Km by 1 Km. Intra-annual variation in water demand is considered by using the demand density function developed in Appendix D.

A feasible policy for the development of groundwater resources in the study area is that which does not violate any of the above mentioned constraints.

7.2.3 The Management Model

The considered system is to be managed on intra-annual basis. The objective is to determine, in space and time, the optimal yield of the system. The management model is essentially that developed in Chapter 3. The approach is the combined simulation-optimization modelling. The boundary element method is the employed simulation technique. The link between simulation and optimization is established through the response functions of the system. The linear programming method is the technique used to solve the optimization problem.

7.3 Simulation Modelling

7.3.1 Input Data

The boundary element method involves modelling only the boundary geometry of the system which reduces, to a great extent, the input data required to run the model. The input data file supplied to the model contains information which defines the boundary geometry of the modelled system, hydraulic characteristics of the aquifer, boundary conditions and any input to or output from the system.

The boundary geometry of the modelled system comprises 12 sides. This is described in the input data file by the coordinates of the 12 corner points which define the modelled area. Each side on the boundary is then subdivided into boundary elements according to the number of elements and the discretization factor specified in the input data file. Boundary nodes, including a double node at each

corner point, are then defined internally by the model as explained in Chapter 5.

Regarding boundary conditions, as described in Chapter 6, geometrical boundaries of the modelled system coincide with the natural hydrogeological boundaries occurring in the system. The open boundary between the aquifer in the modelled area and the Nile Delta main aquifer, a front of 10 Km length between the Ismailia Canal and the major fault in the south, is considered in the model as a first type boundary, i.e. the prescribed heads on this front will always remain unchanged. Along the major fault no flow takes place, thus, a second type boundary condition is assigned to this boundary. Along the Suez Canal, a first type boundary condition is specified in the model as the head is at sea level everywhere on the eastern boundary. A third type boundary condition is specified along the Ismailia Canal. This means that, the parameters governing the flow from the canal into the aquifer, being the depth of water in the canal, the wetted perimeter of the canal and the hydraulic resistance of the seepage surface, should be assigned to the model in the input data file.

The time step and the number of time steps required for the transient flow solution should also be included in the input data file. A time step of 15 days is used in the model, where a calender year is considered as 24 time steps. Values and coordinates of internal point sources and/or point sinks should also be specified. As described in Chapter 5, computer implementation of the model includes automatic discretization of the inside of the modelled area into triangular cells. Thus, any distributed internal input and/or output is specified in the input data file by its strength over the generated internal cells.

Initial conditions as an input data for the transient flow solution are generated by running the model in the

steady state mode. Then, the groundwater levels produced by the steady state solution are used to run the model for transient flow conditions until a dynamic balance is reached. After the model calibration, as discussed in the next section, groundwater levels produced by the transient flow solution, when the dynamic balance is reached, are considered in the model as the existing initial conditions of the system.

The boundary geometry of the modelled area as well as the types of boundary conditions assigned to the model are illustrated in Figure (7.1). A plot of the computer implementation of the automatic generation of boundary elements and internal cells for the modelled area is shown in Figure (7.2). The generated discretization comprises 86 boundary and internal nodes forming 109 internal cells.

7.3.2 Calibration of the Model

Before the model can perform its tasks of predicting the response of the system to any future activities, it must be calibrated. The calibration of a model is the process in which the various model parameters are verified. This means that a check must be made to see whether the developed conceptual model can correctly generate the past behaviour of the real system as it is known from historical records. In principle, results of the model calibration runs are compared to the available field measurements and when a good agreement between them is achieved the model is said to be calibrated. Once the model is calibrated, all its parameters are well defined and can be used with confidence for forecasting the response of the system to the planned activities in the future.

Historical records of water table elevations in the study area, as described in Chapter 6, indicate that the modelled system is in a state of dynamic equilibrium and

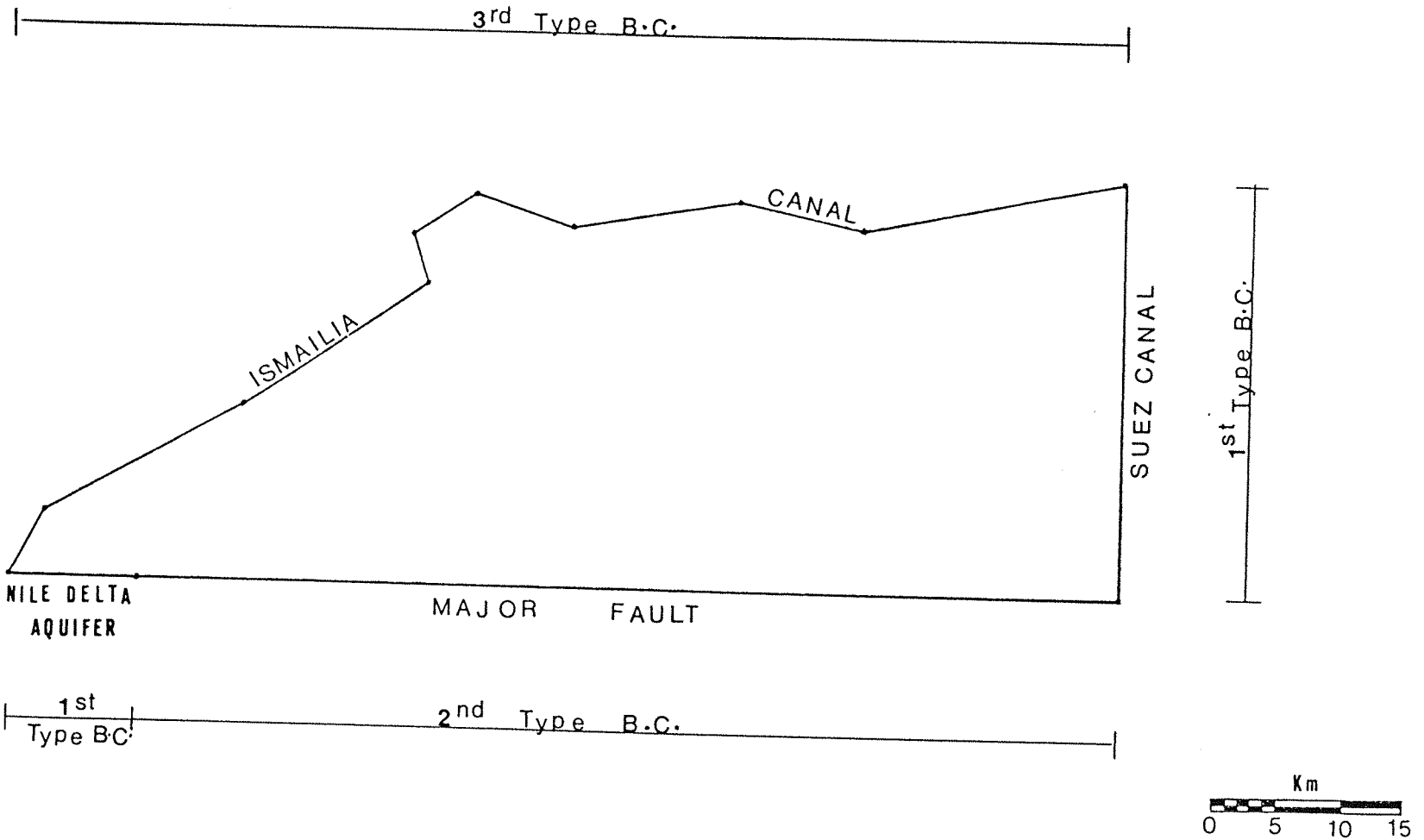

Fig. 7.1 GEOMETRY AND BOUNDARY CONDITIONS

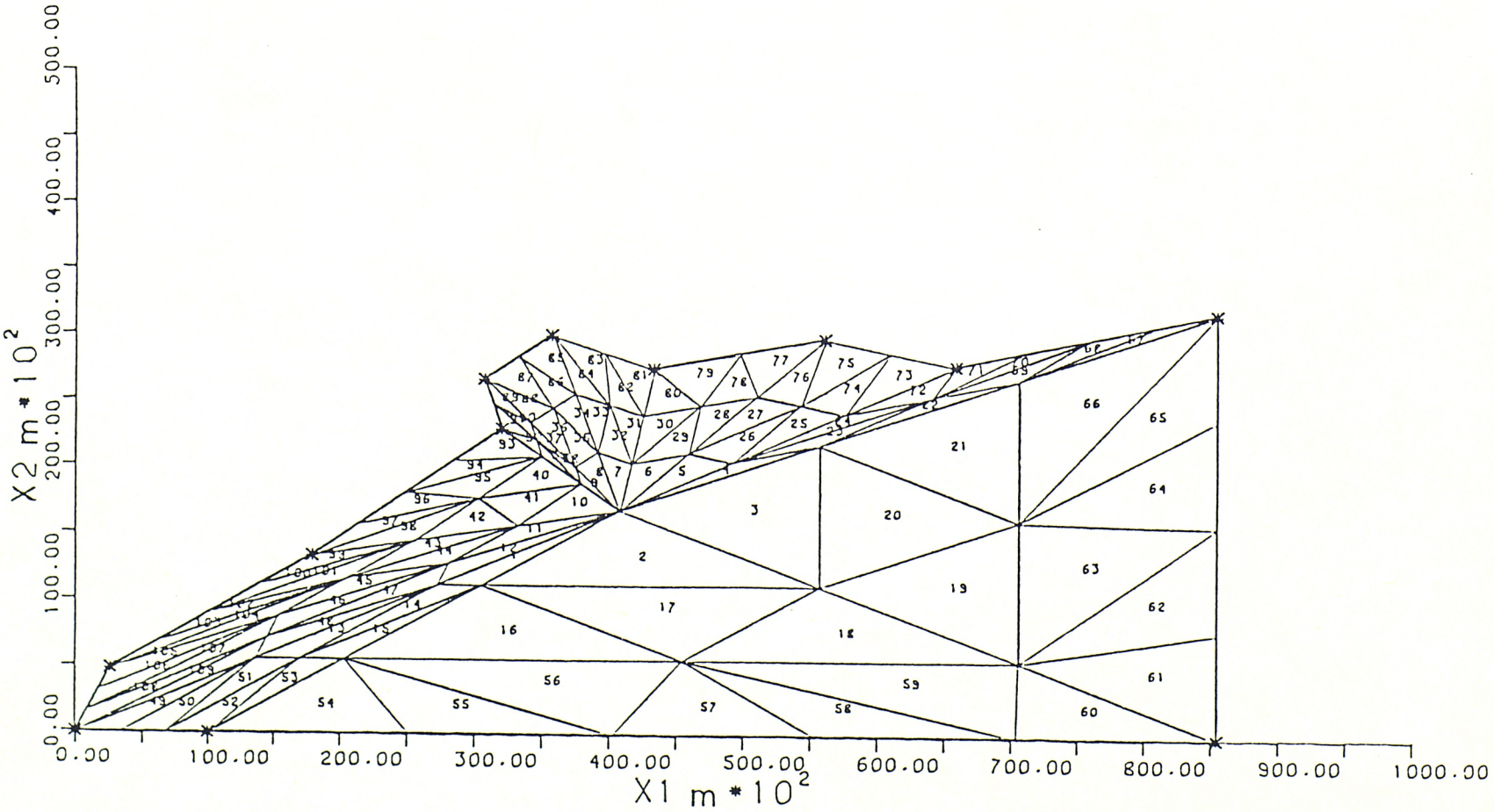

Fig. 7.2 AUTOMATIC GENERATION OF BOUNDARY AND DOMAIN ELEMENTS

approaching steady state conditions. Thus, the calibration is performed via running the model to simulate the existing state of the system. The procedure includes running the model in the steady state mode to generate initial conditions which are used to run the model for transient flow conditions until a dynamic balance is reached. When the dynamic balance is reached, the calculated water table elevations, at the 86 boundary and internal nodes, are used to produce a contour map showing the pattern of the calculated groundwater levels. On the other hand, groundwater levels at six check points, which exist in the study area as observation wells, are calculated. The output from the model also includes the calculated inflow into and outflow from the system. The output from the model is then compared to the available data records.

Several test runs are performed to calibrate the model. The dynamic balance is achieved after 72 time steps, i.e. three years. The calibration is attained by adjusting the hydraulic resistance of the seepage surface at each node on the Ismailia Canal boundary. The calibrated data used to run the model is compiled in the input data sheet shown in Figure (7.3).

The contour map of simulated groundwater levels is shown in Figure (7.4). Comparison of this map with that of the observed groundwater levels (Figure (6.8)) shows that the simulated pattern of groundwater levels is in good agreement with the observed one. For the six check points of observation wells, calculated groundwater levels match the observed levels considerably well as shown in Table (7.1).

The calibrated dynamic balance of groundwater flow in the study area is given in Table (7.2). The inflow components are the seepage from the Ismailia Canal and the flow, from the Nile Delta main aquifer, passing through the

INPUT DATA SHEET

- Number of corner points = 12

- Coordinates of the Corner Points

Point	X_1 m	X_2 m
1	0.0	0.0
2	10000.0	0.0
3	85500.0	0.0
4	85500.0	31700.0
5	65900.0	27726.0
6	56100.0	29716.0
7	43300.0	27444.0
8	35700.0	29942.0
9	30700.0	26625.0
10	32000.0	22842.0
11	17900.0	13345.0
12	2600.0	4850.0

- Number of Boundary Elements on each side

Boundary Side	1	2	3	4	5	6	7	8	9	10	11	12
Number of Boundary Elements	3	5	4	4	2	2	2	2	2	4	4	3

- Total Number of Boundary Elements = 37

- Transmissivity = 1200 m^2/day

- Storativity = 0.012

Fig. (7.3)

INPUT DATA SHEET cont.

- Boundary Data

Node	NCod	H (m)	Q m^2/day	H_s (m)	W.P.(m)	CSP (m)	RIS day
1	1	13.6	-	-	-	-	-
2	1	13.2	-	-	-	-	-
3	1	12.9	-	-	-	-	-
4	2	-	0.0	-	-	-	-
5	2	-	0.0	-	-	-	-
6	2	-	0.0	-	-	-	-
7	2	-	0.0	-	-	-	-
8	2	-	0.0	-	-	-	-
9	2	-	0.0	-	-	-	-
10	4	0.0	-	-	-	-	-
11	1	0.0	-	-	-	-	-
12	1	0.0	-	-	-	-	-
13	1	0.0	-	-	-	-	-
14	1	0.0	-	-	-	-	-
15	1	0.0	-	-	-	-	-
16	1	0.0	-	-	-	-	-
17	5	-	-	6.83	34.22	0.661	2.20
18	5	-	-	7.09	35.07	0.724	2.70
19	5	-	-	7.31	35.61	0.765	4.10
20	5	-	-	7.54	42.70	0.645	5.90
21	5	-	-	7.54	42.70	0.645	5.90
22	5	-	-	7.76	42.79	0.651	19.20
23	5	-	-	7.98	42.88	0.657	4.90
24	5	-	-	7.98	42.88	0.657	4.90
25	5	-	-	8.26	50.10	0.578	20.0
26	5	-	-	8.55	50.10	0.578	7.50

FIG. (7.3) cont.

INPUT DATA SHEET cont.

Node	NCod	H (m)	Q m^2/day	H_s (m)	W.P.(m)	CSP (m)	RIS day
27	5	-	-	8.55	50.10	0.578	7.50
28	5	-	-	8.73	50.10	0.578	6.40
29	5	-	-	8.91	50.10	0.578	7.50
30	5	-	-	8.91	50.10	0.578	7.50
31	5	-	-	9.11	53.89	0.664	9.0
32	5	-	-	9.32	54.83	0.723	7.50
33	5	-	-	9.32	54.83	0.723	7.50
34	5	-	-	9.46	60.10	0.678	9.80
35	5	-	-	9.60	66.32	0.629	1.20
36	5	-	-	9.60	66.32	0.629	1.20
37	5	-	-	9.92	66.41	0.629	9.40
38	5	-	-	10.25	66.50	0.639	12.40
39	5	-	-	10.58	66.59	0.644	14.60
40	5	-	-	10.88	66.68	0.649	0.90
41	5	-	-	10.88	66.68	0.649	0.90
42	5	-	-	11.16	67.04	0.669	0.90
43	5	-	-	11.47	67.17	0.677	0.70
44	5	-	-	11.78	67.30	0.685	2.4
45	5	-	-	12.09	67.44	0.692	0.70
46	5	-	-	12.09	67.44	0.692	0.70
47	5	-	-	12.22	67.48	0.695	1.20
48	5	-	-	12.35	67.57	0.70	4.20
49	51	13.60	-	13.80	69.81	0.833	20.0

H_s = elevation of water surface in the canal
W.P. = wetted perimeter of the canal
CSP = canal section property = $HW^2/W.P\ Sin\alpha$
HW = depth of water in the canal
α = angle of side slopes (side slope is 2:1)
RIS = Hydraulic resistance of the seepage surface

Fig. (7.3) cont.

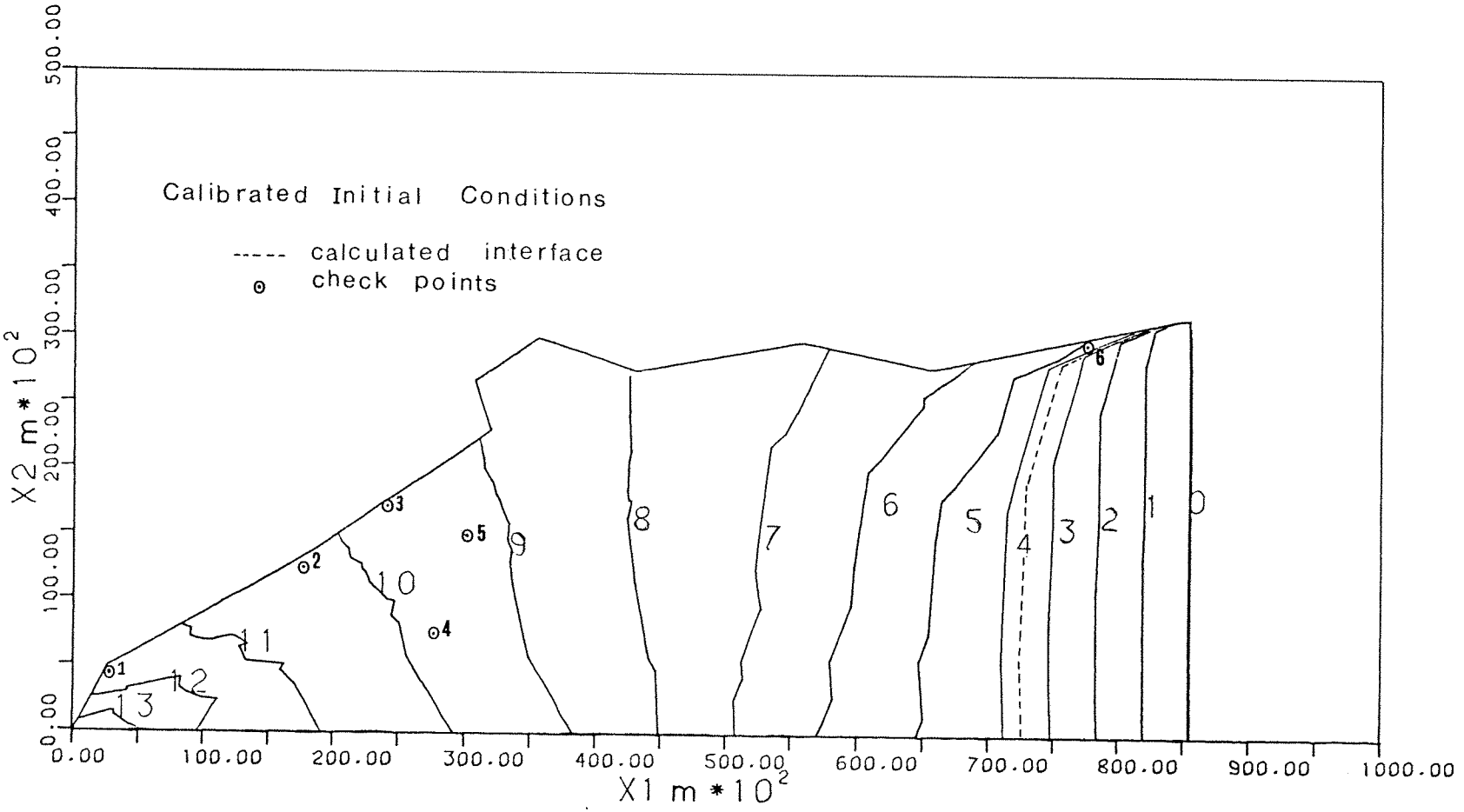

Fig. 7.4 CONTOUR MAP OF CALCULATED GROUNDWATER HEADS

Check Point	Observation Well No.	Observed Groundwater Level (m)	Calculated Groundwater Level (m)	Difference (m)
1	48	11.4	11.25	-0.15
2	49	10.3	10.18	-0.12
3	51	9.6	9.65	+0.05
4	10th Ramadan	9.4	9.43	+0.03
5	Ramsis	9.3	9.31	+0.01
6	59	5.1	5.0	-0.10

Table (7.1) Observed and Calculated Groundwater Levels

Inflow Components	10^3 m^3/day
Recharge from Ismailia Canal	149.21
Recharge from Nile Delta Aquifer	46.38
Total Inflow	195.59

Outflow Components	10^3 m^3/day
Outflow into Suez Canal	149.42
Outflow into Ismailia Canal	44.08
Total Outflow	193.50

Table (7.2) Calibrated Dynamic Balance Flow

limited entrance between the canal and the major fault. Figure (7.5) shows the distribution of the calculated seepage rates from the Ismailia Canal (between Km 28 and Km 128) flowing to the right of the canal into the study area. The annual rate of seepage calculated by the calibrated model amounts to 54.5 million m^3. The calculated seepage is in agreement with the estimate made by RIGW (1977) and the water balance results given by IWAGO-RIGW (1986). The calculated annual flow from the Nile Delta main aquifer into the study area amounts to 17 million m^3. The outflow components are the natural discharge into the Suez Canal and the flow gained by the Ismailia Canal in some reaches. The calculated annual outflow into the Suez Canal is in the same order of magnitude as that of inflow from the Ismailia Canal. Most of this outflow takes place in the northern part of the boundary next to the Ismailia Canal. Calculated outflow from the aquifer into the Ismailia Canal amounts to 16 million m^3/year and occurs mainly in that part opposite to the front of inflow from the Nile Delta main aquifer.

According to the criterion described in Chapter 6, the location of the equipotential line of 3.65 metres above main sea level can be used to express the extent of salt water intrusion in the study area. This is shown in Figure (7.4) using linear interpolation on the contour map of the calculated groundwater levels. The locus of the toe point on the salt-fresh water interface conforms with the path of this equipotential. Although the shape of interface, represented by this equipotential line, is in agreement with the overall pattern of groundwater quality in the study area, shown in Figure (6.9), field investigations in the coastal area of the Suez Canal are needed so that the calculated interface can be calibrated against field measurements in the real system. The calculated interface in the present model calibration provides guide lines for the location of the necessary field investigations.

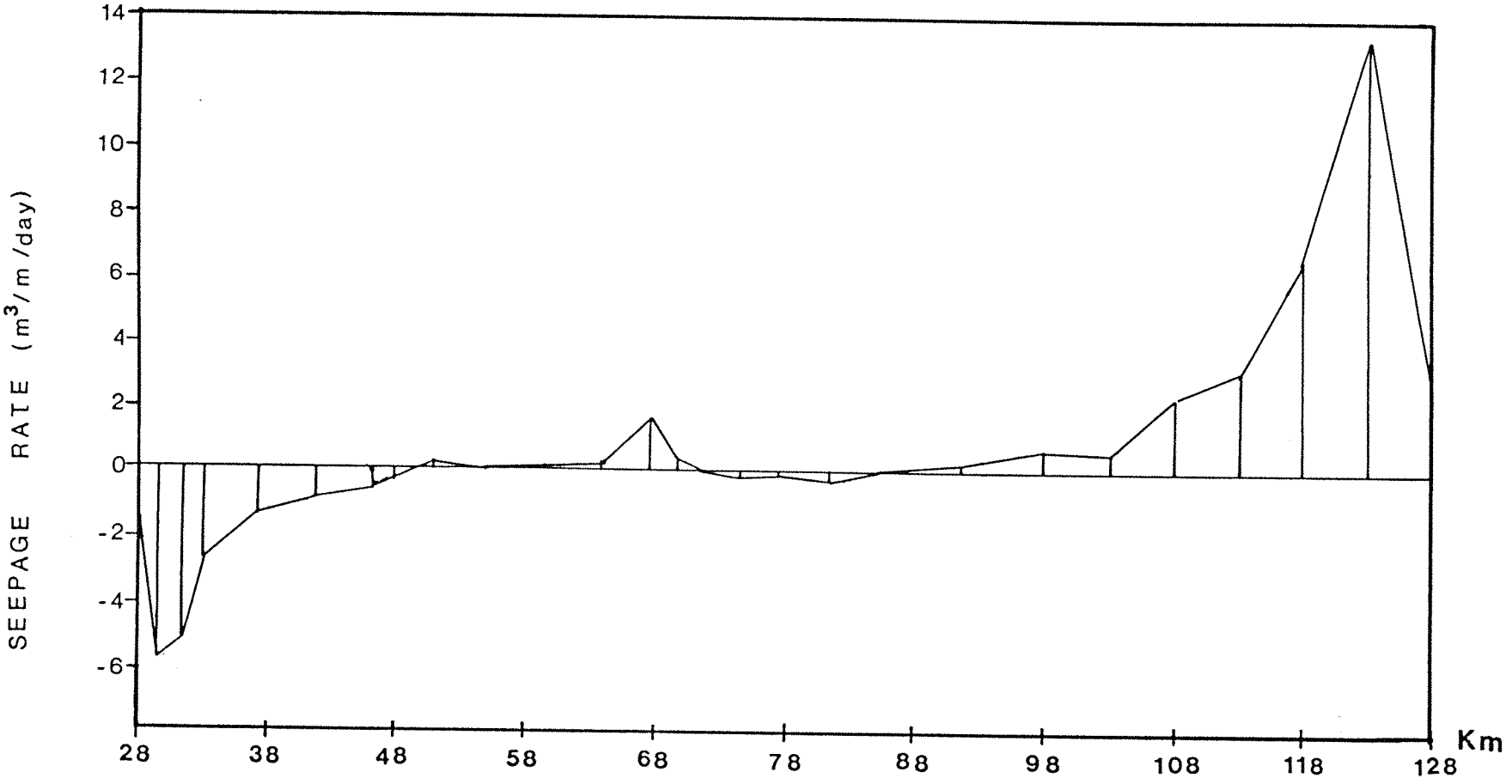

Fig. 7.5 DISTRIBUTION OF THE CALCULATED SEEPAGE

The model calibration shows that the assumption of a homogeneous and isotropic aquifer system in the study area is a satisfactory approximation. Based on the achieved results of calibration, the model can be used with confidence to perform its task of predicting the response of the system to activities in the future.

7.3.3 Application of the Model

The role of the simulation, as described in Chapter 3, is delinated by determining the response coefficients, β, and the interaction parameters, φ, for the considered system. This can be achieved by introducing one unit of pumping in a certain location during the first time step and running the calibrated model for the required number of time steps to calculate the resulting response. The response coefficients β are the calculated drawdowns at all points of interest due to that pumping at the end of each time step. The interaction parameters are the calculated induced flow into the aquifer due to that pumping at the end of each time step. The procedure is repeated for all considered pumping locations to generate the response matrices of $[\beta]$ and $[\varphi]$.

Based on groundwater quality aspects, as presented in section 7.2, the modelled area is divided into two zones; productive and non-productive. Pumping locations considered in developing the response matrices are defined by discretizing the productive zone into a mesh of quadrilateral production cells. Several test runs of the model are carried out to determine the adequate size of a production cell. The size of a production cell is decided such that the response of the system to pumping by a number of wells distributed over the cell can be represented by that resulting from pumping the same amount of water by a fictitious well located in the centre of the cell. This is accomplished by using a 5 Km by 5 Km cell for the arrangement of wells shown in Figure (7.6). Accordingly,

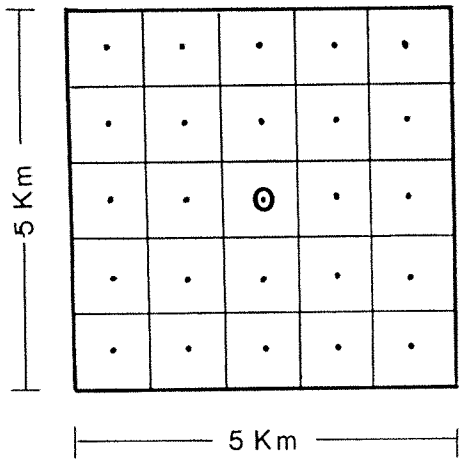

Fig. 7.6 Arrangement of Wells in a Production Cell

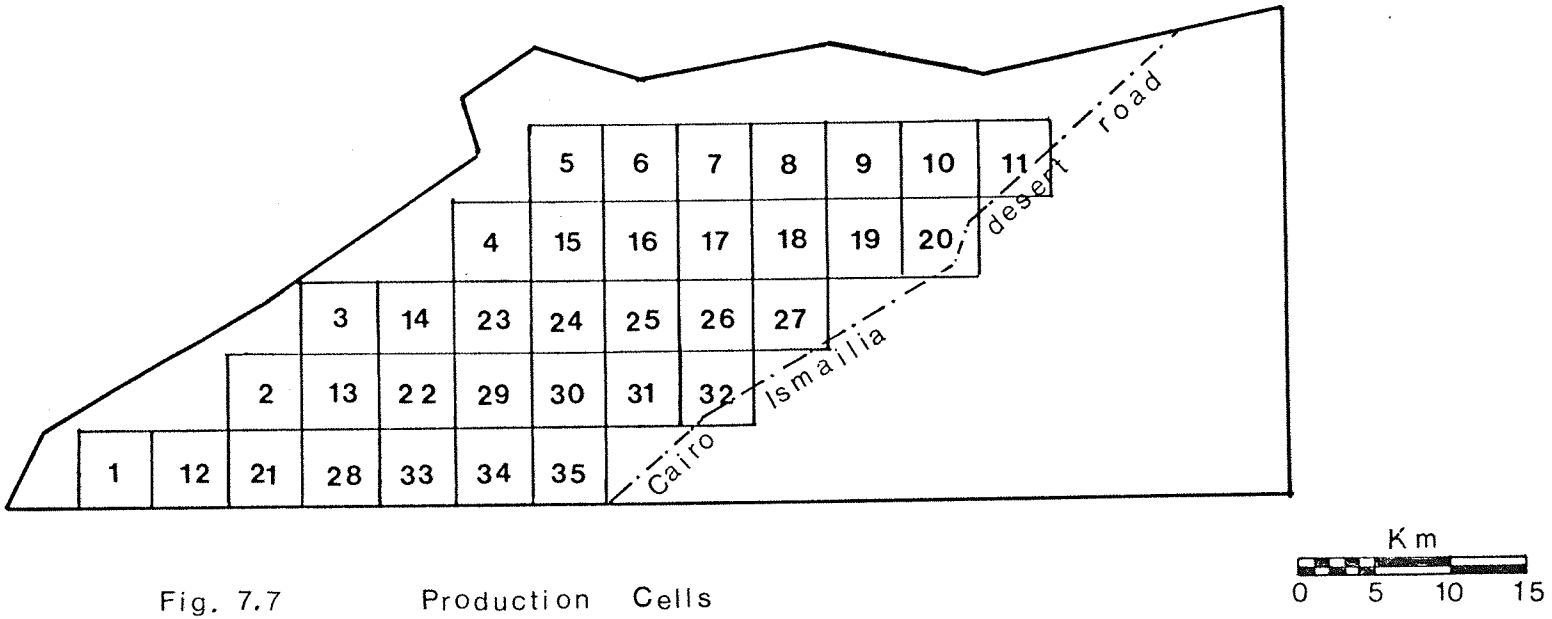

Fig. 7.7 Production Cells

the productive zone is discretized into 35 cells as shown in Figure (7.7). The discretization scheme excludes the narrow strip of old agricultural lands and small villages in the immediate vicinity of the Ismailia Canal and the production cells covers only the new desert lands.

Considering intra-annual operation, the response of the system to pumping in each production cell is generated for the 24 time steps covering the one year operation horizon. A unit point sink of 10,000 cu.m./day is introduced in the centre of a production cell during the first time step and the calibrated model is applied to calculate the resulting drawdowns and the induced flow into the aquifer at the end of each time step. Drawdowns are calculated at the end of each time step in 37 internal nodes. The procedure is repeated for the 35 production cells and the generated response matrices [β] and [φ] are stored in an output data file. The sizes of these matrices are [35x37x24] and [35x24], respectively. Having the system's response to one unit of input per unit time is simulated, it can be extended for any multiplication of input and time units in the range of the assumed linearity of the model.

7.4 Hydraulic Management of the System

7.4.1 Alternative Operating Policies

In the management of the system, development of groundwater resources in the study area aims at providing an accessible source of water in the desert uplands where new large-scale land reclamation projects are planned. These land reclamation projects, as shown in Figure (7.8), can be grouped into three main development areas. Namely, the Agricultural Co-operative Societies, El-Mullak Extension and El-Shabab; referred to later as development area 1,

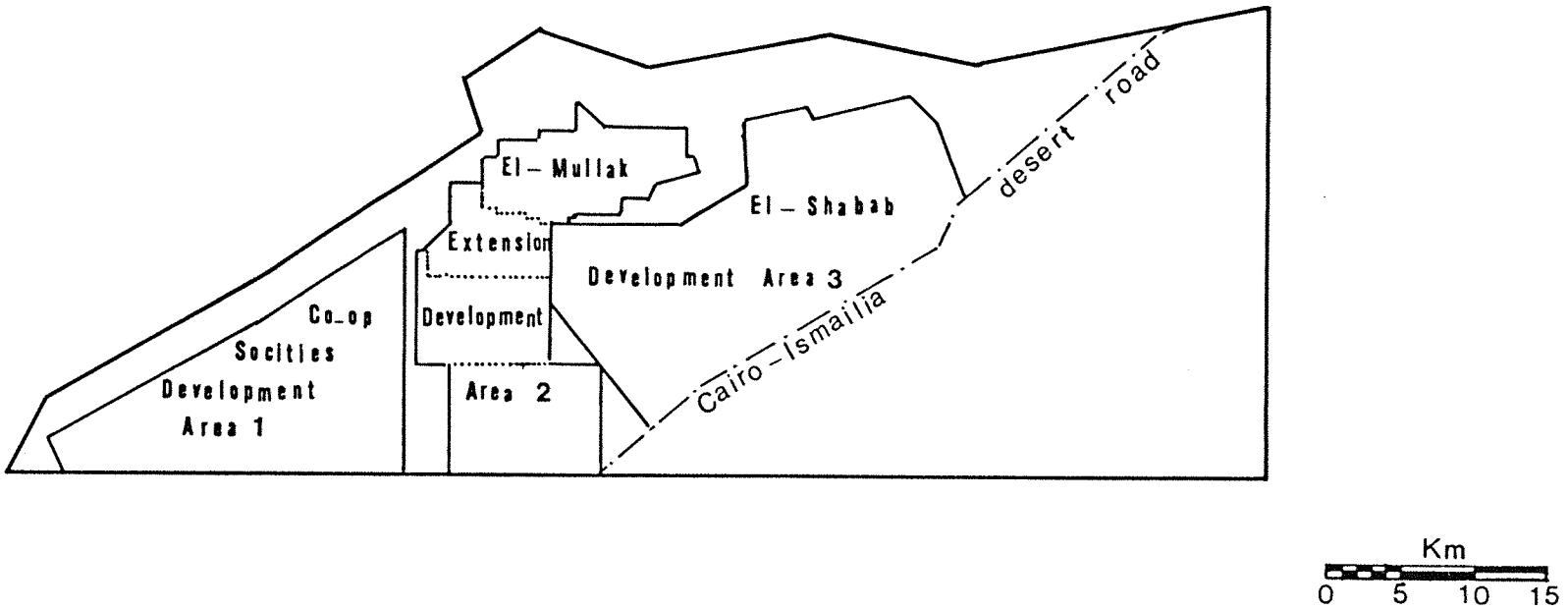

Fig. 7.8 Land Reclamation Projects

development area 2 and development area 3, respectively. The fact that the development areas are located where the productive zone in the aquifer system is identified means that groundwater withdrawn from the aquifer in a certain production cell needs not to be transported outside the cell and advantageously can be used directly where it is produced.

Four possible operating policies are considered in the hydraulic management of the system. In the first policy the optimal yield of the system is to be determined such that pumping could take place in any of the 35 production cells defining the productive zone in the aquifer system. In the other three policies, the approach is to determine the optimal yield of the system on basis of the development areas. This means that the physical space for the second policy is confined to the production cells defining development area 1, the physical space for the third policy is confined to the production cells defining development area 2 and that of the fourth policy is confined to these cells defining development area 3. Figures (7.9a), (7.9b), (7.9c) and (7.9d) show the physical spaces for the alternative operating policies; 1, 2, 3 and 4 respectively. For each operating policy, quantitative distribution of the optimal yield, in space and time, are determined for both conditions of variable and constant demands.

7.4.2 Application of the Management Model

Two input data files are required to run the management model. The first one is the output file from the simulation model which contains the response matrices of the system. The second one specifies numerical values for the constraints imposed on the decision and state variables of the system.

Fig. 7.9a Physical Space of

Policy 1

(35 cells)

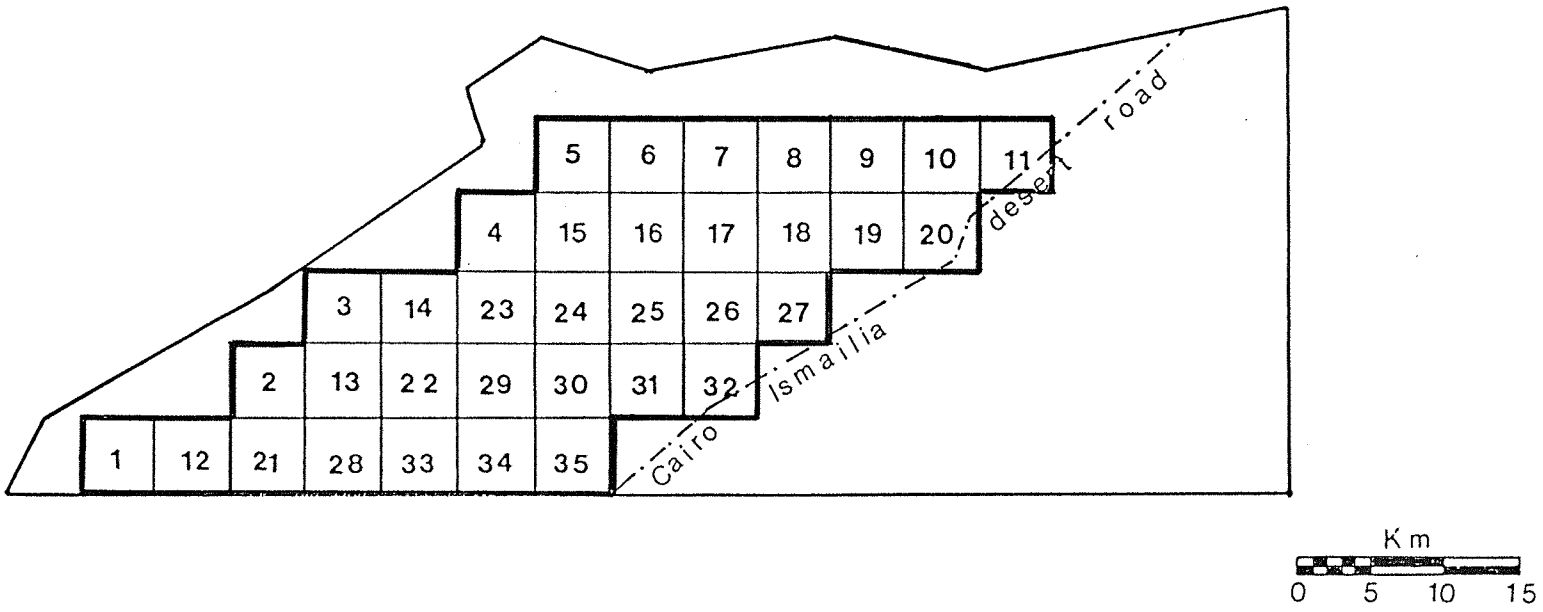

Fig. 7.9b Physical Space of

Policy 2

(10 cells)

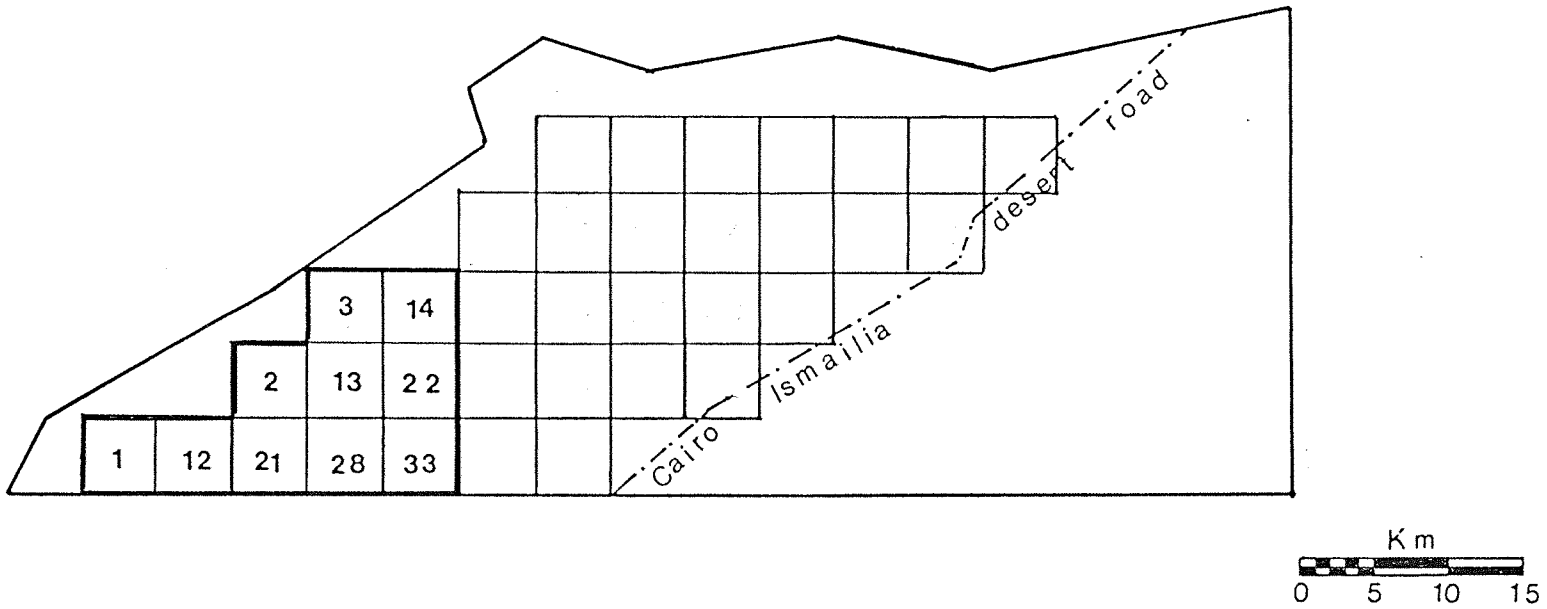

Fig. 7.9c Physical Space of

Policy 3

(15 cells)

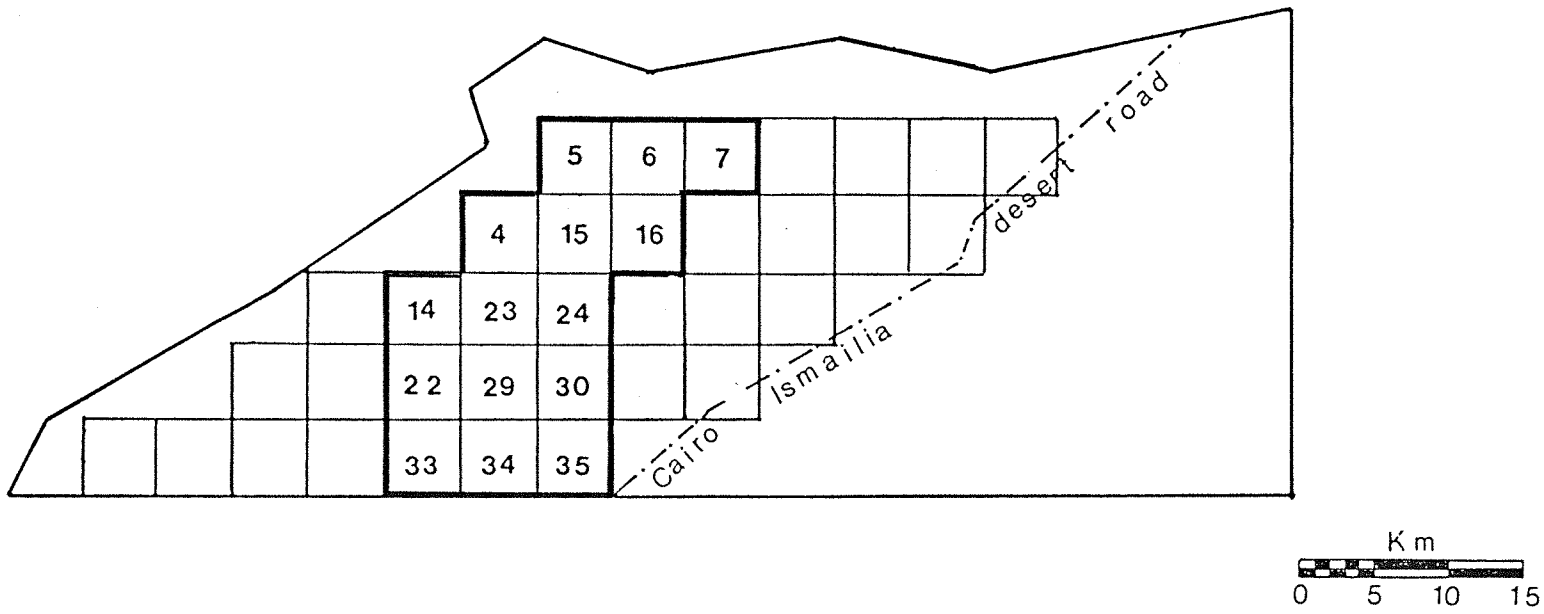

Fig. 7.9d Physical Space of Policy 4

(18 cells)

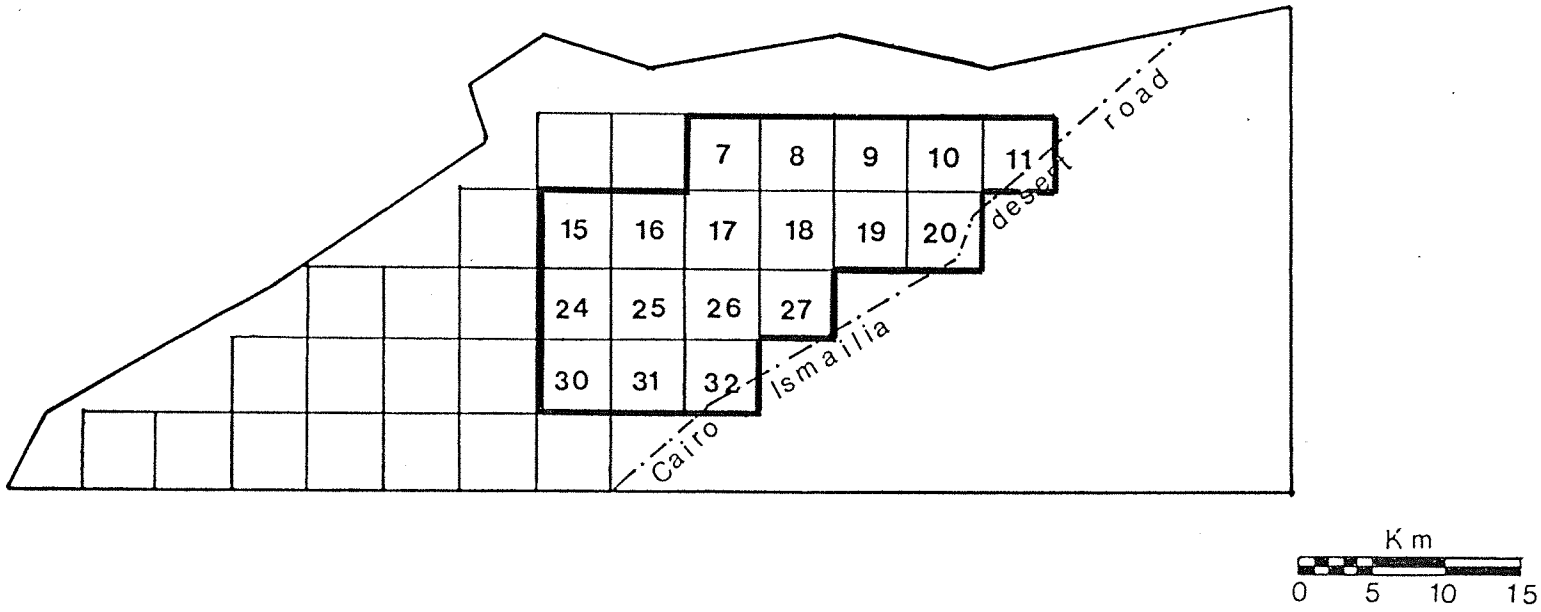

For each operating policy, the number of decision variables during a time step is equal to the number of production cells defining the physical space of the policy. Each decision variable represents the number of pumping units that could be withdrawn from a single production cell during a time step (as specified in the simulation model, a pumping unit is 10,000 cu.m/day, a time step is 15 days and a calender year is 24 time steps). In the case of variable demand, the decision variable in a cell varies from time step to another. This is expressed in the objective function using the demand density function adopted for the system. On the other hand, a constant demand means that the decision variable in a cell remains unchanged throughout the year. Using the maximum allowable capacity of a well and the arrangement of wells shown in Figure (7.5), in a single production cell (5 Km by 5 Km) the constraint imposed on the decision variables, i.e. that imposed on the number of pumping units (NPU) withdrawn from the cell during any time step, is expressed as

$$0 \leq NPU \leq 10$$

This means that the maximum number of pumping units to be assigned by the model in a single production cell is 10 units. Meanwhile, in the search for an optimal yield satisfying other imposed constraints the model is free to assign a zero output from any of the production cells contained by the physical space of the policy.

Maximising the output from the system to achieve an optimal yield involves essentially an increase in the inflow to the system and a reduction in the outflow from it. The increase in the inflow is to be gained by means of the induced recharge from the Ismailia Canal as well as the Nile Delta main aquifer. This recharge is governed in the model by the excitation-response relationship expressed by the interaction parameters. On the other hand, any reduction in

the system's outflow is a decision variable that should be assessed according to its effects on the system. The amount of allowed reduction in the outflow from the system is calculated such that all the outflow into the Ismailia Canal and part of the outflows into the Suez Canal could be withdrawn from the aquifer. Obviously any reduction in the outflow of fresh water to the Suez Canal will cause the existing interface to advance inland and its new position will depend on the allowed reduction. The relationship among the length of salt water intrusion, the outflow to the Suez Canal and the water table elevation above the toe point is expressed by equation (C.15) in Appendix C. Thus, allowing the interface to advance inland a maximum distance of 7.5 Km from its existing position, the resulting reduced outflow, calculated by using equation (C.15), amounts to 61,000 cu.m/day. Accordingly the maximum contribution from aquifer storage into the optimal yield is given by the difference between the natural inflow to the system and the reduced outflow. This difference yields an annual amount of 48.45 million cu.m. This amount is specified in the model as a constraint imposed on the quantity of water to be released from aquifer storage during the year.

The constraints imposed on the state variables of the system are expressed by specifying a value for the allowable drawdowns at the end of the one year management horizon for the 37 interval nodes defined by the simulation model. The contribution from aquifer storage and the extent of salt water intrusion are controlled by controlling the drawdowns in the system. Allowable drawdowns are specified such that water table elevation along the new position of the interface satisfies Ghyben-Herzberg relationship and the drop in groundwater levels at any internal node beyond the interface should not exceed one metre at the end of the year.

The management model is then used to calculate the optimal yield of the system and its quantitative distribution in time and space under the imposed constraints and for each of the alternative operating policies. The results obtained from the model analysis for the considered operating policies are presented in the next chapter.

7.4.3 Feedback Verification

Since the system is managed on intra-annual basis, the optimal yield determined by the management model for an operating policy is granted every year when the policy is implemented. However the resulting drawdowns and the position of the interface, which are necessarily less than or equal to the specified allowable values, describe only the state of the system at the end of the first year of operation. Obviously, changes in the state of the system will continue to take place every year until the steady state conditions are reached. This means that the steady conditions of the state variables for the alternative operating policies should also be assessed and checked against certain allowable limits. These allowable limits are set such that when the steady state conditions are reached the drawdowns at any internal node should not exceed three metres and the interface should not advance inland more than 15 kM from its initial position.

This is achieved via a feedback verification process. In this process, the output from the management model represented by the optimal yield calculated for an operating policy is used by the simulation model as an input to calculate the steady conditions of the state variables. The calculated steady state drawdowns and the location of the interface are then checked against the allowable limits mentioned above. If the allowable limits are not violated, then the output from the management model is satisfactory. On the other hand, the constraints imposed on the decision

and state variables of the system should be adjusted if the allowable limits are violated. Results of the feedback verification for the alternative operating policies are also presented in the next chapter.

CHAPTER 8

CASE STUDY: RESULTS OF THE MANAGEMENT MODEL ANALYSIS

8.1 Introduction

8.2 Optimal Solution
- 8.2.1 Operating Policy 1
- 8.2.2 Operating Policy 2
- 8.2.3 Operating Policy 3
- 8.2.4 Operating Policy 4

8.3 Feedback Verification
- 8.3.1 Steady State Drawdowns
- 8.3.2 Location of the Interface

8.4 Concluding Remarks

CHAPTER 8

CASE STUDY: RESULTS OF THE MANAGEMENT MODEL ANALYSIS

8.1 Introduction

Four alternative operating policies are considered in the hydraulic management of the stream-aquifer system south-east of the Nile Delta. Each operating policy is defined by a certain area of production in the system which is called the physical space of the policy. The optimal yield of the system, according to an operating policy, is determined by the model such that withdrawal from the aquifer will take place only within the area defined by the physical space of the policy.

The physical space of operating policy 1 covers the 35 production cells occupying the entire production zone described in Chapter 7. This means that the model in its search for the optimal solution is free to locate pumping from the aquifer in any of these 35 cells. The physical space of operating policy 2 is confined to the 10 production cells defining development area 1 in the eastern part of the system. The physical space of operating policy 3 comprises the 15 production cells covering development area 2 in the middle part of the system. The physical space of operating policy 4 encompasses the 18 production cells occupying development area 3 in the western part of the system.

The optimal yield of the system according to each operating policy is calculated by the management model on intra-annual basis where both conditions of variable and constant demands are considered in each policy. The model determines the quantitative distribution of the optimal yield in space and time. The distribution in space is determined by locating the operating cells, within the set

of production cells considered in an operating policy, which satisfy the optimal solution. The maximum quantity of water to be withdrawn from each operating cell during each time step is specified by the model and distributed in time according to the demand density function adopted for the condition of variable demand. Obviously, for the condition of constant demand the optimal yield will be uniformly distributed throughout the year.

The optimal yield determined by the model is introduced into the simulation model of the system as a feedback verification process to calculate the resulting steady state drawdowns and to check the extent of salt water intrusion. The optimal yield solution, according to an operating policy, is considered satisfactory if the regional steady state drawdown calculated at any internal node is less than three metres and the intruded length of the interface, measured from its initial position, is less than fifteen kilometres.

Results obtained from the model application and feedback verification for the alternative operating policies considered in the hydraulic management of the system are presented below.

8.2 Optimal Solution

8.2.1 Operating Policy 1

i - Variable demand

The optimal solution produced by the model indicates that the optimal yield, according to this policy under the condition of variable demand, is to be achieved by pumping from the eight operating cells shown in Figure (8.1). The optimal yield supplied by pumping from these cells amounts

Fig. 8.1 Operating Cells

Policy 1

-variable demand-

118.9 Million m^3/year

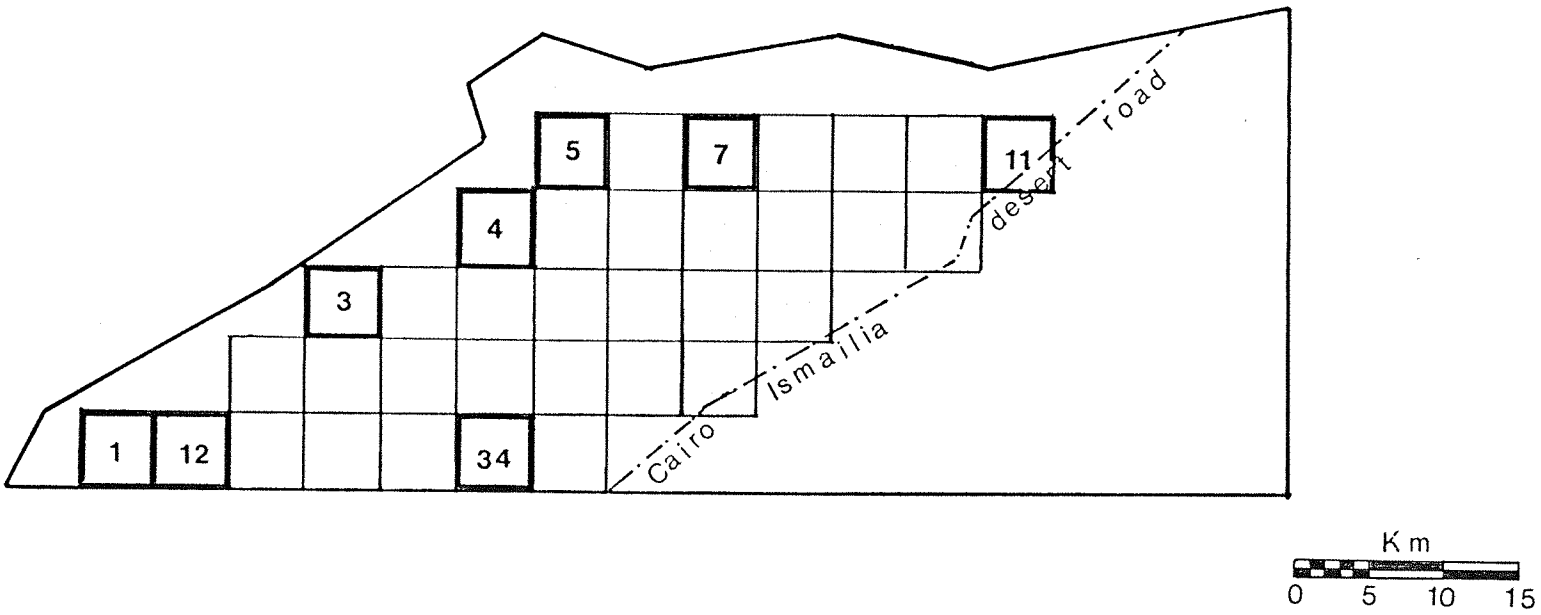

to 118.9 million cu.m. per year. Quantitative distributions of pumping determined by the model over the year are shown in Table (8.1). Results of the model analysis show that the policy permits the optimal yield to include the entire allowable contribution from aquifer storage specified in the model (48.45×10^6 m^3/year). Accordingly, the annual quantity of water diverted from the Ismailia Canal into the aquifer amounts to 70.45 million cu.m. This means that about 59% of the optimal yield is supplied directly from induced recharge by the stream-aquifer interaction during pumping. Figure (8.2) shows the intra-annual contributions to the optimal yield from the aquifer storage and the induced recharge due to pumping from the operating cells.

ii - Constant demand

The optimal solution according to operating policy 1 under the condition of constant demand is achieved by pumping from the ten operating cells as shown in Figure (8.3). The annual optimal yield of the system in this case amounts to 108.98 million cu.m. Optimal pumping rates from these cells are given in Table (8.2). Although this optimal yield is 8.34% less than that determined under the condition of variable demand, the contribution from aquifer storage remains unchanged. Thus the contribution to the optimal yield from induced recharge by the stream-aquifer interaction during pumping amounts to 60.53 million cu.m. per year. This means that about 55% of the optimal yield is diverted from the Ismailia Canal into the aquifer during pumping.

	Optimal Pumping Rates x 10^3 m^3/day							
Month	Cell 1	Cell 3	Cell 4	Cell 5	Cell 7	Cell 11	Cell 12	Cell 34
Jan	32.39	29.65	8.29	15.49	14.54	17.35	31.18	18.02
Feb	38.41	35.16	9.82	18.37	17.24	20.58	36.97	21.37
Mar	48.25	44.16	12.34	23.08	21.65	25.85	46.44	26.85
Apr	82.89	75.87	21.20	39.64	37.20	44.41	79.78	46.12
May	100.00	91.53	25.58	47.82	44.88	53.58	96.25	55.64
Jun	89.64	82.05	22.93	42.87	40.23	48.02	86.28	49.87
Jul	85.27	78.05	21.81	40.78	38.26	45.68	82.07	47.44
Aug	77.58	71.01	19.85	37.10	34.81	41.56	74.67	43.16
Sept	73.85	67.60	18.89	35.32	33.14	39.57	71.08	41.09
Oct	62.18	56.69	15.91	29.74	27.90	33.31	59.85	34.60
Nov	40.98	37.51	10.48	19.60	18.39	21.96	39.44	22.80
Dec	37.70	34.51	9.64	18.03	16.92	20.20	36.29	20.98

Table (8.1) Optimal pumping rates under variable demand conditions, Policy 1

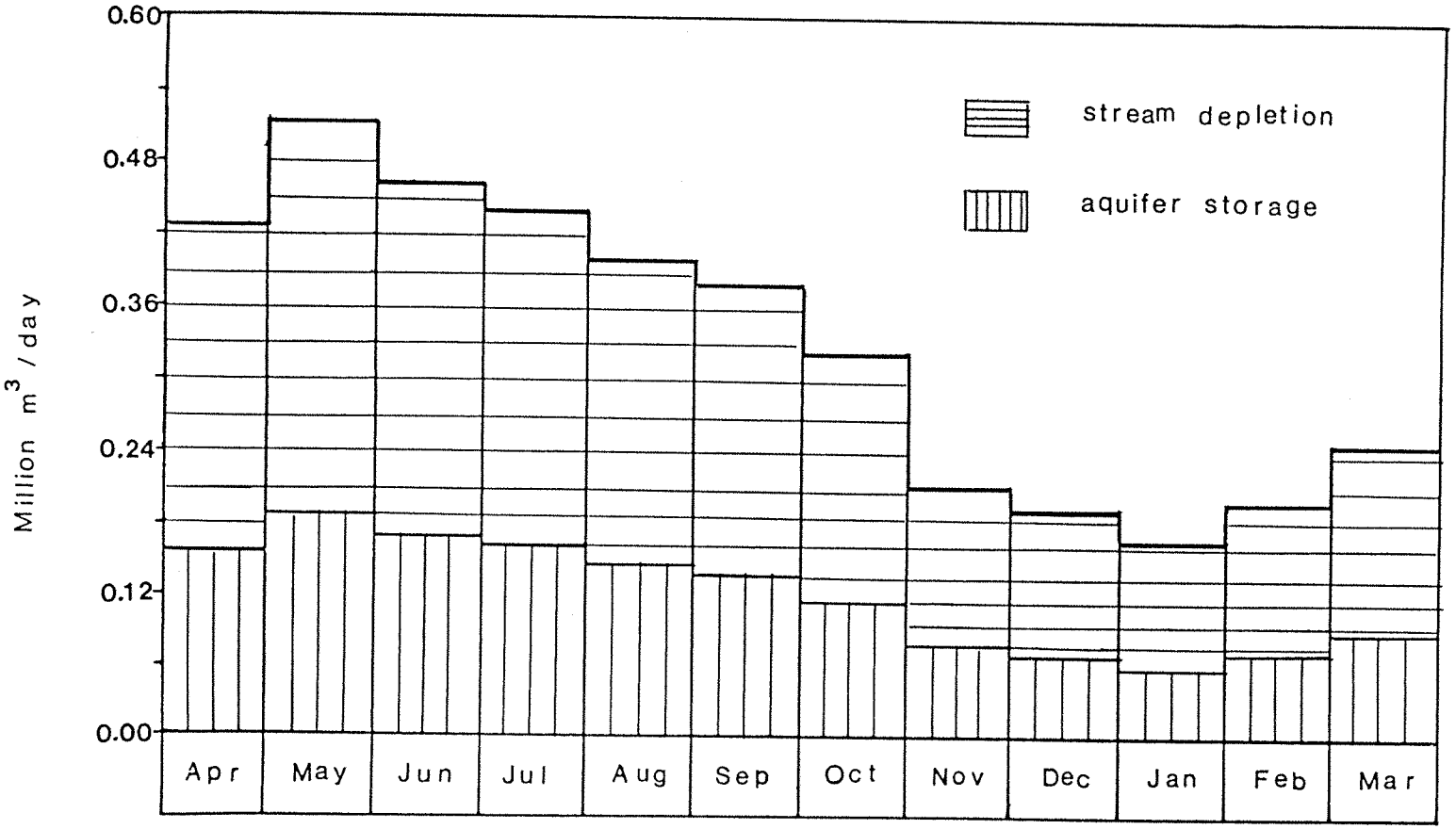

Fig. 8.2 Distribution of the Optimal Yield – policy 1, variable demand –

Fig. 8.3 Operating Cells

Policy 1

-constant demand-

108.98 Million m^3/year

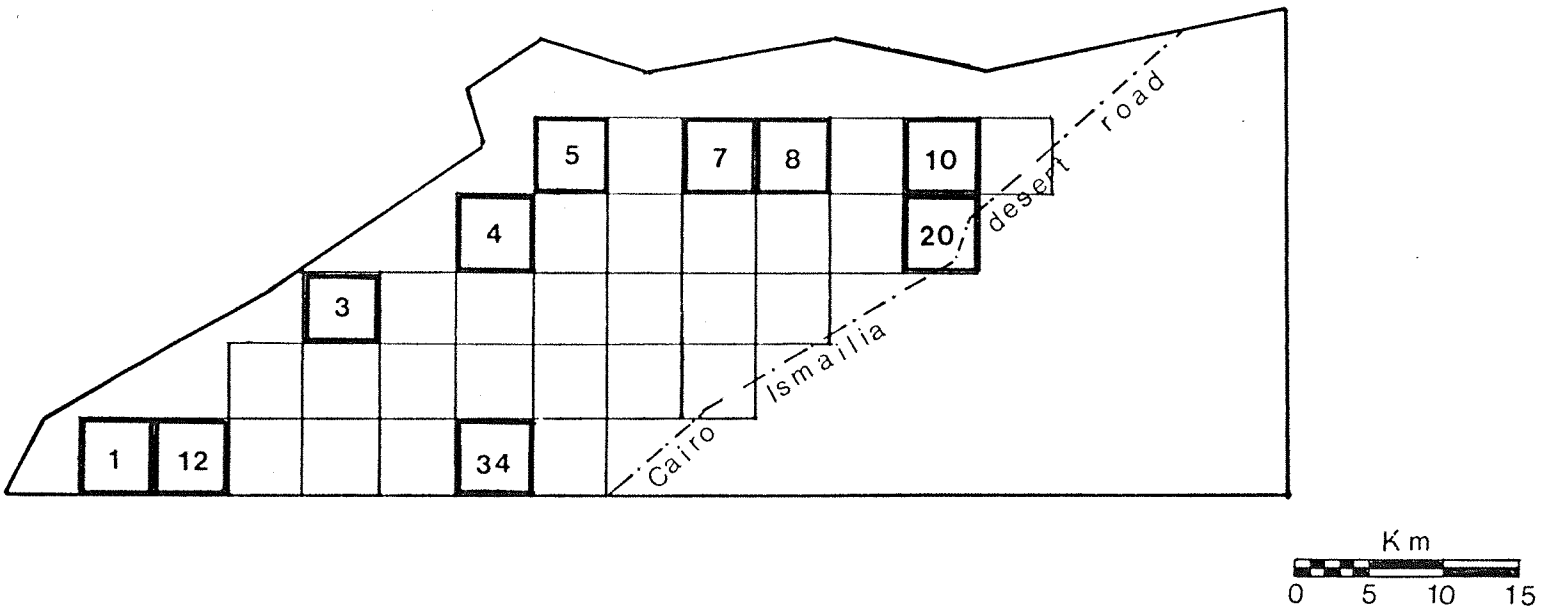

Cell No	Optimal Pumping Rates$\times 10^3$ m^3/day
1	100.00
3	42.89
4	46.07
5	22.77
7	18.69
8	6.15
10	14.30
12	30.95
20	34.84
34	27.55

Table (8.2) Optimal pumping rates under constant demand condition, Policy 1

8.2.2 Operating Policy 2

i - Variable demand

The optimal solution is fulfilled by pumping from the five operating cells shown in Figure (8.4). The annual optimal yield determined by the model is 79.86 million cu.m. Quantitative distributions of the pumping from these cells over the year are given in table (8.3). The policy under this condition permits an annual amount of 29.67 million cu. m. to be withdrawn from the aquifer storage. This amount represents only about 61% of the allowable contribution from aquifer storage specified in the model. Accordingly, 50.19 million cu.m. per year are supplied directly from induced recharge by the stream-aquifer interaction, i.e. about 63% of the optimal yield is diverted from the Ismailia Canal into the aquifer during pumping. The contributions from aquifer storage and induced recharge are illustrated in Figure (8.5).

Fig. 8.4 Operating Cells

Policy 2

-variable demand-

79.86 Million m^3/year

-constant demand-

70.48 Million m^3/year

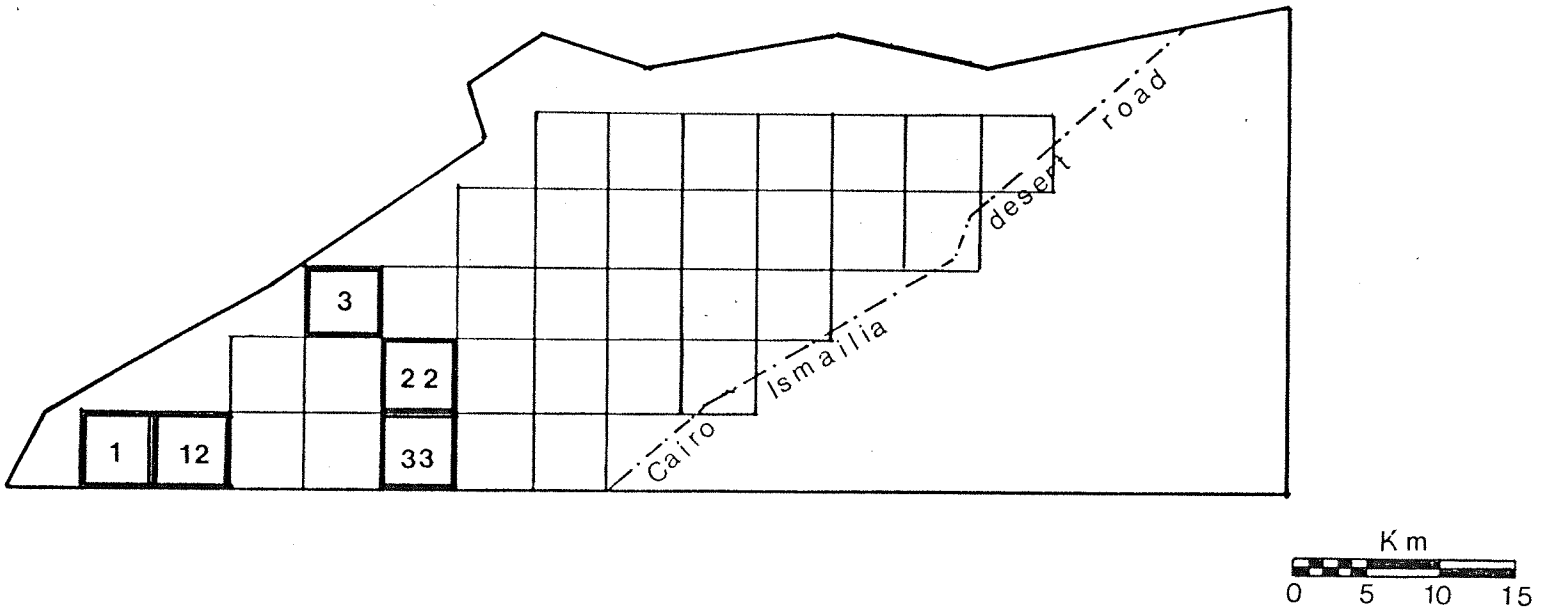

	Optimal Pumping Rates x 10^3 m^3/day				
Month	Cell 1	Cell 3	Cell 12	Cell 22	Cell 33
Jan	32.40	29.96	30.2	10.14	9.40
Feb	38.41	35.53	35.8	12.02	11.19
Mar	48.25	44.63	45.0	15.10	14.05
Apr	82.89	76.67	77.2	25.94	24.14
May	100.00	92.50	93.2	31.30	29.12
Jun	89.64	82.92	83.5	28.06	26.10
Jul	85.27	78.88	79.4	26.69	24.83
Aug	77.58	71.76	72.2	24.28	22.60
Sept	73.85	68.31	68.8	23.11	21.51
Oct	62.18	57.52	58.0	19.46	18.11
Nov	40.98	37.91	38.2	12.83	11.93
Dec	37.70	34.87	35.1	11.80	10.98

Table (8.3) Optimal pumping rates under variable demand conditions, Policy 2

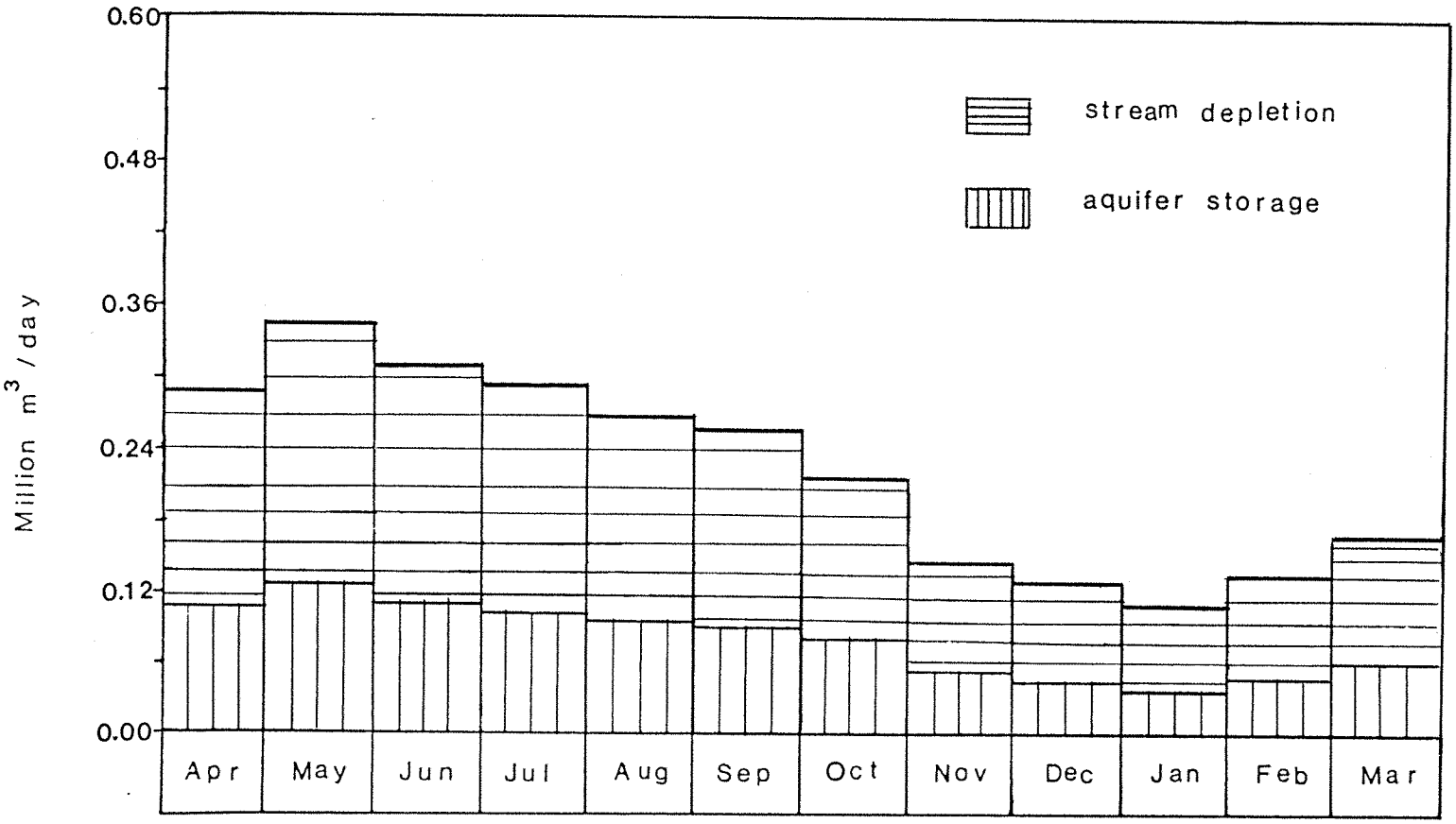

Fig. 8.5 Distribution of the Optimal Yield – policy 2, variable demand –

ii - Constant demand

The optimal solution is achieved under this condition by pumping from the same operating cells located by the model for the condition of variable demand as shown in Figure (8.4). The optimal yield determined by the model in this case is 70.48 million cu.m. per year, i.e.about 11.7% less than that determined under the condition of variable demand. Optimal pumping rates from these cells are given in Table (8.4). The optimal solution permits 24.46 million cu. m. to be withdrawn annually from the aquifer storage. This quantity represents only about 50% of the allowable contribution from aquifer storage specified in the model. The contribution from induced recharge by the stream-aquifer interaction amounts to 46.02 million cu.m. per year, i.e. about 65% of the optimal yield is diverted from the Ismailia Canal into the aquifer during pumping.

Cell No	Optimal Pumping Ratesx10^3 m^3/day
1	100.00
3	43.64
12	30.93
22	15.22
33	6.00

Table (8.4) Optimal pumping rates under constant demand conditions, Policy 2

8.2.3 Operating Policy 3

i - Variable demand

The model locates six operating cells according to this policy as shown in Figure (8.6). The annual optimal yield supplied by pumping from these cells is 79.15 million cu.m. Quantitative distributions of the pumping during the

Fig. 8.6 Operating Cells

Policy 3

-variable demand-

79.15 Million m^3/year

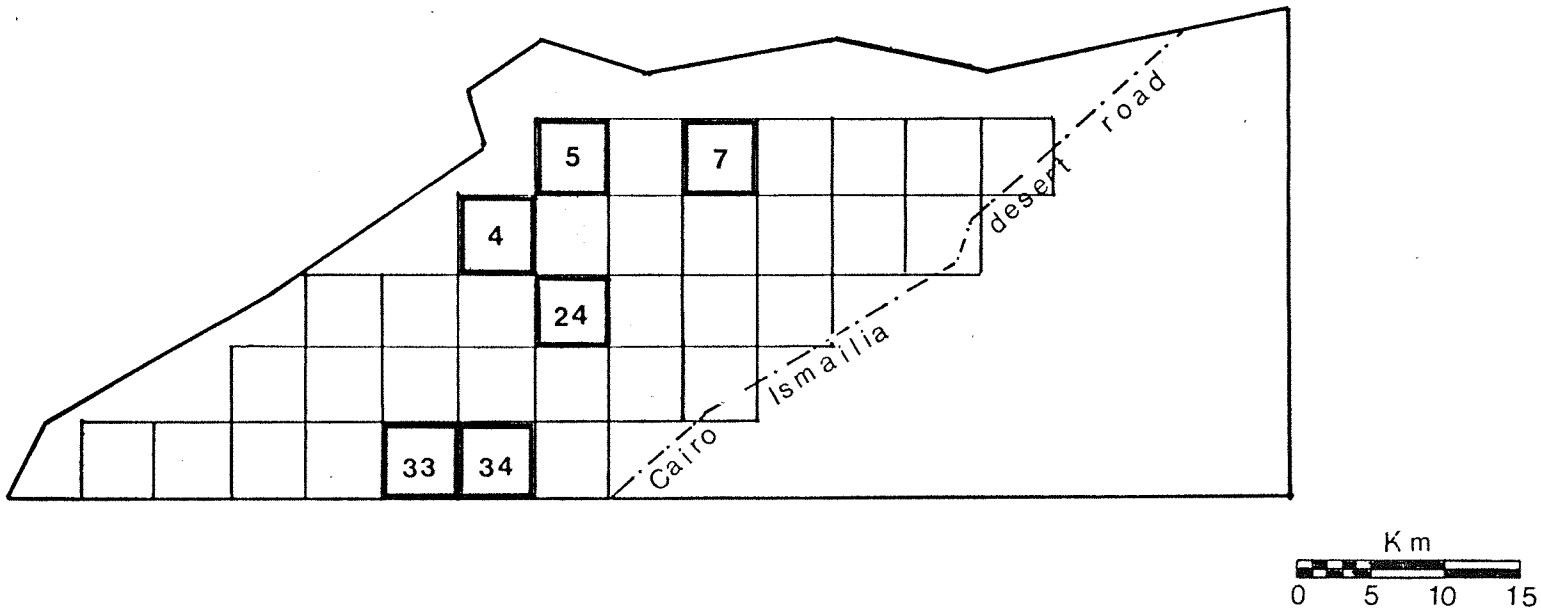

Month	Optimal Pumping Rates x 10^3 m^3/day					
	Cell 4	Cell 5	Cell 7	Cell 24	Cell 33	Cell 34
Jan	3.48	16.17	16.07	10.61	32.40	32.39
Feb	4.13	19.17	19.06	12.58	38.41	38.41
Mar	5.21	24.08	23.94	15.80	48.25	48.25
Apr	8.91	41.37	41.13	27.15	82.89	82.89
May	10.75	49.92	49.62	32.75	100.00	100.00
Jun	9.64	44.74	44.48	29.36	89.64	89.64
Jul	9.17	42.56	42.31	27.93	85.27	85.27
Aug	8.34	38.72	38.49	25.41	77.58	77.58
Sept	7.94	36.86	36.64	24.19	73.85	73.85
Oct	6.68	31.04	30.85	20.37	62.18	62.18
Nov	4.41	20.46	20.33	13.42	40.98	40.98
Dec	4.05	18.82	18.71	12.35	37.70	37.70

Table (8.5) Optimal pumping rates under variable demand conditions, Policy 3

year are given in Table (8.5). The policy permits the optimal yield to include the entire allowable contribution from aquifer storage specified in the model ($48.45 \times 10^6 m^3$/year). Thus, 30.7 million cu.m. per year are supplied directly from the induced recharge, i.e. about 39% of the optimal yield is diverted from the Ismailia Canal during pumping. The contributions from aquifer storage and induced recharge to the optimal yield are shown in Figure (8.7).

ii - Constant demand

The optimal solution is achieved by pumping from the four operating cells shown in Figure (8.8). The annual optimal yield withdrawn from these cells amounts to 66.04 million cu.m. The entire allowable contribution from aquifer storage specified in the model is induced in the optimal yield. Optimal pumping rates from the located cells are given in Table (8.6). The solution indicates that the quantity supplied from induced recharge is 17.59 million cu. m. per year, i.e. about 27% of the optimal yield is diverted from the Ismailia Canal into the aquifer during pumping.

Cell No	Optimal Pumping Rates $\times 10^3$ m^3/day
5	26.48
7	24.91
33	32.05
34	100.00

Table (8.6) Optimal pumping rates under constant demand conditions, Policy 3

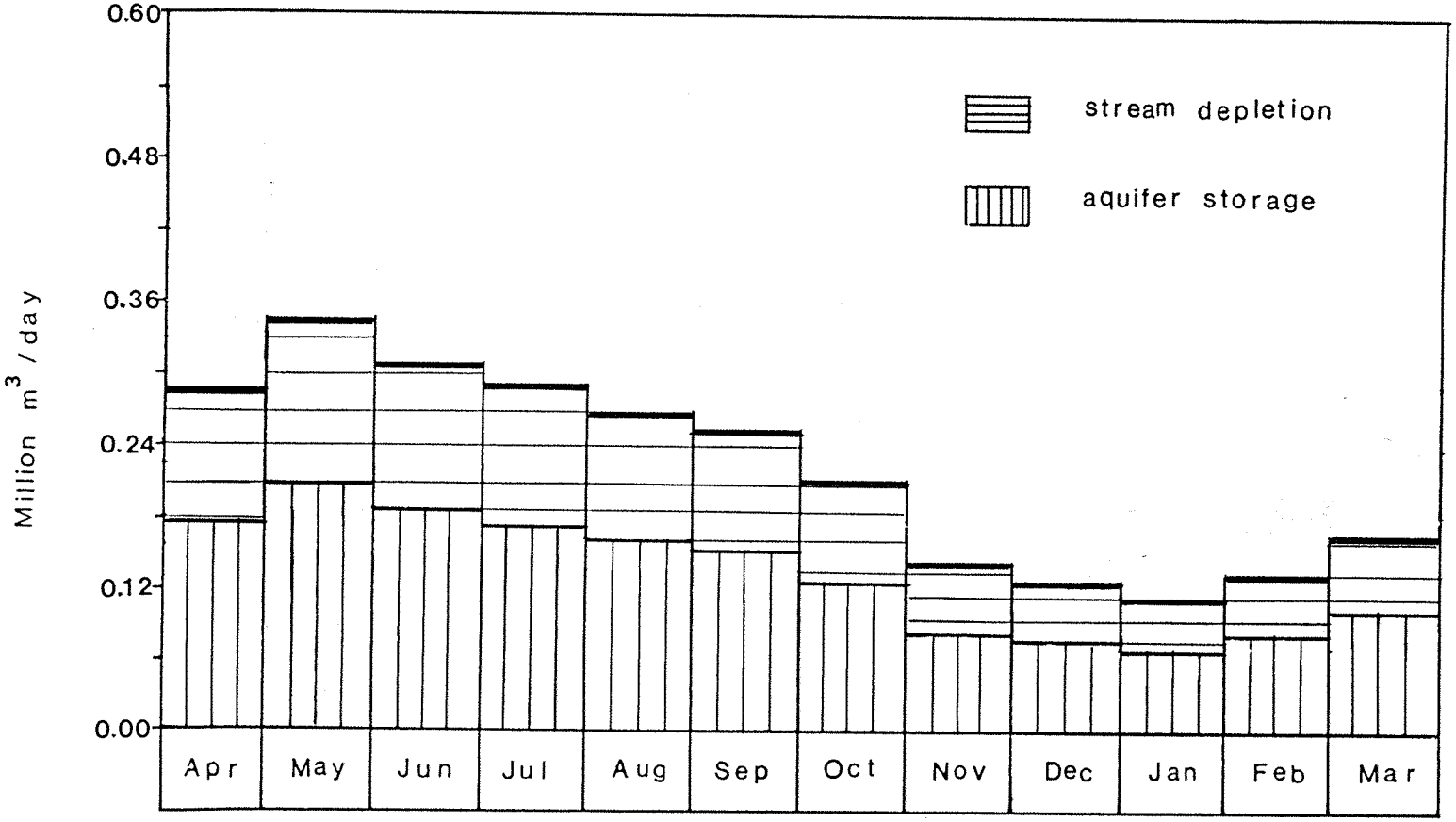

Fig. 8.7 Distribution of the Optimal Yield – policy 3, variable demand –

Fig. 8.8 Operating Cells

Policy 3

-constant demand-

66.04 Million m^3/year

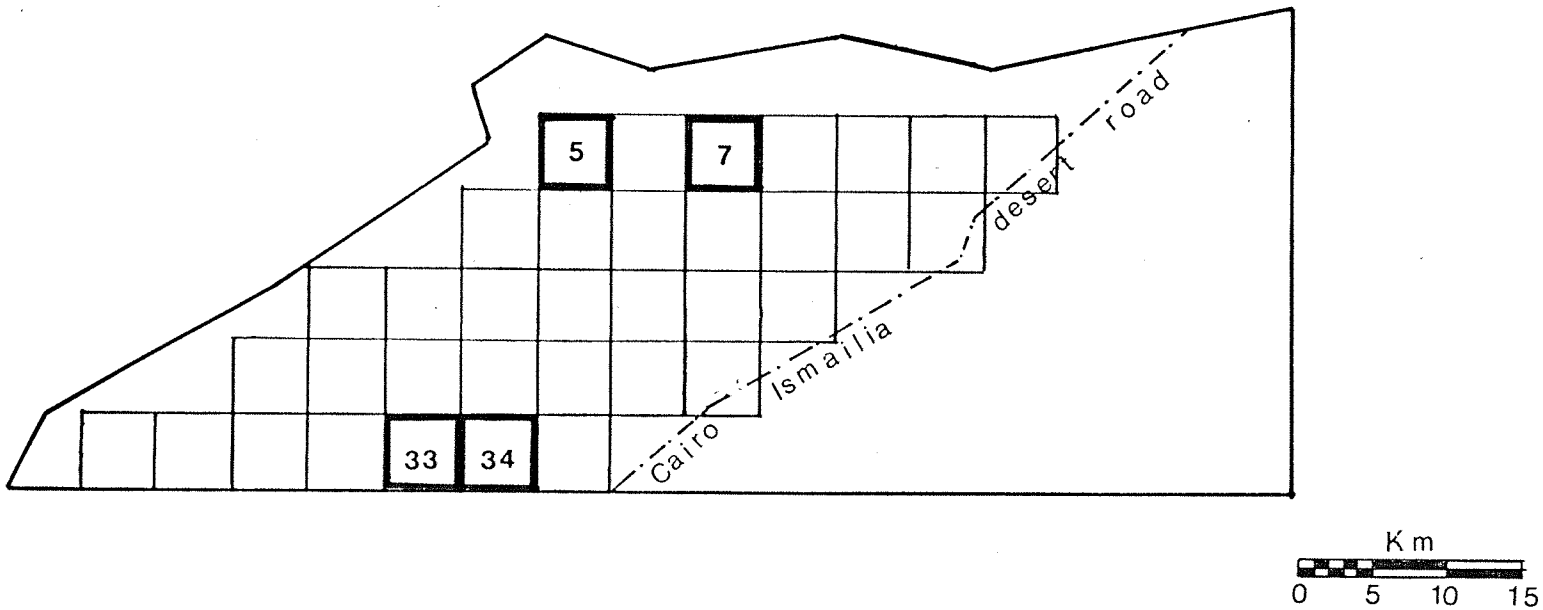

8.2.4 Operating Policy 4

i - Variable demand

The optimal solution is achieved by pumping from the seven operating cells shown in Figure (8.9). The annual optimal yield supplied by pumping from these cells is 71.20 million cu.m. Quantitative distributions of the pumping over the year are shown in Table (8.7). The optimal yield under this condition is permitted to include all the allowable contribution from aquifer storage specified in the model. The quantity supplied from the induced recharge amounts to 22.75 million cu.m. per year, i.e. about 32% of the optimal yield is diverted into the aquifer from the Ismailia Canal during pumping. Figure (8.10) illustrates the contributions from aquifer storage and induced recharge to the optimal yield.

ii - Constant demand

Five operating cells are located by the model under this condition as shown in Figure (8.11). The annual optimal yield determined by the model is 61.22 million cu.m. About 96% of the allowable contribution from aquifer storage specified in the model is included in the optimal yield. Optimal pumping rates from the located cells are given in Table (8.8). The quantity supplied from induced recharge is 14.94 million cu.m. per year, i.e. about 24% of the optimal yield is diverted from the Ismailia canal into the aquifer during pumping.

Fig. 8.9 Operating Cells

Policy 4

-variable demand-

71.2 Million m^3/year

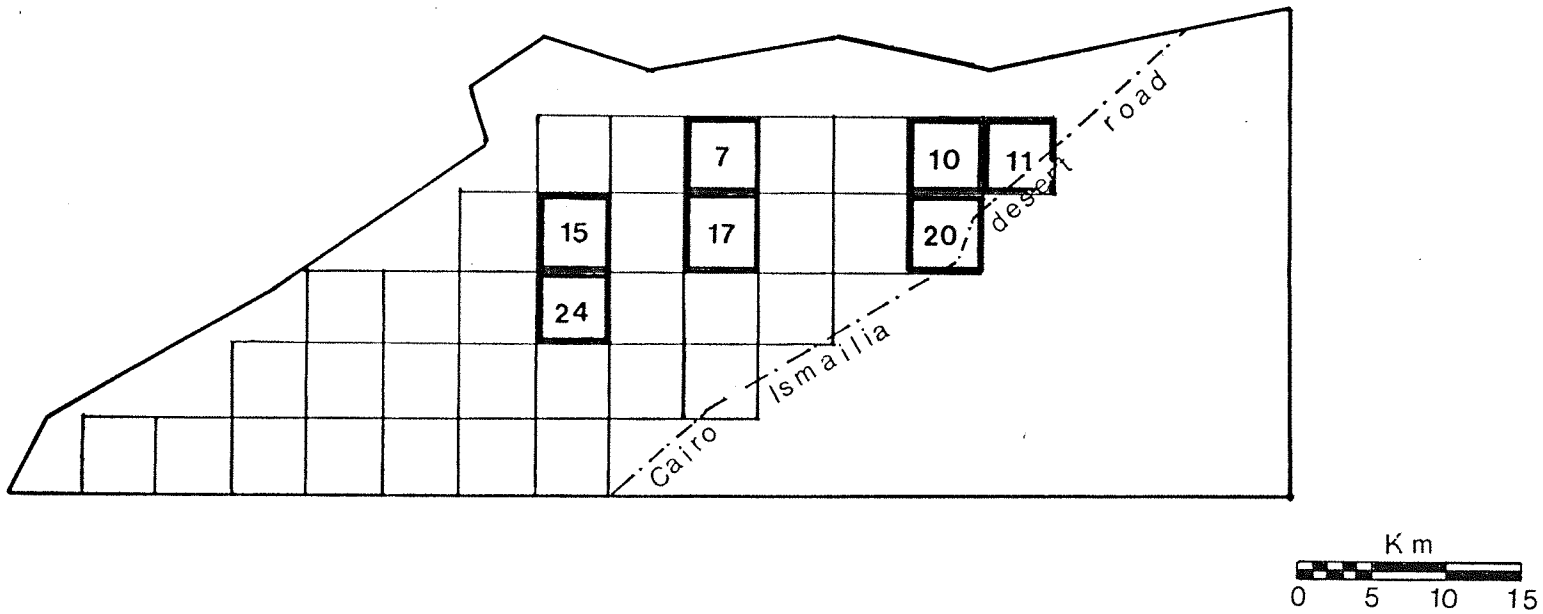

	Optimal Pumping Rates x 10^3 m^3/day						
Month	Cell 7	Cell 10	Cell 11	Cell 15	Cell 17	Cell 20	Cell 24
Jan	2.74	4.67	8.13	6.62	26.10	19.31	32.40
Feb	3.25	5.54	9.64	7.85	30.95	22.90	38.41
Mar	4.08	6.96	12.11	9.86	38.87	28.76	48.25
Apr	7.01	11.95	20.81	16.94	66.78	49.41	82.89
May	8.46	14.42	25.10	20.44	80.57	59.61	100.00
Jun	7.58	12.92	22.50	18.32	72.22	53.43	89.64
Jul	7.21	12.30	21.40	17.43	68.70	50.83	85.27
Aug	6.56	11.18	19.47	15.85	62.50	46.24	77.58
Sept	6.25	10.65	18.54	15.09	50.10	44.02	73.85
Oct	5.26	8.96	15.61	12.71	33.02	37.06	62.18
Nov	3.47	5.91	10.29	8.37	30.37	24.43	40.98
Dec	3.19	5.43	9.46	7.70	26.10	22.47	37.70

Table (8.7) Optimal pumping rates under variable demand conditions, Policy 4

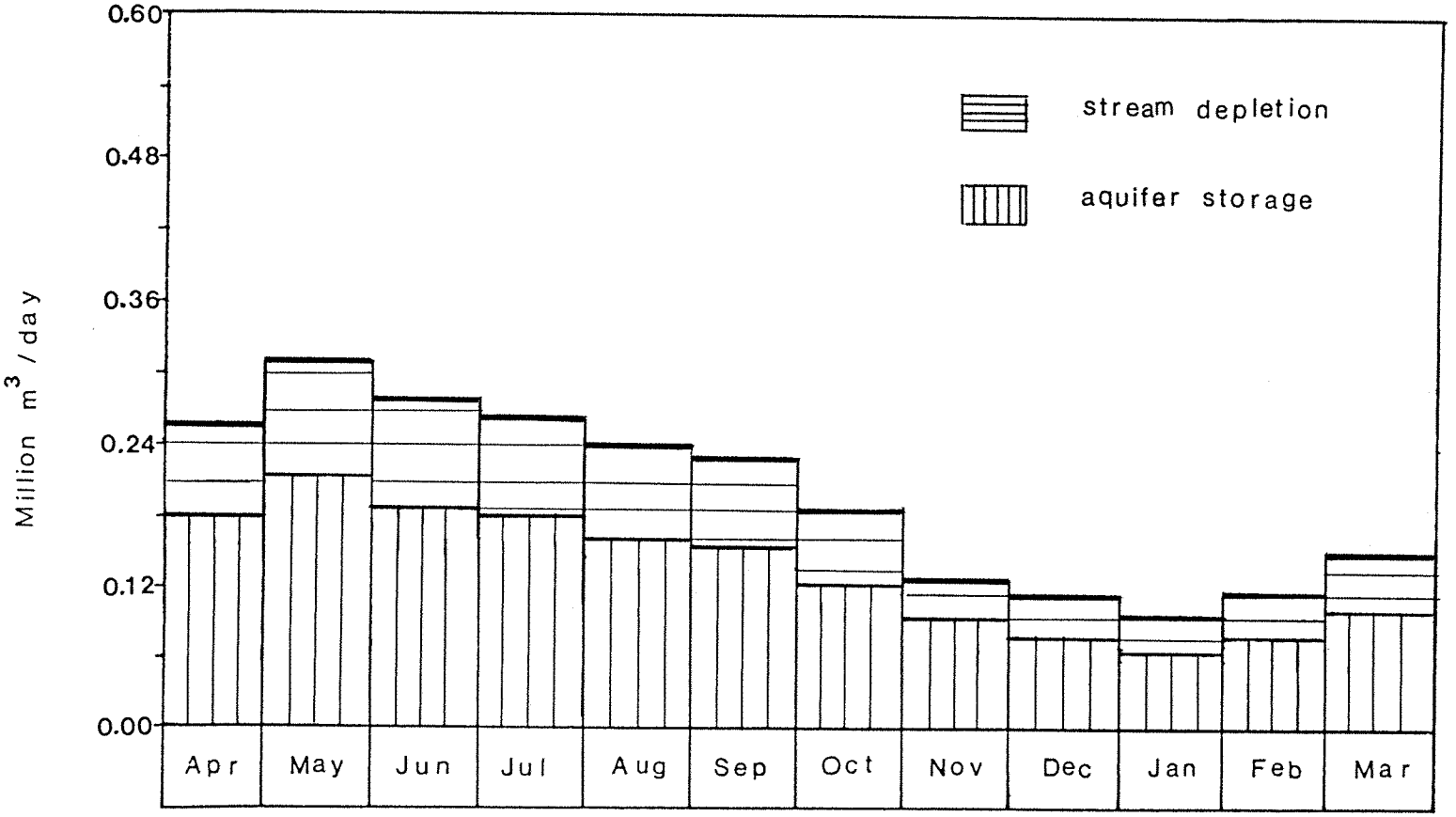

Fig. 8.10 Distribution of the Optimal Yield – policy 4, variable demand –

Fig. 8.11 Operating Cells

Policy 4

-constant demand-

61.22 Million m^3/year

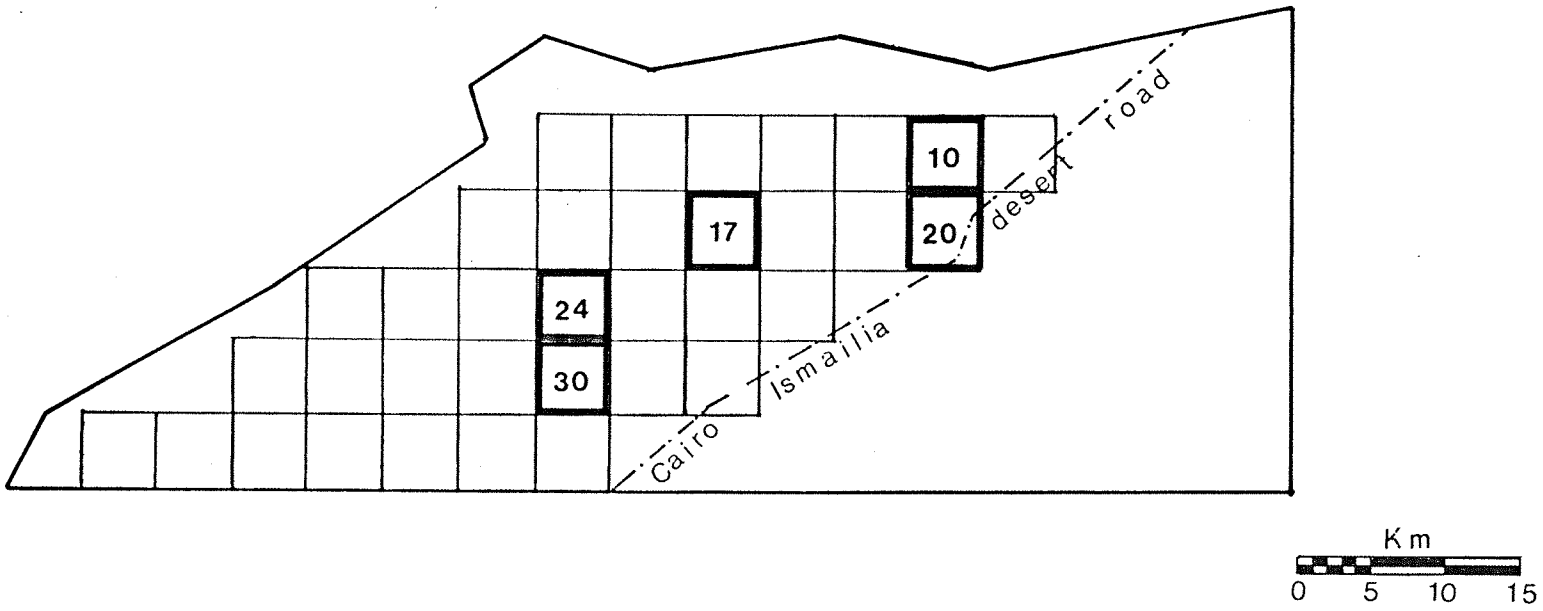

Cell No	Optimal Pumping Ratesx10^3 m^3/day
10	16.59
17	41.53
20	35.50
24	61.63
30	14.82

Table (8.8) Optimal pumping rates under constant demand conditions, Policy 4

8.3 Feedback Verification

8.3.1 Steady-State Drawdowns

Figures (8.12) to (8.19) show contour maps of the steady-state groundwater levels resulting from the considered operating policies. Results of the feedback verification shows that operating policy 1 and operating policy 2 do not violate the specified allowable steady-state drawdown. On the other hand steady-state drawdowns resulting from operating policy 3 and operating policy 4 exceed the three metres allowable limit at several internal nodes.

The fact that operating policies 3 and 4 do not comply with the allowable drawdown condition suggests that, under the constraints imposed originally on the state and decision variables of the system, operating policies 1 and 2 are the only possible alternative policies to operate the system.

8.3.2 Location of the Interface

The fresh water-salt water interface resulting from each operating policy in the steady state conditions is shown on the contour maps of groundwater levels Figures (8.12) to (8.19). For operating policy 1 under both conditions of variable and constant demand the intruded length of the interface, measured from its initial position,

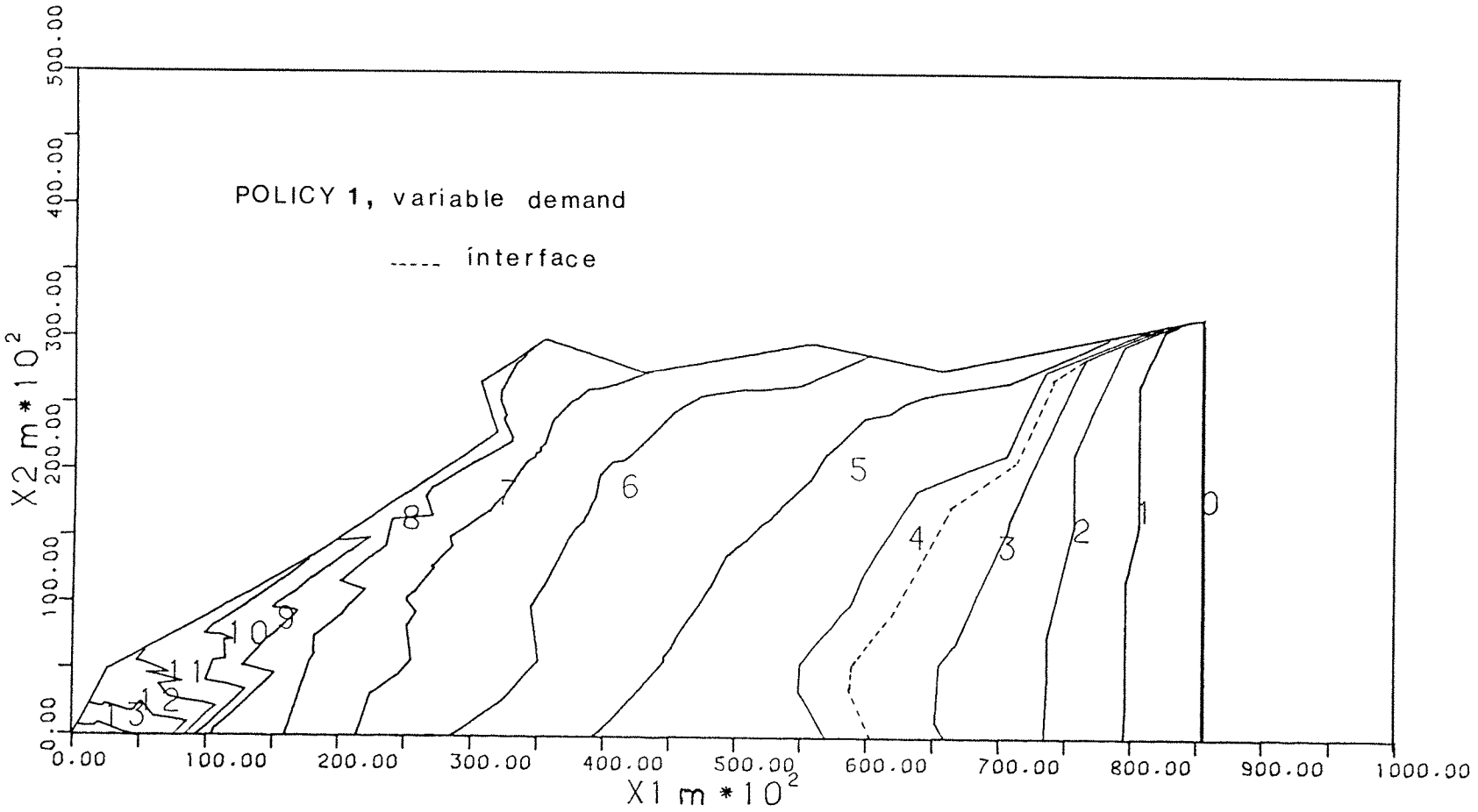

Fig. 8.12 CONTOUR MAP OF CALCULATED GROUNDWATER HEADS

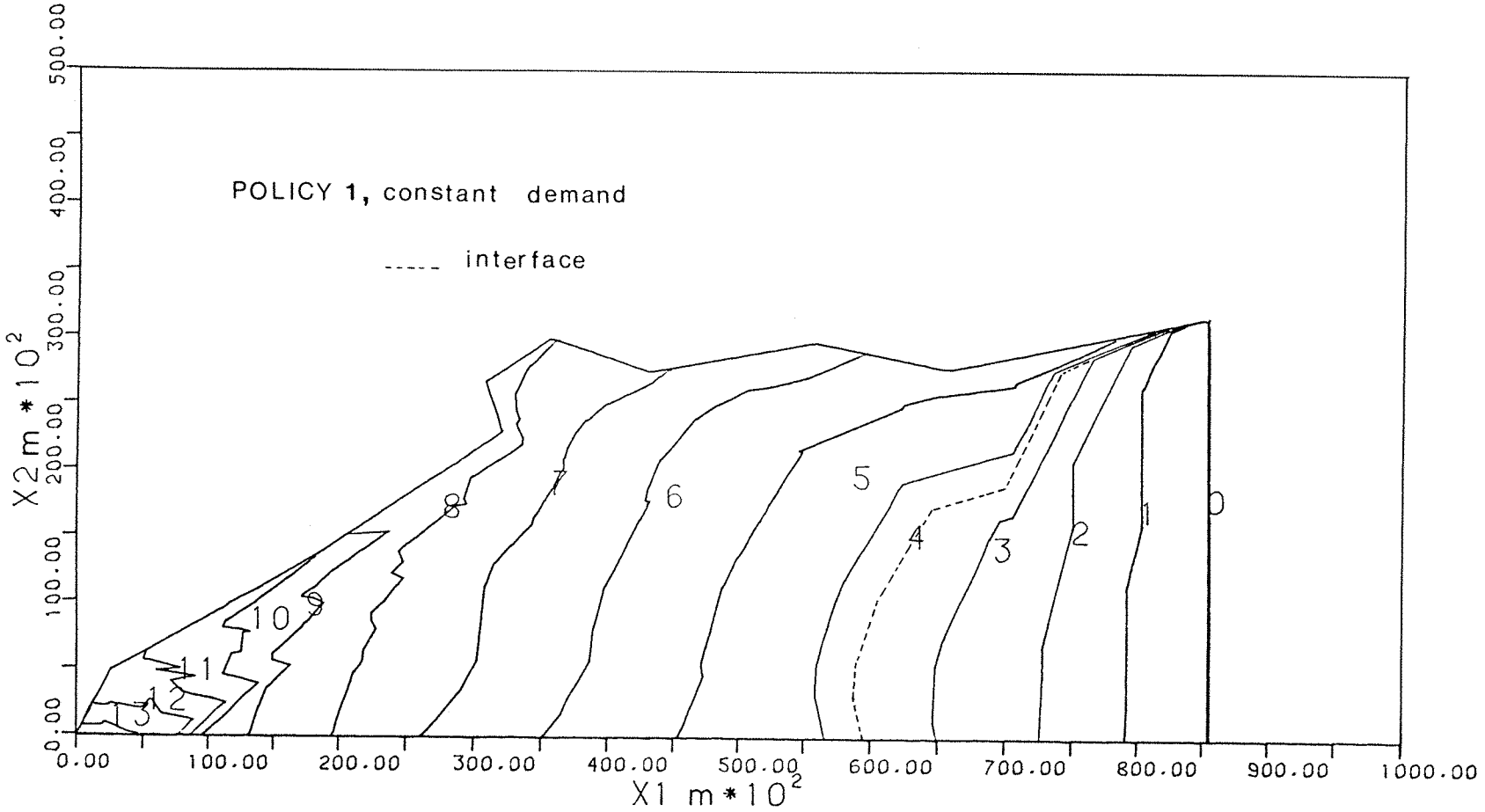

Fig. 8.13 CONTOUR MAP OF CALCULATED GROUNDWATER HEADS

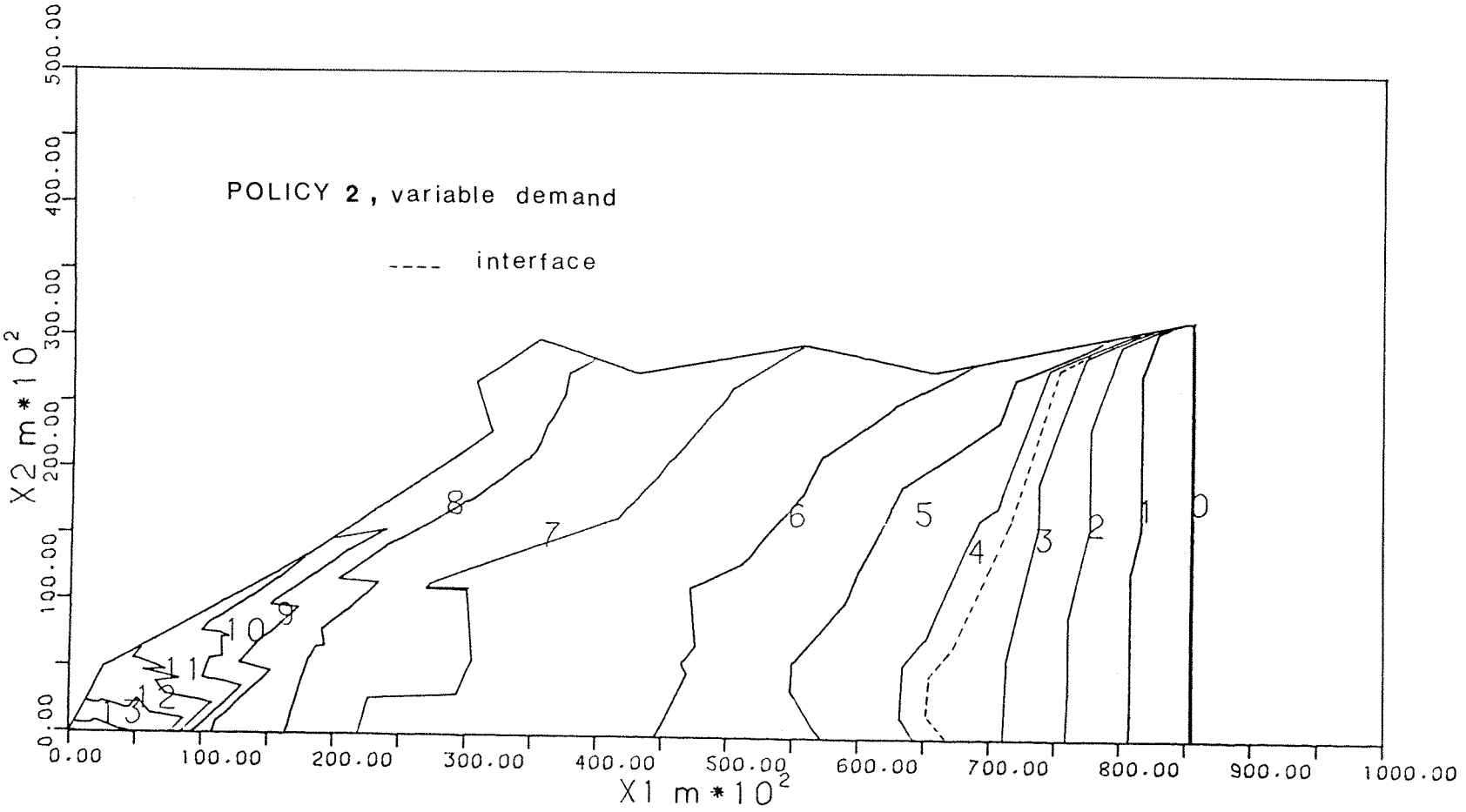

Fig. 8.14 CONTOUR MAP OF CALCULATED GROUNDWATER HEADS

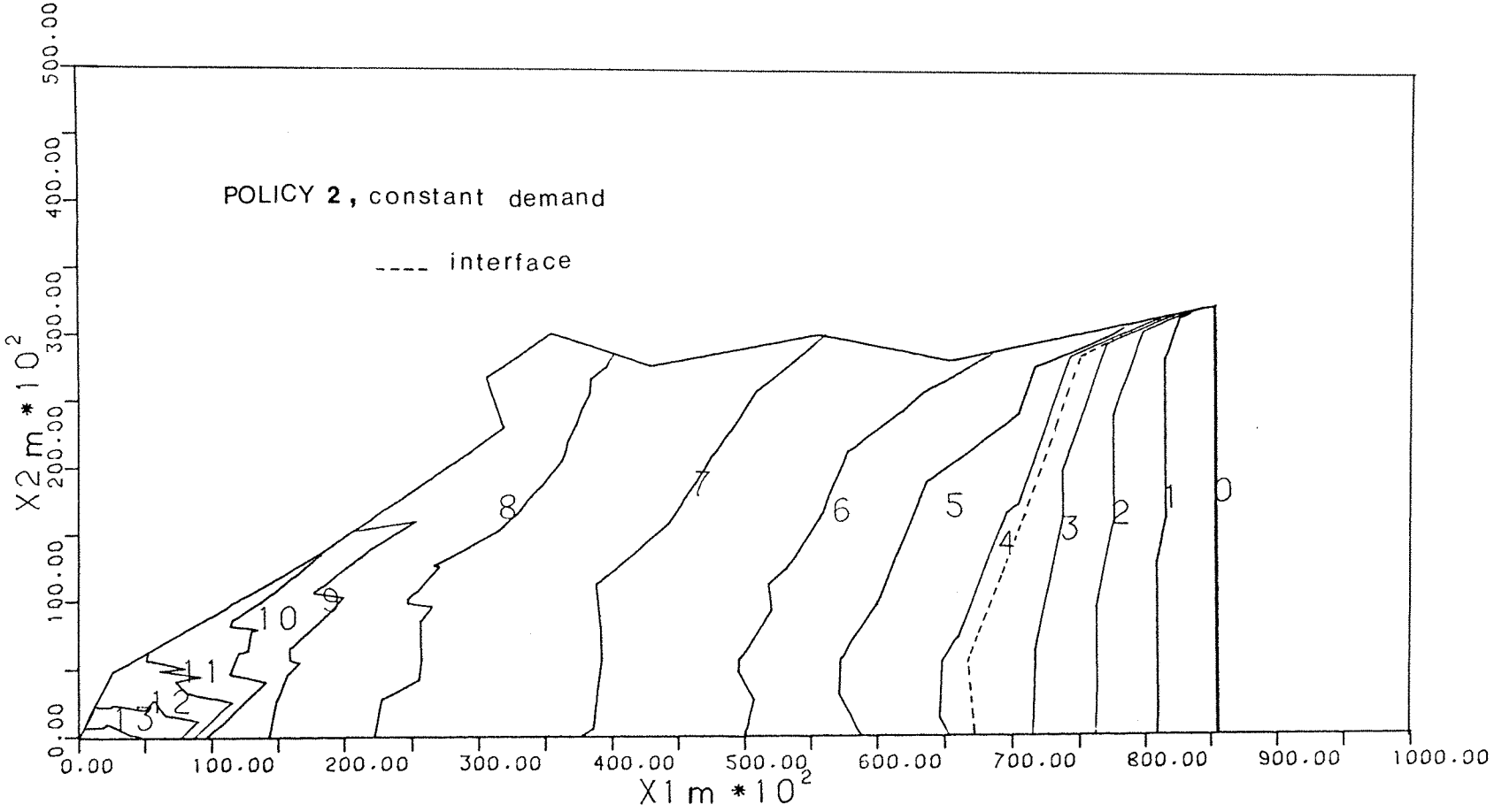

Fig. 8.15 CONTOUR MAP OF CALCULATED GROUNDWATER HEADS

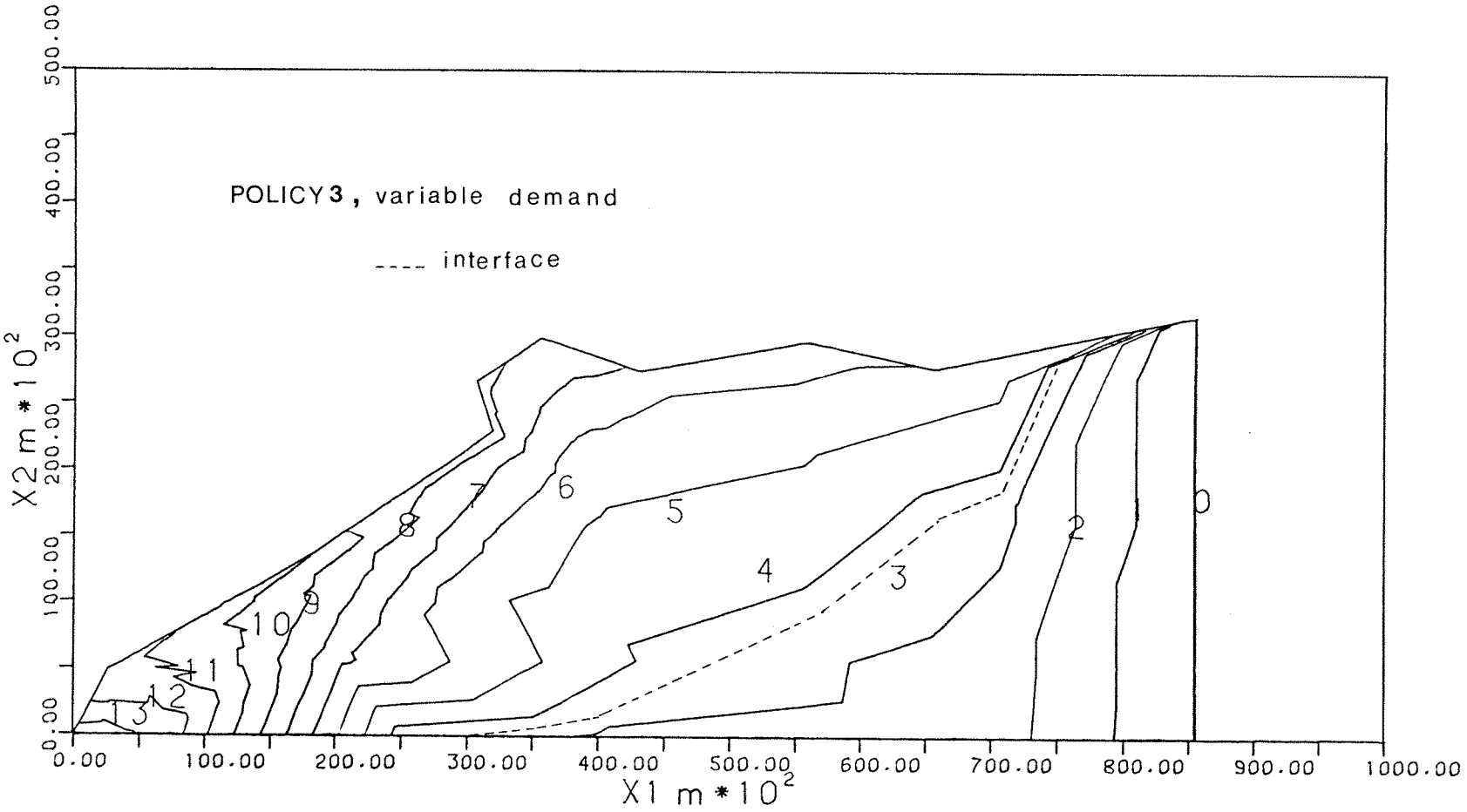

Fig. 8.16 CONTOUR MAP OF CALCULATED GROUNDWATER HEADS

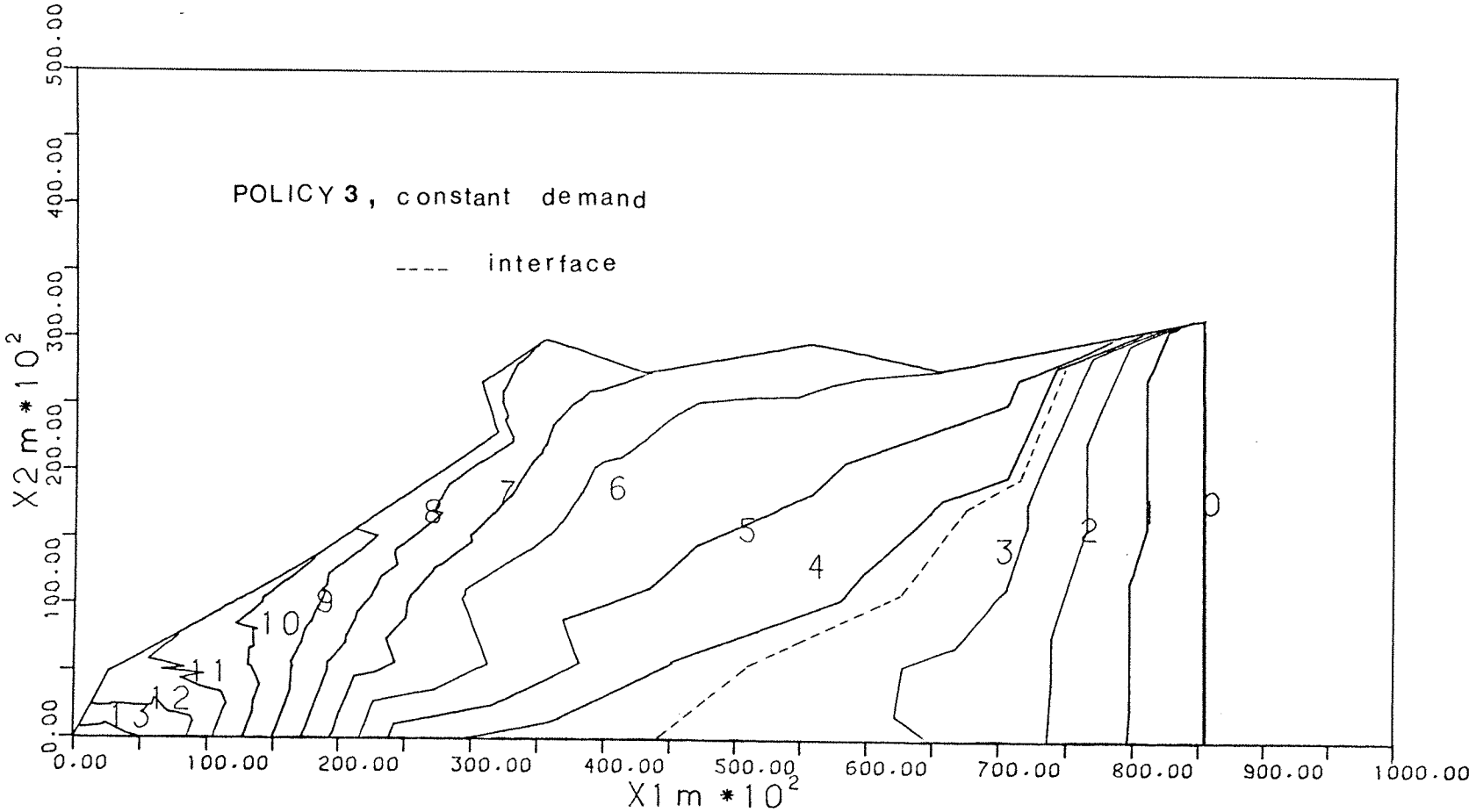

Fig. 8.17 CONTOUR MAP OF CALCULATED GROUNDWATER HEADS

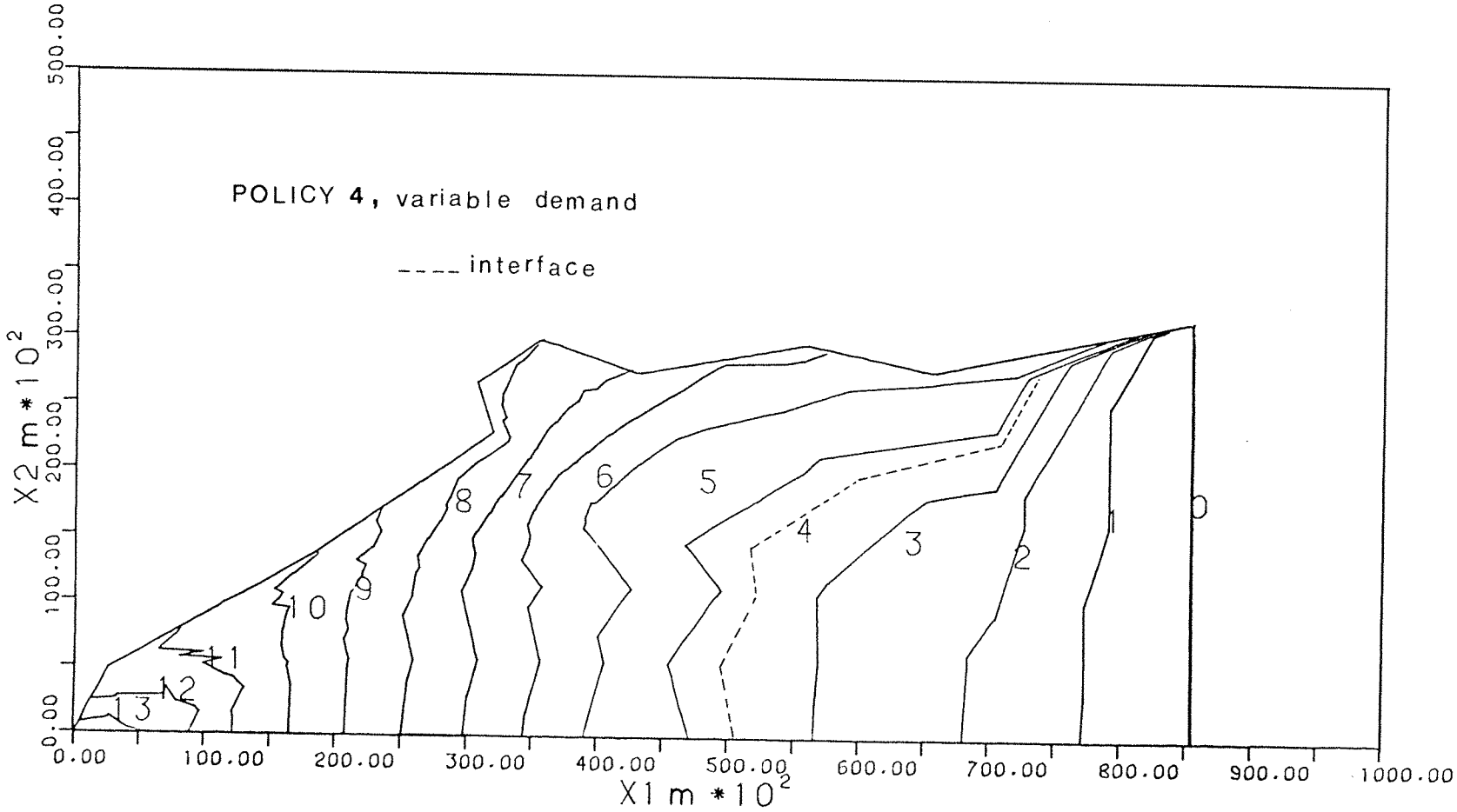

Fig. 8.18 CONTOUR MAP OF CALCULATED GROUNDWATER HEADS

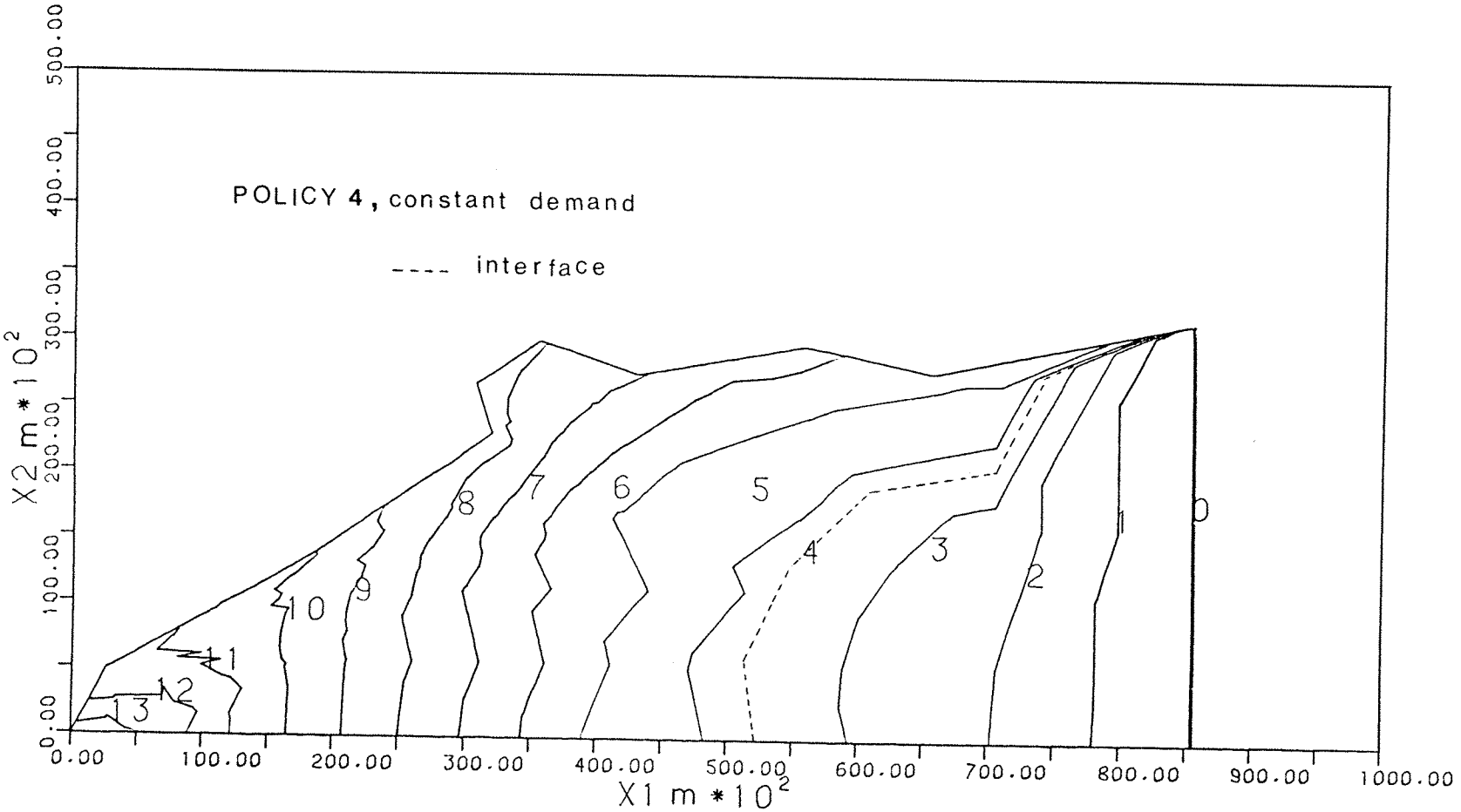

Fig. 8.19 CONTOUR MAP OF CALCULATED GROUNDWATER HEADS

is 12.5 kilometres. For operating policy 2, under the condition of variable demand the intruded length of the interface is 6.25 kilometres whereas under the condition of constant demand the intruded length is 5.0 kilometres. For operating policy 3 the intruded lengths are 42.5 kilometres and 30.0 kilometres for the conditions of variable and constant demand, respectively. For operating policy 4 the intruded length under the condition of variable demand is 22.5 kilometres and under the condition of constant demand it is 20.0 kilometres. These results show that operating policies 1 and 2 comply with the specified limitation on the resulting salt water intrusion whereas policies 3 and 4 violate drastically this limit.

8.4 Concluding Remarks

If the success of the considered four operating policies is to be assessed by their optimal yield determined by the model they will be ranked in the same order as they are numbered. However the feedback verification analysis shows that operating policies 3 and 4 violate drastically the specified steady state limitations on drawdowns and salt water intrusion. Therefore, operating policies 3 and 4 are excluded and policies 1 and 2 are considered the possible alternative ones to operate the system.

Although it seems obvious that operating policy 1 is superior to operating policy 2, since the optimal yield according to the first one is almost 1.5 times the optimal yield from the second one, the later has the advantage that the use of groundwater in the study area will be concentrated in development area 1. However, the decision is up to land reclamation and irrigation authorities within the frame work of the regional development plans.

CHAPTER 9

CONCLUSIONS AND RECOMMENDATIONS

9.1 Conclusions

9.2 Recommendations

CHAPTER 9

CONCLUSIONS AND RECOMMENDATIONS

9.1 Conclusions

A mathematical model, based on the analytical solutions for the case of pumping a single well in a stream-aquifer system, is developed to investigate stream-aquifer interaction. The developed model is used to examine the role of the various variables affecting stream-aquifer interaction and to present quantitative assessment of the excitation-response relationships. The model analysis provides guide lines for the design of groundwater development schemes in a stream-aquifer system.

The management problem of a stream-aquifer system is identified to be a hydraulic management one. A joint simulation and optimization modelling approach is employed to develop the management model. This combined model approach considers the particular behaviour of a given stream-aquifer system and determines the best operating policy under the specified objective and constraints. The complete procedure required to establish the link between simulation and optimization using the response functions technique is presented in the model formulation. The model considers the stream-aquifer interaction as a manageable component of the system. Although the decisions variables are expressed in physical terms the model formulation presented is valid when these variables are interpreted as surrogate economic ones or when explicit economic factors are considered.

The ability to predict the response of a system to any implemented decision in the future is an intrinsic part of the procedure for determining a management problem. This is known as the forecasting problem of the system and mathematical models solved by numerical techniques are often used to solve this problem. Finite difference and finite element techniques are domain methods. When such methods are applied to the forecasting problem of a stream-aquifer system, drawdowns need to be calculated at many grid points for reasonable accuracy to be achieved. The information at the majority of these points may be of no interest and even impossible to be verified in the real system. Apparently, modelling of stream aquifer systems according to domain methods is not particularly efficient in performing the dual service of providing the stream-response to pumping and the drawdowns in the aquifer only at points of interest. The boundary element method holds a promise for reducing computational effort and the data required to solve a problem. Therefore, the method is employed to solve the forecasting problem of a stream-aquifer system.

A complete formulation of the boundary element solutions for two-dimensional steady state and transient groundwater flow in a homogeneous and isotropic aquifer is presented. A computer implementation of the boundary element model is developed. The algorithm is successfully applied to two sample problems and the numerical results are found to be in good agreement with the exact solution. The major part of the computational work is spent in setting up the system of equations for the transient solution. This can be considerably reduced by using a uniform time step. The time marching process used in the algorithm shows it capable of producing considerably accurate solution to transient flow problems even when large time steps are used. In a stream-aquifer system, stream losses to the aquifer as a response to pumping by wells are directly obtained from the solution on the boundary. Once all the boundary variables

are determined, the drawdowns at any subsequently selected interior points can be calculated. The algorithm is thus found to be efficient and accurate in performing the dual service of a stream-aquifer simulation model. This means that, the interaction parameters and the response coefficients required by the management model can be generated efficiently.

The management model is applied to a case study of the stream-aquifer system south-east of the Nile delta. The application demonstrates the procedure for implementing the hydraulic management of a stream-aquifer system using the combined simulation-optimization approach. The application essentially involves calibration of the boundary element model to simulate the real system. The calibration is achieved successfully and the results show that the assumption of a homogeneous and isotropic system is a satisfactory approximation. The model considers the concept of a stationary interface and Ghypen-Herzberg relationship to determine the extent of salt water intrusion in the coastal strip bounded by the Suez Canal in the east. However, field investigations are needed to determine the exact location of the interface so that the calculated location could be checked against field measurements. The calibrated model is then used to generate the system's response coefficients and interaction parameters. The output from the simulation model is used as input into the optimization model to determine on intra-annual basis the optimal yield of the system.

Four alternative operating policies are considered in the hydraulic management of the system. The model is applied successfully and the optimal yield of the system according to each policy is determined for both conditions of variable and constant demand. Quantitative distribution of the optimal yield over the year, under the condition of variable demand, is determined according to the

representative demand density function developed for the system. Up to a 12% increase in the optimal yield of the system could be achieved if the system is operated under the condition of variable demand. Since the optimal yield determined by the model is based on intra-annual operation of the system, a feedback verification process is introduced to check the condition of the system proper when the steady state conditions are reached. In this process the optimal yield determined by the management model is introduced into the simulation model to calculate the steady state drawdown and to check the intruded length of the interface. The feedback verification shows that, under the specified steady state limitations on drawdowns and salt water intrusion, operating policies 3 and 4 are not acceptable and policies 1 and 2 are the possible alternative ones to operate the system. The choice between the two operating policies is up to the land reclamation and irrigation authorities within the framework of the regional development plans.

Generally speaking, the application of the developed model indicates that the boundary element method is a highly efficient technique for solving the forecasting problem of aquifer system in general and stream-aquifer systems in particular and demonstrates that response function approach is applicable to real world systems and is a valuable tool for solving management problems of aquifer system.

9.2 Recommendations

Since the optimal yield determined by the model for the case study is controlled by the extent of salt water intrusion from the Suez Canal, it is recommended to carry out field investigation in the study area to define the actual extent of the problem and to check the location of the interface calculated by the model against field measurements.

Extending the model to include the dynamic presence of salt water intrusion is a recommended future work. Mathematically speaking, the model formulation presented and its implementation are modular and could be extended using the treatment of the problem of zones described in Chapter 4. However, this cannot be achieved unless the field investigations required to calibrate the model and to monitor the movement of the interface are carried out.

REFERENCES

Abramowitz, M., and Stegum, I.A. (1974): Handbook of mathematical functions. Dover, New York.

Alarcon, A., Martin, A., and Paris, F. (1978): Improved boundary element in torsion problems. Proc. Int. Conf. on "Recent Advances in Boundary Element Method", Southampton University, pp. 144-165.

Aguado, E., and Remson, I. (1974): Groundwater hydraulics in aquifer management. J. Hydraul. Div., ASCE, 100(HY1), pp. 103-118.

Arpaci, V. (1966): Conduction heat transfer. Addison-Wesley Inc.

Bachmat, Y., Bredehoeft, J., Andrews, B., Holtz, D., and Sebastian, S. (1980): Groundwater Management: The Use of Numerical Models. Water Resour. Monogr. Ser., Vol. 5, AGU, Washington, D.C.

Banerjee, P.K., and Butterfield, R. (1981): Boundary Element Methods in Engineering Science. McGraw-Hill, London.

Banerjee, P.K., Butterfield, R., and Tomlin, G.R. (1981): Boundry element methods for two-dimensional problems of transient groundwater flow. Int. J.Num.Anal.Meth. Geomech.5, pp. 15-31.

Bathala, C.T., Rao, A.R., and Spooner, J.A. (1980): Linear system models for regional aquifer evaluation studies. Water Resour.Res., 16(2), pp. 409-422.

Bear, J. (1972): Dynamics of Fluids in Porous Media. American Elsevier, New York.

Bear, J. (1979): Hydraulics of Groundwater. McGraw-Hill, New York.

Bear, J., Zaslavsky, D., and Irmay, C. (1968): Physical Principles of Water Percolation and Seepage. Aridzone Research xxix, UNESCO, Paris.

Binnie and Partners (1980): Ismailia Canal Study, Final Report. Ministry of Irrigation, Egypt.

Brebbia, C.A. (1978): The Boundary Element Method for Engineers. Pentech Press, London.

Brebbia, C.A., and Walker, S. (1980): Boundary Element Techniques in Engineering. Newnes-Butterworths, London.

Brebbia, C.A., and Wrobel, L.C. (1980): Steady and unstready potential problems using the boundary element method. Chapter 1 in "Recent Advances in Numerical Methods in Fluids". C. Taylor and K. Morgan, eds. Pineridge Press, U.K.

Bredehoeft, J.D., and Young, R.A. (1970): The temporal allocation of groundwater - A simulation aproach. Water Resour.Res., 6(1), pp. 3-21.

Bronson, R. (1973): Differential Equations. McGRaw-Hill, New York.

Carslaw, H.S., and Jaeger, J.C. (1959): Conduction of Heat in Solids. Clarendon Press, Oxford.

Churchill, R. (1972): Operational Mathematics. McGraw-Hill, New York.

Conner, J.J., and Brebbia, C.A. (1976): Finite Element Techniques for Fluid Flow. Newnes-Butterworths, London.

Cooper, H.H., and Rorabaugh, M.I. (1963): Groundwater movements and bank storage due to flood stages in surface streams. U.S. Geol.Surv.Water Supply Pap., 1536-J, pp., 343-363.

DeWiest, R.J.M. (1969): Flow through Proous Media. Academic Press, New York.

Dubois, M., and Buysee, M. (1980): Transient heat transfer analysis by the boundary integral method. "Proceedings of Second Int. Seminar on Recent Advances in Boundary Element Methods" pp.137-154. C. Brebbia, ed., CML Publications, University of Southampton.

Dupuit, J. (1863): Etudes Theoriques et Partiques sur le Mouvement des Eaux dans les Canaux de Couverts et a Travers les Terrains Permeables. 2nd edn., Dunod, Paris.

El-Fayomy, M.D. (1968): Geology of groundwater supplies in the region east of the Nile Delta and its extension in the North Sinai. Ph.D. Thesis, Cairo University.

Eshett, A., and Bittinger, M.W. (1965): Stream-aquifer system analysis. J. Hydraul.Div., ASCE, 91 (HY6), pp. 153-164.

Fike, C.T. (1968): Comptuer Evaluation of Mathematical Functions. Englewood Cliffs, N.J., Prentice-Hall.

Farid, M.S. (1980): Nile Delta Groundwter Study. M.Sc. thesis, Faculty of Engineering, Cairo University.

Freeze, R.A., and Cherry, J.A. (1979): Groundwater. Englewood Cliffs, N.J., Prentice-Hall.

Glover, R.E. (1960): Groundwater - Surface water relationships. Rep.CER60REG-45, Colo.State Univ., Fort Collins.

Glover, R.E. (1978): Transient Groundwater Hydraulics. Wter Resour. Publications, Fort Collins, Colorado.

Glover, R.E., and Balmer, G.G. (1954): River depletion resulting from pumping a well near a river. Trans. AGU, Vol. 35(3), pp. 468-470.

Gorelick, S.M. (1983): A review of distributed parmeter groundwater managmeent modelling methods. Water Resour. Res., 19(2), pp. 305-319.

Greenberg, M.D. (1971): Application of Green's Functions in Science and Engineering. Prentice-Hall, Englewood Cliffs, N.J.

Haimes, Y.Y. (1977): Hierarchical Analysis of Water Resources Systems. McGraw-Hill, New York.

Hall, F.R., and Moench, A.F. (1972): Application of the convolution eqution to stream-aquifer relationships. Water Resour. Res., 8(2), pp. 487-493.

Hall, W.A., and Dracup, J.A. (1970): Water Resources Systems Engineering. McGraw-Hill, New York.

Hammer, P.C., and Stroud, A.H. (1958): Numerical Evaluation of Multiple Integrals. Math. Tables Aids Comput. 12.

Hantush, M.S. (1955): Discussion of 'River depletion resulting from pumping a well near a river', by R.E. Glover and G.G. Balmer. Trans. AGU, vol.36, pp. 345-346.

Hantush, M.S. (1964): Hydraulcis of Wells. Advances in Hydroscience, vol. 1, V.T. Chow, ed., Academic Press, New York.

Hantush, M.S. (1965): Wells near streams with seimpervious beds. J. Geophys. Res., vol.70, pp.2829-2838.

Hantush, M.S. and Jacob, C.E. (1955): Non-steady Green's functions for an infinite strip of leaky aquifer. Trans. AGU, vol.36, pp. 101-112.

Haskoning (1976): Lining of the Ismailia Canal, A Preliminary Study, Ministry of Irrigation, Egypt.

Hassan, M.M. (1982): Calibration of A One-Dimensional Steady State Sea Water Intrusion Model for Nile Delta Aquifer. M.Sc. thesis, Faculty of Engineering, Cairo University.

Hefny, K., Morsi, A., and Khater, A. (1977): Hydrogeological Investigations for the Ismailia Canal Region. Research Institute for Groundwater, Egypt.

Heidari, M. (1982): Application of linear system's theory and linear programming to groundwater management in Kansas. Water Resour. Bull., 18(6), pp. 1003-1012.

Hornberger, G.M., Ebert, J., and Remson, I. (1970): Numerical solution of the Boussinesq equation for aquifer-stream interactions. Water Resour.Res., 6(2), pp. 601-608.

Huyakorn, P.S., and Pinder, G.F. (1983): Comptuational Methods in Subsurface Flow. Academic Press, New York.

Illangasekare, T.H., and Morel-Seytoux, H.J. (1982): Stream-aquifer influence coefficients for simulation and management. Water Resour.Res., 18(1), pp. 168-176.

Illangasekare, T.H. and Morel-Seytoux, H.J. (1984): Design of a physically based distributed parameter model for arid zone surface-groundwater management. J.Hydrol., 74, pp. 213-232.

IWACO-RIGW (1986): Control of water logging in the western part of Wadi El-Tumilat, Development and Management of Groundwater Resources in the Nile Valley and Delta, Annex F. Research Institute for Groundwater (RIGW), Egypt.

Jaswon, M.A., and Symm, G.T. (1977): Integral Equation Methods in Potential Theory and Elastostatics. Academic Press, New York.

Javandel, I., and Witherspoon, P.A. (1968): Application of the finite element method to transient flow in prous media. Soc.Pet.Eng.J. 8, pp. 241-252.

Jenkins, C.T. (1968a): Techniques for computing rate and volume of stream depletion by wells. Ground Water, vol.6(2), pp. 37-46.

Jenkins, C.T. (1968b): Electric-analog and digital-computer model analysis of stream depletion by wells. Ground Water Vol.6(6), pp. 27-34.

Jenkins, C.T., and Taylor, O.J. (1974): A special planning technique for stream-aquifer systems. U.S. Geol.Surv., Open-File Rep., 47-242.

Khater, A.M.R. (1980): Seepage from canals with a "skin layer". M.Sc. dissertation, Dept. of Civil Eng., University of Southampton.

Kinzelbach, W. (1986): Groundwater Modelling Development in Water Science, Vol. 25, Elsevier, pp. 126-129.

Lachat, J. and Watson, J. (1976): Effective numerical tratment of boundary integral equation. Int. J. Num. Meth. in Eng., Vol 10 pp. 991-1005.

Lanezos, C. (1961): Linear Differential Operators, Van Nostrand, New York.

Liggett, J.A. (1977): Location of free surface in porous media. ASCE, J.Hydraul.Div., 103(HY4), pp. 353-365.

Maddock, T., III. (1972): Algebraic technological functions from a simulation model. Water Resour.Res., 8(1), pp. 129-134.

Maddock, T., III (1973): Management model as a tool for studying the worth of data. Water Resour.Res., 9(2), pp. 270-280.

Maddock, T., III (1974): The operation of stream-aquifer system under stochastic demands. WaterResour.Res., 10(1), pp. 1-10.

Martin, W.E., Burdak, T., and Young, R.A. (1969): Projecting hydrologic and economic relationships in groundwater basin management. Am.J.Agric.Econ., 15(5), pp. 1593-1597.

Ministry of Irrigation (1981): Water Master Plan, "Water Demands", Technical Report 2, UNDP - EGY/73/024.

Morel-Seytoux, H.J. (1975): A simple case of conjunctive surface-ground-water management. Ground Water, vol. 13(6), pp.506-515.

Morel-Seytoux, H.J., and Daly, C.J. (1975):A discrete kernel generator for stream-aquifer studies. Water Resour.Res., 11(2), pp. 253-260.

Moulder, E.A., and Jenkins, C.T. (1969). Analog digital models of stream-aquifer systems. Ground Water, vol.7(5), pp. 19-24.

Pontin, J.H.A. and Weller,J.A., (1979): Prediction of Seepage Losses from the Englarged Ismailia Canal. Report No. OD28, Hydraulic Research Station Wallingford, U.K.

RIGW (1980): Groundwater Studies for the Tenth of Ramadan City, Reserch Instiurte for Groundwater, Egypt.

RIGW-IWACO (1983): Hydrogeological Inventory Study of the Eastern Nile Delta Region. Research Institute for Groundwater, Egypt.

Remson, I., Apple, C.A., and Webster, R.A. (1965): Groundwater models solved by digital computer. ASCE, J.Hydraul. Div., 91(HY3), pp. 133-147.

Remson, I., Hornberger, G.M., and Moltz, F.J. (1971): Numerical Methods in Subsurface Hydrology. Wiley Interscience, New York.

Said, R. (1981): The Geological evaluation of the River Nile. Springer-Verlag.

Schwarz, J. (1971): Linear models for groundwater management.J. Hydrol., 28, pp. 377-392.

SHAW, F. S., and R. V. SOUTHWELL. 1941. Relaxation methods applied to engineering problems: VII. Problems relating to the percolation of fluids through porous materials. *Proc. Roy. Soc. Lond.*, A178, pp. 1–17.

Stroud, A.H., and Secrest, D. (1966): Gaussian Quadrature Formulas. Prentice-Hall, Englewood Cliffs, N.J.

Theis, C.V. (1941): The effect of a well on a nearby stream. Trans. AGU, Pt.3, pp. 734-738.

Todd, D.K. (1959): Ground Water Hydrology. John Wiley, New York.

Venetis, C. (1968): On the impulse response of an aquifer. Bull. Int. Assoc.Sci.Hydrol., 13(3), pp.136-139.

Zienkiewicz, O.C., Mayer, P., and Cheung, Y.K. (1966): Solution of anisotropic seepage problems by finite elements. Proc. ASCE, 92(EM1), pp. 111-120.

A P P E N D I C E S

APPENDIX A

COMPUTER PROGRAMS

As has been discussed in Chapter 2, the following computer programs are developed to solve the computation schemes of the mathematical model of stream-aquifer interaction. The notation used in the model formulation is also used in writing the computer programs. Each program is preceded by a description of its function and is explained in the program listing by means of comment statements.

Computation Scheme (i)

The following program implements computation scheme (i) by solving equations (2.1) and (2.9). The equations are solved for values of the overall parameter (Z) running between zero and 2.0 with a 0.02 increment. The computed values of the dimensionless ratios (QR) and (VR) are used to produce the graphic output of Figure (2.1).

```
C  THIS  PROGRAMME  CALCULATES RATIOS OF FLOW RATE & VOLUME
DEPLETED
C FROM A STREAM BY PUMPING A SINGLE WELL IN AN IDEAL SYSTEM
C
C
      REAL X,Z,V,ZS,EZSN,ZRPI,ALPHA,BETA,QR,VR
      WRITE (6,6)
      DATA PI/3.1415927/
      V= 0.0
20    Z=V
      IF (Z .EQ. 0.0) GO TO 25
      ZS= Z**2
      ALPHA= 1+(2*ZS)
      EZSN= EXP(-ZS)
      ZRPI= Z* SQRT(PI)
      BETA= 2*ZS* ((EZSN/ZRPI) -1)
25    QR= 1- ERF(Z)
      WRITE(4,*)Z,QR
      VR= 1.0
      IF (Z .EQ. 0.0) GO TO 27
      VR= 1- (ALPHA* ERF(Z) + BETA)
27    WRITE (6,8) Z,QR,VR
      WRITE(8,*) Z,VR
      V=V+0.02
      IF (Z .GE. 1.98) GO TO 30
      GO TO 20
30    STOP
6     FORMAT(1H1,T18,1HZ,T38,2HQR,T57,2HVR)
8     FORMAT(1H0, 10X, F10.5, 10X, F10.5,10X, F10.5)
      END
```

```
C
C
C
      FUNCTION ERF(X)
      REAL X,X2,SUM,SUM1,TERM
      INTEGER I
      DATA TOL/1.0E-5/,SQRTPI/1.772454/
      ERF= 0.0
      IF (X .EQ. 0.0) GO TO 99
      ERF= 1.0
      IF (X .GT. 3.0) GO TO 99
      X2 =X*X
      SUM= X
      TERM= X
      I= 0
10    I=I+1
      SUM1= SUM
      TERM= TERM*X2/(I+0.5)
      SUM= TERM + SUM1
      IF (TERM .GE. TOL*SUM) GO TO 10
      ERF = 2*SUM*EXP(-X2) / (SQRTPI)
99    RETURN
      END
```

Computation Scheme (ii)

The following program implements computation scheme (ii) by solving equations (2.11) to calculate the ratio of depletion rate after cessation of pumping (RQR). The time ratio (TR)/(TT) should be supplied by the user. The computed values of the ratio (RQR) for the selected values of the time ratio (TR)/(TT) are used to produce the graphic output of Figure (2.2).

```
C THIS PROGRAMME CALCULATES RATIO OF DEPLETED STREAM FLOW
C ( RQR ) AFTER CESSATION OF PUMPING.
C
C
C THE FOLLOWING NOTATIONS ARE USED;
C
C RTS = TR/TT
C ZTT = A/SQRT(4*ALPHA*TT)
C ZTR = A/SQRT(4*ALPHA*TR)
C PARA= RQR
C                    WHERE; RQR=QRTT-QRTR
C QRTT= STRAM DEPLETION RATIO AT A TOTAL TIME (TT)
C  QRTR=  STREAM  DEPLETION  RATIO  AT  A  TIME  (TR) AFTER
CESSSATION OF
C       PUMPING
C                    WHERE; TT= TP + TR
C                               TP= PUMPING TIME
C
      DIMENSION RTS(7),RZS(7),TZ(41),ZTR(7,41),
     *RZ(7,41),RQR(7,41)
      REAL MAX
      INTEGER I,J
      DO 5 I=1,7
      RTS(I)=0.0
      RZS(I)=0.0
      DO 5 J=0,40
      TZ(J)=0.0
      ZTR(I,J)=0.0
      RZ(I,J)=0.0
5     RQR(I,J)=0.0
      I=1
      MAX=3.1
10    READ(5,*) RTS(I)
      WRITE(6,8) RTS(I)
8     FORMAT (1H1,T25,11HRTS=RT/TT =,2X,F7.4)
      RZS(I)= SQRT(RTS(I))
```

```
C
      J=0
      ZTT=0.0
      WRITE(6,16)
16    FORMAT(1H0,//,T20,3HZTT,T40,3HRQR)
20    TZ(J)= ERF(ZTT)
      IF(RZS(I) .LE. 0.0) GO TO 30
      ZTR(I,J)=ZTT/RZS(I)
      IF(ZTR(I,J) .GE.2.0) GO TO 111
      GO TO 33
30    ZTR(I,J)=MAX
33    RZ(I,J)= ERF(ZTR(I,J))
      GO TO 112
111   RZ(I,J)=1.0 - ERFC(ZTR(I,J))
112   RQR(I,J)=RZ(I,J) - TZ(J)
      WRITE(6,18) ZTT,RQR(I,J)
      WRITE(4,*)ZTT,RQR(I,J)
18    FORMAT(1H0,T18,F7.4,T37,F7.4)
      ZTT=ZTT+0.05
      J=J+1
      IF(J .GT. 40) GO TO 40
      GO TO 20
40    I=I+1
      IF(I .LT. 7) GO TO 10
      STOP
      END
C
C
C
      FUNCTION ERF(X)
      REAL X,X2,SUM,SUM1,TERM
      INTEGER I
      DATA TOL/1.0E-5/,SQRTPI/1.772454/
      ERF=0.0
      IF(X .EQ. 0.0) GO TO 99
      ERF=1.0
      IF(X .GT. 3.0) GO TO 99
      X2=X*X
```

```
      SUM=X
      TERM=X
      I=0
10    I=I+1
      SUM1=SUM
      TERM=TERM*X2/(I+0.5)
      SUM=TERM+SUM1
      IF(TERM .GE. TOL*SUM) GO TO 10
      ERF=2*SUM*EXP(-X2)/(SQRTPI)
99    RETURN
      END
C
C
      FUNCTION ERFC(X)
      REAL X,X2,SUM,U,V,SQRTPI
      INTEGER I,J,TERMS
      DATA SQRTPI/1.772454/,TERMS/12/
C
      X2=X*X
      V= 0.5/X2
      U= 1.0+ V*(TERMS+1)
      DO 10 J=1,TERMS
      I=TERMS - J+1
      SUM= 1.0+ I*V/U
      U=SUM
10    CONTINUE
      ERFC=EXP(-X2)/(X* SUM *SQRTPI)
      RETURN
      END
```

Computation Scheme (iii)

The following program implements computation scheme (iii) by solving equation (2.13) to calculate the ratio of total volume of depletion (TRVR) and the ratio of aquifer rewatering volume after cessation of pumping (ARR). The equation is solved for values of the time ratio (TR)/(TT) running between zero and 1.0 with a 0.05 increment. Values of the overall parameter (ZTT) should be supplied by the user. The computed values of (TRVR) and (ARR) for the selected values of (ZTT) are used to produce the graphic output of Figures (2.3) and (2.4), respectively.

```
C THIS PROGRAMME CALCULATES RATIO OF DEPLETED STREAM
C VOLUME AFTER CESSATION OF PUMPING.
C
C
      DIMENSION
ZTT(8),ZTTS(8),ALPHAT(8),BETAT(8),TZ(8),VRTT(8)
                                                    DIMENSION
ZTR(21),RZS(21),ZTRS(21),ALPHAR(21),BETAR(21)
      DIMENSION TN(21),RZ(21),VRTR(21),PARA(8,21)
      DIMENSION XPT(8),XPR(21),ZTRPI(8),ZRRPI(21),AVR(21)
      DIMENSION
ZTP(21),ZTPS(21),ALPHAP(21),BETAP(21),XPP(21)
                                                    DIMENSION
ZPRPI(21),PZ(21),VRTP(21),RVR(8,21),ARR(8,21)
      REAL RTS,MAX
      INTEGER I,J
      DATA PI/3.1415927/
C INITIALIZATION OF ARRAYS
C
      DO 50 I= 1,8
      ZTT(I)=0.0
      ZTTS(I)=0.0
      ALPHAT(I)=0.0
      XPT(I)=0.0
      ZTRPI(I)=0.0
      BETAT(I)=0.0
      TZ(I)=0.0
      VRTT(I)=0.0
      DO 50 J= 0,21
      ZTP(J)=0.0
      ZTPS(J)=0.0
      ALPHAP(J)=0.0
      BETAP(J)=0.0
      XPP(J)=0.0
      ZPRPI(J)=0.0
      PZ(J)=0.0
      VRTP(J)=0.0
```

```
      ZTR(J)=0.0
      RZS(J)=0.0
      ZTRS(J)=0.0
      ALPHAR(J)=0.0
      XPR(J)=0.0
      ZRRPI(J)=0.0
      BETAR(J)=0.0
      TN(J)=0.0
      RZ(J)=0.0
      VRTR(J)=0.0
      AVR(J)=0.0
      PARA(I,J)=0.0
      RVR(I,J)=0.0
50    ARR(I,J)=0.0
C
      I=1
      MAX=3.1
10    READ (5,*) ZTT(I)
      WRITE (6,8) ZTT(I)
8     FORMAT (1H1,T30,5HZTT =,2X,F7.4)
      ZTTS(I)= (ZTT(I))**2
      ALPHAT(I)= 1.0+(2*(ZTTS(I)))
      XPT(I)= EXP(-ZTTS(I))
      ZTRPI(I)= ZTT(I)*SQRT(PI)
      BETAT(I)= 2*ZTTS(I)*((XPT(I)/ZTRPI(I))-1.0)
      TZ(I)= ERF(ZTT(I))
      VRTT(I)= 1.0-(ALPHAT(I)*TZ(I) +BETAT(I))
C
      J=0
      RTS=0.0
      WRITE(6,16)
16
FORMAT(1H0,//,T5,5HTR/TT,T16,5HTR/TP,T30,7HZTT/ZTR,T48,4HTR
V
     *R,T63,3HRVR,T78,3HARR)
20    RZS(J)=SQRT(RTS)
      TN(J)= RTS/(1.0-RTS)
      IF(RZS(J) .LE. 0.0) GO TO 30
```

```
      ZTR(J)=ZTT(I)/RZS(J)
      GO TO 33
30    ZTR(J)= MAX
      ZTP(J)=ZTT(I)*SQRT(TN(J)+1)
      GO TO 34
33    ZTP(J)=ZTR(J)*SQRT(TN(J))
34    ZTPS(J)=(ZTP(J))**2
      ALPHAP(J)=1.0+(2*ZTPS(J))
      XPP(J)= EXP(-ZTPS(J))
      ZPRPI(J)=ZTP(J)*SQRT(PI)
      BETAP(J)=2*ZTPS(J)*((XPP(J)/ZPRPI(J))-1.0)
      IF(ZTP(J) .GE. 2.0) GO TO 111
      PZ(J)= ERF(ZTP(J))
      GO TO 112
111   PZ(J)=1.0 - ERFC(ZTP(J))
112   AVR(J)=(ALPHAP(J)*PZ(J) +BETAP(J))
      VRTP(J)= 1.0- AVR(J)
      IF(VRTP(J) .LE. 0.0) GO TO 40
      ZTRS(J)=(ZTR(J))**2
      ALPHAR(J)=1.0+(2*ZTRS(J))
      XPR(J)=EXP(-ZTRS(J))
      ZRRPI(J)= ZTR(J)* SQRT(PI)
      BETAR(J)=2*ZTRS(J)*((XPR(J)/ZRRPI(J)) -1.0)
      IF(ZTR(J) .GE. 2.0) GO TO 121
      RZ(J)= ERF(ZTR(J))
      GO TO 122
121   RZ(J)=1.0 - ERFC(ZTR(J))
122   VRTR(J)=1.0-(ALPHAR(J)*RZ(J) +BETAR(J))
      IF(VRTR(J) .LT. 0.0) VRTR(J)=0.0
      PARA(I,J)=TN(J)*(VRTT(I)-VRTR(J)) +VRTT(I)
      RVR(I,J)=PARA(I,J)-VRTP(J)
      ARR(I,J)= RVR(I,J) / AVR(J)
                                              WRITE(6,18)
RTS,TN(J),RZS(J),PARA(I,J),RVR(I,J),ARR(I,J)
18
FORMAT(1H0,T5,F7.4,T15,F7.4,T30,F7.4,T45,F7.4,T60,F7.4,
     *T75,F7.4)
      WRITE(4,*)RTS,PARA(I,J)
```

```
      WRITE(8,*)RTS,ARR(I,J)
      WRITE(10,*)RTS,RVR(I,J)
      RTS=RTS+0.05
      J=J+1
      IF(J .GE. 20) GO TO 40
      GO TO 20
40    I=I+1
      IF(I .LT. 8) GO TO 10
      STOP
      END
C
C
C
C
      FUNCTION ERF(X)
      REAL X,X2,SUM,SUM1,TERM
      INTEGER I
      DATA TOL/1.0E-5/,SQRTPI/1.772454/
      ERF=0.0
      IF(X .EQ. 0.0) GO TO 99
      ERF=1.0
      IF(X .GT. 3.0) GO TO 99
      X2=X*X
      SUM=X
      TERM=X
      I=0
10    I=I+1
      SUM1=SUM
      TERM=TERM*X2/(I+0.5)
      SUM=TERM+SUM1
      IF(TERM .GE. TOL*SUM) GO TO 10
      ERF=2*SUM*EXP(-X2)/(SQRTPI)
99    RETURN
      END
C
C
      FUNCTION ERFC(X)
      REAL X,X2,SUM,U,V,SQRTPI
```

```
      INTEGER I,J,TERMS
      DATA SQRTPI/1.772454/,TERMS/12/
C
      X2=X*X
      V= 0.5/X2
      U= 1.0+V*(TERMS+1)
      DO 10 J=1,TERMS
      I=TERMS -J+1
      SUM=1.0 +I*V/U
      U=SUM
10    CONTINUE
      ERFC=EXP(-X2)/(X* SUM *SQRTPI)
      RETURN
      END
```

Computation Scheme (iv)

The following three programs are used to implement computation scheme (iv) for the considered three hypothetical patterns of cyclic pumping. Although the computation procedure to solve equations (2.11), (2.12) and (2.13) for any pumping pattern is the same, a separate program for each pattern is required to perform superposition of the solution according to the recurrence relations of particular considered pattern. The obtained results are used to produce the graphic output of Figures (2.5), (2.6) and (2.7).

```
C THIS PROGRAMME CALCULATES RATIO OF DEPLETED STREAM FLOW
C FOR A CASE OF INTERMITTENT PUMPING.
C
C THE WELL IS PUMPED FOR 12 HOURS A DAY AND THE PROCESS
C IS REPEATED FOUR SUCCESSIVE DAYS A WEEK.
C  CALCULATION  IS  PERFORMED FOR THE FIRST SUCCESSIVE FOUR
WEEKS.
C
C
                                                      DIMENSION
ZP(4,60,4),TP(4,60,4),TT(4,60,4),TR(4,60,4),
     *ZT(4,60,4),ZR(4,60,4),QR(4,60,4),RQR(4,60,4)
      DIMENSION ZPS(4,60,4),ZRS(4,60,4),ZTS(4,60,4)
      DIMENSION
ALPHAP(4,60,4),ALPHAR(4,60,4),ALPHAT(4,60,4),

*XP(4,60,4),XR(4,60,4),XT(4,60,4),ZPPI(4,60,4),ZRPI(4,60,4)
,

*ZTPI(4,60,4),BETAP(4,60,4),BETAR(4,60,4),BETAT(4,60,4),
     *VR(4,60,4),VRT(4,60,4),VRR(4,60,4),RVR(4,60,4)
      INTEGER I,J,K
      DATA C/3.0/,PI/3.1415927/
      TP0=0.0
      QR0=0.0
      VR0=0.0
      DO 100 K=1,4
      DO 200 I=1,4
      J=1
10    IF(I .GT. 1) GO TO 400
      TP(I,J,K)=0.50
      ZP(I,J,K)= C/SQRT(TP(I,J,K))
      ZPS(I,J,K)=ZP(I,J,K) **2
      ALPHAP(I,J,K)=1.0 + 2*ZPS(I,J,K)
      XP(I,J,K)= EXP(-ZPS(I,J,K))
      ZPPI(I,J,K)=ZP(I,J,K)*SQRT(PI)
```

```
BETAP(I,J,K)=2*ZPS(I,J,K)*((XP(I,J,K)/ZPPI(I,J,K))-1.0)
      IF(J .GT. 1) GO TO 77
      IF (ZP(I,J,K) .GE. 2.0) GO TO 88
      QR(I,J,K)= (1.0 - ERF(ZP(I,J,K)))/16

VR(I,J,K)=(1.-(ALPHAP(I,J,K)*ERF(ZP(I,J,K))+BETAP(I,J,K)))/
16
      GO TO 99
88    QR(I,J,K)= (ERFC(ZP(I,J,K)))/16

VR(I,J,K)=(1.0-(ALPHAP(I,J,K)*(1.-ERFC(ZP(I,J,K)))+BETAP(I,
J
     *,K)))/16
99    IF(K .GT. 1) GO TO 101
      GO TO 102
101   TP(I,J,K)=TP(I,J,K-1) +7.0
      QR(I,J,K)=QR(I,J,K) + RQR(4,J+8,K-1)
      VR(I,J,K)=VR(I,J,K)+RVR(4,J+8,K-1)
      TP0=7*(K-1)
      QR0=RQR(4,8,K-1)
      VR0=RVR(4,8,K-1)
102   WRITE(6,*)TP0,QR0
      WRITE(6,*)TP(I,J,K),QR(I,J,K)
      WRITE(8,*)TP0,VR0
      WRITE(8,*)TP(I,J,K),VR(I,J,K)
      J=J+1
      TT(I,J,K)= 1.0
      TEMP=TT(I,J,K)
      TR(I,J,K)= TT(I,J,K) - 0.50
      GO TO 76
77    TT(I,J,K)=TT(I,J-1,K) +0.5
      TEMP=TT(I,J,K)
      TR(I,J,K)=TT(I,J-1,K)
76    ZT(I,J,K)= C/SQRT(TT(I,J,K))
      ZTS(I,J,K)=ZT(I,J,K)**2
      ALPHAT(I,J,K)=1.+2*ZTS(I,J,K)
      XT(I,J,K)= EXP(-ZTS(I,J,K))
      ZTPI(I,J,K)=ZT(I,J,K)*SQRT(PI)
```

```
BETAT(I,J,K)=2*ZTS(I,J,K)*((XT(I,J,K)/ZTPI(I,J,K))-1.0)
      ZR(I,J,K)= C/SQRT(TR(I,J,K))
      ZRS(I,J,K)= ZR(I,J,K)**2
      ALPHAR(I,J,K)=1.+2*ZRS(I,J,K)
      XR(I,J,K)= EXP(-ZRS(I,J,K))
      ZRPI(I,J,K)=ZR(I,J,K)*SQRT(PI)

BETAR(I,J,K)=2*ZRS(I,J,K)*((XR(I,J,K)/ZRPI(I,J,K))-1.0)
      IF(ZT(I,J,K) .GE. 2.0 .OR. ZR(I,J,K) .GE.2.0)  GO  TO
66
      RQR(I,J,K)=(ERF(ZR(I,J,K)) - ERF(ZT(I,J,K)))/16

VRT(I,J,K)=(1.-(ALPHAT(I,J,K)*ERF(ZT(I,J,K))+BETAT(I,J,K)))
/
     *16

VRT(I,J,K)=(1.-(ALPHAT(I,J,K)*ERF(ZT(I,J,K))+BETAT(I,J,K)))
     */16

VRR(I,J,K)=(1.-(ALPHAR(I,J,K)*ERF(ZR(I,J,K))+BETAR(I,J,K)))
     */16

RVR(I,J,K)=((TEMP-.5)/.5)*(VRT(I,J,K)-VRR(I,J,K))+VRT(I,J,K
)
      GO TO 55
66    RQR(I,J,K)=(ERFC(ZT(I,J,K)) - ERFC(ZR(I,J,K)))/16

VRT(I,J,K)=(1.-(ALPHAT(I,J,K)*(1.-ERFC(ZT(I,J,K)))+BETAT(I,
     *J,K)))/16

VRR(I,J,K)=(1.-(ALPHAR(I,J,K)*(1.-ERFC(ZR(I,J,K)))+BETAR(I,
     *J,K)))/16

RVR(I,J,K)=((TEMP-.5)/.5)*(VRT(I,J,K)-VRR(I,J,K))+VRT(I,J,K
)
55    IF(K .GT. 1) GO TO 65
      GO TO 67
```

```
65    RQR(I,J,K)=RQR(I,J,K)+RQR(4,J+8,K-1)
      TT(I,J,K)=TT(I,J,K)+7*(K-1)
      RVR(I,J,K)= RVR(I,J,K) + RVR(4,J+8,K-1)
      IF(TT(I,J,K) .GT. 28.0) GO TO 68
67    WRITE(6,*) TT(I,J,K),RQR(I,J,K)
      WRITE(8,*) TT(I,J,K),RVR(I,J,K)
68    TT(I,J,K) = TEMP
      GO TO 300
400   IF(J .GT. 1) GO TO 401
      TP0=TP(I-1,J,K)+0.5
      QR0=RQR(I-1,J+1,K)
      VR0=RVR(I-1,J+1,K)
      WRITE(6,*)TP0,QR0
      WRITE(8,*) TP0,VR0
      TP(I,J,K)=TP(I-1,J,K) +1.0
      QR(I,J,K)=QR(1,J,1) +RQR(I-1,J+2,K)
      VR(I,J,K)=VR(1,J,1) +RVR(I-1,J+2,K)
      WRITE(6,*) TP(I,J,K),QR(I,J,K)
      WRITE(8,*) TP(I,J,K),VR(I,J,K)
      J=J+1
401   TT(I,J,K)=TT(I-1,J,K) + 1.0
      IF(K .GT. 1) TT(I,J,K)=TT(I,J,1)+ 7*(K-1)
      RQR(I,J,K)=RQR(1,J,1)+RQR(I-1,J+2,K)
      RVR(I,J,K)=RVR(1,J,1)+RVR(I-1,J+2,K)
      IF(TT(I,J,K) .GT. 28.0) GO TO 300
      WRITE(6,*)TT(I,J,K),RQR(I,J,K)
      WRITE(8,*)TT(I,J,K),RVR(I,J,K)
300   J=J+1
      IF(J .LE. 56) GO TO 10
200   CONTINUE
100   CONTINUE
      STOP
      END
C
C
C
      FUNCTION ERF(X)
      REAL X,X2,SUM,SUM1,TERM
```

```
      INTEGER I
      DATA TOL/1.0E-5/,SQRTPI/1.772454/
      ERF=0.0
      IF(X .EQ. 0.0) GO TO 99
      ERF=1.0
      IF(X .GT. 3.0) GO TO 99
      X2=X*X
      SUM=X
      TERM=X
      I=0
10    I=I+1
      SUM1=SUM
      TERM=TERM*X2/(I+0.5)
      SUM=TERM+SUM1
      IF(TERM .GE. TOL*SUM) GO TO 10
      ERF=2*SUM*EXP(-X2)/(SQRTPI)
99    RETURN
      END
C
C
      FUNCTION ERFC(X)
      REAL X,X2,SUM,U,V,SQRTPI
      INTEGER I,J,TERMS
      DATA SQRTPI/1.772454/,TERMS/12/
C
      X2=X*X
      V= 0.5/X2
      U= 1.0+ V*(TERMS+1)
      DO 10 J=1,TERMS
      I=TERMS - J+1
      SUM= 1.0+ I*V/U
      U=SUM
10    CONTINUE
      ERFC=EXP(-X2)/(X* SUM *SQRTPI)
      RETURN
      END
```

```
C THIS PROGRAMME CALCULATES RATIO OF DEPLETED STREAM FLOW
C FOR A CASE OF INTERMITTENT PUMPING.
C
C THE WELL IS PUMPED FOR ONE DAY, SHUT DOWN THE NEXT DAY
C AND THE PROCESS IS REPEATED TWICE A WEEK.
C
C  CALCULATION  IS  PERFORMED FOR THE FIRST SUCCESSIVE FOUR
WEEKS.
C
C
                                                    DIMENSION
ZP(4,60,4),TP(4,60,4),TT(4,60,4),TR(4,60,4),
     *ZT(4,60,4),ZR(4,60,4),QR(4,60,4),RQR(4,60,4)
      DIMENSION ZPS(4,60,4),ZRS(4,60,4),ZTS(4,60,4)
      DIMENSION
ALPHAP(4,60,4),ALPHAR(4,60,4),ALPHAT(4,60,4),

*XP(4,60,4),XR(4,60,4),XT(4,60,4),ZPPI(4,60,4),ZRPI(4,60,4)
,

*ZTPI(4,60,4),BETAP(4,60,4),BETAR(4,60,4),BETAT(4,60,4),
     *VR(4,60,4),VRT(4,60,4),VRR(4,60,4),RVR(4,60,4)
      INTEGER I,J,K
      DATA C/3.0/,PI/3.1415927/
      TP0=0.0
      QR0=0.0
      VR0=0.0
      DO 100 K=1,4
      DO 200 I=1,2
      J=1
10    IF(I .GT. 1) GO TO 400
      IF(J .GT. 2) GO TO 77
      TP(I,J,K)=0.50
11    TTP=TP(I,J,K)
      ZP(I,J,K)= C/SQRT(TP(I,J,K))
      ZPS(I,J,K)=ZP(I,J,K) **2
      ALPHAP(I,J,K)=1.0 + 2*ZPS(I,J,K)
```

```
      XP(I,J,K)= EXP(-ZPS(I,J,K))
      ZPPI(I,J,K)=ZP(I,J,K)*SQRT(PI)

BETAP(I,J,K)=2*ZPS(I,J,K)*((XP(I,J,K)/ZPPI(I,J,K))-1.0)
      IF (ZP(I,J,K) .GE. 2.0) GO TO 88
      QR(I,J,K)= (1.0 - ERF(ZP(I,J,K)))/8

VR(I,J,K)=(1.-(ALPHAP(I,J,K)*ERF(ZP(I,J,K))+BETAP(I,J,K)))/
8
      GO TO 99
88    QR(I,J,K)= (ERFC(ZP(I,J,K)))/8

VR(I,J,K)=(1.0-(ALPHAP(I,J,K)*(1.-ERFC(ZP(I,J,K)))+BETAP(I,
J
     *,K)))/8
99    IF(K .GT. 1) GO TO 101
      GO TO 102
101   TP(I,J,K)=TP(I,J,K-1) +7.0
      QR(I,J,K)=QR(I,J,K) + RQR(2,J+10,K-1)
      VR(I,J,K)=VR(I,J,K)+RVR(2,J+10,K-1)
      TP0=7*(K-1)
      QR0=RQR(2,10,K-1)
      VR0=RVR(2,10,K-1)
102   IF(J .GT. 1) GO TO 103
      WRITE(6,*) TP0,QR0
      WRITE(8,*) TP0,VR0
103   WRITE(6,*)TP(I,J,K),QR(I,J,K)
      WRITE(8,*)TP(I,J,K),VR(I,J,K)
      J=J+1
      TP(I,J,K)=TTP+0.5
      IF (J .LE. 2) GO TO 11
      TT(I,J,K)= 1.5
      TEMP=TT(I,J,K)
      TR(I,J,K)= TT(I,J,K) - 0.50
      GO TO 76
77    TT(I,J,K)=TT(I,J-1,K) +0.5
      TEMP=TT(I,J,K)
      TR(I,J,K)=TT(I,J-1,K)
```

```
76      ZT(I,J,K)= C/SQRT(TT(I,J,K))
        ZTS(I,J,K)=ZT(I,J,K)**2
        ALPHAT(I,J,K)=1.+2*ZTS(I,J,K)
        XT(I,J,K)= EXP(-ZTS(I,J,K))
        ZTPI(I,J,K)=ZT(I,J,K)*SQRT(PI)

BETAT(I,J,K)=2*ZTS(I,J,K)*((XT(I,J,K)/ZTPI(I,J,K))-1.0)
        ZR(I,J,K)= C/SQRT(TR(I,J,K))
        ZRS(I,J,K)= ZR(I,J,K)**2
        ALPHAR(I,J,K)=1.+2*ZRS(I,J,K)
        XR(I,J,K)= EXP(-ZRS(I,J,K))
        ZRPI(I,J,K)=ZR(I,J,K)*SQRT(PI)

BETAR(I,J,K)=2*ZRS(I,J,K)*((XR(I,J,K)/ZRPI(I,J,K))-1.0)
        IF(ZT(I,J,K) .GE. 2.0 .OR. ZR(I,J,K) .GE.2.0)  GO  TO
66
        RQR(I,J,K)=(ERF(ZR(I,J,K)) - ERF(ZT(I,J,K)))/8

VRT(I,J,K)=(1.-(ALPHAT(I,J,K)*ERF(ZT(I,J,K))+BETAT(I,J,K)))
/
      *8

VRT(I,J,K)=(1.-(ALPHAT(I,J,K)*ERF(ZT(I,J,K))+BETAT(I,J,K)))
      */8

VRR(I,J,K)=(1.-(ALPHAR(I,J,K)*ERF(ZR(I,J,K))+BETAR(I,J,K)))
      */8

RVR(I,J,K)=((TEMP-.5)/.5)*(VRT(I,J,K)-VRR(I,J,K))+VRT(I,J,K
)
        GO TO 55
66      RQR(I,J,K)=(ERFC(ZT(I,J,K)) - ERFC(ZR(I,J,K)))/8

VRT(I,J,K)=(1.-(ALPHAT(I,J,K)*(1.-ERFC(ZT(I,J,K)))+BETAT(I,
      *J,K)))/8

VRR(I,J,K)=(1.-(ALPHAR(I,J,K)*(1.-ERFC(ZR(I,J,K)))+BETAR(I,
      *J,K)))/8
```

```
RVR(I,J,K)=((TEMP-.5)/.5)*(VRT(I,J,K)-VRR(I,J,K))+VRT(I,J,K
)
55    IF(K .GT. 1) GO TO 65
      GO TO 67
65    RQR(I,J,K)=RQR(I,J,K)+RQR(2,J+10,K-1)
      TT(I,J,K)=TT(I,J,K)+7*(K-1)
      RVR(I,J,K)= RVR(I,J,K) + RVR(2,J+10,K-1)
67    IF(TT(I,J,K) .GT. 28.0) GO TO 299
      WRITE(6,*) TT(I,J,K),RQR(I,J,K)
      WRITE(8,*) TT(I,J,K),RVR(I,J,K)
299   TT(I,J,K) = TEMP
      GO TO 300
400   IF(J .GT. 2) GO TO 401
      IF(J .EQ. 2) GO TO 402
      TP0=TP(I-1,J,K)+1.5
      QR0=RQR(I-1,J+3,K)
      VR0=RVR(I-1,J+3,K)
      WRITE(6,*)TP0,QR0
      WRITE(8,*) TP0,VR0
402   TP(I,J,K)=TP(I-1,J,K) +2.0
      QR(I,J,K)=QR(1,J,1) +RQR(I-1,J+4,K)
      VR(I,J,K)=VR(1,J,1) +RVR(I-1,J+4,K)
      WRITE(6,*) TP(I,J,K),QR(I,J,K)
      WRITE(8,*) TP(I,J,K),VR(I,J,K)
      J=J+1
      IF (J .LE. 2) GO TO 10
401   TT(I,J,K)=TT(I-1,J,K) + 2.0
      IF(K .GT. 1) TT(I,J,K)=TT(I,J,1)+ 7*(K-1)
      RQR(I,J,K)=RQR(1,J,1)+RQR(I-1,J+4,K)
      RVR(I,J,K)=RVR(1,J,1)+RVR(I-1,J+4,K)
      IF(TT(I,J,K) .GT. 28.0) GO TO 300
      WRITE(6,*)TT(I,J,K),RQR(I,J,K)
      WRITE(8,*)TT(I,J,K),RVR(I,J,K)
300   J=J+1
      IF(J .LE. 56) GO TO 10
200   CONTINUE
100   CONTINUE
```

```
      STOP
      END
C
C
C
      FUNCTION ERF(X)
      REAL X,X2,SUM,SUM1,TERM
      INTEGER I
      DATA TOL/1.0E-5/,SQRTPI/1.772454/
      ERF=0.0
      IF(X .EQ. 0.0) GO TO 99
      ERF=1.0
      IF(X .GT. 3.0) GO TO 99
      X2=X*X
      SUM=X
      TERM=X
      I=0
10    I=I+1
      SUM1=SUM
      TERM=TERM*X2/(I+0.5)
      SUM=TERM+SUM1
      IF(TERM .GE. TOL*SUM) GO TO 10
      ERF=2*SUM*EXP(-X2)/(SQRTPI)
99    RETURN
      END
C
C
      FUNCTION ERFC(X)
      REAL X,X2,SUM,U,V,SQRTPI
      INTEGER I,J,TERMS
      DATA SQRTPI/1.772454/,TERMS/12/
C
      X2=X*X
      V= 0.5/X2
      U= 1.0+ V*(TERMS+1)
      DO 10 J=1,TERMS
      I=TERMS - J+1
      SUM= 1.0+ I*V/U
```

```
      U=SUM
10    CONTINUE
      ERFC=EXP(-X2)/(X* SUM *SQRTPI)
      RETURN
      END
```

Computation Scheme (v)

The following program implements computation scheme (v) which applies the method of images to the solution of equations (2.1) and (2.9). The solution is performed for values of the overall parameter (Z) running between zero and 2.0 with a 0.05 increment. Values of the boundary ratio (XB)/(XS) should be supplied by the user. The computed values of altered (QR) and (VR), due to the presence of a no-flow boundary, are used to produce the graphic output of Figures (2.8) and (2.9).

```
C THIS PROGRAMME CALCULATES RATIOS OF FLOW RATE & VOLUME
C DEPLETED FROM A STREAM BY PUMPING A SINGLE WELL IN A
C  STREAM_AQUIFER  SYSTEM  WITH  THE  PRESENCE OF A NO FLOW
BOUNDARY.
C
C
C
                                                      DIMENSION
F(5),ZFAC(50),ZNEW(50),ZNEWS(50),ALPHA(50),EZSN(50)
     *,ZRPI(50),BETA(50),QR(50),VR(50),QRC(2),VRC(2)
      REAL TEMP,SUMQ,SUMV,TEMPQ,QRNET,VRNET,Z
      INTEGER N,I,J,M
C
C
      N=0
10    N=N+1
      READ(5,*) F(N)
      WRITE(6,6) F(N)
6     FORMAT(1H1,T20,19HPROXIMITY  RATIO  =,F7.4)
C
C
      WRITE(6,8)
      Z=0.05
15    TEMP=1.0-(4+2*F(N))
      M=1
20    J=0
      I=1
      SUMQ=0.0
      SUMV=0.0
25    IF(I .EQ. J) GO TO 50
      ZFAC(I)= TEMP + (4+2*F(N))
      J=J+2
      GO TO 100
50    ZFAC(I)= TEMP + ( 2*F(N))
100   TEMP= ZFAC(I)
      ZNEW(I)= Z*ZFAC(I)
      ZNEWS(I)= ZNEW(I)**2
```

```
      ALPHA(I)= 1+(2*ZNEWS(I))
      EZSN(I)= EXP(-ZNEWS(I))
      ZRPI(I)= ZNEW(I) * SQRT(3.1415927)
      BETA(I)= 2*ZNEWS(I)*((EZSN(I)/ZRPI(I))-1.0)
      IF(ZNEW(I) .GE. 2.0) GO TO 111
      QR(I)= 1.0 - ERF(ZNEW(I))
      VR(I)= 1.0 - (ALPHA(I)*ERF(ZNEW(I)) + BETA(I))
      GO TO 112
111   QR(I)=ERFC(ZNEW(I))
      VR(I)=1.0 - (ALPHA(I)*(1.0-ERFC(ZNEW(I))) + BETA(I))
112   IF(VR(I).LT. 0.0) VR(I)=0.0
      TEMPQ=SUMQ
      SUMQ= SUMQ + QR(I)
      SUMV= SUMV + VR(I)
      DIF= SUMQ - TEMPQ
      IF(DIF .EQ. 0.0) GO TO 150
      I=I+1
      GO TO 25
150   QRC(M)=SUMQ
      VRC(M)=SUMV
      IF(M .EQ. 2) GO TO 200
      TEMP=-1.0
      M=M+1
      GO TO 20
200   QRNET= QRC(1)-QRC(2)
      TOL=1.0-QRNET
      IF( ABS(TOL) .LT. 7.5E-3) QRNET=1.0
      VRNET= VRC(1)-VRC(2)
      IF(VRNET .GT. 1.0) VRNET=1.0
      WRITE(6,16) Z,QRNET,VRNET
8     FORMAT(1H0,T18,1HZ,T38,2HQR,T57,2HVR)
16    FORMAT(1H0,10X,F10.5,10X,F10.5,10X,F10.5)
C
      WRITE(8,*)Z,QRNET
      WRITE(10,*)Z,VRNET
C
      Z=Z+0.05
      IF(Z .GE. 2.0) GO TO 250
```

```
      GO TO 15
250   IF(N .LE. 4) GO TO 10
      STOP
      END
C
C
C
C
      FUNCTION ERF(X)
      REAL X,X2,SUM,SUM1,TERM
      INTEGER I
      DATA TOL/1.0E-5/,SQRTPI/1.772454/
      ERF=0.0
      IF(X .EQ. 0.0) GO TO 99
      ERF=1.0
      IF(X .GT. 3.0) GO TO 99
      X2=X*X
      SUM=X
      TERM=X
      I=0
10    I=I+1
      SUM1=SUM
      TERM=TERM*X2/(I+0.5)
      SUM=TERM+SUM1
      IF(TERM .GE. TOL*SUM) GO TO 10
      ERF= 2*SUM*EXP(-X2)/(SQRTPI)
99    RETURN
      END
C
C
      FUNCTION ERFC(X)
      REAL X,X2,SUM,U,V,SQRTPI
      INTEGER I,J,TERMS
      DATA SQRTPI/1.772454/,TERMS/12/
C
      X2=X*X
      V=0.5/X2
      U=1.0+ V*(TERMS+1)
```

```
      DO 10 J=1,TERMS
      I=TERMS-J+1
      SUM=1.0+I*V/U
      U=SUM
10    CONTINUE
      ERFC=EXP(-X2)/(X*SUM*SQRTPI)
      RETURN
      END
```

Computation Scheme (vi)

The following program implements computation scheme (vi) by solving equations (2.14) and (2.15). The equations are solved for values of the overall parameter (Z) running between zero and 2.0 with a 0.05 increment. Values of the parameter (F), which is expressed in the computer program as the retardation ratio R(I), should be supplied by the user. Computer values of (QR) and (VR) are used to produce the graphic output of Figures (2.10) and (2.11).

```
C  THIS  PROGRAMME  CALCULATES RATIOS OF FLOW RATE & VOLUME
DEPLETED
C  FROM  A  STREAM  BY  PUMPING  A  SINGLE  WELL  IN  A
STREAM_AQUIFER
C  SYSTEM  WITH  THE  PRESENCE  OF  IMPERFECT  HYDRAULIC
CONNECTION
C
C
      DIMENSION R(5),W(5),WS(5),QR(5),VR(5)
                                                          REAL
Z,ZS,EZSN,ZRPI,ALPHA,BETA,T1,T2,T3,SEG,SEGS,EXVAL,PARA1,
     *PARA2
      INTEGER I
      DATA PI/3.1415927/
      I= 0
10    I= I+1
      READ (5,*) R(I)
      WRITE (6,6)R(I)
6     FORMAT(1H1,T20,20HRETARDATION  RATIO =,F7.4)
      WRITE (6,8)
      Z =0.05
C
15    T1=0.0
      T2=0.0
      T3=0.0
      SEG=0.0
      PARA1=0.0
      PARA2=0.0
      ZS= Z**2
      W(I)=(R(I)/2.0)/Z
      WS(I)=W(I)**2
      SEG=Z+W(I)
      WRITE(6,*) SEG
      SEGS=SEG**2
      EXVAL=-ZS+SEGS
      IF (EXVAL .GT.90) GO TO 20
          T1=1.0 - ERF(Z)
```

```
      T2=EXP(EXVAL)
      IF (SEG .GE. 2.0) GO TO 111
          T3=1.0 - ERF(SEG)
      GO TO 112
111       T3= ERFC(SEG)
112   QR(I)=T1-(T2*T3)
      ALPHA= 1+(2*ZS)
      WRITE(6,*) EXVAL,T1,T2,T3
      EZSN= EXP(-ZS)
      ZRPI= Z* SQRT(PI)
      BETA= 2*ZS* ((EZSN/ZRPI) -1)
      PARA1= 1- (ALPHA* ERF(Z) + BETA)
      PARA2= QR(I)/WS(I)
      PARA3= 2*((-Z*T1)+(EZSN/SQRT(PI)))/W(I)
      WRITE(6,*)PARA1,PARA2,PARA3
      VR(I)= PARA1+PARA2-PARA3
      IF(ABS(QR(I)) .LT. 0.002 ) QR(I)=0.0
      IF(QR(I) .LE.0.0) VR(I)=0.0
      IF(VR(I) .LT.0.0) VR(I)=0.0
      WRITE(6,16) Z,QR(I),VR(I)
8     FORMAT(1H0,T18,1HZ,T38,2HQR,T57,2HVR)
16    FORMAT(1H0,10X,F10.5,10X,F10.5,10X,F10.5)
      WRITE(8,*)Z,QR(I)
      WRITE(10,*)Z,VR(I)
      IF(QR(I) .LE.0.0 .AND. VR(I) .LE.0.0) GO TO 10
20    Z=Z+0.05
      IF(Z .LE. 2.0)GO TO 15
      IF(I .GE. 6) GO TO 50
      GO TO 10
50    STOP
      END
C
C
C
      FUNCTION ERF(X)
      REAL X,X2,SUM,SUM1,TERM
      INTEGER I
      DATA TOL/1.0E-5/,SQRTPI/1.772454/
```

```
      ERF= 0.0
      IF (X .EQ. 0.0) GO TO 99
      ERF= 1.0
      IF (X .GT. 3.5) GO TO 99
      X2 =X*X
      SUM= X
      TERM= X
      I= 0
10    I=I+1
      SUM1= SUM
      TERM= TERM*X2/(I+0.5)
      SUM= TERM + SUM1
      IF (TERM .GE. TOL*SUM) GO TO 10
      ERF = 2*SUM*EXP(-X2) / (SQRTPI)
99    RETURN
      END
C
C
      FUNCTION ERFC(X)
      REAL X,X2,SUM,U,V,SQRTPI
      INTEGER I,J,TERMS
      DATA SQRTPI/1.772454/,TERMS/12/
C
      X2= X*X
      V=0.5/X2
      U=1.0+V*(TERMS+1)
      DO 10 J=1,TERMS
      I=TERMS - J +1
      SUM=1.0 + I*V/U
      U=SUM
10    CONTINUE
      ERFC= EXP(-X2)/(X*SUM*SQRTPI)
      RETURN
      END
```

APPENDIX B GREEN'S IDENTITIES

There are many linear problems in mathematical physics in which it is possible to write the solution as an integral consisting of the product of an auxiliary function and the given information data, which may be the boundary or initial conditions. Such an auxiliary function is called "Green's function". It is dependent on the differential operator and on the geometry of the problem, but not on the given auxiliary information. The construction of the Green's function is often accomplished with the help of three Green's identities, which are briefly reviewed below. More detailed information on Green's function can be found in Greenberg (1971).

The three Green's identities are the consequences of the divergence theorem, which may be stated as follows:

Let (F_1, F_2) be two components of a vector function F defined over a two dimensional region Ω. If the functions F_1 and F_2 are continuously differentiable, then the integral of the divergence of F over any surface is equal to the outward flux of F over the boundary Γ of that surface, i.e.

$$\int_{\Omega} \partial F_i / \partial X_i \, d\Omega = \int_{\Gamma} F_i n_i \, d\Gamma \qquad \text{(B.1)}$$

where $d\Omega = dX_1 \, dX_2$, n_i denotes components of the outward unit normal vector to the boundary Γ, and repeated indices denote summation.

Green's first identity is obtained by setting $F_i = H \, \partial G / \partial X_i$ and substituting in equation (B.1), i.e.

$$\int_{\Omega} \frac{\partial}{\partial X_i} \left(H \frac{\partial G}{\partial X_i}\right) d\Omega = \int_{\Gamma} H \frac{\partial G}{\partial X_i} n_i \, d\Gamma \qquad (B.2)$$

Equation (B.2) may be written in the form

$$\int_{\Omega} H \frac{\partial^2 G}{\partial X_i \partial X_i} d\Omega = \int_{\Gamma} H \frac{\partial G}{\partial X_i} n_i \, d\Gamma - \int_{\Omega} \frac{\partial H}{\partial X_i} \frac{\partial G}{\partial X_i} d\Omega \qquad (B.3)$$

If the roles of G and H in equation (B.3) are interchanged and the resulting equation is subtracted from (B.3), this yields

$$\int_{\Omega} \left(H \frac{\partial^2 G}{\partial X_i \partial X_i} - G \frac{\partial^2 H}{\partial X_i \partial X_i}\right) d\Omega = \int_{\Gamma} \left(H \frac{\partial G}{\partial X_i} - G \frac{\partial H}{\partial X_i}\right) n_i \, d\Gamma \qquad (B.4)$$

which is known as Green's second identity. Green's third identity is derived from the second identity as follows

Let G = Ln r, where as depicted in Figure (B.1), r is the distance from some fixed point $p(\xi_1, \xi_2)$ to any other point $Q(X_1, X_2)$. Because G is infinite when r=0, equation (B.4) can only be applied to the domain Ω^*, which results from Ω where the point P is excluded from Ω by a small circle with radius ε, which in the limits shrinks to zero. Applying (B.4) yields

$$\int_{\Omega} \left(H \frac{\partial^2}{\partial X_i \partial X_i} (Lnr) - Lnr \frac{\partial^2 H}{\partial X_i \partial X_i}\right) d\Omega$$

$$= \int_{\Gamma} \left(H \frac{\partial}{\partial n} (Lnr) - Lnr \frac{\partial H}{\partial n}\right) d\Gamma$$

$$+ \lim_{\varepsilon \to o} \int_{C} \left(H \frac{\partial}{\partial n} (Lnr) - Lnr \frac{\partial H}{\partial n}\right) dC \qquad (B.5)$$

It can be shown that the integration of equation (B.5) gives

$$H(\xi_1,\xi_2) = \frac{1}{2\pi} \int_\Gamma [\, H(X_1,X_2)\, \frac{\partial}{\partial n}\, (\mathrm{Ln}\ r) - \mathrm{Ln}\ r\, \frac{\partial}{\partial n}\, H(X_1,X_2)\,]\, d\Gamma \qquad (B.6)$$

which is known as Green's third identity.

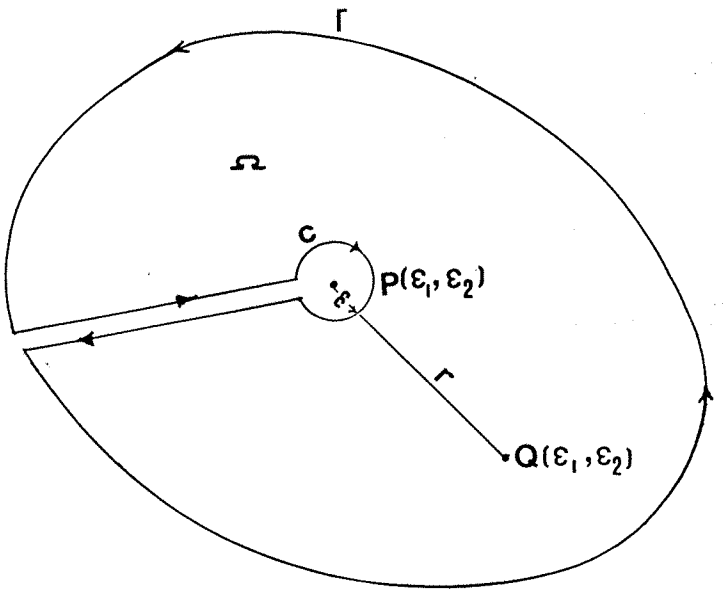

Fig. B.1 Solution Domain

APPENDIX C SALT WATER INTRUSION IN THE CASE STUDY AREA - A THEORETICAL BACKGROUND

.1 OCCURRENCE

In the aquifer system, in the case study area, a hydraulic gradient exists toward the Suez Canal which serves as a recipient for the excess of its fresh water. Owing to the presence of salt water in the aquifer formation under the canal bottom, a zone of contact is formed between the fresh water flowing to the canal and the underlying salt water. In such case, the body of salt water is often in the form of a wedge underneath the fresh water.

Fresh water and salt water are actually miscible fluids and therefore the zone of contact between them takes the form of a transition zone caused by hydrodynamic dispersion. However, under certain conditions, the width of this zone is relatively small, so that an abrupt interface approximation can be introduced. The assumption of an abrupt interface, specially when certain assumptions related to horizontal flow are also introduced, greatly, simplifies the problem in many cases of practical interest.

Under natural undisturbed conditions in a coastal aquifer, a state of equilibrium is maintained, with a stationary interface and a fresh water flow to the sea above it. At every point on this interface, the elevation and slope are determined by the fresh water potential and gradient. If the water table in the vicinity of the coast is lowered, by pumping from the aquifer, to the extent that the head in the fresh water body becomes less than in the adjacent sea water wedge, the interface will start to advance inland until a new equilibrium is reached. This phenomenon is known as salt water intrusion. When the

advancing interface reaches inland pumping wells, the latter become contaminated. When pumping takes place in a well located above the interface, the latter upcones towards the pumping well. In this case, salt water will eventually enter the pumped well, unless the rate of pumping is carefully controlled.

Since a relationship between the rate of fresh water flow to the sea and the extent of salt water intrusion exists, salt water intrusion can be viewed as a part of the management problem of an aquifer system. This is explained by the fact that the fresh water flow to the sea is the difference between the rate of recharge and that of pumping.

.2 MATHEMATICAL STATEMENT OF THE PROBLEM

The mathematical statement is that of a flow problem involving two subdomains of liquids with the assumption that they are separated by an abrupt interface as shown in Figure (C.1).

Assuming that water in both subdomains is incompressible, the piezometric head, h_f, in the fresh water subdomain, Ω_1, and the piezometric head, h_s, in the salt water subdomain, Ω_2, are given by

$$h_f = X_3 + P/\gamma_f \qquad \text{(C.1a)}$$

$$h_s = X_3 + P/\gamma_s \qquad \text{(C.1b)}$$

where γ_f and γ_s are the specific weights of fresh and salt water, respectively.
Then the problem is to determine h_f in Ω_1 and h_s in Ω_2 such that

$$\frac{\partial}{\partial X_i}\left(K_f \frac{\partial h_f}{\partial X_i}\right) = S_o \frac{\partial h_f}{\partial t}, \quad (i=1,2,3) \text{ in } \Omega_1 \qquad (C.2a)$$

$$\frac{\partial}{\partial X_i}\left(K_s \frac{\partial h_s}{\partial X_i}\right) = S_o \frac{\partial h_s}{\partial t}, \quad (i=1,2,3) \text{ in } \Omega_2 \qquad (C.2b)$$

where $K_f = K\gamma_f/\mu_f$, $K_s = K\gamma_s/\mu_s$, K is the intrinsic permeability, $_f$ and $_s$ are the dynamic viscosity of the fresh and salt water and S_o is the specific storativity assumed constant.

In addition, initial conditions for h_f in Ω_1 and h_s in Ω_2 have to be specified. Boundary conditions for h_f on Γ_1 and h_s on Γ_2 are the usual ones encountered in the flow of single fluid. The boundary condition on the interface requires special attention since the location of an interface is unknown until the problem is solved. the sought location and shape of an interface may be expressed in the form

$$F(X_i,t) = 0, \quad (i=1,2,3) \qquad (C.3)$$

Denoting the elevation of points on the interface by $\xi = \xi(X_1,X_2,t)$, the relationship for F becomes

$$F \equiv X_3 - \xi(X_1,X_2,t) = 0 \qquad (C.4)$$

The pressure at a point $P(X_1,X_2,\xi)$ on the interface is the same when approached from both sides. Hence, from the definitions of h_f and h_s,

$$\gamma_f(h_f-\xi) = \gamma_s(h_s-\xi)$$

or

$$\xi(X_1,X_2,t) = h_s(\gamma_s/\Delta\gamma)-h_f(\gamma_f/\Delta\gamma);$$

$$(\Delta\gamma = \gamma_s-\gamma_f) \qquad (C.5)$$

Once the distributions $h_f = h_f(X_i,t)$ and $h_s = h_s(X_i,t)$ are known, equation (C.4) becomes the sought equation for $F(X_i,t)$.

$$F \equiv X_3-h_s(\gamma_s/\Delta\gamma)+h_f(\gamma_f/\Delta\gamma) = 0 \qquad (C.6)$$

The boundary conditions on the interface are

(a) same specific discharge on both sides;
$(q_n)_f = (q_n)_s$ on F

(b) same pressure on both sides;
$\gamma_f(h_f-\xi) = \gamma_s(h_s-\xi)$ on F

Since the interface is a material surface with fluid particles remaining always on it, the substantial derivative dF/dt is given by Bear, 1972 as

$$dF/dt \equiv (\partial F/\partial t) + V_f(\partial F/\partial X_i) = 0$$
$$, (\partial F/\partial t) + V_s(\partial F/\partial X_i) = 0 \qquad (C.7)$$

where $V_f = -\frac{K_f}{n}\frac{\partial h_f}{\partial X_i}$, $V_s = -\frac{K_s}{n}\frac{\partial h_s}{\partial X_i}$; (i=1,2,3)

By combining (C.6), (C.7), the following expressions for boundary conditions are obtained (Bear, 1972)

$$n(\gamma_f/\Delta\gamma)\frac{\partial h_f}{\partial t} - n(\gamma_s/\Delta\gamma)\frac{\partial h_s}{\partial t} - K_f\left[\frac{\partial X_3}{\partial X_i} - (\gamma_s/\Delta\gamma)\frac{\partial h_s}{\partial X_i}\right.$$

$$\left. + (\gamma_f/\Delta\gamma)\frac{\partial h_f}{\partial X_i}\right] \cdot \frac{\partial h_f}{\partial X_i} = 0 \qquad \text{(C.8a)}$$

$$n(\gamma_f/\Delta\gamma)\frac{\partial h_f}{\partial t} - n(\gamma_s/\Delta\gamma)\frac{\partial h_s}{\partial t} - K_s\left[\frac{\partial X_3}{\partial X_i} - (\gamma_s/\Delta\gamma)\frac{\partial h_s}{\partial X_i}\right.$$

$$\left. + (\gamma_f/\Delta\gamma)\frac{\partial h_f}{\partial X_i}\right] \cdot \frac{\partial h_s}{\partial X_i} \qquad \text{(C.8b)}$$

Thus, the boundary conditions on an interface take the form of two nonlinear partial differential equations in h_f and h_s. This is the reason why the derivation of the shape and position of an interface by solving the exact mathematical statement expressed by the partial differential equations (C.2a) and (C.2b) subject to the boundry conditions (C.8a) and (C.8b) on the surface defined by (C.4), is practically impossible and even numerical methods fail here.

Instead of solving the exact mathematical statement of the balance equations in three dimensional space with the nonlinear interface boundary conditions, the hydraulic approach can be employed to average the three dimensional balance equations (C.2a) and (C.2b) over the vertical. Using the nomenclature of Figure (C.2), it can be shown that (Bear, 1979)

$$-\frac{\partial}{\partial X_i} Q_f - n\frac{\partial}{\partial t}(\xi_2 - \xi_1) = 0 \qquad \text{(C.9a)}$$

$$- \frac{\partial}{\partial X_i} Q_s - n \frac{\partial}{\partial t} (\xi_1) = 0 \qquad \text{(C.9b)}$$

where

$$Q_f = -B_f K_f \frac{\partial h_f}{\partial X_i} \quad , (i=1,2) \qquad \text{(C.10a)}$$

$$Q_s = -B_s K_s \frac{\partial h_s}{\partial X_i} \quad , (i=1,2) \qquad \text{(C.10b)}$$

$$B_f = \xi_2 - \xi_1 \qquad \text{(C.11a)}$$

$$B_s = \xi_1 - \xi_0 \qquad \text{(C.11b)}$$

$$\xi_1 = \left(\frac{\gamma_s}{\Delta_\gamma}\right) h_s - \left(\frac{\gamma_f}{\Delta\gamma}\right) h_f \qquad \text{(C.12a)}$$

$$\xi_2 = h_f \qquad \text{(C.12b)}$$

In view of equation (C.12a), initial and boundary conditions for both subdomains are dependent. If initial fresh water levels $h_f = h_f(X_1,X_2,0) \equiv \xi_2(X_1,X_2,0)$ and salt water levels $h_s = h_s(X_1,X_2,0)$ are specified, then the interface elevation $\xi_1(X_1,X_2,0)$ will be dictated by equation (C.12a). Initial conditions are usually obtained from field observations. However, because of the approximation involved, there is no unique way of expressing the boundary conditions for the fresh water and salt water boundaries along the coast. Useful considerations regarding this problem are given by Bear (1979).

Equations (C.9a) and (C.9b) are two equations in $h_f(X_1,X_2,t)$ and $h_s(X_1,X_2,t)$ that have to be solved simultaneously, subject to appropriate boundary conditions

on h_f and h_s in the X_1X_2 plane. For most problems of practical interest the solution is derived by numerical methods. Once h_s and h_f are knwon, the position and shape of interface can eb obtained from equation (C.12a).

.3 STATIONARY INTERFACE

Badon-Ghyben (1988) and Herzberg (1901) presented their model of a stationary interface in a coastal phreatic aquifer as shown in Figure (C.3). The model, essentiall,y assumes static equilibrium and a hydrostatic pressure in the fresh water region, with stationary sea water. However, dynamic equilirbum also may beassumed, i.e., steady flow, but with horizontal flow in the fresh water region. This means that equipotentials are vertical lines identical to the Dupuit assumption. Thus, under these conditions

$$h_s = \left(\frac{\gamma_f}{\Delta\gamma}\right) h_f \qquad (C.13)$$

For $\gamma_s = 1.025$ gr/cm^3, $\gamma_f = 1.0$ gr/cm^3; $\left(\frac{\gamma_f}{\Delta\gamma}\right)$ will be 40 and at any distance form the sea, the depth of a stationary interface below sea level is 40 times the height of fresh water above it. Obviously, as the coast is approached, vertical flow components can no longer be neglected. Meanwhile, the assumptionof vertical equipotentials leaves no room for the fresh water flow to the sea. The actual flow conditions near the coast will be as shown in Figure (C.4), and the actual depth of the interface near the coast is greater than that predicted by Ghyben-Herzberg model.

Notwithstanding the inaccuracy near the coast, the Ghyben-Herzberg model has been shown by Bear and Dagan (1964) to give a good approximation of the salt water intrusion into a horizontal confined auqifer of a thickness

D to within 5% error, provided $\pi KD\Delta\gamma/Q\gamma_f > 8$, where Q is the fresh water discharge to the sea.

Obviously, there exists a relationship between the rate of fresh water flow to the sea and the extent of salt water intrusion. Therefore, salt water intrusion can be viewed as a part of the hydraulic management problem of the aquifer system as the fresh water flow to the sea is the difference between the rate of recharge and that of pumping. The relationship between the extent of salt wter intrusion and the flow of fresh water to the sea can be explained by considering Dupuit's assumption of horizontal flow and the Ghyben-Herzberg relationship (C.13), continuity leads to

$$Q = - K (h_s+h_f)\frac{\partial h_f}{\partial X_i} = - K (1 + \frac{\gamma_f}{\Delta\gamma}) h_f \frac{\partial h_f}{\partial X_i} \qquad (C.14)$$

Integrating (C.14) with X = 0 and h_s = B, at the toe, yields

$$Q[X]_0^L = \tfrac{1}{2}K(1 + \frac{\gamma_f}{\Delta\gamma}) [h_f^2(X)]_{X=0}^L \qquad (C.15)$$

which shows that the interface has the form of a parabola with vertex at $h_f = 0$ and passes through X = 0 and X = L. Above the toe if follows that

$$L = \tfrac{1}{2}K (1 + \frac{\gamma_f}{\Delta\gamma}) \frac{h_f^2}{Q} \qquad (C.16)$$

The relationship among the length L of salt water intrusion, the discharge Q to the sea and the piezometric head h_f abvoe the toe, is clearly expressed by (C.16). As Q increases L decreases. This means that the extent of salt

water intrusion, expressed by L, is a decision variable in the hydraulic management problem of the aquifer. Thus, the extent of salt water intrusion is controlled via controlling the recharge and/or pumping in the coastal aquifer strip.

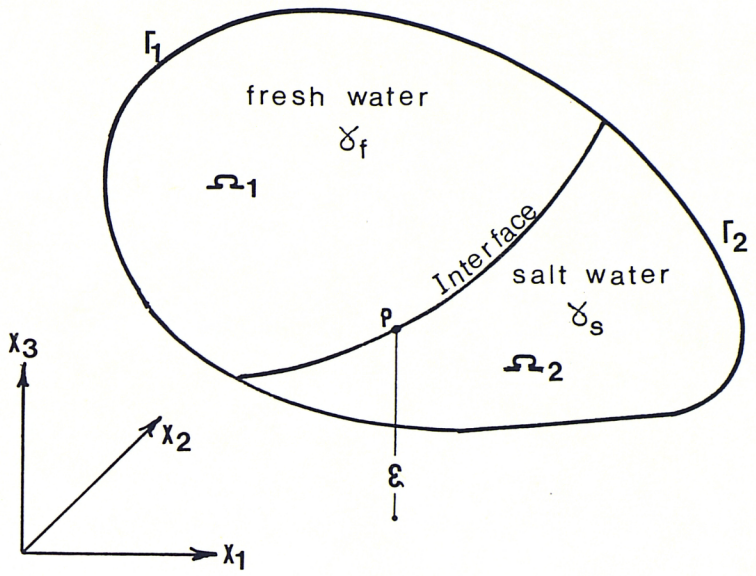

Fig. C.1 fresh water and salt water subdomains

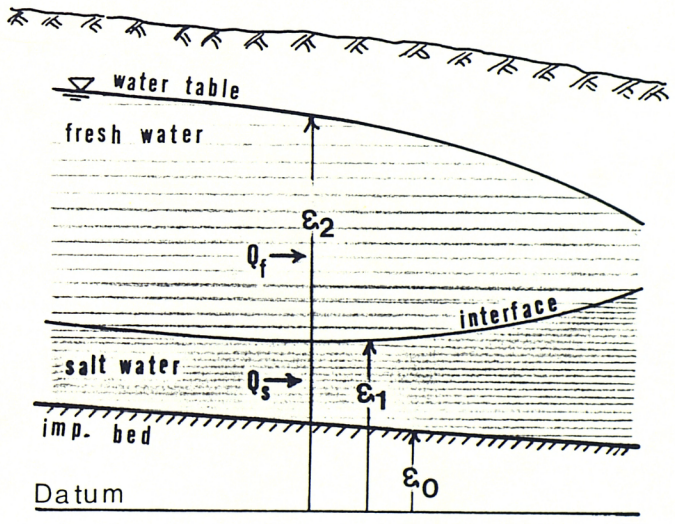

Fig. C.2 nomenclature

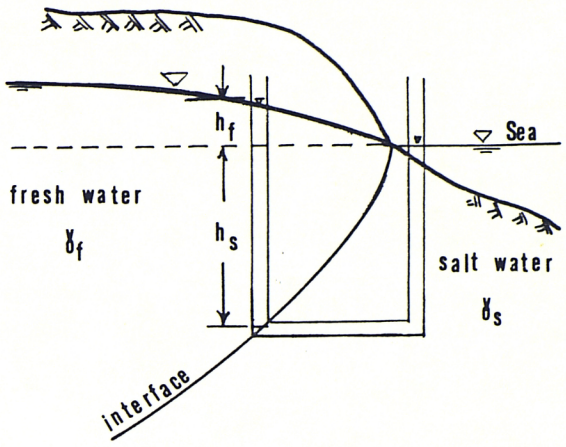

Fig. C.3 Ghyben - Herzberg Model

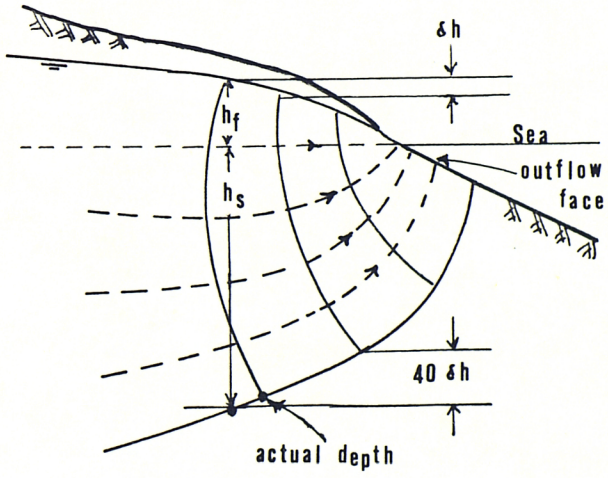

Fig. C.4 Actual Flow Pattern

APPENDIX D FORMULATION OF A REPRESENTATIVE DEMAND DENSITY FUNCTION FOR IRRIGATION REQUIREMENT IN THE CASE-STUDY AREA

Agriculture in the eastern region of the Nile Delta comprises two main categories, that of the "old" lands, which occupies virtually the whole of the present irrigated areas north of the case-study area, and the relatively small areas of "new" lands on the desert soils outside the alluvial zone. For the development of a representative demand density function for irrigation requirement in the case-study area. The main concern is the present agricultural practice on the "new" lands.

In the higher desert areas outside of the Ismailia Canal command, several projects to reclaim new lands are taking place. Most of these projects require water to be pumped, from the Ismailia Canal, a considerable height up to 100 metres. Because of the light free draining soils, irrigation is usually by sprinkler and/or trickle methods. Operation of these projects is quite different to the normal traditional agriculture practised on the "old" lands. Capital costs are high and they are commonly operated on a large scale commercial basis.

Salheya, Shabab and Ramsis land reclamation projects, Table (D.1), are representative examples of the present agricultural practice on the "new" lands in the eastern region of the Nile Delta.

PROJECT	CROPPED AREA Feddan*	IRRIGATION METHOD AND % OF CROPPED AREA
Salheya	14000	Central pivot sprinkler systems, 75% Trickle, 25%
Shabab	12000	Central pivot sprinkler systems, 83% Trickle, 17%
Ramsis	1800	Trickle, 100%

* 1 feddan = 0.42 hectare

Table (D.1) Large Scale Land Reclamation Projects in the Eastern Region of the Nile Delta

Compiled information on cropping patterns and irrigation requirements in these projects (RIGW AND IWACO, 1986), and those proposed by the Ministry of Land Reclamation and the Ministry of Irrigation (MOI, 1980) are used to formulate representative density function for water demands in the study area.

Density of water demand at any month throughout a year can be obtained by expressing the monthly water requirement as a percentage of the annual water requirements. Densities of water demand for five main cropping patterns as practised on the "new" lands in the above mentioned projects are shown in Table (D.2). The arithmetic means of the densities of monthly water demands can be considered as a satisfactory representation of the expected demand densities in the study area.

	CROPPING PATTERN	MONTHLY WATER DEMAND EXPRESSED AS A PERCENTAGE OF ANNUAL DEMAND D(i) %											
		J	F	M	A	M	J	J	A	S	O	N	D
1	Alfalfa $\frac{1}{3}$, Barley and Peanut $\frac{1}{3}$, Vegetables $\frac{1}{3}$	4.151	5.057	5.521	10.961	12.802	10.76	10.41	9.811	10.27	8.674	5.747	5.836
2	Alfalfa $\frac{1}{3}$, Barley and Peanut $\frac{1}{3}$, Citrus $\frac{1}{3}$	5.213	5.763	5.107	9.727	12.31	12.543	12.673	11.667	10.46	5.737	4.427	4.373
3	Alfalfa $\frac{1}{3}$, Vegetables $\frac{1}{3}$, Citrus $\frac{1}{3}$	3.838	4.594	6.938	11.412	13.236	10.757	9.68	9.021	9.42	9.328	6.044	5.732
4	Barley and Peanut $\frac{1}{3}$, Vegetables $\frac{1}{3}$, Citrus $\frac{1}{3}$	3.551	4.658	6.398	11.286	13.359	11.213	10.567	9.435	9.26	9.484	5.724	5.065
5	Citrus	4.30	4.90	7.40	10.50	13.30	13.00	12.10	10.50	8.60	7.20	4.70	3.50
	AVERAGE D(i)	4.2106	4.9944	6.2728	10.7772	13.0014	11.6546	11.0860	10.0868	9.6020	8.0846	5.3284	4.9012

Table (D.2) Densities of water demand for five main cropping patterns as practised on the "new land" in the eastern region of the Nile Delta.

A demand density function, (i), can then be developed such that the value of (i) at any month, i, is given by

$$\alpha(i) = \frac{D(i)}{D_{max}} \quad , \quad (i=1,12) \qquad (D.1)$$

where D(i) is the density of monthly demand at any month, i, and D_{max} is the density of maximum monthly demand through the year.

Calculated values of $\alpha(i)$ for the study area are shown in Table (D.3).

Accordingly, monthly supply by pumping from groundwater, S(i), at any month, i, can be expressed as

$$S(i) = S_{max}\ \alpha(i) \quad , \quad (i=1,12) \qquad (D.2)$$

where S_{max} is the maximum allowable supply from groundwater during the same month of maximum demand.

Month (i)	D(i)	α(i)
Jan	4.2106	0.3239
Feb	4.9944	0.3841
Mar	6.2728	0.4825
Apr	10.7772	0.8289
May	13.0014	1.0
Jun	11.6546	0.8964
Jul	11.0860	0.8527
Aug	10.0868	0.7758
Sep	9.6020	0.7385
Oct	8.0846	0.6218
Nov	5.3284	0.4098
Dec	4.9012	0.3770

Table (D.3) Values of the demand density function, α(i)

Considering an agricultural year where summer planting starts in April, Figure (D.1) shows a graphical representation of the demand density function α(i) chronologically arranged according to the crop calender.

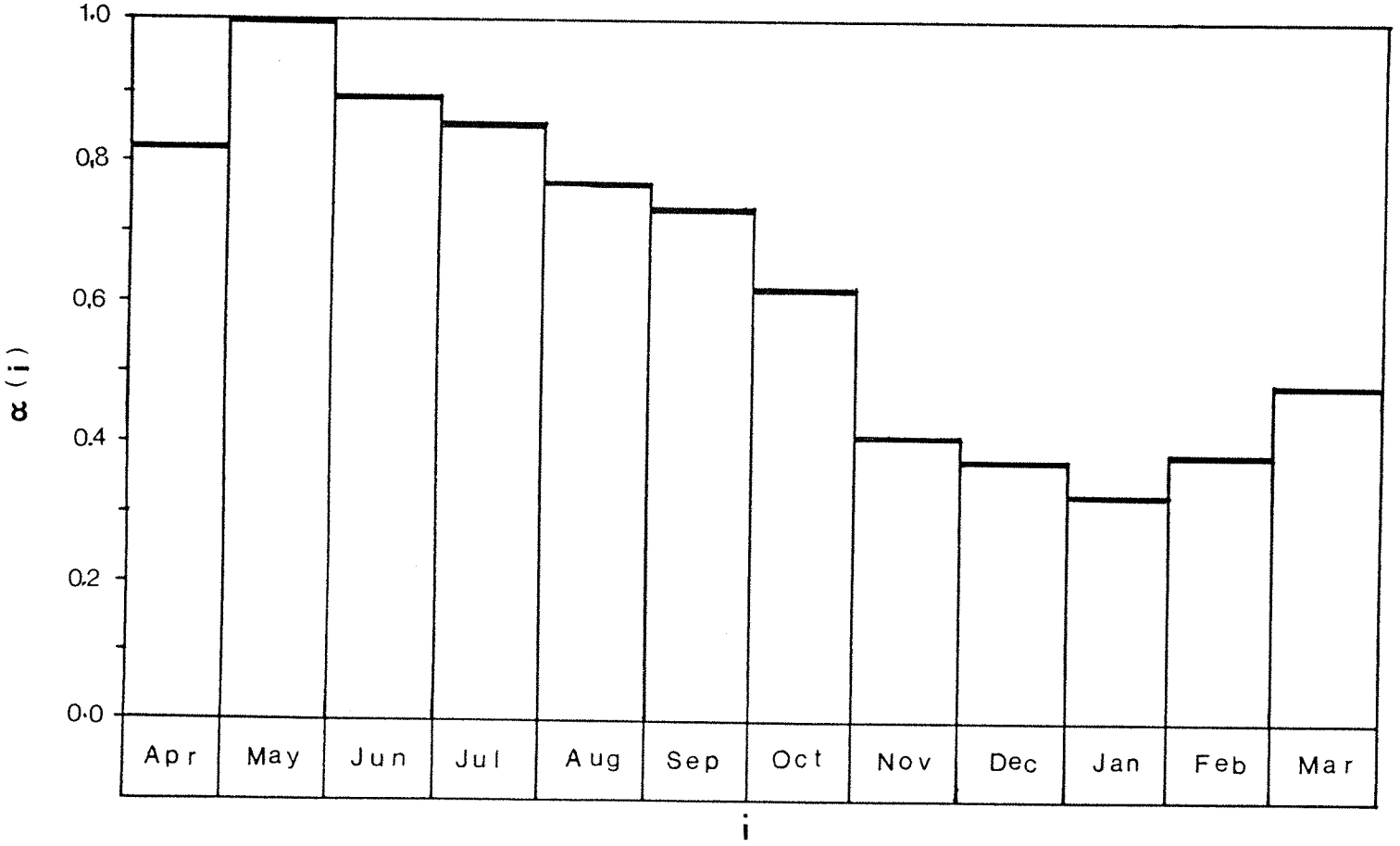

Fig. D.1 Values of the Demand Density Function, $\alpha(i)$

APPENDIX E

LIST OF SYMBOLS

Symbol	Definition	Units
A	Coefficient as defined by eqn. (2.10a)	
A	Area of a triangular cell	L^2
A_1	Angle	
A_2	Angle	
AR,AT	Coefficients as defined by eqn. (2.13)	
ARR	Ratio of aquifer rewatering	
$A^e_{i,j}$	Boundary integrals	
a	Retardation factor defined by K/(k/b)	L
a	A variable defined by eqn. (4.23)	
B	Coefficient as defined by eqn. (2.10b)	
BI	Boundary integral	
BR,BT	Coefficients as defined in eqn. (2.13)	
B_1	Angle	
B_2	Angle	
$B^e_{i,j}$	Boundary integrals	
b	Semi-pervious layer thickness	L
b	Half width of a stream bed	L
C	Hydraulic resistance	T
C^c	Domain integrals contributed by a cell	
C^e	Boundary integrals contributed by a linear element	
c	Circular arc	L
D	Aquifer thickness	L
D	Drawdown in the aquifer	L
D( )	Monthly water demand expressed as a percentage of the annual demand	
DI	Domain integral	
D_a	Allowable drawdown	L
$D^c_{i,j}$	Domain integrals	
d	The normal distance between a base point and a linear element	L
$E^c_{i,c}$	Domain integrals	
Ei[ ]	The exponential integral function	
erf	Error function	
erfc	Complementary error function	
F	Parameter defined by X/a	
F	Vector function	
F_1,F_2	Components of a vector function	
F_j	Linear interpolation function	
f	Flux per unit length of a stream boundary	L^2T^{-1}
G	Green's function	
G_o	Green's function	

Symbol	Definition	Units
H	Hydraulic head	L
H_o	Initial hydraulic head	L
H_s	Surface water elevation in a stream above impermeable bed	L
H_w	Depth of water in a stream	L
h_f	Piezometric head in fresh water subdomain	L
h_s	Piezometric head in salt water subdomain	L
I	Quantity of water induced from a stream	L^3T^{-1}
i	Time interval unit	T
J	Jacobian of transformation	
K	Hydraulic conductivity	LT^{-1}
K	Intrinsic permeability	L^2
k	Hydraulic conductivity of a semi-pervious layer	LT^{-1}
k	Location of an observation well	
L	Length	L
L	Number of pumping locations	
L_e	Length of a boundry element	L
ℓ	A pumping location	
ℓ	A time level	
M	Number of domain integration cells	
N	Pumping rate from a well	L^3T^{-1}
N	Time ratio defined by (TR/TP)	
N_*	Number of boundary elements	
N^*	Quantity of water withdrawn from aquifer during the time interval of maximum demand	L^3T^{-1}
n	Summation variable	
n	Number of time interval units	
n	Porosity	
n	Outward normal	
n, ℓ	Local coordinates	
P_i	A base point	
P_j	Boundary node point	
Q	Rate of pumping	L^3T^{-1}
Q	Flow of fresh water to the sea	L^3T^{-1}
QR	Ratio of the rate of stream depletion	
q	Rate of stream depletion	L^3T^{-1}
q	Flux defined by $-T\ \partial H/\partial n$	L^2T^{-1}
q	Dummy gradient of flux at a corner point	
q^*	Defined as $-T\ \partial G/\partial n$	
q_r	Rate of stream depletion after cessation of pumping	L^3T^{-1}
R	Natural Recharge	L^3T^{-1}
RQR	Ratio of the rate of stream depletion after cessation of pumping	

Symbol	Definition	Units
r	Distance from a base point to a field point	L
S	Specific yield	
T	Transmissivity	L^2T^{-1}
TP	Pumping time	T
TR	Time after cessation of pumping	T
TRVR	Ratio of the volume of stream depletion after cessation of pumping	
TT	Time defined by (TP+TR)	T
TVS	Total volume of stream depletion	L^3
t	Time	T
U	Variable defined by eqn. (2.4b)	
V	Parameter defined by $1/2Z^2$	
VR	Ratio of the volume of stream depletion	
V_d	Induced stream depletion during pumping	L^3T^{-1}
V_p	Quantity of water removed from aquifer storage and stream by pumping wells	L^3T^{-1}
V_r	Induced stream depletion after cessation of pumping	L^3T^{-1}
V_s	Quantity of water removed from aquifer storage	L^3T^{-1}
W	Parameter defined by (F/2Z)	
W_i	Weighting factor for Gaussian quadrature	
X	Distance from pumped well to a stream	L
X_1, X_2	Global Cartesian coordiantes	L
Z	Parameter defined by eqn. (2.4a)	
α	Coefficient as defined by eqn. (2.5)	
α	Angle	
$\alpha( )$	Demand density function	
α_a	Angle	
α_b	Angle	
α, β, γ	Coefficients defined by eqn. (4.47)	
$\alpha_i, \beta_i, \gamma_i$	Coefficients defined by eqn. (4.45)	
$\beta( )$	Stream-aquifer response coefficients	
Γ	Boundary of solution domain	
Γ_D	Dividing boundary in a two-zone domain	
Γ_e	Linear boundary element	
γ_f	Specific weight of fresh water	FL^{-3}
γ_s	Specific weight of salt water	FL^{-3}
$\Delta\gamma$	Difference in specific weight $(\gamma_s - \gamma_f)$	FL^{-3}
$\delta( )$	The Dirac delta function	
ε	Radius of a small circle	L
η	Local dimensionless coordinate system	
η_1, η_2	Local oblique coordinates	L
θ	Interior boundary angle	

Symbol	Definition	Units
λ	Coefficients defined by eqn. (4.11)	
μ	Variable defined by eqn. (4.37)	
μ_f	Dynamic viscosity of fresh water	FTL^{-2}
μ_s	Dynamic viscosity of salt water	FTL^{-2}
ν	Variable defined by eqn. (4.35)	
ξ_1, ξ_2	Coordinates of a base point	L
σ	Coefficient of hydraulic connection	LT^{-1}
τ	Time variable	T
$\psi(\ )$	Stream-aquifer interaction parameters	
Ω	Interior of the solution domain	
Ω_1	Fresh water subdomain	
Ω_2	Salt water subdomain	
Ω_c	Internal integration cell	